

NASA SP-332

N73-31731

THE GUM NEBULA  
AND RELATED PROBLEMS

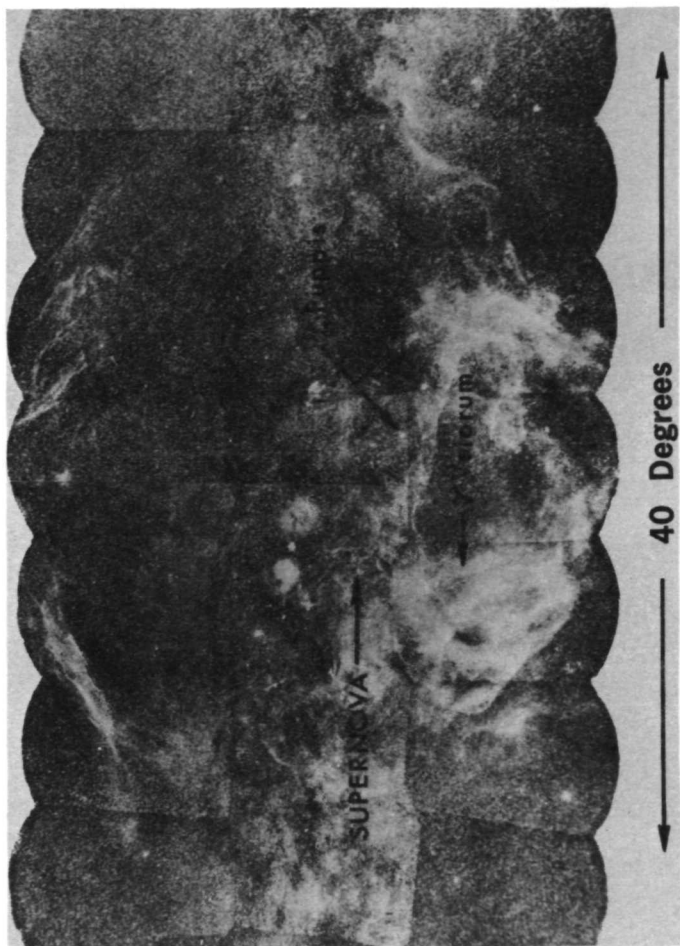
CASE FILE  
COPY

A symposium held at  
GODDARD SPACE FLIGHT CENTER  
May 18, 1971



NATIONAL AERONAUTICS AND SPACE ADMINISTRATION

**THE GUM NEBULA  
AND RELATED PROBLEMS**



Frontispiece - The Gum Nebula in H-alpha was portrayed in the conference poster, as discussed on page 10. The mosaic photograph is taken from An Atlas of H-alpha Emission in the Southern Milky Way, by A. W. Rodgers, C. T. Campbell, J. B. Whiteoak, H. H. Bailey, and V. O. Hunt, published in 1960 by the Australian National University.

# THE GUM NEBULA AND RELATED PROBLEMS

*The proceedings of a symposium held at the  
NASA Goddard Space Flight Center, May 18, 1971*

*Prepared by Goddard Space Flight Center*



*Scientific and Technical Information Office*

1973  
NATIONAL AERONAUTICS AND SPACE ADMINISTRATION  
Washington, D.C.



---

For sale by the National Technical Information Service  
Springfield, Virginia 22151  
Price \$3.00  
*Library of Congress Catalog Card Number 73-6000176*

## PREFACE

This volume constitutes the proceedings of a symposium held at the Goddard Space Flight Center in Greenbelt, Maryland on May 18, 1971. A preliminary edition of the proceedings was distributed in September, 1971 to scientists actively engaged in this field, in view of the observing programs then being planned for the austral summer. Since that time, several papers have been corrected or slightly revised in accord with the instructions of the authors, and the article by Dr. Westerhout has been added, as has the index.

The papers by Webster, by Reynolds et al., and by Blamont and Levasseur are invited contributions that were not actually presented at the Symposium. A few of the other articles discuss their respective subjects at much greater length than was possible at the meeting. Although the discussion sections have been summarized from tape recordings, none of the papers was prepared in this fashion; all of the papers are based on manuscripts supplied by the authors. It should be noted, however, that Figure 3 of the Gott and Ostriker article was prepared by us from a video recording of a blackboard sketch by Mr. Gott. The illustrations for Prof. Bok's paper were chosen by us from the collection of photographs that he has generously made available to astronomers working in this field and we have also made a few changes in these illustrations and those that accompany several other articles.

Mr. Howard Caulk supervised editorial work on the illustrations, and Mrs. Margaret A. Becker was in charge of the production of the preliminary edition. We thank Mr. Milton Kalet and Mrs. Mozelle Bird for their help in organizing the symposium.

Stephen P. Maran  
John C. Brandt  
Theodore P. Stecher

**Page Intentionally Left Blank**

## INTRODUCTION

Stephen P. Maran  
*Laboratory for Solar Physics*  
*Goddard Space Flight Center*  
*Greenbelt, Maryland 20771*

Taken separately, the Gum Nebula, the Vela X supernova remnant, the hot stars gamma Velorum and zeta Puppis, the B-associations in Vela-Puppis and the pulsar PSR 0833-45 are each a fascinating subject for astrophysical investigation. Viewed collectively, with the remnant Puppis A and several slow pulsars apparently in the background, this appears to be one of the most interesting regions of the sky.

Leafing through these proceedings, one is perhaps most impressed by the way in which each of many disciplines has played a significant role. It is clear that both our present understanding and future progress depend on ground-based optical and radio astronomy, rocket and satellite observations in the radio, visible, ultraviolet, and x-ray regimes, and on the solution of a great many theoretical problems in the physical state of the interstellar medium, in stellar evolutionary processes and perhaps also in the dynamics of runaway stars.

The reader may wish to consult the reports on the symposium that appear in the August, 1971 issue of Sky and Telescope and in the September, 1971 Physics Today. A popular account of research in this field appears in the February, 1972 edition of Smithsonian.

A portrait of Colin Gum appears here as Figure 1, and his career is described in Prof. Kerr's paper that follows this Introduction. Gum's work in exploring the nebula is also described in the December, 1971 Scientific American.

Since this conference was held, George Wallerstein and Joseph Silk have measured the expansion rate of Vela X, as revealed by high velocity absorption lines in the spectra of two distant stars. Inspired by the work of McCray and Schwarz, as summarized in these proceedings, Brandt and I have searched for observational counterparts to the older kind of Gum Nebulae that they predict. We believe that the galactic radio spurs or "giant loops" may be the sought-for objects; a similar conclusion has been drawn independently by Minas Kafatos and Philip Morrison. The OSO-7 satellite, launched on

Sept. 29, 1971, carried a gamma ray spectrometer developed by Edward Chupp of the University of New Hampshire. This instrument is searching for the emission lines predicted by Ramaty and Boldt in these proceedings. Surely new discoveries can be expected as astronomers continue to unravel the problems of the Gum Nebula and related phenomena.



Figure 1. Colin S. Gum (courtesy of Ewart Gale).

# CONTENTS

Introduction	
<i>Stephen P. Maran</i> . . . . .	vii
Colin Gum and the Discovery of the Gum Nebula	
<i>F. J. Kerr</i> . . . . .	1
Identification of the Gum Nebula as the Fossil Strömgren	
Sphere of the Vela X Supernova	
<i>John C. Brandt</i> . . . . .	4
The Size and Shape of Gum's Nebula	
<i>Hugh M. Johnson</i> . . . . .	12
Formation of Giant H II Regions Following Supernova Explosions	
<i>L. Sartori</i> . . . . .	20
Radio Astronomy Explorer-1 Observations of the Gum Nebula	
<i>J.K. Alexander</i> . . . . .	31
A Discussion of the Ground-Based Radio Observations	
<i>F. J. Kerr</i> . . . . .	38
Runaway Stars in the Gum Nebula	
<i>J. Richard Gott, III and Jeremiah P. Ostriker</i> . . . . .	42
Structure and Evolution of Fossil H II Regions	
<i>Richard McCray and Joseph Schwarz</i> . . . . .	56
The Velocity and Composition of Supernova Ejecta	
<i>Stirling A. Colgate</i> . . . . .	68
Cosmic Rays from Supernovae and Comments on the	
Vela X Pre-Supernova	
<i>A. G. W. Cameron</i> . . . . .	74
Cosmic-Ray Effects in the Gum Nebula	
<i>R. Ramaty and E. A. Boldt</i> . . . . .	89

The Early Evolution of Giant H II Regions Formed by Supernova Explosions <i>Minas C. Kafatos</i> .....	103
Three Proposed B-Associations in the Vicinity of Zeta Puppis <i>Edward K. L. Upton</i> .....	119
Comments on an Association in Vela <i>W. C. Straka</i> .....	126
A Discussion of the H-Alpha Filamentary Nebulae and Galactic Structure in the Cygnus Region <i>Thomas A. Matthews and S. Christian Simonson, III</i> .....	128
Radiofrequency Recombination Lines from the Interstellar Medium <i>A. K. Dupree</i> .....	139
The Appearance of the Gum Nebula <i>Bart J. Bok</i> .....	148
The Difficulty of Ultraviolet Emission from Supernovae <i>Stirling A. Colgate</i> .....	152
A Note on the Possible Importance of the Gum Nebula <i>D. P. Cox</i> .....	155
X-Rays from the Vela-Puppis Complex <i>A. N. Bunner</i> .....	158
The Basic Assumption <i>Theodore P. Stecher</i> .....	167
Low-Intensity H-Beta Emission from the Interstellar Medium <i>R. J. Reynolds, F. Roesler, F. Scherb, and E. Boldt</i> .....	169
Large Nebular Complexes in the Northern Portion of the Galaxy <i>William J. Webster, Jr.</i> .....	193

Preliminary Results of an H-Alpha Map of the Gum Nebula Obtained with the D-2-A Satellite <i>J. E. Blamont and A. C. Levasseur</i> . . . . .	203
How to Recognize and Analyze Gum Nebulae <i>Gart Westerhout</i> . . . . .	211



# COLIN GUM AND THE DISCOVERY OF THE GUM NEBULA

F. J. Kerr

*Astronomy Program, University of Maryland  
College Park, Maryland 20742*

As some later speakers will be talking of a proposed time scale of tens of thousands of years, it is appropriate to begin this symposium with a brief sketch of some recent history. Most of the people in this room do not know who Colin Gum was. As a former colleague and personal friend of his, I want to give a short outline of his career and scientific work. He made three principal contributions to astronomy, and it is interesting that all three of these are relevant to today's symposium.

Colin Gum lived from 1924 to 1960. He graduated with a Bachelor of Science Honours degree in physics at the University of Adelaide in South Australia, and later received his Ph.D. at the Australian National University for work done at the Mount Stromlo Observatory. He then spent three years in my group at the CSIRO Radiophysics Laboratory in Sydney, followed by a year in Pasadena as a Carnegie Fellow. In fact, I believe that his was the first Ph.D. in astronomy to be awarded at ANU. It is an interesting historical sidelight that his flight to California in 1959 was the first commercial jet service across the Pacific – a Boeing 707 operated by the Australian airline Qantas. The passengers all received special V.I.P. treatment.

His first project at Mount Stromlo was a radio survey at 200 MHz (Figure 1), carried out with C. W. Allen who is now at the University of London and is well known for his compendium entitled Astrophysical Quantities. This was one of the first large-scale radio surveys. Although carried out with a Yagi antenna with a beamwidth of  $25^\circ$ , it was not superseded for several years. It includes the part of the sky that is being considered at this symposium.

Colin Gum's Ph.D. project was a photographic survey for H II regions in the Southern Milky Way from longitude ( $l^{\text{II}}$ )  $220^\circ$  to  $20^\circ$ . He used an f:1 Schmidt with a 10-cm aperture, and an  $11^\circ$  field. Photographs were taken in a  $250 \text{ \AA}$  band centered on H $\alpha$ , and in a  $600 \text{ \AA}$  comparison band nearby. Exposure times were 20-60 minutes, which enabled him to get down to emission measures as low as 600. Some of these observations were taken at Mount Stromlo, and others during site testing work in the Flinders Range in South Australia, where he had very good skies. He also took slit spectra with a nebular spectrograph to confirm the reality of some of the very faint regions.



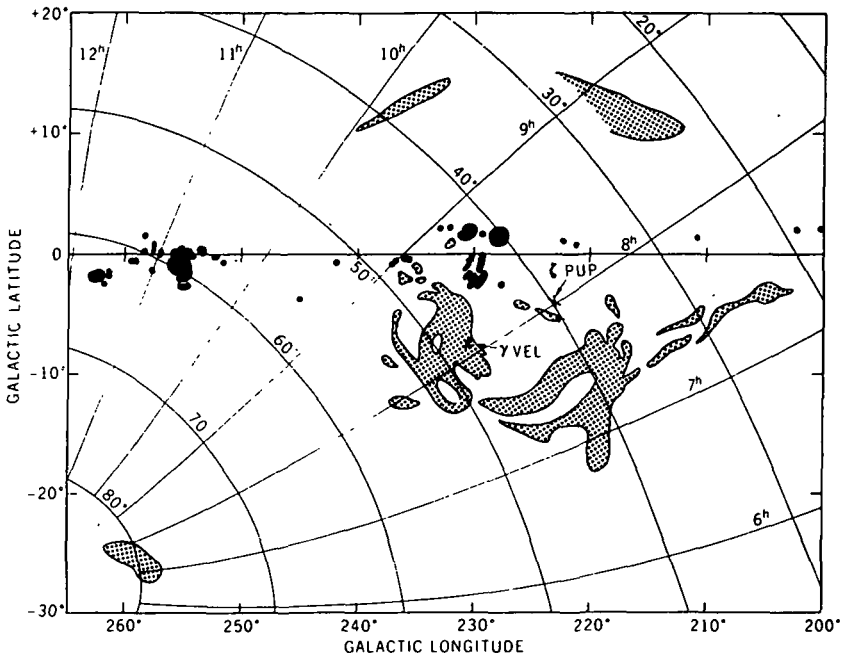


Figure 2. Gum's (1956) sketch of the "large H II region excited by  $\gamma^2$  Vel and  $\zeta$  Pup," with the constituents indicated by half-tone areas. Other galactic nebulosities at greater distances are shown as solid black areas. (Old galactic coordinates.)

Colin Gum was killed in a skiing accident in Switzerland at the age of 36. He had a short scientific life, but he completed several important studies in both optical and radio astronomy, and his name is well entrenched in the sky through the famous nebula that is the center of today's discussions.

#### References

- Allen, C. W., and Gum, C. S. 1950, "Survey of Galactic Radio Noise at 200 Mc/s," Aust. J. Sci. Res., **3A**, 224.
- Gum, C. S. 1955, "A Survey of Southern H II Regions," Mem. Roy. Astron. Soc., **67**, 155.
- Gum, C. S. 1956, "The Extent and Excitation of the Large H II Region in Vela-Puppis," Observatory, **76**, 150.
- Gum, C. S., Kerr, F. J., and Westerhout, G. 1960, "A 21-cm Determination of the Principal Plane of the Galaxy," Mon. Not. Roy. Astron. Soc., **121**, 132.
- Pawsey, J. L., and Bracewell, R. N. 1955, Radio Astronomy, (Oxford: Clarendon Press), p. 258.

# IDENTIFICATION OF THE GUM NEBULA AS THE FOSSIL STRÖMGREN SPHERE OF THE VELA X SUPERNOVA

John C. Brandt

*Laboratory for Solar Physics  
Goddard Space Flight Center  
Greenbelt, Maryland 20771*

I will briefly outline the evidence for the fact that the Gum Nebula undoubtedly is not ionized by gamma Velorum and zeta Puppis, but was produced by some other source, which we have identified as the Vela X supernova (Brandt et al. 1971).

Figure 1 is a photographic mosaic from the Mount Stromlo H-alpha survey (Rodgers et al. 1960) which gives an impression of the size and extent of the Gum Nebula. This is probably only part of the nebula; however, its extent is more fully indicated in the chart of H-alpha emission given by Johnson (1971). The most probable angular dimension in the plane of the galactic equator is about  $90^\circ$  and the dimension perpendicular to the plane is about  $40^\circ$ .

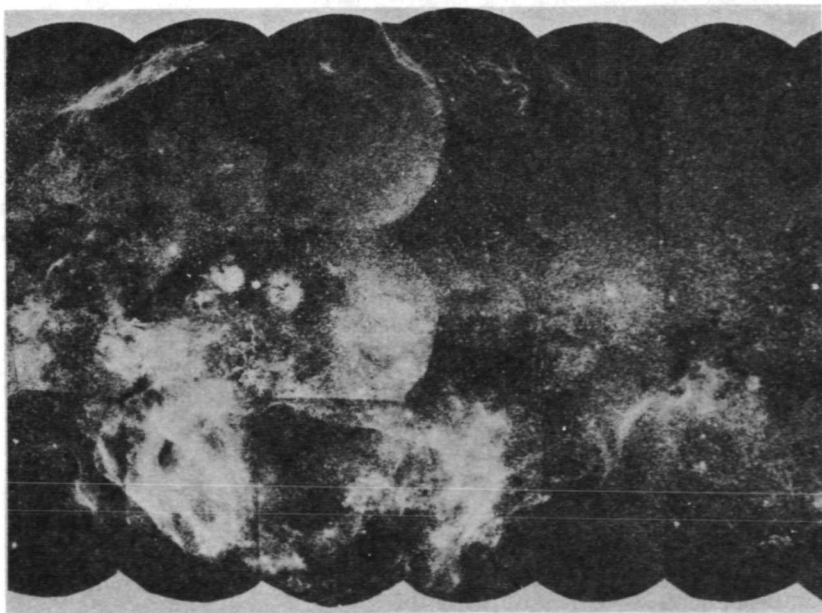


Figure 1. Mosaic of the Gum Nebula in H-alpha, from Rodgers et al. (1960).

Any attempt to determine what excites this nebula must be based on a model. Table 1 lists the "observed" quantities. The emission measure can be disputed, but it is undoubtedly not too far off. The emission measure that we have adopted can be verified to within a factor of 2 by taking the pulsar dispersion measure and scaling it up by some factor that takes account of the clumpiness. The dispersion measure in Table 1 is an average quantity for the path to the central region of the nebula, based on PSR 0833-45, which is in that region, and on three other pulsars that are probably on the other side of the nebula, and which have roughly double the dispersion measure of PSR 0833-45, as one would expect. These pulsars are MP 0736, MP 0835, and MP 0940. The hydrogen measure, that is, the amount of hydrogen between the Sun and the stars gamma Velorum and zeta Puppis (which also lie in the central region of the nebula), is based on rocket measurements of Lyman-alpha absorption and is nearly the same for the two stars.

Table 1  
The Gum Nebula — Observational Data

$EM = \int n_e^2 ds = 1300 \text{ cm}^{-6} \text{ pc}$
$DM = \int n_e ds = 63 \text{ cm}^{-3} \text{ pc}$
$HM = \int n_H ds = 25 \text{ cm}^{-3} \text{ pc}$
Distance: 460 pc
Temperature: $\gtrsim 50,000^\circ \text{K}$

By photometry of the B-star component of gamma Velorum and of a related small group of B stars that appears to be an association, we found a distance of 460 parsecs to the central region of the nebula (Brandt *et al.* 1971), in agreement with the estimated distance to the supernova remnant Vela X (Milne 1968).

The nebular temperature (Table 1) is derived from low frequency radio astronomy measurements (Alexander *et al.* 1971), as discussed in detail by Alexander (1971).

Table 2 illustrates the assumptions involved in the model building. Basically, we suppose that the line of sight from the Sun through the nebula encounters mostly neutral hydrogen near the Sun, passes a boundary and then goes into a fully ionized region. These assumptions allow us to derive a model for the Gum Nebula on the basis of the quantities given in Table 1, providing that we adopt a value for the mean neutral hydrogen density near the Sun. Since we know the hydrogen measure, that will immediately give us the distance to the edge of the nebula, and hence also the radius of the nebula. The size

can then be checked against the observations. This comparison is given in Table 3. The radio astronomy evidence cited in Brandt *et al.* implied that the neutral hydrogen density near the Sun is  $0.4 \text{ cm}^{-3}$ . Later, Alexander *et al.* took into account the OGO-5 satellite measurements that give a neutral hydrogen density of  $0.1 \text{ cm}^{-3}$ . This quantity refers to hydrogen streaming into the solar system and illuminated by solar Lyman-alpha; it is a very local measurement. So, in a "burst of creativity," we simply averaged these two values and adopted  $0.25 \text{ cm}^{-3}$ . This number implies a nebula with a mean dimension of  $90^\circ$ , as required by the observations. (The angular size was calculated to be  $\arcsin L/460 \text{ pc} + \arctan L/460 \text{ pc}$  because we don't know exactly how the boundary of the nebula should appear.)

Table 2  
Assumptions in Model Building

$L$  = radius of nebula

$\ell$  = distance to edge of nebula

$L + \ell = 460 \text{ pc}$

Ionized Region	Neutral Region
$n_H \ll n_e$	$n_e \ll n_H$
$EM = 2L \langle n_e^2 \rangle$	$HM = \langle n_H \rangle \ell$
$DM = L \langle n_e \rangle$	

Table 3  
Implications of Three Assumed Values of  $\langle n_H \rangle$

$\langle n_H \rangle (\text{cm}^{-3})$	$\ell (\text{pc})$	$L (\text{pc})$	Angular Diameter of Nebula
0.4	60	400	$110^\circ$
0.25	100	360	$90^\circ \sqrt{\sqrt{}}$
0.1	240	220	$55^\circ$

The result is our model of the nebula as shown in Figure 2. This diagram is intended to provoke discussion, and shows schematically that the boundary is irregular and the structure is filamentary (clumpy). The clumpiness factor  $X$  is 1 for a homogeneous nebula and greater if the clumpiness is important.

It is a simple calculation to see if gamma Velorum and zeta Puppis could maintain the ionized region. They fail, by at least one order of magnitude, if  $\langle n_e^2 \rangle^{1/2} = 1 \text{ cm}^{-3}$  (Spitzer 1968). Hence, something else ionized the Gum Nebula.

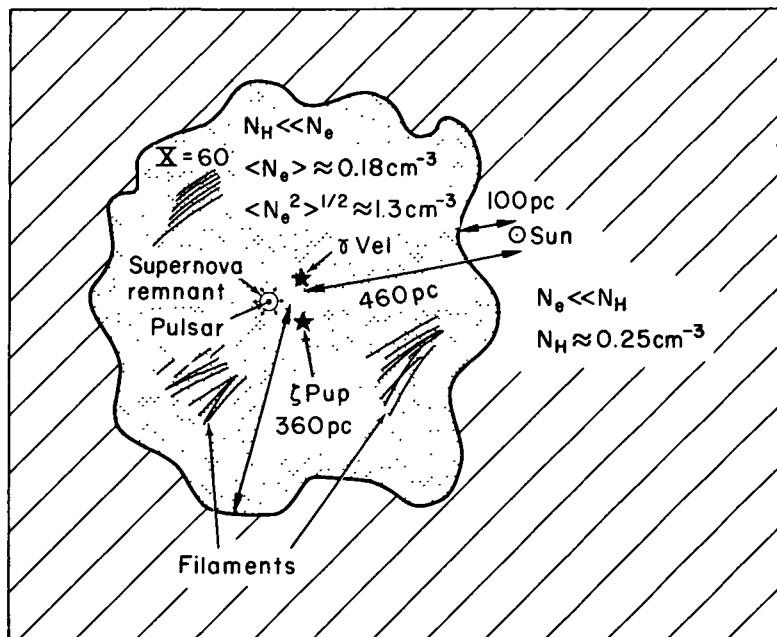


Figure 2. Schematic representation of the derived model for the Gum Nebula.

The culprit is probably a supernova and there is considerable evidence for it. There is the pulsar PSR 0833-45 (Large *et al.* 1968), the nonthermal extended radio source (Milne 1968), and the X-ray source (Seward *et al.* 1971). The photograph by Bok (1971) of the radio source region shows the striking nebulosity that appears to be a supernova remnant located within the Gum Nebula.

The remaining calculation concerns the energy requirements, and the numbers are given in Table 4. If we assign a radius of 360 parsecs to the nebula, a height of 100 parsecs, and compute the volume of the cylinder, it comes out to be about  $1.2 \times 10^{63} \text{ cm}^3$ . We know the average electron density, and, hence, can estimate that the nebula contains about  $2 \times 10^{62}$  electrons. If we assume 15 eV per ionization, we immediately find that  $5 \times 10^{51}$  erg, or to the accuracy appropriate for a calculation such as this one,  $10^{52}$  erg, are required to ionize our model Gum Nebula. This is our suggestion — the supernova produced the energy to ionize this nebula. There are obviously many questions to be answered. In particular, we hope this symposium will stimulate a thorough discussion of the different ways of supplying energy to produce the nebula.

Table 4  
Energy Requirements for Single Ionization  
of the Gum Nebula

<u>Nebular volume</u> Radius: 360 pc Height: 100 pc $V \approx 1.2 \times 10^{63} \text{ cm}^3$
<u>Number of electrons in nebula</u> $V \langle n_e \rangle \approx 2 \times 10^{62} \text{ electrons}$
<u>Energy required</u> 15 eV per ionization, $E \approx 5 \times 10^{51} \text{ erg}$

I will add in closing that there is another observation that may possibly exist, which would be of great interest. The age of the pulsar as inferred from its spin-down rate (Reichley et al., 1970) leads one to believe that there might have been a very bright supernova around 9000 B. C. The apparent magnitude may have been  $m_v \approx -10$ , which is comparable to the quarter moon, and much brighter than the Crab supernova as observed by the Chinese. We are pursuing the admittedly outside chance that evidence of such an observation may exist in the archaeological record; such data would hopefully yield a much more accurate estimate for the age of the pulsar and the Gum Nebula than is presently available.



## References

- Alexander, J. K. 1971, this volume.
- Alexander, J. K., Brandt, J. C., Maran, S. P., and Stecher, T. P. 1971, Ap. J., 167, 487.
- Bok, B. J. 1971, this volume.
- Brandt, J. C., Stecher, T. P., Crawford, D. L., and Maran, S. P. 1971, Ap. J. (Letters), 163, L99.
- Johnson, H. M. 1971, this volume.
- Large, M. I., Vaughan, A. E., and Mills, B. Y. 1968, Nature, 220, 340.
- Milne, D. K. 1968, Austral. J. Phys., 21, 201.
- Reichley, P. E., Downs, G. S., and Morris, G. A. 1970, Ap. J. (Letters), 159, L35.
- Rodgers, A. W., Campbell, C. T., Whiteoak, J. B., Bailey, H. H., and Hunt, V. O. 1960, An Atlas of H-alpha Emission in the Southern Milky Way (Canberra: Australian National University).
- Seward, F. D., Burginyon, G. A., Grader, R. J., Hill, R. W., Palmieri, T. M., and Stoering, J. P. 1971, Ap. J., 169, 515.
- Spitzer, L. 1968, Diffuse Matter in Space (New York: Interscience).

## DISCUSSION

*A. POVEDA:*

If one takes the naive point of view that the H II region is just what we see in the photographs, then the volume is much smaller than the one that you have chosen and therefore the amount of energy needed to ionize it is correspondingly smaller.

*J. C. BRANDT:*

Gum quoted  $60^\circ \times 30^\circ$  in one paper and other outlying H II regions have been discovered subsequently. The column density of electrons is an observed quantity, so if we take a smaller volume, the total electron content is only slightly reduced.

*B. J. BOK:*

I am worried by the assumption that there is one Gum Nebula. From the photographic work that I have done, looking at the composite and the Schmidt photographs, I have the impression that there are two or three things that are going on in this region. First of all, there is the big emission blob around gamma Vel. That blob, which has a bite out of it due to a nearby dark nebula, is centered on gamma Vel and looks like an ideal Strömgren sphere. There is a similar nebulosity near zeta Pup. Then there is the entirely different nebulosity [Vela X] which looks like what we find in Cygnus; it appears that we have a big explosion, a shock wave affair. It is well to the north of the bright, normal-appearing blobs. Finally, there is the nebulosity that seems to outline the outer part of the Gum Nebula. I think one should be very careful before one calls the Gum Nebula a single unit. Note also that zeta Pup is the brightest O-star (05) and gamma Vel is one of the best known Wolf-Rayet stars (Lindsey Smith has determined its distance with considerable accuracy). The emission measure of this region isn't a single number; it's a complex affair and has to be studied carefully. We also have to be careful about the distance: 460 pc is a fine figure but it's an upper limit; 350 pc may be more accurate. One of the most important things to do today is to point out that the observations of this part of the sky are still incomplete. In summary, the upper part of the poster photo [see frontispiece] looks like it may be excited by the supernova, the lower part looks like normal H II regions, and the central part looks like it is of completely different nature [supernova remnant].

*BRANDT:*

Obviously gamma Vel and zeta Pup contribute to the ionization in this region but probably not more than 10 percent of it. I don't think that they can maintain the entire region.

*S. VAN DEN BERGH:*

I think that it would be wise to remember that there are two optical supernova remnants located near the center of the Gum Nebula: Vela X and Puppis A (Baade and Minkowski 1954). There is no a priori reason to regard Vela X, which is roughly centered on the Vela pulsar (PSR 0833-45) as the more likely source of ionization for the Gum Nebula. Intercomparison of a recent 48-inch Schmidt plate of the Vela X remnant with the prints of the Whiteoak Sky Survey shows no evidence for expansion of the supernova remnant. This result indicates that the shell of the Vela supernova has either been decelerated or that it has an age  $t \gtrsim 10,000$  years. Reference: Baade, W., and Minkowski, R. 1954, Ap. J., 119, 206.

## THE SIZE AND SHAPE OF GUM'S NEBULA

Hugh M. Johnson

*Lockheed Missiles and Space Company  
Palo Alto, California 94304*

The title of the original paper by Brandt *et al.* (1971) is deceptively simple. The H II region is certainly not a sphere, and we shall examine this important fact. Nor is it a fossil if it shows the recombination spectrum of hydrogen. Rather it was the ionizing light of the causative supernova which is now "fossilized" in the still live though failing H II region.

H-alpha has been recorded spectrographically in Gum's nebula by Gum (1952, 1955). However, Gum used a spectrograph which was probably incapable of resolving H-alpha and [N II] 6548, 6583 Å. Large interstellar regions may show [N II] 6583 Å in emission without H-alpha (cf.: Rubin and Ford 1970) so that it is probably still uncertain how much H-alpha is radiated in Gum's nebula.

The critical point in the paper by Brandt *et al.* is the energy required to produce the observed ionization of the nebula. This is estimated in that paper by granting 15 eV per photon and by equating the minimum number of photons to the number of electrons in the nebula. The latter is nebular volume  $V$  times a mean electron density  $\langle n_e \rangle$ , where  $V$  was represented by a circular cylinder of radius 400 pc and height 100 pc and where  $\langle n_e \rangle = \langle DM \rangle / L$ .  $\langle DM \rangle = 63 \text{ cm}^{-3} \text{ pc}$  is estimated from observations of four pulsars, one taken to be in the center of the nebula and three to be beyond it. Path length  $L$  is equated to the radius of the model nebula for the central pulsar or  $2L$  for the three supposedly distant pulsars. Thus, all of the dispersion is said to occur in the nebula, and the nebula is said to occupy 400/460 of the distance to the center at the Vela pulsar, taken to be  $r_\odot = 460 \text{ pc}$ . The good point about this procedure is the apparently unbiased sampling of coordinates in the nebula, and it is interesting that the rms error of  $\langle n_e \rangle$  is only  $\pm 8$  percent despite the patchy structure of the gas. Of course, the rms error would be much increased by almost any other arbitrary assumption of the relative values of path length to be assigned for computing the DM of each pulsar.

Brandt *et al.*'s derivation of  $L = 400 \text{ pc}$  for nebular radius is contradicted by the observed angular radii.  $\text{Arc sin } 400/460 = 60^\circ$ , the angular radius of the model cylinder, is far larger than the known nebula. Gum (1956) estimated total dimensions of  $30^\circ \times 60^\circ$ . A second paper by Alexander *et al.* (1971) revises the angular diameter downward.

If the center is at the Vela pulsar, the nebula is somewhat asymmetrical with the most distant fragment reported by Gum (1956)  $40^\circ$  from center, around  $\ell = 292^\circ$ ,  $b = -25^\circ$ . Another fragment reported by Johnson (1959) is about  $45^\circ$  from center around  $\ell = 284^\circ$ ,  $b = -38^\circ$ . Other possible fragments are RCW 63 (Rodgers, Campbell, and Whiteoak 1960) at  $\ell = 297^\circ$ ,  $b = +7^\circ$ ; the nebula catalogued by Lynds (1965) at  $\ell = 244^\circ.20$ ,  $b = +34^\circ.18$ ; and S 313 (Sharpless 1959) = A 35 (Abell 1966) at  $\ell = 304^\circ$ ,  $b = +40^\circ$ , a nebula which Hromov and Kohoutek (1968) regard as not a planetary. The I.A.U. system of galactic coordinates is used here. Figure 1 shows the nebulae in the ranges of  $220^\circ < \ell < 310^\circ$  and  $-24^\circ < b < +24^\circ$ , as outlined schematically (and impartially with respect to this conference) by Rodgers, Campbell, Whiteoak, Bailey, and Hunt (1960), to which the outlying fragments mentioned above are added. The fragments at large radii are at high latitudes.

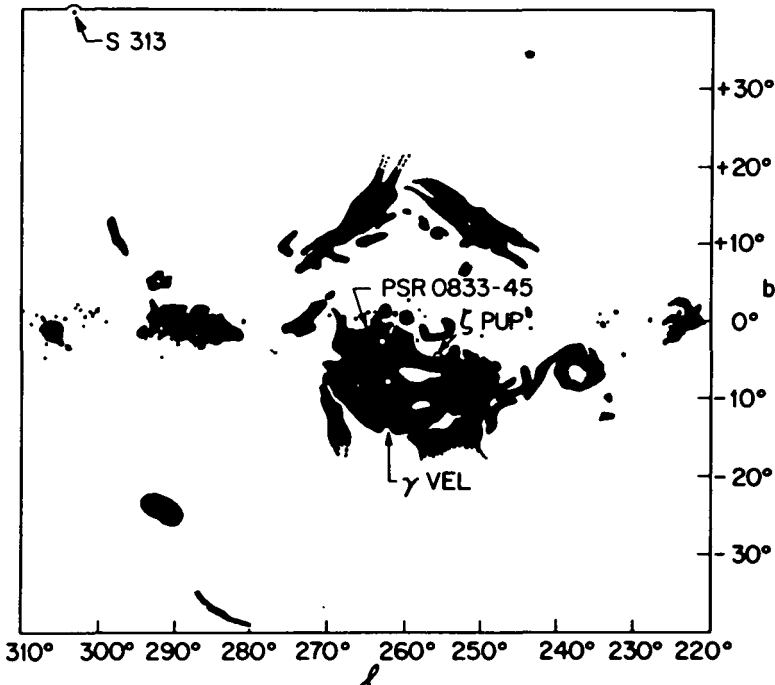


Figure 1. Gum's nebula and all field nebulae from the map by Rodgers, Campbell, Whiteoak, Bailey, and Hunt (1960), with some outlying fragments and some stellar objects added to their picture.

The main body of the nebula certainly suggests a hollow center or shell-form with a characteristic radius about half the distances of the outlying fragments. The edges of the main-body patches are typically sharp and are often bright parts. Figure 2 illustrates these remarks. In places an outer edge of dust was suggested by a close inspection of the original 8-inch Schmidt plates at the Mount Stromlo Observatory in 1959. These observations imply a "front" of some kind more definite than the limit of ionization, as though expansion of the gas was under way. The spin-down age of the Vela pulsar,  $1.1 \times 10^4$  years (Reichley, Downs, and Morris 1970) is the available time for expansion and shock-front formation, without making special hypotheses. The apparent hollowness of the formation might be a consequence of lower Balmer-line emissivity at higher electron temperature if the center has been heated most. We conclude that the structure of the Gum Nebula appears to be dependent on the event of ionization and possibly on the details of heating; and it is not now an unstructured ambient medium as it may have been before the recent ionization. The alternative of a structured ambient medium requires special hypotheses. One of them is structuring by previous supernova events near the site of the Vela pulsar. At a rate of one randomly distributed supernova per galaxy per 100 years, about 5 supernova events per million years are predicted within the volume of the nebula ionized at present. The effects of such events may be cumulative and not relaxed between events.

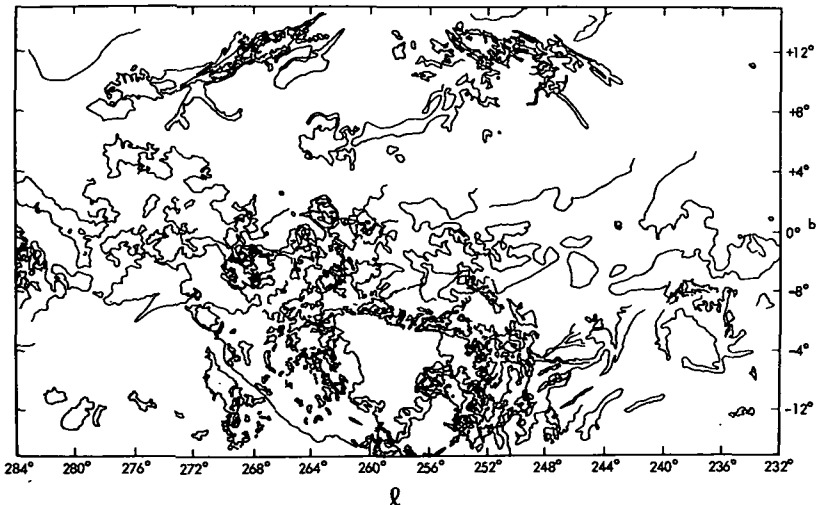


Figure 2. Mosaic of maps of Gum's nebula made with a bandpass of  $326\text{\AA}$  around H-alpha. The original maps give measured intensities of the isophotes (Johnson 1960).

Another hypothesis is that Gum's nebula, by accident of its present state, reveals the cross-section of the neutral-hydrogen arm in Vela at the distance of 460 pc. It has not been shown elsewhere or by other means that galactic arms tend to be tubular with fairly sharp perimeters, as this hypothesis suggests.

The great size of Gum's nebula must reflect the gradient of ambient interstellar density normal to the galactic plane, and possibly in the orthogonal directions, if the Vela supernova event or events did not perturb the interstellar structure very much. According to Kerr (1969) the thickness of the H I layer between points at half the density in the galactic plane is 200 pc in the range 4-10 kpc from the galactic center. For an exponential  $z$ -distribution, the scale height  $H = 144$  pc. If hydrogen obeys the distribution  $n_H(z) = n_0 \exp(-z/H)$  in smooth strata of large extent, and if it is photoionized by any source near the galactic plane to a radius  $r = 230$  pc in the galactic plane, then the H II zone is bounded as shown in Figure 3, where the Strömgen radii  $S$  are computed from the definition

$$\int_0^S n_H^2(r) r^2 dr = \text{constant}.$$

The radii of photoionization are unbounded in the cone of radius  $55^\circ$  around the axis normal to the plane of the Galaxy at the Vela pulsar. This shape is quite different from that of the observed main body of the nebula. For example, hydrogen may be photoionized at  $b = +90^\circ$  and at  $|z| > 270$  pc by the agent of Gum's nebula. The emission measure of the galactic polar Gum nebula with smooth, exponential  $z$ -distribution of the mass is

$$\text{EM}(b = \pm 90^\circ) = \int_{270}^{\infty} n_0^2 \exp(-2z/H) dz$$

$= 1.69 n_0^2 \text{ cm}^{-6} \text{ pc}$ , where  $n_0^2$  is the mean-square electron density at  $z = 0$ . Outlying clouds of the kind discussed earlier, or fainter fragments, may be expected over a large part of the sky on the model of an exponential  $z$ -distribution of the interstellar gas. The Sun remains sheltered in H I, but it is partially enveloped by the nebula as Gum intuitively suspected. The shape and size of the nebula for other agents of ionization should also be computed.

The mean electron density of the nebula near the galactic plane is  $\langle n_e \rangle = (DM)/L = 0.27 \text{ cm}^{-3}$ , and the equivalent volume  $V_{eq}$  at this density is the sphere of radius  $L = 230$  pc so that  $V_{eq} \langle n_e \rangle = 4 \times 10^{62}$  electrons. The

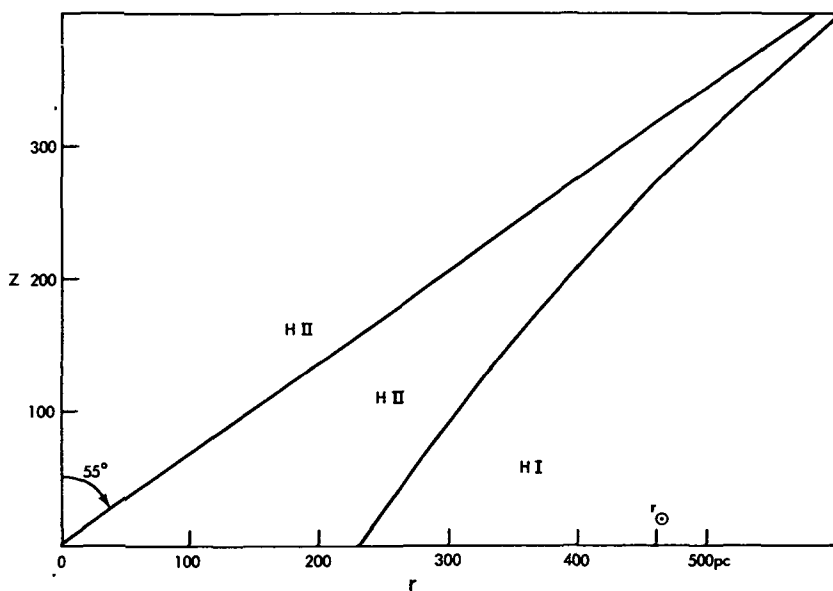


Figure 3. Cross-section of a plane which contains the center of Gum's nebula at the origin, the Sun at  $r = 460$  pc on the abscissa axis, and the ordinate  $z$ -axis normal to the galactic plane. The ambient interstellar gas is ionized to  $r = 230$  pc at  $z = 0$  and elsewhere to the curved boundary which approaches asymptotically to the cone of radius  $55^\circ$  around the ordinate axis. In this cone the radius of ionization is unbounded.

predicted value of the emission measure in the direction of the center of Gum's nebula is  $EM = 2 L n_0^2 = 34 \text{ cm}^{-6} \text{ pc}$  for uniform density. Nebular irregularities, as observed on photographs, would increase the predicted EM at the same mean  $\langle n_0 \rangle$ . The question of maximum EM in Gum's nebula is complicated by the presence of  $\zeta$  Pup and  $\gamma^2$  Vel, which are nearer the brightest parts than the Vela pulsar is. There is no reliably observed mean  $\langle EM \rangle$  in the nebula for use in the determination of  $\langle n_e^2 \rangle$ , and no  $\langle EM_0 \rangle$  for the determination of  $\langle n_e^2 \rangle$ . Thus  $X = \langle n_e^2 (EM) \rangle / \langle n_e (DM) \rangle^2$  and  $X_0$  are very poorly known.

In conclusion, we draw attention to an apparent giant complex of nebulae which is nearly opposite to Gum's nebula in the sky. According to Lynds' (1965) map and catalogue of bright nebulae, which she produced from an inspection of all of the Palomar Sky Survey charts, the complex may be defined inside a circle of about  $45^\circ$  radius centered near  $\ell = 110^\circ$ ,  $b = 0^\circ$ .



These nebulae are obviously distinct from the brighter and much more compact Cygnus complex of radius  $8^\circ$  centered near  $\ell = 75^\circ$ ,  $b = 0^\circ$ , and also distinct from many other distant nebulae which lie in the circle but quite close to the galactic equator (see Figure 4). The complex lies, like Gum's nebula, near a node of Gould's Belt or the "local system" of OB stars and interstellar matter. This distinguishes its members from the many nearby nebulae at moderately high latitudes in Scorpius and Taurus. The distance of the proposed complex is not known, but we suggest tentatively that its significance is similar to that of Gum's nebula.

This work has been done under the Lockheed Independent Research Program.

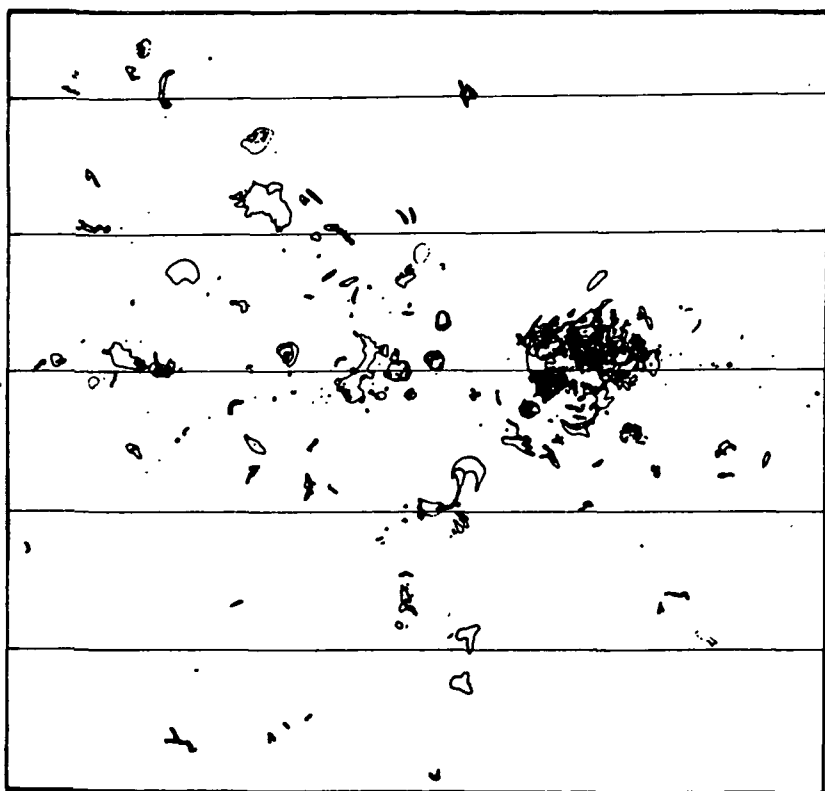


Figure 4. Nebulae on the map by Lynds (1965) centered near  $\ell = 110^\circ$ ,  $b = 0^\circ$ . The grid of galactic latitudes (interval =  $20^\circ$ ) has been added to the illustration published by The University of Chicago Press. Copyright 1965 by The University of Chicago; all rights reserved.

## References

- Abell, G. O. 1966, Ap. J., 144, 259.
- Alexander, J. K., Brandt, J. C., Maran, S. P., and Stecher, T. P. 1971, Ap. J., 167, 487.
- Brandt, J. C., Stecher, T. P., Crawford, D. L., and Maran, S. P. 1971, Ap. J. (Letters), 163, L99.
- Gum, C. S. 1952, Observatory, 72, 151.
- Gum, C. S. 1955, Mem. R.A.S., 67, 155.
- Gum, C. S. 1956, Observatory, 76, 150.
- Hromov, G. S., and Kohoutek, L. 1968, B.A.C., 19, 90.
- Johnson, H. M. 1959, Pub. A.S.P., 71, 342.
- \_\_\_\_\_ 1960, Mem. Mount Stromlo Observatory, No. 15.
- Kerr, F. J. 1969, Ann. Rev. Astron. and Ap., 7, 39.
- Lynds, B. T. 1965, Ap. J. Suppl., 12, 163.
- Reichley, P. E., Downs, G. S., and Morris, G. A. 1970, Ap. J. (Letters), 159, L35.
- Rodgers, A. W., Campbell, C. T., and Whiteoak, J. B. 1960, M.N., 121, 103.
- Rodgers, A. W., Campbell, C. T., Whiteoak, J. B., Bailey, H. H., and Hunt, V. O. 1960, An Atlas of H-Alpha Emission in the Southern Milky Way (Canberra: Mount Stromlo Observatory).
- Rubin, V. C., and Ford, W. K., Jr. 1970, Ap. J., 159, 379.
- Sharpless, S. 1959, Ap. J. Suppl., 4, 257.

## DISCUSSION

*T. P. STECHER:*

We haven't said much yet about the two stars (gamma Vel and zeta Pup) themselves. I observed them with a rocket-borne scanner to determine their temperatures. With no correction for interstellar absorption, the temperatures were about 30,000 °K. There is very little absorption in this direction, so I set an upper limit of about 40,000 °K. If this temperature is correct, these stars are not capable of ionizing the Gum Nebula. This result was confirmed by Hanbury Brown and colleagues, using the optical interferometer in Australia; in fact, they obtained an even lower temperature.

*B. J. BOK:*

If the Strömgren sphere of these stars had a radius of 50 to 60 pc, it could account for the brightest part of this region, and one must be very careful about estimating the emission measures of the faint outer parts; they may be much fainter, as indicated by Poveda and by Johnson.

*S. P. MARAN:*

The emission measure in the brightest parts is about 3000; Brandt et al. took a mean of 1300 and other values are discussed by Alexander et al.

## FORMATION OF GIANT H II REGIONS FOLLOWING SUPERNOVA EXPLOSIONS\*

L. Sartori

*Department of Physics and Center for Space Research  
Massachusetts Institute of Technology  
Cambridge, Massachusetts 02139*

Theoreticians are notoriously adept at cooking up schemes to explain observations, particularly in astronomy, where the parameters that go into a theory are often determined observationally only within rather wide limits. The theorist is therefore afforded considerable leeway in choosing the parameters of his model so as to match the properties of an observed object.

It is a somewhat different matter to calculate the properties of something that has not been observed. Then you have to put your cards on the table before the other fellow has shown his hand. If an object is subsequently discovered that exhibits all the properties predicted by your theory, that certainly doesn't prove the theory is right, but it does put you one up on the people whose models come after the discovery.

It was therefore with considerable satisfaction that Phil Morrison and I greeted the recent news about the Gum Nebula, since the object described by Brandt et al. (1971) is almost exactly what should surround every type I supernova remnant according to our fluorescence theory of supernova light (Morrison and Sartori 1966, 1969). Inasmuch as that theory has been more or less politely ignored by the astronomical community since we presented it a few years ago, I am going to take advantage of this opportunity to propagandize a little in its behalf. I shall first summarize the principal ideas of the theory as it pertains to the optical observations over the first few years, and then discuss the implications for the giant H II regions that are the subject of today's symposium.

The principal optical properties of type I supernovae (SN I) can be briefly summarized as follows:

---

\*Supported in part by NASA Grant NGL-22-009-019, and also in part by NSF Grant GP-11453.

i) Light curve. The photographic light curve shows a rapid rise and decline within some 10-20 days, followed by an exponential-like tail with a time constant of 50-100 days. The latter, the most reliable signature of a type I event, persists at least two years, the longest period over which a supernova has been followed. The decay times vary by a factor 2 or 3 between one supernova and another. The integrated energy under the photographic light curve is about  $10^{49}$  erg.

ii) Spectrum. The spectra consist of broad bands, a couple of hundred Angstroms wide, with very little continuum. Several of the major bands are observed to shift with time toward the red, the total shift over a few months being of order a hundred Angstroms. The most prominent feature, which contains about half the photographic power, has its maximum around  $\lambda$  4640Å in the early spectra and shifts eventually to something over  $\lambda$  4700Å. The spectrum bears very little resemblance to that of a blackbody. More detailed discussion is found in many review articles (cf.: Minkowski 1964, Zwicky 1965).

According to our theory, the observed light is principally fluorescence, excited in the medium surrounding the supernova by ultraviolet radiation originating from the explosion. The actual emission at a given point takes place over a very short interval (10-20 days or less), but the observed light at the earth is spread out over a much longer period because of the difference in total travel time for the various possible paths. If the initiating UV pulse is considered a  $\delta$ -function, the locus of points seen by the observer at a given time is an expanding ellipsoidal surface (Fig. 1). The time dependence of the observed fluorescent intensity is determined by the spatial attenuation of the exciting pulse which includes a  $1/r^2$  geometrical factor and an exponential factor from the absorption. In the simplest model, that of a single fluorescent line in a uniform medium, the time dependence is the exponential integral  $E_1(ct/2\Lambda)$ , where  $\Lambda$  is the mean free path for the exciting photons, i.e.:

$$\Lambda = (\sigma n)^{-1} \quad (1)$$

where  $n$  is the density of the fluorescing material and  $\sigma$  the cross-section for the transition that excites the fluorescence. In the simplest version we therefore have a one-parameter theory. Figure 2 shows the fit to the measured light curves; the three cases shown include the longest-measured one, IC 4182, which constitutes the most sensitive test and ought to be included in any comparison of theoretical light curves with observations. It is clear that the  $E_1$  function, whose asymptotic behavior is  $e^{-x}/x$ , provides a better fit than does a simple exponential, since it reproduces approximately the observed curvature in the light curve during the period 40 days  $\lesssim t \lesssim$  100 days.

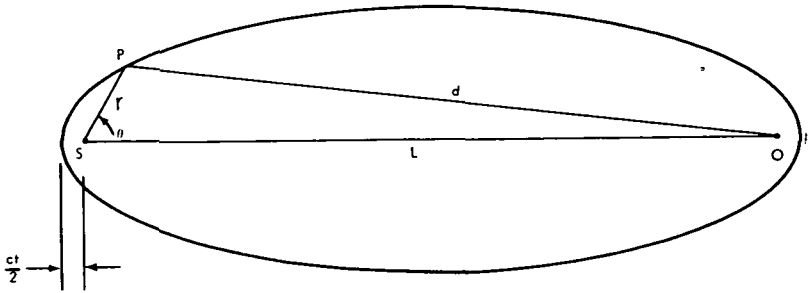


Figure 1. Locus of points from which fluorescent emission reaches observer O at a given time  $t$ , for a  $\delta$ -function pulse originating at S;  $t$  is measured from the arrival time of the direct signal, i.e.: from time  $L/c$  after the explosion. The surface is an expanding ellipsoid, given by  $r + d = L + ct$ . (From Morrison and Sartori 1969, published by the U. of Chicago Press. Copyright 1969 by the University of Chicago. All rights reserved.)

I shall return to the light curves in a moment, but first I want to discuss the spectrum. The dominant photographic feature, already mentioned, is in our view He II 4686Å, the Paschen-alpha (4-3) transition. This identification is not new with us; it was suggested long ago by Minkowski. According to our geometrical picture, all the fluorescent lines are Doppler-shifted because of the (essentially) radial motion of the emitting atoms. During early times, most of the radiation observed comes from the forward part of the ellipsoid of Fig. 1; consequently, the line ought to be observed as blueshifted. With time, an increasing fraction of the observed light comes from the back; the line is therefore redshifted. Thus the observed redshift of the principal features is a natural feature of the fluorescence theory.

If the observed light is principally He II fluorescence, we can calculate from eq. (1) the density of helium required to give the mean free path  $\Lambda$  the indicated value. The result is  $n_{\text{He}^+} \sim 1.5 \text{ cm}^{-3}$ . This is more helium than can reasonably be expected to be found as ordinary interstellar material, but can quite comfortably be understood as material ejected from the star during its entire pre-supernova history. The total mass of helium required for a region about a light year in radius is a tenth of a solar mass or so. The variation among measured decay times reflects, in this picture, differences in the amount of ejected helium (or its distribution).

I will not discuss the remainder of the spectrum, which is treated in our 1969 paper, and turn to the last important feature of the model. The fluorescence theory evidently demands a lot of singly-ionized helium, and we can't afford

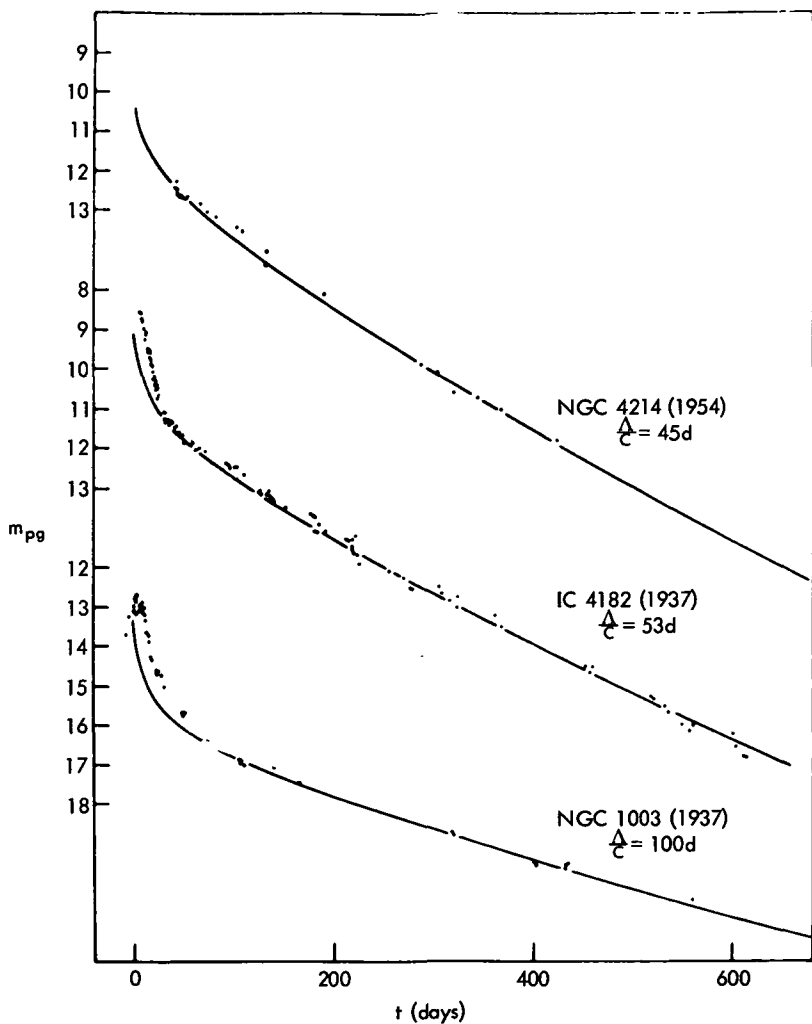


Figure 2. Theoretical fit (on the basis of the model with uniform density,  $\delta$ -function excitation pulse, and a single absorption line) to the photographic light curves of type I supernovae in three galaxies. The parameter  $\Lambda/c$  in the luminosity function,  $L(t) \sim E_1(ct/2\Lambda)$  is shown for each light curve. (From Morrison and Sartori 1969, published by the U. of Chicago Press. Copyright 1969 by the University of Chicago. All rights reserved.)

to let it lose that second electron. (The recombination time is impossibly long, and each  $\text{He}^+$  must emit of the order of  $10^5$  fluorescent photons.) This requires that the spectrum that impinges on the fluorescent medium while the emission is taking place must fall abruptly across the Lyman edge of  $\text{He II}$ , i.e., at 54 eV. (After a few days, when the fluorescence has been emitted, we don't care if the whole thing gets ionized.) Such a "filtering" action is plausibly provided by a much denser internal region, rich in helium, immediately surrounding the exploding object. This will form a Strömgren sphere during the time the intense UV pulse is passing through it. (Not to be confused with the huge fossil Strömgren sphere we are seeing today.) The optical depth for ionizing photons is very great, and recombination is rapid. An appreciable fraction of the recombinations takes place to excited states, each such event effectively converting an ionizing photon into two or more photons below the edge. This is what happens in ordinary H II regions, planetary nebulae, etc., which filter out all radiation above the hydrogen Lyman edge.

The amount of material required to accomplish the desired filtering in the SN I case, calculated with the formulas that apply to static Strömgren spheres, is a few tenths of a solar mass. Obviously the conditions in the region we have in mind are very different from these in a classical Strömgren sphere. The energy input is very intense and very brief, and one does not even know the form in which the primary energy arrives; it could, for example, be carried by particles. Nonetheless, the simple estimates suffice to convince us that the filtering action can occur. This aspect of the problem must be looked at in greater detail.

The dense region serves one other purpose — it slows down the photons below the edge by Thomson scattering, thereby spreading out the UV pulse in time. Even if the initial pulse was very short, a characteristic time of order 10 days is produced by this mechanism, without appreciably altering the spectrum. With a diffusion-broadened input of this nature, the divergence at  $t = 0$  in the light curve calculated with a  $\delta$ -function input is removed, and the early part of the light curve is in fact quite accurately reproduced. Figure 3 shows a composite of the light curves of six SN I, plotted as a function of  $t/\Lambda$ , where  $\Lambda$  is obtained from the late-time behavior. The universality of the SN I phenomenon is strikingly demonstrated by this plot, and the fit provided by the two-parameter version of the fluorescence theory is seen to be quite good. We wish to emphasize, however, that whereas the filtering action of the dense region is absolutely essential to the theory, the time diffusion is not. The pulse could be broadened by some other mechanism; or the early luminosity could contain a substantial non-fluorescent contribution.



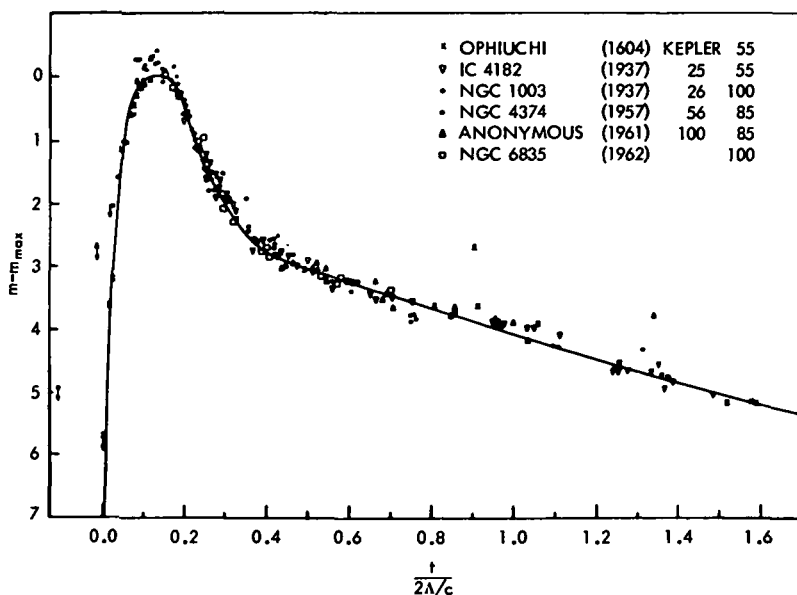


Figure 3. Composite photographic light curve for type I supernovae. The luminosity is plotted as a function of the dimensionless variable  $1/2 \text{ ct}/\Lambda$ . The name, date, Zwicky Number (where applicable) and  $\Lambda$  are given for each supernova. The points for Kepler's supernova are from visual observations, but they probably include a substantial amount of the 4600 Å radiation that dominates the photographic light curve of a SN I. (From Morrison and Sartori 1969, published by the U. of Chicago Press. Copyright 1969 by the University of Chicago. All rights reserved.)

A number of other details of the theory are discussed in our paper. The feature of interest here today is of course the ultraviolet radiation which the theory implies, and the ultimate effect of these UV photons in producing the Gum Nebula. The energetic argument is quite straightforward. Each 3-volt photon from the He II 4-3 transition requires a 50-volt photon to excite the initial state. When one takes into account the rather small fluorescent yield for the transition in question, the over-all conversion efficiency (output visible energy/excitation UV energy) turns out to be about 1/200. With an integrated measured energy in the dominant 4686 Å feature of about  $5 \times 10^{48}$  erg, this implies about  $10^{51}$  erg of excitation energy, concentrated in a band a few eV wide in the vicinity of 50 volts. We have no idea as to the detailed shape of the primary spectrum, but can hardly expect all the energy to be concentrated in so narrow a band. Assuming that the fraction of photons in the excitation band is of order 10%, we arrived at  $10^{52}$  erg as our estimate

of the total UV energy incident on the fluorescent medium. If you like, you can say that the bolometric correction for this unusual emitter is some eight magnitudes! The bulk of the energy is found in the form of He II Lyman-alpha radiation ( $h\nu = 40$  eV), He II Balmer lines, and continuum below 54 volts.

What happens to all these UV photons? A few of them make the observed fluorescence. But the majority (including all the He II Lyman-alpha) escape from the neighborhood of the supernova and ionize the surrounding gas as far as they can reach. That is to say, they make a Gum Nebula. Our estimate of  $10^{52}$  erg implies about  $10^{62}$  photons, which make an equal number of ions. This is just about the number deduced by Brandt *et al.* from the observations. The numerical agreement is closer than we have any right to expect, but it seems fair to say that the predicted extent of the ionized region is consistent with the observations on the Gum Nebula.

The H II region formed by this mechanism is initially quite hot. When a He II Lyman-alpha photon ionizes a hydrogen atom there is 27 eV of kinetic energy left over; thus when the system comes to thermal equilibrium the temperature will be  $\approx 9$  eV or roughly  $10^5$  °K. The system will then cool gradually and expand. The time evolution of such an object is discussed by Kafatos (1971).

At least two other mechanisms for the production of the ionization in the Gum Nebula have been proposed. Tucker (1971) considers the shock wave associated with the expansion of the supernova shell, and argues that this will eventually radiate copiously in the UV. By an appropriate choice of parameters, he can get enough UV to ionize the nebula.

The other idea, due to Ramaty *et al.* (1971), is that the nebula is ionized not by radiation but by collision with heavy particles, of energy  $\sim 10$  MeV, ejected in the supernova event. The production of these particles is a consequence of Colgate's theory of the explosion (Colgate and McKee 1969, Colgate 1971).

I shall not give a detailed critique of the competing theories, but I do wish to make a few general remarks. The first one is this: The Morrison-Sartori theory deals exclusively with the post-explosion supernova. We recognize that many of the most interesting phenomena take place earlier, as the pre-supernova rushes through the final states of its evolutionary track. The period before and during the explosion has received much theoretical attention, and deservedly so. But the calculations involve many assumptions and are very complicated; unfortunately the results are not subject to direct observational test. Our theory, on the other hand, is very simple (in fact, surely oversimplified), but it can be tested observationally and seems to pass every major

test. When the simplest version of a theory, with very few adjustable parameters, accounts for the principal features of a phenomenon, one is encouraged to believe that it forms the basis for the correct explanation. This does not mean the model is correct in every detail.

When we first proposed the fluorescence theory, our estimate of  $10^{52}$  erg of ultraviolet energy was held to be excessively high. Colgate (1971) argues on the basis of hydrodynamic calculations, that the UV we require cannot possibly be produced in the explosion. We find such an argument unconvincing, because it rests on assumptions for which there is no observational evidence. We take the point of view that the observed properties of the post-explosion object (among which the Gum Nebula now plays a prominent role) strongly suggest that at least  $10^{52}$  erg of UV is indeed produced. If the hydrodynamic model cannot come up with the required energy, perhaps the supernova is even more clever.

Incidentally, we are quite willing to concede comparable amounts of energy to cosmic rays, to kinetic energy of expansion, shocks, flywheel mass loss, or other channels. We see no reason why a total energy release several times  $10^{52}$  erg should be considered unacceptable ( $1 M_{\odot} c^2 = 2 \times 10^{54}$  erg).

The principal difference between an ionized region produced by our mechanism and one produced à la either Tucker or Ramaty et al. is the time scale for production. Our Strömgren sphere is produced instantaneously — the ionization front expands at essentially the speed of light. Both of the other mechanisms require much more time; according to them, the Gum Nebula is a newly-formed object. In fact, if the age is  $\sim 10^4$  years there is some difficulty in ionizing the outer parts on the cosmic-ray hypothesis.

An obvious means for investigating the formation time is to look at a young supernova remnant. The best candidate is Tycho, 400 years old, and identified as SN I on the basis of evidence which is suggestive although not conclusive. If Tycho is indeed a SN I, its "Gum Nebula" should already have formed, according to our picture, whereas according to the others the ionization is just getting started. Unfortunately, even if Tycho were a fully formed Gum Nebula it would be a far less spectacular object. In the first place it is much further away ( $\sim 5$  kpc). Moreover, being 100 pc out of the plane, the gas density in the vicinity of Tycho is fairly small which would make its emission measure very low unless some clouds were included. And at an age of 400 years, the nebula would still be very hot, making it very hard to observe in H-alpha, although some forbidden lines may be observable. (See Kafatos 1971.)

Some very tentative evidence for the presence of an ionized sphere around the Tycho remnant is provided by the observation of a "hole" in the 21-cm emission (Williams 1971) just at the position of the supernova. Unfortunately, many such holes are found in places where no known supernova remnant resides, so the evidence is far from convincing. It may be, however, that this undramatic sign is the only one by which such a young and distant Gum Nebula identifies itself.

All the ideas presented here have been developed jointly with my collaborator, Philip Morrison. Conversations with Minas Kafatos have been very useful.

### References

- Brandt, J. C., Stecher, T. P., Crawford, D. L., and Maran, S. P. 1971, Ap. J. (Letters), 163, L99.
- Colgate, S. A. 1971, this volume.
- Colgate, S. A., and McKee, C. 1969, Ap. J., 157, 623.
- Kafatos, M. C. 1971, this volume.
- Minkowski, R. 1964, Ann. Rev. Astron. Astrophys., 2, 247.
- Morrison, P., and Sartori, L. 1966, Phys. Rev. Letters, 16, 414.
- Morrison, P., and Sartori, L. 1969, Ap. J., 158, 541.
- Ramaty, R., Boldt, E. A., Colgate, S. A., and Silk, J. 1971, Ap. J., 169, 87.
- Tucker, W. H. 1971, Ap. J. (Letters), 167, L85.
- Williams, D. R. 1971, private communication, quoted by Kafatos, this volume.
- Zwicky, F. 1965, in Stellar Structure, Vol. 8, ed. L. H. Aller and D. B. McLaughlin (Chicago: U. of Chicago Press), p. 367.

## DISCUSSION

*A. G. W. CAMERON:*

It seems to me that there are many supernova light curve theories that would predict a great deal of ultraviolet emission, so the discovery of a fossil Strömgren sphere is not necessarily evidence for your theory. One should attempt rather to argue in reverse. That is, are there features of the Gum Nebula which specifically yield more information than just that there was an ultraviolet burst.

*S. A. COLGATE:*

[Dr. Colgate gave the arguments against great ultraviolet emission from a supernova that he presents in detail elsewhere in this volume. — Editor.]

*A. G. W. CAMERON:*

Dr. Colgate has not included the pulsar, which should have  $10^{52}$  erg in rotational energy initially, which it will shed in a time scale comparable to that of the supernova light curve.

*L. SARTORI:*

It seems more appropriate to start from our deduction (for the Gum Nebula) that  $10^{62}$  ultraviolet photons were produced by the supernova, and to place this as a condition on supernova theories, than to argue on purely theoretical grounds that  $10^{62}$  ultraviolet photons cannot be produced.

*T. L. PAGE:*

What are the requirements of your theory as to the production of helium in the pre-supernova evolution?

*SARTORI:*

About 0.1 solar mass has to be produced over the stellar lifetime and diffuse out to a distance of about one light year. It need not happen only in the last stages of evolution. The uniform helium distribution that we have assumed represents a zero order model, but it is not necessary to have a strictly uniform helium density in order to get good agreement with the light curve.

*A. POVEDA:*

The observations of bright supernovae, when a reasonable bolometric correction is made, do not imply more than  $5 \times 10^{50}$  erg in radiation.

*SARTORI:*

According to our view, the spectrum is completely unlike that of a blackbody and the bolometric correction is 8 magnitudes. In the optical wavelengths, the observed spectrum has strong emission bands and does not resemble a blackbody.

*D. REAMES:*

Does the Doppler-shift interpretation require that the material be moving radially before the photons get to it?

*SARTORI:*

The theory is consistent whether the material is already in motion or not, for velocities less than 0.01 or 0.02 times the speed of light.

*D. P. COX:*

The mean free path is only one scattering; is that correct?

*SARTORI:*

The simple version of our theory, in which we get good agreement with the light curve, takes only a single fluorescence into account. If we wish to include the effects of multiple scattering, the mathematical problem becomes much more complicated. It is not obvious how the light curve would be affected. Any effect of secondary fluorescence will be delayed with respect to the first one.

# RADIO ASTRONOMY EXPLORER-1 OBSERVATIONS OF THE GUM NEBULA

J. K. Alexander  
*Radio Astronomy Branch*  
*Laboratory for Extraterrestrial Physics*  
*Goddard Space Flight Center*  
*Greenbelt, Maryland 20771*

Low frequency radio waves propagating in the interstellar medium are attenuated due to free-free absorption by thermal electrons in regions of interstellar H II. This process is so efficient that at frequencies below 1 MHz ( $\lambda > 300$  m) one reaches unit optical depth at a distance of only a few hundred parsecs along a typical line of sight. Since the free-free absorption coefficient is a function of the density and temperature of the thermal electrons along the line of sight, one can attempt to use measurements of low frequency radio wave absorption to study the properties of the ionized component of the interstellar medium.\*

When Brandt et al. (1971) proposed that the Gum Nebula should appear as an object subtending an angle as great as  $90^\circ$  in the galactic plane with an average electron density of about  $0.16 \text{ cm}^{-3}$  it became obvious that free-free absorption effects should occur in the nebula. Such a region should appear on low frequency radio continuum maps of the southern sky as an area of relatively low brightness since much of the background galactic synchrotron radiation coming from beyond the nebula should be absorbed by the ionized gas in the nebular region. If one could construct a spectrum of the nonthermal radiation coming from the direction of the Gum Nebula and detect the expected absorption, then it should be possible to measure the average optical depth over the nebula.

The optical depth for free-free absorption is given by

$$\tau_\nu = \frac{3.1 \times 10^4 \langle n_e^2 L \rangle}{T_e^{3/2} \nu^2} \left[ 3.9 + \ln \frac{T_e^{3/2}}{\nu} \right]$$

---

\*The results presented in this paper appear in condensed form in Alexander et al. (1971).

where  $\nu$  is the radio frequency in MHz,  $\langle n_e^2 L \rangle$  is the emission measure in  $\text{cm}^{-6}$  pc, and  $T_e$  is the electron temperature in  $^{\circ}\text{K}$ . Since the emission measure of the Gum Nebula can be estimated independently, a measurement of  $\tau$  provides an estimate of  $T_e$ .

Although this procedure is simple in principle, its utility is tempered by a number of complicating factors. For example, in compiling an average spectrum for the Gum Nebula one has to take into account the radiation from the supernova remnants in the direction of the nebula which are likely to have a different spectrum from the background radiation from the nebular region. Fortunately, the supernova remnants subtend a solid angle of less than  $\sim 10$  sq. deg., and therefore they occupy a very small fraction of the total area of the nebula. By using radio surveys of high angular resolution the average spectrum of the galactic synchrotron radiation from the direction of the nebula can be estimated while minimizing the contributions due to the discrete supernova remnant sources.

A second complicating factor in the analysis of the spectrum arises from the fact that the absorption law for radiation originating from beyond the nebula will differ from that for radiation generated within the nebula. Galactic background radiation generated at distances greater than about 900 pc will be absorbed by a factor  $e^{-\tau}$ . Radiation by cosmic ray electrons that lie within the nebula in the same region as the absorbing thermal electrons will be attenuated by a factor  $(1 - e^{-\tau})/\tau$ . Uncertainties in estimating the relative contributions of these two components to the total spectrum will place a corresponding uncertainty on the optical depth derived.

A third complicating factor is the Razin effect, which results in a low-frequency cutoff to the spectrum of synchrotron radiation by particles in a thermal plasma. Such is the case for the component of nonthermal radiation by cosmic ray electrons in the highly ionized gas in the Gum Nebula. For a magnetic field  $B \simeq 2 \mu\text{G}$  and an electron density  $n_e \simeq 0.18 \text{ cm}^{-3}$ , the frequency of the Razin effect cutoff (corresponding to an effective Razin effect optical depth of unity) will be

$$\nu_R \simeq \frac{20 n_e}{B} = 1.8 \text{ MHz.}$$

Hence the spectrum of the radiation component from within the nebular radius will be likely to fall off at low frequencies more rapidly than if free-free absorption alone were important.



The net result of the complicating factors mentioned above is to cause a tendency to over-estimate the amount of absorption occurring in the nebula, and hence we can only get an upper limit to the optical depth. Consequently, we determine a lower limit to the temperature of the region.

The average spectrum for the Gum Nebula region at low radio frequencies is shown in Figure 1. The brightness at each frequency was obtained by averaging the observed brightness distribution given in continuum maps over the region  $240^\circ < \ell < 280^\circ$ ,  $-15^\circ < b < 15^\circ$ . The error bars shown are generally larger than the absolute uncertainty of the original published surveys and reflect the additional uncertainty due the averaging process and the removal of the supernova remnant radiation. A list of the surveys used to compile the spectrum and their angular resolution (antenna beamwidth) is given in Table I.

Table I  
Southern Sky Surveys Used to Compile  
Gum Nebula Spectrum

Frequency	Beam Size	Reference
150 MHz	$2.2^\circ \times 2.2^\circ$	Landecker and Wielebinski (1970)
85	$3.5^\circ \times 3.8^\circ$	Yates (1968)
55	$14^\circ$	Rohan and Soden (1970)
30	$11^\circ$	Mathewson <i>et al.</i> (1965)
18.3	$17^\circ$	Shain and Higgins (1954)
6.55	$14^\circ \times 34^\circ$	RAE-1
4.7	$3^\circ \times 11^\circ$	Ellis and Hamilton (1966)
3.93	$23^\circ \times 52^\circ$	RAE-1
2.1	$7^\circ$	Reber (1968)

The points at 3.93 and 6.55 MHz were obtained from measurements with the Radio Astronomy Explorer-1 satellite. The brightness values were obtained by using maps produced by the RAE 229-m travelling-wave V antenna calibrated by absolute measurements of the average sky brightness with the satellite's 37-m dipole antenna. Details of the RAE-1 instrumentation are discussed by Weber *et al.* (1971). The brightness values at 2.1 and 4.7 MHz were obtained by normalizing to the values observed at high latitudes and calibrating with the absolute spectral data from RAE. Both the satellite measurements and the two lowest-frequency ground-based surveys at 2.1 and 4.7 MHz distinctly show regions of low brightness approximately centered on the Gum Nebula. This is illustrated in Figure 2 which shows a map of the region at

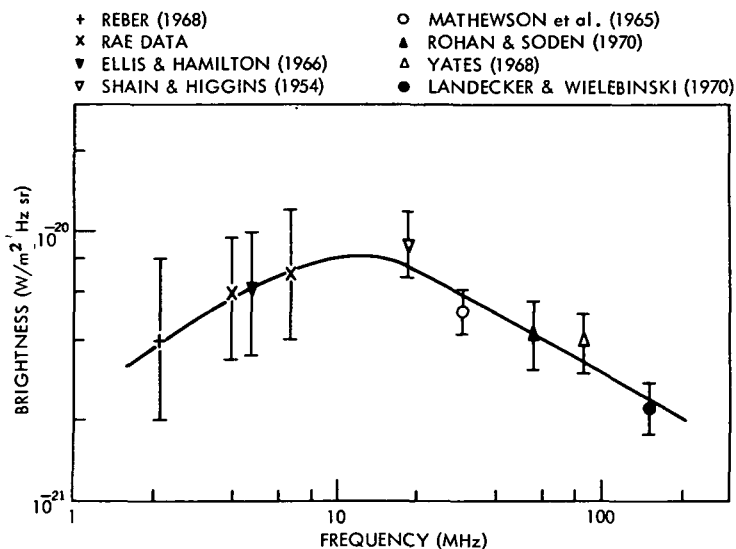


Figure 1. Radio spectrum of the region of the Gum Nebula.

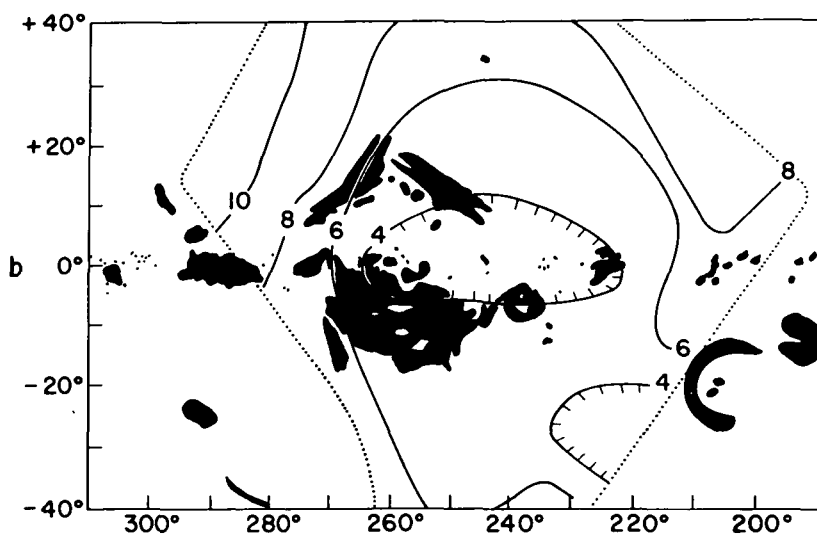


Figure 2. Preliminary map of the Gum Nebula region at 3.93 MHz from the RAE-1 satellite. The area enclosed by the dotted boundaries denotes the region for which there are satellite data for two separate surveys with orthogonal antenna beam orientations. The contours show isophotes of relative antenna temperature; one unit corresponds to a brightness temperature  $\sim 3 \times 10^5$  K.

3.93 MHz from RAE-1. The fact that the center of the "low" in the isophotes is shifted to slightly smaller longitudes than the center of the nebula is probably due to beam-smearing effects arising from the presence of a second nearby H II region located at  $\ell \approx 200^\circ$ ,  $b \approx -20^\circ$ . Although its size and shape cannot be unambiguously determined from the satellite measurements, the Gum Nebula region is one of the most pronounced features in the sky observed with RAE-1. That this is so is indicative of the very large area that must be subtended by the diffuse ionized gas associated with the nebula.

As one can see from Figure 1, the brightness in the direction of the nebula is down by about a factor of three at  $\nu = 4$  MHz from a straight-line extrapolation of the high frequency emission spectrum. At 2 MHz the brightness would appear to have fallen by a factor of  $\sim 8$ . After making allowance for the difference in the form of the absorption law for foreground and background radiation and for the possibility of a Razin effect cutoff at  $\nu \sim 2$  MHz, we estimate that the average optical depth for the nebula at 4 MHz is

$$\tau_4 \lesssim 3 \pm 1.$$

The average electron temperature of the nebula corresponding to  $\tau_4 = 3$  is shown as a function of emission measure in Figure 3. If we take the average emission measure of the visible filaments estimated by Brandt *et al.* (1971),  $\langle n_e^2 L \rangle = 1300 \text{ cm}^{-6} \text{ pc}$ , then the lower limit to the temperature of the nebula is  $(5.7^{+1.8}_{-1.0}) \times 10^4 \text{ }^\circ\text{K}$ . If, instead, we estimate the emission measure by using the value of  $\langle n_e \rangle$  obtained from the pulsar dispersion measures and typical values of the clumpiness in H II regions such as the Orion Nebula (Spitzer 1968), we find  $\langle n_e^2 L \rangle \approx 900 \text{ cm}^{-6} \text{ pc}$  which gives  $T_e \gtrsim 4.5 \times 10^4 \text{ }^\circ\text{K}$ . As an extreme case, one could argue that the visible, high-density filaments occupy such a small fraction of the total area of the nebula that one should use the electron density derived from the pulsar dispersion measures to estimate the average emission measure implying a nearly uniform electron distribution. Then,  $\langle n_e^2 L \rangle \approx 25 \text{ cm}^{-6} \text{ pc}$  and  $T_e \gtrsim 4 \times 10^3 \text{ }^\circ\text{K}$ . This number, of course, is the absolute lower limit to the nebular temperature. We are led to conclude that the average emission measure for the Gum Nebula is most probably  $\gtrsim 600 \text{ cm}^{-6} \text{ pc}$  so that for  $\tau_4 \lesssim 3 \pm 1$ ,  $T_e \gtrsim (4 \pm 1) \times 10^4 \text{ }^\circ\text{K}$ .

### Acknowledgments

Many important contributions to the analysis of the RAE-1 satellite data were made by my colleagues L. W. Brown, T. A. Clark, M. L. Kaiser, R. G. Stone, and R. R. Weber. I also gratefully acknowledge discussions with J. C. Brandt, S. P. Maran, and T. P. Stecher.

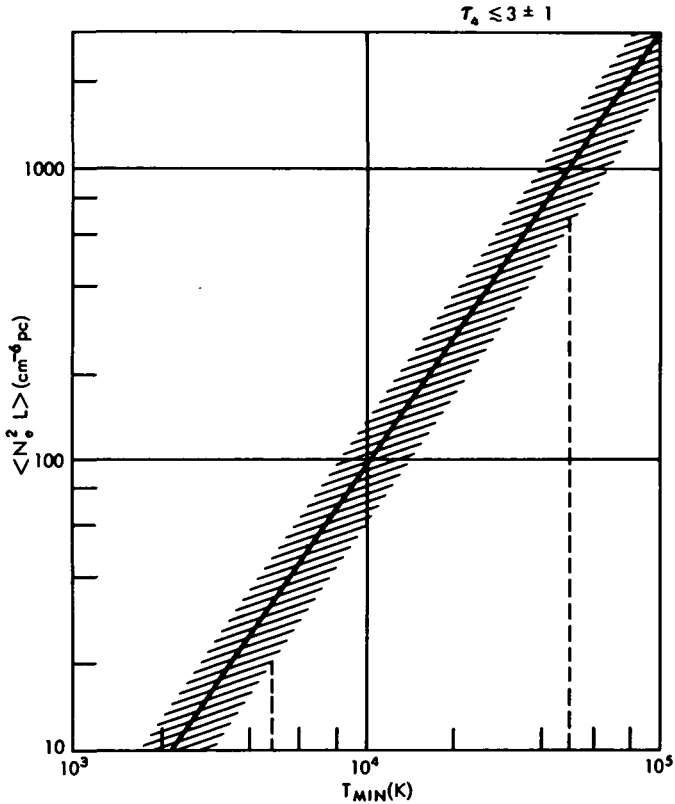


Figure 3. Plot of the average temperature of the Gum Nebula as a function of emission measure for  $\tau_4 = 3$ . The shaded area denotes the uncertainty in  $T_e$  corresponding to an uncertainty in  $\tau_4$  of  $\pm 1$ .

### References

- Alexander, J. K., Brandt, J. C., Maran, S. P., and Stecher, T. P. 1971, Ap. J., 167, 487.
- Brandt, J. C., Stecher, T. P., Crawford, D. L., and Maran, S. P. 1971, Ap. J. (Letters), 163, L99
- Ellis, G. R. A., and Hamilton, P. A. 1966, Ap. J., 143, 227.
- Gum, C. S. 1955, Mem. R. A. S., 67, 155.
- Johnson, H. M. 1971, this volume.

- Landecker, T. L., and Wielebinski, R. 1970, Aust. J. Phys., Astrophys. Sup., No. 16.
- Mathewson, D. S., Broten, N. W., and Cole, D. J. 1965, Aust. J. Phys., 18, 665.
- Reber, G. 1968, J. Franklin Inst., 285, 1.
- Rohan, P., and Soden, L. B. 1970, Aust. J. Phys., 23, 223.
- Shain, C. A., and Higgins, C. S. 1954, Aust. J. Phys., 7, 138.
- Spitzer, L. 1968, Diffuse Matter in Space, (New York: Interscience), p. 32.
- Weber, R. R., Alexander, J. K., and Stone, R. G. 1971, Radio Sci., 6, 1085.
- Yates, K. W. 1968, Aust. J. Phys., 21, 167

## A DISCUSSION OF THE GROUND-BASED RADIO OBSERVATIONS

F. J. Kerr

*Astronomy Program, University of Maryland  
College Park, Maryland 20742*

I wish to present a somewhat different interpretation of the radio observations. By way of preamble, I would like to remind ourselves of Bok's comment that this is not one single nebula, but rather it appears to be composed of several different entities.

I have examined all the southern surveys in the continuum, recombination line, H I, and OH. About 20 surveys are available altogether, although half of these do not go far enough in longitude or latitude to cover the region we are especially concerned with today.

Figure 1 shows a diagram by Mathewson, Healey, and Rome (1962) at a wavelength near 21 cm with a beamwidth of  $0^{\circ}.8$ . It shows a large extended region near the equator with some compact centers, covering a latitude range from  $-8^{\circ}$  to  $+4^{\circ}$ ; this is the region of "the small Gum Nebula," the bright portion. A similar result was obtained in recent 11-cm observations at Parkes by Day and others. I have done some computations on a preliminary form of their diagram, but these observations have not yet been published.

The striking point is the large amount of high-frequency radio emission from this region, the "small nebula." In fact, the total is comparable with the amount seen in the direction of the Carina spiral arm, leading to the suggestion that there is much more in this direction than just the Gum Nebula. Hugh Johnson also remarked earlier that this region is somewhat reminiscent of an end-on spiral arm.

The continuum results at longer wavelengths have essentially been shown in the previous talk by Alexander. I believe that at all frequencies it is the fairly small nebula that we are seeing. At the lower frequencies, the antenna resolutions are not as good, and therefore the nebula of small angular size is going to spread out on the sky and resemble the shape of the big nebula. Again, in 21-cm H I data and in recombination-line observations the smaller feature can be seen, but not the large Gum Nebula.

I submit that the outer part of the Gum Nebula has not been seen in any radio observations so far, and only the inner part has been observed. I don't think it is justifiable to work out any parameters for the whole Gum Nebula through

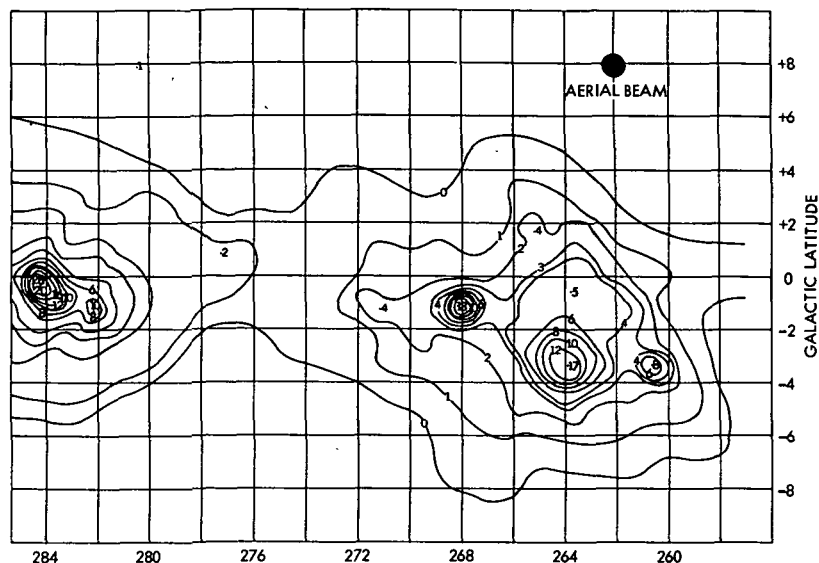


Figure 1. Isophotes of portion of the Southern Milky Way at 1440 MHz, with 50 arc min beamwidth (Mathewson, Healey, and Rome 1962).

taking an average over the whole solid angle subtended by the big nebula. There appears to be a large difference in density between the small nebula and the big one.

The possibility of such a density difference has not been mentioned by the earlier speakers. It may well be, for example, that most of the electrons that are doing the pulsar dispersion in this region are in the smaller volume occupied by the brighter nebula. In that case, we do not need as much ionization as has been suggested.

I believe the problem is more complicated than has been suggested so far. We need more observations in the whole region, both radio and optical, and I think we should reserve judgment on some points as far as properties of the whole nebula are concerned.

#### Reference

Mathewson, D. S., Healey, J. R., and Rome, J. M. 1962, Aust. J. Phys., 15, 354.

## DISCUSSION

*R. McCRAY:*

What is the distinction between the large nebula and the small nebula?

*F. J. KERR:*

The diameter of the small nebula is about  $30^\circ$  and the diameter that has been suggested for the large nebula is  $90^\circ$ .

*H. M. JOHNSON:*

It seems to me that the deductions so far made to compare dispersion and emission measures and to get the so-called clumpiness factor (X) — must still be very uncertain. I don't think the factor 65 is at all well-established. It is my personal opinion that it could be different by a factor of 10, and my only credential is Bart Bok's encouragement.

*B. J. BOK:*

Your work on Orion changed the whole picture.

*JOHNSON:*

The Orion region is so much denser that it doesn't necessarily have the same sort of structures that we are seeing here. In particular, Orion is concentrated toward the center, whereas this region seems to be hollow toward the center. So it seems to me that both the kind and the amount of clumpiness could be different.

*A. K. DUPREE:*

What recombination line sources did Dr. Kerr refer to?

*KERR:*

In Tom Wilson's catalog there are three sources in this general region.

*J. K. ALEXANDER:*

The temperatures from the recombination lines range from  $7000^\circ\text{K}$  to  $11,000^\circ\text{K}$ , and there are about five transitions that have been measured in the 6-18 cm wavelength range.



*R. N. MANCHESTER:*

I would like to make two points. First, for the pulsars used in the Gum Nebula model described by Brandt (other than PSR 0833-45), the dispersion measures are those obtained when the pulsars were discovered at Molonglo. There the instrument is limited to a bandwidth of 4 MHz at 408 MHz and dispersions were measured from analog recordings. Consequently the dispersion measures obtained are not very accurate. For example, the Molonglo value for PSR 0818-13 was  $25 \pm 10$  whereas I now obtain  $40.8 \pm 0.2$ . Similarly for PSR 1929 + 10 we have  $8 \pm 4$  and  $3.176 \pm 0.003$ . One point in favor of Brandt's discussion is that the error tends to be independent of the size of the dispersion measure and so proportionally smaller for pulsars with large dispersion measures. However, for PSR 0736-40, which is one of the pulsars that was used, the Molonglo observers quote an error of  $\pm 10\%$  but say that the measurement was made from "a few weak pulses," so, in fact it is probably not very accurate.

In principle, it is of course possible to measure these dispersion measures more accurately at Parkes or elsewhere. However, the large estimated errors in declination and period together with the weakness of many of the pulsars (the east-west arm of the Molonglo cross has over five times the collecting area of the 210-foot antenna at Parkes) make the measurements difficult. The second point is more fundamental and probably impossible to overcome; it is that the observed dispersion measure (even when accurately determined) does not necessarily yield a representative value of the mean electron density in the nebula. Because of irregularities in the medium, distances obtained from dispersion measures are probably uncertain by at least a factor of two. For example, Brandt *et al.* (1971) quote a "clumpiness factor" of 65 for the Gum Nebula. If the clump or filament diameter were about 1 pc, then the average line of sight would only intercept about 6 filaments. Obviously this number is very uncertain. However, it is clear that one must expect large differences in dispersion measures from pulsars at a given distance, especially when they are behind or within something like the Gum Nebula.

*T. P. STECHER:*

I would like to propose an observational test. Certainly around gamma Vel and zeta Pup there would be a small H II region formed long ago, with the standard temperature of 10,000 °K. If the Morrison and Sartori picture is correct, that H II region should be unaffected by the blast, as it was already ionized. Thus it would remain relatively cool, and recombination lines would be observed from it.

# RUNAWAY STARS IN THE GUM NEBULA

J. Richard Gott, III and Jeremiah P. Ostriker

*Princeton University Observatory*

*Princeton, New Jersey 08540*

## Abstract

We propose that the two pulsars PSR 0833-45 (the Vela pulsar) and MP 0835 are runaways from a common binary system originally located in the B association around  $\gamma$  Velorum. We present arguments in favor of a simple model of the Gum Nebula in which two distinct ionized regions are present. The first consists of the Strömgren spheres of  $\gamma$  Velorum and  $\zeta$  Puppis while the second is a larger, more filamentary region ionized by the supernova explosion associated with PSR 0833-45. Using this model and the available dispersion measures, we estimate the distances to the two pulsars and they are found to be compatible with a runaway origin. The position angle of the rotation axis of PSR 0833-45 is also compatible with a runaway origin. The masses of the parent stars of the two pulsars can be deduced from the runaway star dynamics and an assumed age for MP 0835. We conclude that the masses of the parent stars were in excess of  $10 M_{\odot}$ . The dynamically-determined parent star masses are in agreement with the values one would expect for evolved members of the B association around  $\gamma$  Velorum. Several observations are suggested which can further test this runaway star model for these two pulsars.

---

Runaway stars are produced when a supernova occurs in a binary star system. This process is illustrated schematically in Figure 1. Initially, we have two massive stars with masses  $M_1$  and  $M_2$  in a close binary system. Such systems typically have nearly circular orbits and  $M_1$  and  $M_2$  may have orbital velocities of the order of  $100 \text{ km sec}^{-1}$ .  $M_1$  is the more massive of the two stars and evolves first, eventually becoming a supernova. In the supernova explosion of  $M_1$  a neutron star of mass  $M_{N1}$  is produced and a shell of matter of mass  $(M_1 - M_{N1})$  is ejected. Figure 1a shows the initial binary system  $(M_1, M_2)$ , Figure 1b shows the ejection of the shell of matter which is presumed to take place in a time that is short compared with the orbital period of  $(M_1, M_2)$ . Once the shell has expanded beyond the position of  $M_2$ , as in Figure 1b, it no longer exerts any gravitational force on  $M_{N1}$  and  $M_2$ . So  $M_{N1}$  and  $M_2$  move freely under their mutual gravitational attraction and as initial conditions

have their initial separation and their initial orbital velocities. If more than half of the total initial mass of the binary system is ejected, then simple virial theorem arguments show that  $M_2$  and  $M_{N1}$  will follow unbound trajectories. Thus, the resulting system becomes unbound if

$$M_1 - M_2 > 2M_{N1}.$$

In this case, the trajectories of  $M_{N1}$  and  $M_2$  are as depicted in Figure 1c. Both are left as runaways with translational velocities comparable with their initial orbital velocities. Note that both  $M_2$  and  $M_{N1}$  move off the diagram in the upward direction so as to balance the momentum in the downward direction carried away by the ejected matter of the supernova explosion.

Zwicky (1957) and Blaauw (1961) have proposed that the high-velocity O and B "runaway" stars are in fact stars like  $M_2$  which have escaped from binary systems in the manner described above. These "runaway" stars are found to have space velocities in the range  $40 \text{ km sec}^{-1} < V < 200 \text{ km sec}^{-1}$  and are always single stars that have normal spectra. Often such a runaway star is found to be moving directly away from a known O association. Blaauw (1961) and Boersma (1961) have made a very careful study of runaway stars as escapees from binary systems and this explanation is now generally accepted.

After a time  $T$ , which one can take to be essentially the difference in main-sequence lifetimes of  $M_1$  and  $M_2$ , the star  $M_2$  will reach the end of its life and become a supernova, ejecting most of its mass and forming a neutron star of mass  $M_{N2}$ . Thus, both  $M_{N1}$  and  $M_{N2}$  are left as high velocity objects. We would accordingly expect many pulsars to be high-velocity runaways with velocities in the same range as those of the runaway stars found by Blaauw.

Gunn and Ostriker (1970) noticed that the older, longer-period pulsars are found at generally greater distances from the galactic plane than the younger, shorter-period ones. After a careful statistical study they concluded that the data were best fit by assuming that the parent stars of the pulsars had a scale height of  $\sim 80 \text{ pc}$  and that the pulsars received velocities of the order of  $100 \text{ km sec}^{-1}$  at birth. The scale height of the parent stars corresponds to that of the massive, Population I O and B stars, which have a scale height of  $\sim 50 \text{ pc}$  (O'Connell 1958) and the high velocities are explained by the runaway-star process.

Recent radio studies of interstellar scintillations of pulsars have confirmed that they are high velocity objects. Ewing *et al.* (1970) measured three pulsars and deduced that all three possess transverse velocities of approximately  $100 \text{ km sec}^{-1}$  with respect to the interstellar medium. Since interstellar medium velocities with respect to the earth are much smaller than this, they concluded

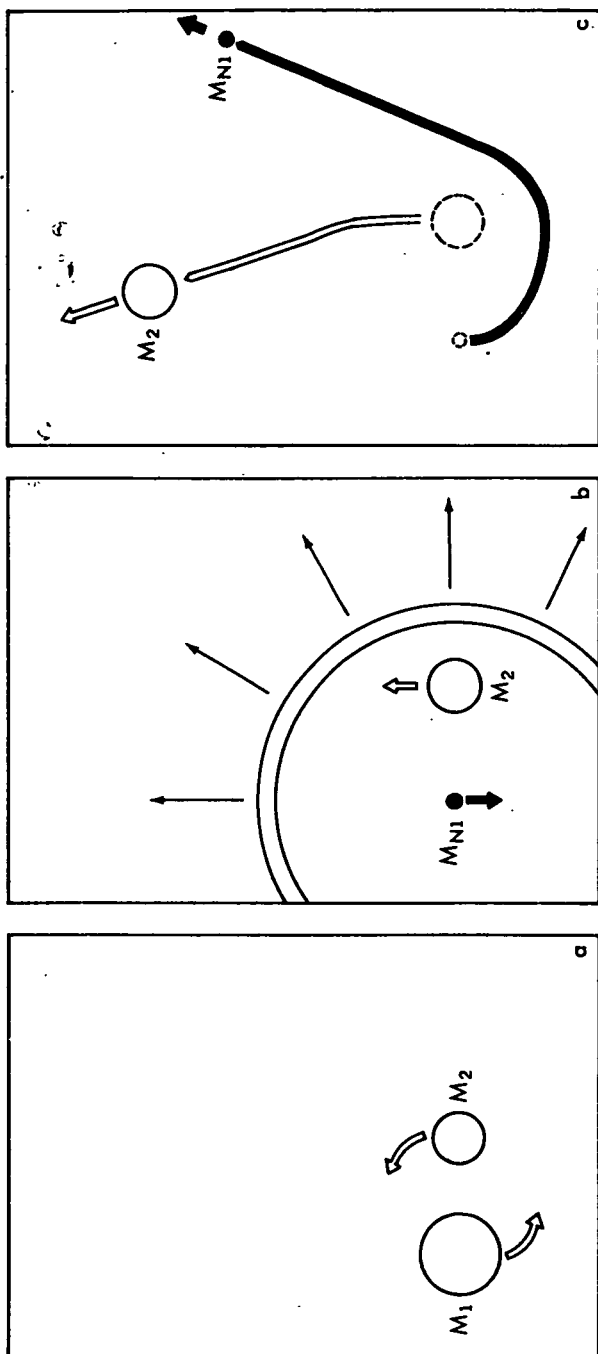


Figure 1. The runaway star process: (a) Initial binary system, (b) Supernova explosion of star  $M_1$ , (c) Trajectories of the second star ( $M_2$ ) and the neutron star ( $M_{N1}$ ); both are left as high velocity runaway objects.

that the effect was due to the motion of the pulsars with respect to both the interstellar medium and the earth. Lang (1971) has obtained similar observational results.

PSR 0833-45 (the Vela pulsar), and MP 0835 appear to be runaways from a binary system originally located in the B association around  $\gamma$  Vel. Using the nomenclature introduced above we wish to identify the old pulsar MP 0835 (period = 0.765 sec) with  $M_{N1}$  and the young Vela pulsar PSR 0833-45 (period = 0.0892 sec) with  $M_{N2}$ .

In a recent paper Brandt *et al.* (1971) have proposed that the Gum Nebula is a fossil Strömgren sphere produced by the supernova that gave birth to the Vela pulsar and the Vela X supernova remnant.

Brandt *et al.* described a photometric survey of the region around  $\gamma$  Vel and reported a B association around it. They list 10 stars, all having a distance of approximately 460 pc and all having spectral types earlier than B3. These stars form a cluster with a diameter of about  $8^\circ$  centered on  $\gamma$  Vel. All the stars listed must have masses in excess of  $7 M_\odot$  which is the approximate mass of a B3 V star. The 07 star which is a component of  $\gamma$  Vel must have a mass of the order of  $35 M_\odot$ . This cluster appears too young to have any definite turn-off point in its Hertzsprung-Russell diagram. Surely any evolved star associated with this group such as the parent star of the Vela pulsar must have been a massive star, probably with  $M > 10 M_\odot$ .

Now the Vela pulsar and MP 0835 both lie just off the N.E. edge of the B association found by Brandt *et al.* (see Figure 2), making them good candidates for runaways from the association. We know that the distance to  $\gamma$  Vel and its B association is 460 pc (Brandt *et al.* 1971) so to establish our runaway case we need to determine the distances to the Vela pulsar and MP 0835.

Brandt *et al.* noticed that the dispersion measure of the Vela pulsar is roughly half of that of nearby pulsars and concluded that the Vela pulsar is at the center of the ionized region corresponding to the Gum Nebula. This seems very reasonable. Using averages of 21-cm data, they concluded that the neutral hydrogen density in the vicinity of the sun is  $n_H \sim 0.4 \text{ cm}^{-3}$ . From Ly  $\alpha$  absorption in  $\gamma^2$  Vel and  $\xi$  Pup they concluded that there is  $\sim 60$  pc of neutral hydrogen between us and the front edge of the Gum Nebula. They then assume that the Vela pulsar lies at a distance of 460 pc as does  $\gamma$  Vel. So the ionized region corresponding to the Gum Nebula is found to have a diameter of  $\sim 800$  pc.

There is strong evidence against such a large ionized region. Its angular extent would be such as to cover almost half of the sky. This is much larger than the extent of the strong H  $\alpha$  emission from the Gum Nebula which one can observe

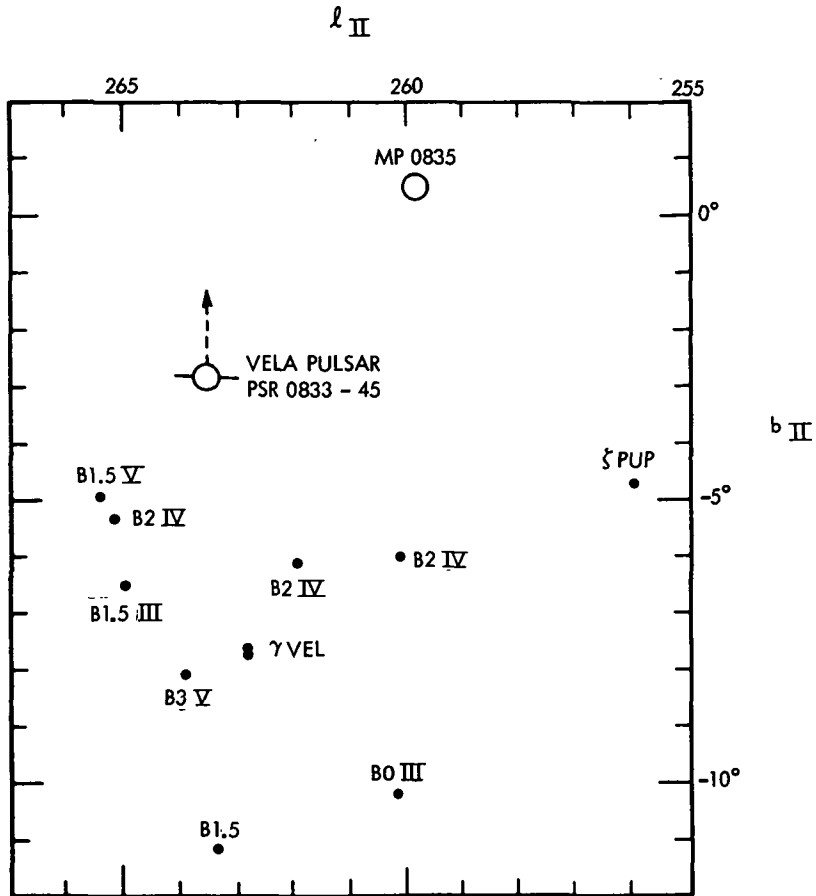


Figure 2. Region of the sky around  $\gamma$  Velorum showing the B association and the two pulsars PSR 0833-45 and MP 0835. Solid line shows the rotation axis of PSR 0833-45 and the dotted line shows its proposed direction of motion.

in *An Atlas of H-alpha Emission in the Southern Milky Way* (Rodgers *et al.* (1960). We see that, if we include the prominent filaments north of the galactic plane as part of the nebula, then the Gum Nebula is roughly circular in shape and lies between approximately  $-18^\circ < b_{II} < 18^\circ$  and  $241^\circ < l_{II} < 277^\circ$ . So it has an apparent radius of approximately  $18^\circ$ . This H $\alpha$  emission would certainly seem to define the size of the ionized region. Also, if the ionized region were as large as Brandt *et al.* suggest, then we would expect to

find a significant amount of ionized matter between us and CP 0834, which lies about  $45^\circ$  from the center of the Gum Nebula. Lang (1971), from interstellar scintillation studies, found that the distance to CP 0834 is about 362 pc and from its dispersion measure he concluded that the mean electron density along the line of sight is  $\langle n_e \rangle = 0.035$ . This is just the value one obtains for neutral hydrogen regions. In addition, PSR 0628-28 and MP 0818 which are both about  $30^\circ$  from the center of the Gum Nebula show dispersion measures less than half that of the Vela pulsar (Terzian 1970). Thus, it seems likely that the ionized region of the Gum Nebula is confined to the region outlined by the H $\alpha$  emission and has an apparent radius of about  $18^\circ$ .

We can obtain a consistent model if we use a better estimate of the local neutral hydrogen density. Jenkins and Morton (1967) have measured Ly  $\alpha$  absorption between the sun and three stars in Orion at a distance of 460 pc and found a mean column density of  $1.6 \times 10^{20} \text{ cm}^{-2}$ . This corresponds to a mean neutral hydrogen density along the line of sight of  $n_H \sim 0.1 \text{ cm}^{-3}$ . Since  $\gamma$  Vel and the Gum Nebula are in the same general area of the sky, the above value seems to be the best one to take for the neutral hydrogen density between us and the near edge of the Gum Nebula. Smith (1970) and Jenkins (1971) have also measured the hydrogen column density to  $\zeta$  Pup and found  $7 \times 10^{19} \text{ cm}^{-2}$ . With  $n_H = 0.1 \text{ cm}^{-3}$ , this means that the near edge of the Gum Nebula lies at a distance of 230 pc from the sun. If we assume the Gum Nebula is spherical, then its center is at a distance of  $330 \text{ pc} = 230 \text{ pc} / (1 - \sin 18^\circ)$  and its radius is 100 pc. The center of the Gum Nebula is thus 130 pc closer to the sun than  $\gamma$  Vel and  $\zeta$  Pup and therefore does not seem to have been produced by them (see Figure 3). The only other reasonable source for ionizing the Gum Nebula is the Vela X supernova event which gave birth to the Vela pulsar as Brandt *et al.* (1971) have pointed out. The ionization could have been caused either by photons below the Lyman limit or by low-energy cosmic rays from the supernova. The age of the Vela pulsar is estimated to be  $1.1 \times 10^4$  yrs. by Reichley, Downs, and Morris (1970). With the supernova event occurring only this long ago, Brandt *et al.* (1971) have shown that recombination within the Gum Nebula has not yet occurred.

Thus, we find that PSR 0833-45 (the Vela pulsar) is at the center of the Gum Nebula and lies at a distance of 330 pc from the sun. (Note: even if the Vela pulsar has a velocity of  $100 \text{ km sec}^{-1}$  it has had time to move only 1 pc since its birth.) This distance estimate is certainly consistent with the distance estimate of 500 pc to the Vela X supernova remnant according to Milne (1968 a, b) because of the great uncertainties in Milne's estimate.

The Vela pulsar has a dispersion measure of  $69.2 \text{ cm}^{-3} \text{ pc}$  (Ables *et al.* 1970).<sup>1</sup> We expect  $\langle n_e \rangle \sim 0.03 \text{ cm}^{-3}$  in the neutral hydrogen region between us and

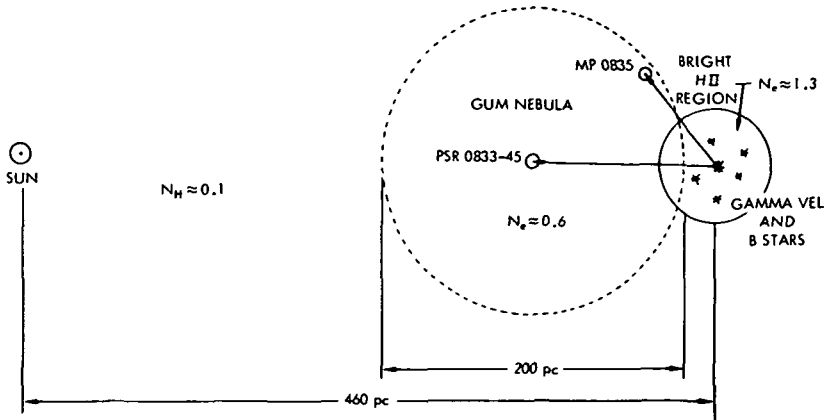


Figure 3. Schematic representation of the adopted model for the Gum Nebula region.

the Gum Nebula, so within the large spherical nebula region we find  $\langle n_e \rangle \sim 0.63$ . Using this value we find that MP 0835 with a dispersion measure of  $120 \text{ cm}^{-3} \text{ pc}$  (Terzian 1970) lies at a distance of  $\sim 410 \text{ pc}$  from the sun. (Note: The distances of the Vela pulsar and MP 0835 have been determined completely independently of any assumptions regarding their connection with the B association around  $\gamma \text{ Vel}$ .)

$\gamma \text{ Vel}$  (WC8 + 07) with its B association and  $\zeta \text{ Pup}$  (05) will each produce Strömgren spheres somewhat less than  $50 \text{ pc}$  in radius behind the Gum Nebula and joining with it if the local hydrogen density is of the order of  $\sim 3 \text{ cm}^{-3}$  (Spitzer 1968). This additional ionization at higher density would explain the increased  $H\alpha$  emission observed in the half of the Gum Nebula south of the galactic plane near these stars.

The above model of the region fits all the observations and also provides the expected increase in hydrogen density (from  $0.1 \text{ cm}^{-3}$  to  $0.63 \text{ cm}^{-3}$  to  $3 \text{ cm}^{-3}$ ) as we approach the star-forming region of the young B association.

We now know the distances and the positions in the sky of the center of the B association ( $\gamma \text{ Vel}$ ), the Vela pulsar, and MP 0835, so we can compute the lengths of the sides of the triangle they form in space and check our runaway hypothesis. The Vela pulsar is obviously the younger of the two pulsars and thus corresponds to  $M_{N2}$ , while MP 0835 corresponds to  $M_{N1}$ . The runaway star dynamics (Gott, Gunn and Ostriker 1970), tell us that if they shared a



common binary origin, the two pulsars and  $\gamma$  Vel (taken to be their approximate point of origin) should form a right triangle in space, with the right angle at MP 0835. The results are as follows: the sides of the triangle are approximately 80 pc, 90 pc, and 130 pc; the angle at MP 0835 is  $\sim 100^\circ$  and the angle at  $\gamma$  Vel is  $\sim 40^\circ$ , see Figure 1c and Figure 3.

Considering the uncertainties in the distances involved, this is a good agreement with the prediction offered by the runaway star dynamics.

We can make one check of the model immediately. Close binaries preferentially have rotation axes perpendicular to the orbital plane of the binary system. If no significant torques occur in the supernova explosions then the pulsars should have their rotation axes approximately perpendicular to the initial orbital plane, which is also the plane of the right triangle discussed above. We can compute that to be perpendicular to this plane, the rotation axis of the Vela pulsar should have a position angle in the sky of approximately  $\theta = 300^\circ$ . Now if pulsars are oblique magnetic rotators (Gunn and Ostriker 1969) and if the pulses originate in the regions of the magnetic poles, then a simple geometrical model such as proposed by Wampler, Scargle, and Miller (1970) shows that the linear polarization of the pulse should sweep in position angle as the magnetic pole rotates by our line of sight. Radhakrishnan *et al.* (1969) have observed just such a classic pattern in the Vela pulsar; the linear polarization in the pulse sweeps through  $45^\circ$  in position angle during the pulse. The simple geometric models mentioned above also indicate that if the pulse is exactly centered over the magnetic pole, then the position angle of the average intrinsic linear polarization should be perpendicular to the position angle of the rotation axis of the pulsar. Ekers *et al.* (1969) have taken out the Faraday rotation to find the position angle of the intrinsic linear polarization of the Vela pulsar. From this we deduce an "observed" value of the position angle of the rotation axis:  $\theta = 327^\circ \pm 6^\circ$  which agrees satisfactorily with our predicted value of  $\theta = 300^\circ$ . Uncertainties are introduced by the fact that the pulsar axis may not be perpendicular to the orbital plane and by the fact that the pulse may not be located exactly over the magnetic pole, which introduces an observational uncertainty of about  $\pm 1/2$  ( $45^\circ$ ).

The difference in main-sequence lifetimes of the parent stars of MP 0835 and the Vela pulsar ( $M_1, M_2$ ), is essentially equal to the age of MP 0835. If we knew this age we could compute the masses of the two parent stars  $M_1$  and  $M_2$ . We assume that  $M_{N1} \sim 1.5 M_\odot$ . The runaway star dynamics give us one relation between  $M_1$  and  $M_2$ , while the difference in main-sequence lifetimes as a function of  $M_1$  and  $M_2$  gives us another. The rate of change of the period of MP 0835 has not been reported, so we cannot estimate its age directly. MP 0835 has a period of 0.765 sec and we might expect its age to be similar

to that of other pulsars with similar periods. Now HP 1508 and CP 0329 are two such pulsars with periods of 0.740 sec and 0.715 sec respectively and ages  $(\frac{1}{2}P(dP/dt))^{-1}$  of  $2.3 \times 10^6$  years and  $5.5 \times 10^6$  years respectively. It seems reasonable to suppose that the age of MP 0835 lies in this range. If the age of MP 0835 is approximately  $6 \times 10^6$  years, then we would find  $M_1 \sim 20 M_\odot$  and  $M_2 \sim 10 M_\odot$ ; if the age is approximately  $2 \times 10^6$  years then we would find  $M_1 \sim 50 M_\odot$  and  $M_2 \sim 30 M_\odot$ .

Since we do not expect MP 0835 to be much older than  $6 \times 10^6$  years, it is clear that  $M_1$  and  $M_2$  must both be more massive than  $10 M_\odot$ ; this is what one would expect from the masses of the unevolved stars in the B association. If MP 0835 is a fairly young pulsar with an age of say  $2 \times 10^6$  years, then  $M_1$  and  $M_2$  were just about as massive as the most massive unevolved stars we see in the cluster. Either result would be possible because the association is so young. An experimental determination of the rate of change of the period of MP 0835 would allow us to estimate its age and determine the parent star masses.

Several observational tests of the possible binary origin of the Vela pulsar and MP 0835 can be made. The position angle of the rotation axis of MP 0835 can be deduced from measurements of its linear polarization at different frequencies. If it is from the same original binary system as the Vela pulsar we would expect its rotation axis to be approximately parallel to that of the Vela pulsar. Secondly, the transverse velocities of the Vela pulsar and MP 0835 can be measured by interstellar scintillation techniques and compared with the predictions offered by the binary origin model. Finally our distance estimates for the two pulsars, based on dispersion measures, can be complemented by distance estimates from interstellar scintillation techniques.

In conclusion, we propose that the Vela pulsar and MP 0835 are runaways from the B association around  $\gamma$  Vel. Taking a simple model of the Gum Nebula it is possible to use the dispersion measures to find the distances of the two pulsars. Their positions in space found in this way are consistent with a common origin as runaways from a binary system in the B association. The masses of the parent stars of the two pulsars are found from this model to be in excess of  $10 M_\odot$  which is consistent with what we would expect from the unevolved stars in the B association. The observed position of the rotation axis of the Vela pulsar is consistent with this binary origin model. We also propose additional observational tests of the model.

#### Acknowledgments

One of us (J. R. G.) wishes to acknowledge a National Science Foundation Graduate Fellowship.

## References

- Ables, J. G., Komesaroff, M. M., and Hamilton, P. A. 1970, Ap. Letters, 6, 147.
- Blaauw, A. 1961, B.A.N., 15, 265.
- Boersma, J. 1961, B.A.N., 15, 291.
- Brandt, J. C., Stecher, T. P., Crawford, D. L., and Maran, S. P. 1971, Ap. J., (Letters), 163, L99.
- Ekers, R. D., Lequeux, J., Moffet, A. T., and Seielstad, G. A. 1969, Ap. J., (Letters), 156, L21.
- Ewing, M. S., Batchelor, R. A., Friefeld, R. D., Price, R. M., and Staelin, D. H. 1970, Ap. J. (Letters), 162, L169.
- Gott, J. R., III, Gunn, J. E., and Ostriker, J. P. 1970, Ap. J. (Letters), 160, L91.
- Gunn, J. E., and Ostriker, J. P. 1970, Ap. J., 160, 979.
- Jenkins, E. B. 1971, Ap. J., 169, 25.
- Jenkins, E. B., and Morton, D. C. 1967, Nature, 215, 1257.
- Lang, K. R. 1971, Ap. J., 164, 249.
- Milne, D. K. 1968a, Australian J. Physics, 21, 201.
- . 1968b, ibid., p. 501.
- O'Connell, D. J. K. 1958, Ric. Astr. Specola Vaticana, 5.
- Ostriker, J. P., and Gunn, J. E. 1969, Ap. J., 157, 1395.
- Radhakrishnan, V., Cooke, D. J., Komesaroff, M. M., and Morris, D. 1969, Nature, 221, 443.
- Reichley, P. E., Downes, G. S., and Morris, G. A. 1970, Ap. J. (Letters), 159, L35.
- Rodgers, A. W., Campbell, C. T., Whiteoak, J. B., Bailey, H. H., and Hunt, V. O. 1960, An Atlas of H-alpha Emission in the Southern Milky Way (Canberra: Australian National University).

Smith, A. M. 1970, Ap. J., 160, 595.

Spitzer, L., Jr. 1968, Diffuse Matter in Space, (New York: John Wiley & Sons), p. 117.

Terzian, Y. 1970, private communication.

Wampler, E. J., Scargle, J. D., and Miller, J. S. 1969, Ap. J. (Letters) 157, L1.

Zwicky, F. 1957, Morphological Astronomy (Berlin: Springer-Verlag), p. 258.

## DISCUSSION

*A. G. W. CAMERON:*

What made you assume an age of less than  $6 \times 10^6$  years for MP 0835? Does it concern runaway velocity or a general age theory for pulsars?

*J. R. GOTT:*

It is an assumption based on the theory (Gunn and Ostriker) of the upper age limits for pulsars.

*CAMERON:*

Then, if we disregard that theory, you could make the age much greater and the pre-supernova masses much lower.

*S. A. COLGATE:*

Have you considered the rocket effect when a supernova goes off close to another star? If the mass ratio does not exceed 2 to 1, then at  $10^5$  km/sec something like 30 times more energy is deposited in the rocket effect than just in the separation of orbits by mass.

*GOTT:*

We have not considered the rocket effect.

*A. POVEDA:*

It should be pointed out that explosion in a binary system is not the only way to produce runaway stars. They can be produced by dynamical interactions in compact systems. In the Crimean catalog of runaway stars there are about 5 runaway stars in the Gum Nebula region.

*GOTT:*

It should also be noted that there are other pulsars in this region that might be runaway objects. We are also checking on zeta Pup.

*S. P. MARAN:*

To me, the most interesting aspect of this paper is the model, which takes the Gum Nebula diameter to be smaller than that derived by Brandt (although it is thereby more in accord with the predictions of Morrison and Sartori), and

which takes the Gum Nebula to be closer than derived by Brandt, and to lie in front of the normal H II region around gamma Vel which Bok mentioned. Would someone comment on the acceptability of this model?

*J. K. ALEXANDER:*

This model has to contend with the low-frequency radio measurements. If the nebula had  $n_e \approx 0.6 \text{ cm}^{-3}$  and were as close as suggested by Gott and Ostriker, it would be quite opaque at low frequencies. If we divide the observed brightness at a frequency at which it is opaque by the distance at which we no longer get background radiation from beyond the opaque portion of the nebula, then that gives us the volume emissivity of cosmic ray electrons along that path. If we then compare the emissivity thus deduced with the interstellar synchrotron emissivity expected for cosmic ray electrons, we find the volume emissivity very high compared to direct measurements of cosmic ray electrons. To resolve this apparent discrepancy, we must either raise the nebular temperature so that the path length through the nebula up to the point where it becomes opaque can be increased, or we must increase the distance to the nebula, or we must accept the idea of large spatial gradients in the interstellar cosmic ray electron distribution such that there is an enhanced density of radiating electrons in the vicinity of the Gum Nebula. Although these problems do not make this model impossible, they raise some rather difficult questions.

*S. SOBIESKI:*

I wonder if the amount of mass loss suggested by the binary star/supernova theory presented here is consistent with the observations, which suggest that the total mass of material in this region is less than one solar mass.

*A. B. UNDERHILL:*

Yes, if the great amount of mass loss mentioned by Gott is distributed in this small region, we ought to be able to see it.

*EDITOR'S NOTE:*

At this point Dr. A. B. Underhill criticized the pre-supernova masses assumed by Gott as being too high, and Dr. A. G. W. Cameron criticized them as being too low!

*VOICE:*

If there are other runaway stars in this region, then why must we suppose that the two pulsars are related to each other as a runaway pair?

*GOTT:*

The positions of the two pulsars, both being on the same side of the B-association, and their distances influenced this assumption by us. The rotation axis directions and transverse velocities, when they are known, will be valuable for checking this.

*K. HENIZE:*

There is no real evidence that these two pulsars are high velocity objects is there?

*GOTT:*

No, that is correct. It would be very desirable to obtain such evidence. However, there is statistical evidence that pulsars in general are high velocity objects. First, statistically one finds that old pulsars are further from the galactic equator. Second, the interstellar scintillation observations, such as those of Ewing et al. indicate typical transverse velocities of 100 km/sec for pulsars.

# STRUCTURE AND EVOLUTION OF FOSSIL H II REGIONS\*

Richard McCray  
and

Joseph Schwarz  
*Harvard College Observatory  
Cambridge, Massachusetts 02138*

## Abstract

We consider the structure and evolution of a fossil H II region created by a burst of ionizing radiation from a supernova. If  $10^{51}$  erg in UV and soft X-ray continuum radiation are released into a homogeneous gas of density  $n_0 = 1 \text{ cm}^{-3}$ , the resulting structure is a fully ionized zone of radius roughly 70 pc at temperature  $\sim 2 \times 10^5 \text{ }^\circ\text{K}$  surrounded by a partially ionized shell at temperature  $\sim 10^4 \text{ }^\circ\text{K}$  extending some 70 pc further. The whole region cools to  $10^4 \text{ }^\circ\text{K}$  in about  $10^4$  years. The fully ionized zone further cools to  $\sim 30 \text{ }^\circ\text{K}$  in about  $10^5$  years, while the partially ionized shell remains at  $10^4 \text{ }^\circ\text{K}$ . The cooling time scale for the shell is about  $10^6$  years. We suggest that superposition of million-year-old fossil H II regions may account for the temperature and ionization of the interstellar medium.

Fossil H II regions are unstable to growth of thermal condensations. Highly ionized filamentary structures (scale length  $\sim 0.1$  pc,  $T \sim 10^4 \text{ }^\circ\text{K}$ ) form and dissipate in about  $10^4$  years. Partially ionized clouds (scale length 1-10 pc,  $T \sim 30 \text{ }^\circ\text{K}$ ) form and dissipate in about  $10^6$  years.

## I. Introduction

The suggestion that giant relict H II regions, or "fossil Strömgren spheres," are created by supernova outbursts has been put forward recently in several different contexts. Morrison and Sartori (1969) calculated from their He II fluorescence model that approximately  $10^{62}$  ionizing (40 eV) photons would be produced during the visible outburst. Bottcher *et al.* (1970) proposed that the temperature and electron density in the interstellar gas are due to a superposition of fossil H II regions (most of which are about  $10^6$  years old) that

---

\*Partly supported by the National Science Foundation.



are recombining and cooling; the interpretation requires approximately  $10^{62}$  ionizations per supernova if the mean interval for supernova outbursts in the galaxy is 30 years. Brandt et al. (1971) suggested that the Gum Nebula is a fossil H II region created by the supernova outburst responsible for the Vela X supernova remnant and for the pulsar PSR 0833-45. If so, the outburst must have produced of order  $10^{62}$  ionizations at the time that the event occurred, which according to the pulsar deceleration rate was some  $1.1 \times 10^4$  years ago. Less than one percent of the interstellar matter would have recombined in the time elapsed since the ionization occurred, unless most of the matter is concentrated in dense filaments.

Several of us\* at Harvard College Observatory have been working on topics closely related to the structure and evolution of fossil H II regions. Our work can be divided into three closely related problems: (1) the temperature and ionization structure of a region exposed to a "sudden" burst of ionizing radiation; (2) the subsequent time evolution of "fossil H II regions," and the role that such regions play in the ionization and thermal balance of the interstellar medium; and (3) the formation of condensations such as filaments and clouds in this context.

## II. Supernovae as Ionization Sources

The mechanism whereby a supernova explosion might create a fossil H II region is a controversial subject. The ionization of the Gum Nebula region requires an energy of at least  $3 \times 10^{51}$  erg ( $E_{51} = 3$ ), and more likely  $E_{51} = 10$ . In terms of the total energetics of supernovae, this is a reasonable value. If supernovae occur at a rate  $(30 \text{ year})^{-1}$  in the galaxy, each one must release about  $10^{51}$  erg in high energy ( $\gtrsim 100$  MeV) cosmic rays in order to account for the origin of cosmic rays in the galaxy (assuming an escape time of  $3 \times 10^6$  years). Also, an interpretation of several supernova remnants according to the spherical blast wave theory suggests that supernovae release between  $10^{50}$  and  $10^{51}$  erg in mechanical energy (Minkowski 1968; Shklovsky 1968).

There is little evidence that supernovae release comparable energy in ionizing radiation. The observed optical (2-5 eV) output integrated over the light curve of the outburst is typically  $3 \times 10^{49}$  erg. If the spectrum extended out to 500 eV as a flat bremsstrahlung continuum from an optically-thin plasma at  $5 \times 10^6$  °K, it would release  $3 \times 10^{51}$  erg in ionizing radiation. Color temperatures and bolometric corrections obtained from the optical spectrum are of little value in estimating the ionizing part of the supernova spectrum.

---

\*Christopher Bottcher, Alexander Dalgarno, Michael Jura, Richard McCray, and Joseph Schwarz.

Morrison and Sartori (1969) have suggested, on the basis of a He II fluorescence model for the supernova light curve, that roughly  $10^{52}$  erg in 40.8 eV UV radiation accompanies a type I supernova outburst.

Yet another way in which a supernova might create a fossil H II region is by radiation from the blast wave associated with the remnant (Tucker 1971a). The blast wave converts its mechanical energy ( $E_{51} \approx 1$ ) into ionizing radiation with almost complete efficiency in a time scale of order  $3 \times 10^4$  years. This process may be occurring now in the Gum Nebula (Tucker 1971b).

It may be that the Gum Nebula region is ionized by low energy cosmic rays instead of radiation (Ramaty *et al.* 1971). We doubt it, because low energy cosmic rays cannot propagate freely through an H II region (Cesarsky 1971). Their streaming velocity is limited to the Alfvén velocity, and they can propagate only a few parsecs from their source before dissipating their energy.

The physical nature of the supernova outburst is quite uncertain at present. Perhaps, as Ostriker and Gunn (1971) suggest, the outburst is driven electromagnetically by a newly-formed pulsar. At any rate, it seems premature to adopt a firm opinion as to the relative efficiencies of the supernova event in producing ionizing radiation, mechanical energy, and fast particles. Our approach has been to work out the consequences of various models for the ionizing source. We have worked mainly with photoionizing burst models because their consequences can be described with few parameters. However, most of the conclusions discussed in sections IV and V apply also to regions suddenly ionized by cosmic rays.

### III. Structure of Photoionized Fossil H II Regions

An ultraviolet or soft X-ray burst that releases an energy  $E_{51} \times 10^{51}$  erg of ionizing radiation into an initially cold H I region of hydrogen density  $n_0 \text{ cm}^{-3}$  will create a fully ionized zone of radius roughly

$$R_1 \simeq 70 \left( \frac{E_{51}}{n_0} \right)^{1/3} \text{ pc}, \quad (1)$$

containing a mass of roughly  $3 \times 10^4 E_{51}$  solar masses. This radius is much larger than the maximum radius ( $\sim 10 \text{ pc}$ ) of the supernova remnant.

If the duration of the ionizing flux is less than  $10^5$  years, the zone can be described as "fossil," but it is not a "Strömgren sphere," for two reasons. First, the spectrum of ionizing radiation is not at all like a blackbody spectrum.

It may be quite hard, with the consequence that the transition from H II to H I is not a sharp boundary at all, in contrast to the Strömgren case. Also, the ionization occurs in a time short compared to the recombination time scale, so that recombinations play no role in determining the structure of the zone. The radius of the zone is set by the total number of ionizing photons emitted during the outburst rather than by the recombination rate.

In order to find the structure of the zone, it is necessary to calculate the ionization (including secondary ionization) and associated heating for each radial distance  $r$ . The problem is complicated by the fact that, as the inner zone becomes more ionized, the optical depth  $\tau_\nu(r, t)$  decreases with time. If the source spectrum is not monochromatic, the only photons that reach a given radius initially are the hard ones, for which the optical depth is small ( $\tau_\nu \propto \nu^{-3}$ ). Later, the same radius may be exposed to soft photons. The number of secondary ionizations per primary ionization and the heating per ion pair are functions of the primary photon spectrum and of the ionized fraction  $x = n_e/n_0$ , where  $n_0 = n_{\text{H I}} + n_{\text{H II}}$  ( $\text{cm}^{-3}$ ). These functions have been calculated in detail by Jura (1971).

We have solved the coupled equations for heating and ionization by a sudden burst for the idealized model of a pure hydrogen gas exposed to various simple source spectra, such as a monochromatic spectrum, power law spectra, and a bremsstrahlung spectrum. The results for the last case provide an interesting example. We find that for  $R$  less than  $R_1$  of equation (1),  $x \approx 1$  and  $T \approx 2 \times 10^5$  °K. The ionized fraction begins to decrease slowly for  $R > R_1$ , but it is still significant at  $R = 2R_1$  where  $x \approx 0.05$  and  $T \approx 10^4$  °K. The partially ionized region is generally thinner for monochromatic UV spectra or decreasing power law spectra, but the results are otherwise similar. A photoionized fossil H II region consists of a fully-ionized zone at a temperature roughly  $2 \times 10^5$  °K, surrounded by a thick, partially ionized shell, the temperature of which is above  $10^4$  °K if  $x > 0.05$ .

The inclusion of processes involving helium modifies the temperature and ionization structure of the region quantitatively but not qualitatively. Photoionization of trace elements such as oxygen does not significantly change the initial structure of the region, but it does have important effects on the subsequent evolution of the region, as we shall presently see.

#### IV. Evolution of Fossil H II Regions; Relation to Structure of the Interstellar Medium

To make the calculations described in the last section we assumed that heating and ionization occurred in a time short compared to the cooling and

recombination time scales of the gas. Then the structure of the zone after the ionizing burst may be adopted as the initial condition for the subsequent evolution of the fossil H II region.

The power radiated per unit mass by a low density plasma can be written  $P = (n_0/m_H) \Lambda(x, T)$ . The function  $\Lambda$  ( $\text{erg cm}^3 \text{sec}^{-1}$ ) for a gas of normal cosmic abundance has been calculated by Cox and Tucker (1969) for  $T_4 = T/10^4 \text{ }^\circ\text{K} > 1$ , and by Jura (1971) for  $T_4 < 1$ . It is displayed in Figure 1.

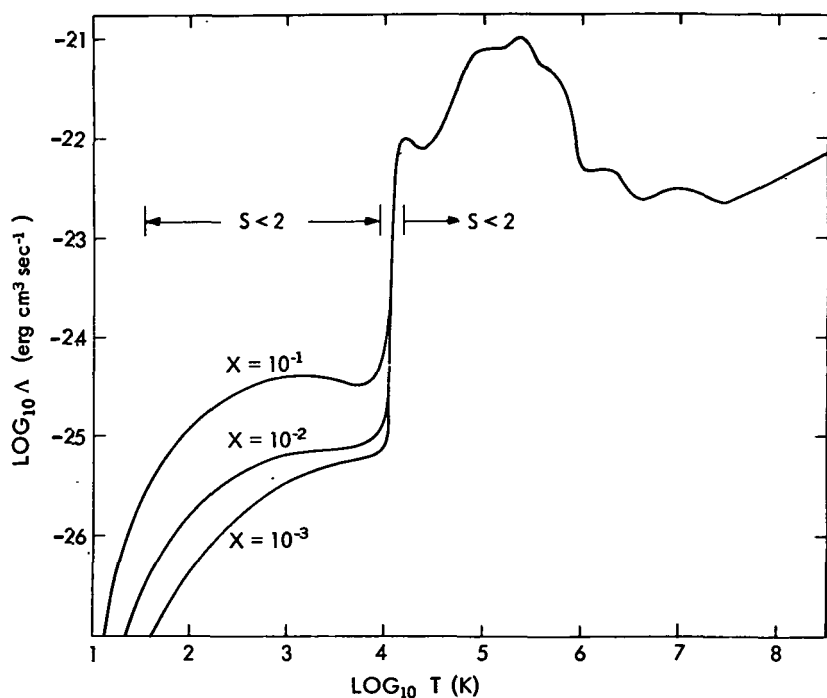


Figure 1. Cooling of a low density plasma with cosmic abundances. The power radiated per unit mass is given by  $p = n_0 \Lambda / m_H$ . For  $\log T < 4$ ,  $\Lambda$  is given for three values of the ionized fraction  $x = n_e / n_0$ . Temperature ranges favoring thermal condensation (logarithmic slope  $s < 2$ ) are indicated.

Cooling in the high temperature range ( $1 < T_4 < 30$ ) is dominated by electron impact excitation of atomic lines of H I, He I, He II, multiply-ionized oxygen, and other trace elements. In this temperature range hydrogen is ionized by thermal collisions, so that the free electron concentration is a function of temperature. We may represent this cooling by defining a cooling time scale  $\tau_c \equiv T/(dT/dt)$ . Very roughly,

$$\tau_c \approx \frac{2000}{n_0} \text{ years; } 1 < T_4 < 30. \quad (2)$$

Kafatos (1971) has shown that the Cox and Tucker results approximate the actual time-dependent cooling fairly well.

Cooling in the low temperature range ( $T_4 < 1$ ) is dominated by electron impact excitation of infrared fine structure transitions in trace constituents such as  $C^+$ , O, and  $Fe^+$ . In this temperature range hydrogen is not thermally ionized. Hence, the ionized fraction of interstellar gas is not necessarily a function of temperature alone. In Figure 1, the cooling rate is plotted for three different values of the ionized fraction  $x$ . The cooling at a given temperature is linear with  $x$  for  $x > 10^{-2}$  because electron impact excitation dominates. In this case, the cooling time scale can be written

$$\tau_c \approx \frac{2 \times 10^4 T_4}{n_0 x} \text{ years} \quad 10^{-2} < T_4 < 1. \quad (3)$$

For temperatures below 100°K, the cooling time scale becomes long again. For very low fractional ionizations ( $x < 10^{-3}$ ), the cooling becomes independent of  $x$  because impact excitation by neutral hydrogen becomes dominant.

We may apply these results to the evolution of the fossil H II region described in section III. Consider a medium that has been suddenly heated and partially ionized. The hydrogen recombination time scale  $\tau_R \equiv x/(dx/dt)$  is longer than the cooling time scale for all  $T < 30^\circ\text{K}$ :

$$\tau_R \approx \frac{10^5 T_4^{1/2}}{n_0 x} \text{ years.} \quad (4)$$

Therefore, it is a fairly good approximation to assume that the medium will maintain its initial ionized fraction until its temperature drops below  $100^\circ\text{K}$ .

On a time scale that we might call "recent prehistory" ( $t < 10^4$  years), only the high temperature material ( $T_4 > 1$ ) has time to cool. In a few times  $\tau_c$  (equation 2), all matter that was initially hotter than  $10^4$  °K will cool to roughly  $10^4$  °K, with no significant recombination. This would be the case for the Gum Nebula, for which  $t = 1.1 \times 10^4$  years (Reichley, Downs, and Morris 1970).

Cooling of the fossil H II region below  $T_4 = 1$  (equation 3) occurs on a longer time scale which varies according to the initial ionized fraction  $x$ . Jura (1971) has calculated time-dependent cooling and recombination curves for initial temperature  $T_4 \approx 1$  and various initial ionized fractions  $x$ , including the effect of ionizing trace elements, which lengthens the cooling time scale. With a density  $n_0 = 1 \text{ cm}^{-3}$ , the inner, fully ionized zone will cool to roughly  $30^\circ\text{K}$  and begin to recombine within  $10^5$  years, while the outer, partially ionized zone remains at  $T_4 \approx 1$ . On a still longer time scale, which we might call "Pleistocene" ( $t \approx 10^6 - 10^7$  years), the outer shell will also cool to  $30^\circ\text{K}$ .

Bottcher *et al.* (1970) suggested that these "Pleistocene" fossil H II regions play a major role in keeping the general interstellar medium heated and partially ionized. The argument is simple: every time an ionizing burst occurs, it sets up approximately  $3 \times 10^5 E_{51}$  solar masses of interstellar matter in a hot ionized condition. This matter then begins to cool and recombine. The frequency of supernova outbursts in the galaxy (Shklovsky 1968) is roughly  $(30 \text{ years})^{-1}$ . If we assume the same frequency for ionizing bursts, each with  $E_{51} = 1$ , we have  $10^3 M_\odot/\text{year}$  interstellar matter returned to the initial condition. The total galactic content of interstellar matter is roughly  $2 \times 10^9 M_\odot$ , which means that any given region of the galaxy is likely to be cycled back to the initial condition after a time scale of order  $2 \times 10^6$  years. Accordingly, most of the interstellar medium at present would be composed of Pleistocene fossil H II regions.

A model for the interstellar medium composed of a superposition of these regions would have a distribution of temperature and ionization that agrees reasonably well with observations. The central regions would have  $x \approx 10^{-2}$ ,  $T \approx 30^\circ\text{K}$ , and the outer shells would have  $x \approx 10^{-1}$ ,  $T \approx 10^4$  °K. Very little matter would be expected with  $10^2$  °K  $< T < 10^3$  °K, because the time to cool through that temperature range is short, according to equation (3). The resulting sharp division of temperature that occurs in a fossil H II region model for the interstellar medium will resemble that in hydrostatic models in which clouds and intercloud medium are maintained in thermodynamic balance by

a hypothetical flux of low energy ( $\sim 2$  MeV) cosmic rays (Field, Goldsmith and Habing 1969; Hjellming, Gordon and Gordon 1969; Jura 1971) or ionizing photons (Habing and Goldsmith 1971; Bergeron and Souffrin 1971; Jura 1971).

The earlier time-dependent model of Bottcher *et al.* (1970) for the interstellar medium did not agree very well with observations because the authors assumed that ultraviolet bursts created fully ionized zones, which cool too fast. For that reason, Jura (1971) proposed cosmic rays as an additional source of heating. The model described here, in which a substantial part of the H II region is partially ionized by soft X-rays, fits the observations better than that of Bottcher *et al.* Such a soft X-ray burst model was first suggested by Werner, Silk and Rees (1970).

All models for heating and ionizing the interstellar medium have difficulties. It is doubtful that a spatially homogeneous flux of low energy cosmic rays can exist (Bottcher *et al.* 1970). The observed soft X-ray background fails by at least one order of magnitude to provide the necessary flux (Silk and Werner 1969). Discrete X-ray sources also seem inadequate. If the galaxy contained X-ray stars in sufficient quantity to heat the medium, we should see roughly 50 sources brighter than Sco X-1. Given these circumstances, it is gratifying to see in the Gum Nebula fossil H II region at least one observed member of a class of sources that is potentially capable of ionizing and heating the interstellar medium to the necessary degree. Indeed, a Gum Nebula ( $E_{51} = 10$ ) type event every 30 years would provide too much heating and ionization.

We have not considered possible fluid motions, despite the fact that the fossil H II regions will have pressures that are two or three orders of magnitude greater than their surroundings. The associated pressure gradients can move matter at velocities comparable to the sound velocity  $c$ . Substantial changes in density over a scale length  $\lambda$  can occur in a time  $t_3 \sim \lambda/c$ . For scale lengths typical of the model fossil H II regions described here ( $\lambda \sim 20$  pc),  $t_3 \simeq 2 \times 10^6 T_4^{1/2}$  years. This time scale is long compared to most cooling time scales associated with fossil H II regions. As a result, large scale fluid motions that occur during the cooling time scale of the medium have little effect. We may therefore assume that, on a large scale, the region cools at constant density (isochorically). The partially ionized shell may be an exception; the shell may expand (both inward and outward) substantially as it cools.

#### V. Thermal Condensations in Fossil H II Regions; Formation of Filaments and Clouds

Perhaps the most interesting type of fluid motion that occurs in fossil H II regions involves density perturbations of scale length smaller than that of the

region. Matter that is set up in an initially hot condition and subsequently cools by radiation almost always favors the growth of thermal condensations. Regions of enhanced density cool faster than their surroundings, and condense further as the medium attempts to maintain pressure equilibrium. Gravity plays no role in the initial development of these condensations – only thermal pressure is effective. This process provides a natural mechanism whereby fossil H II regions can spawn filaments and clouds.

In order to study the growth of the condensations, we have modified the linearized theory of thermal instability (Field 1965) to take account of the fact that the fluctuations are departures from a nonequilibrium initial state (the isochorically cooling region). In this case, density fluctuations can grow in a time comparable to the cooling time scale whenever the slope of the cooling curve  $s \equiv d \ln \Lambda / d \ln T$  is less than 2. (By contrast, Field's analysis of development of perturbations from an initial state of heating balanced by cooling requires  $s < 1$  for instability.) Figure 1 shows that, except for narrow temperature bands near  $T = 10^4$  °K, and below about 30°K, our model region favors the growth of thermal condensations.

Condensations that result from high-temperature cooling (equation 2) and those that result from low-temperature cooling (equation 3) will grow in two different time scales, and will be characterized by different length scales. The linearized theory shows that isobaric perturbations of all wavelengths  $\lambda$  less than  $\tau_c c$  grow at nearly the same rate. Perturbations of longer wavelength grow more slowly. Physically, we can see that the condition  $\lambda < \tau_c c$  is necessary for the condensation to develop isobarically, since pressure equilibrium is re-established in the sound travel time across the condensation. This time must be small compared to the cooling time. We may apply these general considerations to formation of condensations in fossil H II regions in (a) the inner, fully ionized central region:  $x = 1$ ,  $T_0 \approx 2 \times 10^5$  °K,  $n = n_0$ ; and (b) the outer, partially ionized shell:  $x < 1$ ,  $T_0 \approx 10^4$  °K,  $n = n_0$ .

In case (a), condensations with a scale length roughly  $0.1/n_0$  pc will grow in the cooling time scale  $2000/n_0$  years. The growth of smaller condensations is suppressed by thermal conduction. The condensations can reach a maximum density enhancement of order 10, and they remain highly ionized at a temperature  $10^4$  °K. We expect these condensations to dissipate in a time scale comparable to their formation time scale. A condensation that cools to  $10^4$  °K before its surroundings will remain at that temperature while the surrounding medium also cools to  $10^4$  °K, because of the abrupt increase in cooling time scale. The condensation will then expand in order to re-establish pressure equilibrium.



Some of the filamentary structures in the Gum Nebula may be a manifestation of this process (but not the filaments associated with the Vela supernova remnant, which must be related to mechanical shock waves). If there is a fossil H II region surrounding the Tycho supernova remnant, as Kafatos and Morrison (1971) suggest, we do not expect to see filamentary structures in it, because the filaments have not had enough time to form.

On the longer time scale associated with cooling below  $10^4$  °K (case b) the gas is again unstable to growth of condensations, but the scale length is considerably larger than for case (a). The maximum scale length of a condensation is roughly  $\lambda_m \approx 0.5/n_0 x$  pc, typical of interstellar clouds. The larger clouds will be formed in the outer shell of the fossil H II region, where the initial ionized fraction  $x$  is less than one. The clouds cool to about 30°K and reach a maximum density enhancement of order 100. At that point the instability shuts off ( $s > 2$ ), and the clouds begin to dissipate again.

The formation of interstellar clouds is a natural consequence of the fossil H II regions. Clouds will be transient phenomena that are formed and then dissipated in time scales of the order of millions of years.

A number of important questions remain concerning the morphology of thermal condensations. For example, in case (b) the growth rate is approximately constant for a range of wavelengths from  $10^{-2} \lambda_m$  to  $\lambda_m$ . We are not sure to what extent a condensation that starts with a wavelength  $\lambda_m$  will fragment into subcondensations as it forms. Two-dimensional instabilities might also cause fragmentation when the condensation becomes nonlinear. We do not know to what extent condensations will tend to be one-, two-, or three-dimensional. A preferred axis provided by, say, a magnetic field or an initial temperature gradient may cause the condensations to form in sheets. These questions can be answered properly only by nonlinear hydrodynamic calculations, which have yet to be performed.

Fragmentation does not prevent the condensation process from running its course and forming clouds at 30°K. However, our discussion suggests that the structure of such clouds will be complicated.

## References

- Bergeron, J., and Souffrin, S. 1971, Astron. Astrophys., 8, 329.
- Bottcher, C., McCray, R., Jura, M., and Dalgarno, A. 1970, Astrophys. Letters, 6, 237.
- Brandt, J. C., Stecher, T. P., Crawford, D. L., and Maran, S. P. 1971, Astrophys. J. (Letters), 163, L99.
- Cesarsky, C. 1971, private communication.
- Cox, D. P., and Tucker, W. H. 1969, Astrophys. J., 157, 1157.
- Field, G. B. 1965, Astrophys. J., 142, 531.
- Field, G. B., Goldsmith, D. W., and Habing, H. 1969, Astrophys. J. (Letters), 155, L149.
- Habing, H., and Goldsmith, D. W. 1971, Astrophys. J., 166, 525.
- Hjellming, R., Gordon, C. P., and Gordon, K. J. 1969, Astron. Astrophys., 2, 202.
- Jura, M. 1971, doctoral dissertation, Harvard Univ.
- Kafatos, M. 1971, this volume.
- Kafatos, M., and Morrison, P. 1971, Astrophys. J., 168, 195
- Minkowski, R. L. 1968, in Stars and Stellar Systems, Vol. 7, eds. B. M. Middlehurst and L. H. Aller, chap. 11 (Chicago: University of Chicago Press).
- Morrison, P., and Sartori, L. 1969, Astrophys. J., 158, 541.
- Ostriker, J. P., and Gunn, J. E. 1971, Astrophys. J. (Letters), 164, L95.
- Ramaty, R., Boldt, E. A., Colgate, S. A., and Silk, J. 1971, Astrophys. J., 169, 87.
- Reichley, P. E., Downs, G. S., and Morris, G. A. 1970, Astrophys. J. (Letters), 159, L35.
- Shklovsky, I. S. 1968, Supernovae (London: Wiley and Sons).
- Silk, J., and Werner, M. W. 1969, Astrophys. J., 158, 185.
- Tucker, W. H. 1971a, Science, 172, 372.
- 1971b, Astrophys. J. (Letters), 167, L85.
- Werner, M. W., Silk, J., and Rees, M. J. 1970, Astrophys. J., 161, 965.

## DISCUSSION

*T. L. PAGE:*

On this model, the center of the Gum Nebula would not yet be cooler than the outer region?

*R. McCRAY:*

No, on the 10,000-year time scale it is still in the high-temperature cooling regime. The interior would probably still be somewhat hotter.

# THE VELOCITY AND COMPOSITION OF SUPERNOVA EJECTA

Stirling A. Colgate

*New Mexico Institute of Mining and Technology  
Socorro, New Mexico 87801*

## I. Velocity Distribution

The explosion of a supernova is generally agreed upon to take place at the end of stellar evolution. Hence all models of supernova explosions depend upon a highly condensed star. In some models, especially those depending upon thermonuclear detonation, no remnant such as a neutron star is left behind. For the case in question of the Gum Nebula, a pulsar — a presumed neutron star, is believed to be a relic of the explosive event. Regardless of the mechanism of the explosion, whether a thermonuclear detonation or a neutron star-neutrino transport model, the velocity distribution and composition of the ejected matter will be roughly the same. This is because the available energy is 1 to 4 MeV per nucleon ( $1.4$  to  $3 \times 10^9$  cm/sec) depending upon the contribution from the neutron star binding energy and, in addition, all models start from at least the density of carbon synthesis,  $\geq 10^7$  g/cm<sup>3</sup>.

If the energy were released uniformly throughout the stellar mass, if the density were uniform and gravity neglected, then a uniform spherical expansion would take place with the density independent of radius out to a surface. The non-uniform energy release, non-uniform initial density distribution and, finally, gravity all perturb this simple picture, but to a surprisingly small degree. The explosion shock wave has a strong leveling effect. The detonation in the high density central regions drives a shock wave into the lower density, lower energy regions. The expansion behind the shock reduces the energy and density at the site of origin and compresses and adds energy to the site of shock traversal. Furthermore, the specific energy behind the shock is large compared to gravitational binding and so gravity can be neglected. Therefore, to a surprising degree the expansion appears uniform.

There are two modifications to this simple picture of some importance. First, in the case of neutron star formation a fraction (25 to 50%) of the initially expanding matter falls backward and reimplodes onto the surface of the neutron star, thereby removing from observation and the universe, matter that would otherwise be offensively neutron rich. For this matter, gravity is clearly important.

The outer layers of the star are progressively lower in density, and hence for the outer 10 to 15% mass fraction, the strong shock of finite compression ratio cannot possibly compensate for the density gradient, and so a change in shock strength occurs. Again, roughly speaking, the shock wave speeds up in the outer layers in just that fashion such that the final velocity distribution is described by velocity  $\propto F^{-1/4}$ , where  $F$  is the mass fraction external to the point in question. This velocity distribution results in a fair approximation to the observed, demodulated low energy cosmic rays. The combined velocity distribution is shown in Figure 1, where the reimplosion mass fraction cut-off is shown along with the modification in shock behavior due to relativity.

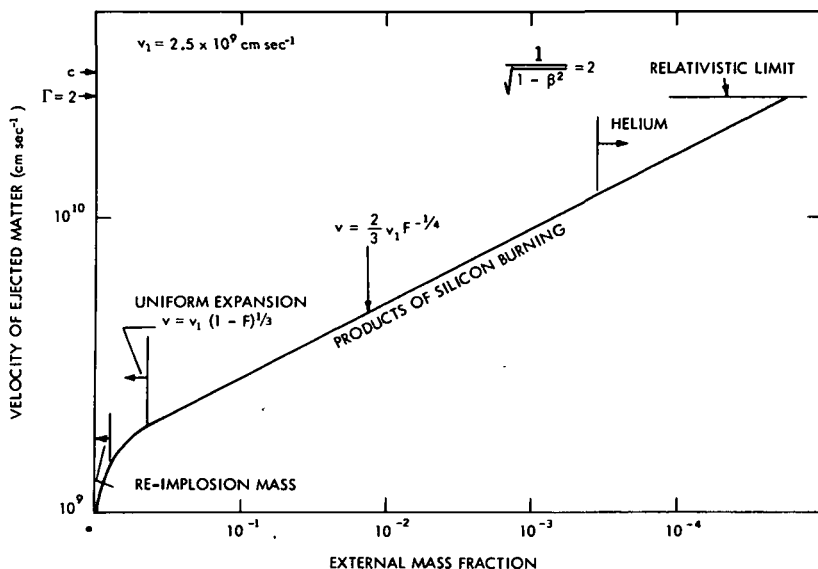


Figure 1. The mass fractions and velocities of ejecta from three regions – the inner re-implosion, the region of products of silicon burning, and the outer shell of helium.

## II. Composition

The reimploding mass fraction is presumed to be neutron rich. The bulk of the explosion is presumed to take place in matter that is predominantly either carbon, oxygen or the products of partial burning of carbon and oxygen. In either case, the product of the detonation or sudden shock heating of such material is described as quasi-equilibrium silicon burning. The

final composition is presumed to be roughly one-third iron and two-thirds silicon with many and various small fractions of elements from helium to iron.

The ejected mass of these elements is reasonably consistent with supernova models, supernova frequency, past galactic history, and iron content of the galaxy. The mass fraction of iron in the sun is about  $1.5 \times 10^{-3}$ , and the additional synthesis since the formation of the sun might be at most 25%, or a mass fraction of iron in the active galaxy of  $1.8 \times 10^{-3}$ . Roughly 50% of the iron of the galaxy is tied up in white dwarfs formed early in the history of the galaxy, and containing significantly less iron than the active mixed matter, and so for  $10^{11} M_{\odot}$  per galaxy, there must be  $10^8 M_{\odot}$  of iron formed. One half of this was presumably formed in the first 10% of the age of the galaxy so that  $5 \times 10^7 M_{\odot}$  have presumably been injected into the galaxy by supernovae during  $10^{10}$  years. The frequency of supernovae of type I is variously estimated to be one per 40 years to one per 400 years depending upon the galaxy type. For our galaxy, which is of the large active spiral type, the higher rate is presumably more nearly correct, and so  $2.5 \times 10^8$  supernovae must inject  $0.2 M_{\odot}$  of iron per event to make the observed iron content. In addition,  $0.4 M_{\odot}$  of silicon must be injected which results in an ejected mass fraction of  $0.6 M_{\odot}$ . This is a reasonable estimate for type I supernovae and is self-consistent with the generation of the optical light curve by the radioactive heat of the  $^{56}\text{Ni} \rightarrow ^{56}\text{Co} \rightarrow ^{56}\text{Fe}$  decay.  $0.2 M_{\odot}$  of  $^{56}\text{Co}$  decay is also consistent with the observed large flux of low energy positrons.

Although the ejection of a relatively large mass of silicon-burning products is self-consistent for the above reasons, it definitely is not consistent with the measurements of the composition of low energy cosmic rays. If silicon-burning products were ejected with the power law of Figure 1, they would either be observed as the dominant source of low energy cosmic rays, or have to be absorbed by a relatively large factor ( $\sim 1/100$ ) since the compositions are so radically different. The cosmic ray composition corresponds to roughly a 10 times enrichment above solar composition of all elements of  $Z \geq 6$ , relative to hydrogen. This composition could arise from the shock ejection of an outer layer of enriched helium, but not from an outer layer of carbon, oxygen, magnesium or iron. The hydrogen is produced as the surviving product of all spallation processes.

### III. Mass Fraction of Helium-Burning Shell

The termination of helium shell burning occurs because the shell is expanded and cooled by radiation stress.

Let  $\Delta m$  = mass per unit area of helium shell. Then in hydrostatic equilibrium

$$\Delta m g = P = \rho RT + \frac{aT^4}{3},$$

but

$$\Delta m = h\rho, \text{ where } h = \left( \frac{1}{\rho} \frac{d\rho}{dr} \right)^{-1}$$

The radiation flux  $\phi$  becomes

$$\phi = \frac{c}{3\kappa\rho} \frac{d}{dr} (aT^4) = \frac{4c}{3\kappa\rho} (aT^4) \frac{1}{T} \frac{dT}{dr}.$$

For a polytrope of index 3 and/or a radiative zero solution envelope,  $\rho \sim T^3$  and

$$\frac{1}{\rho} \frac{d\rho}{dr} = 3 \frac{1}{T} \frac{dT}{dr},$$

so that

$$\phi = \frac{4c(aT^4)}{9\kappa\rho h} = \frac{4c(aT^4)}{9\kappa\Delta m}.$$

Kutter, Savedoff, and Schuerman (1969) have shown that the critical luminosity  $\phi_c$  at which hydrostatic equilibrium is exceeded by the radiation stress (including  $\rho RT$ ) is 1/3 the purely radiative condition so that

$$\phi_c = \frac{gc}{3\kappa}.$$

We apply this condition at the helium-burning zone, recognizing that mass loss will proceed further out in the envelope prior to the burning layer reversal because  $\kappa$  will be larger than the Compton opacity near the surface layer. Then termination of helium shell burning should occur when

$$\phi = \phi_c, \text{ or}$$

$$\Delta m = \frac{4(aT^4)}{3g}.$$

The mass fraction of the helium layer becomes

$$F = \frac{4 \pi r^2 \Delta m}{M} = \frac{\frac{4}{3} a T^4 4 \pi r^4}{M^2 G}$$

Taking  $T = 2.4 \times 10^9$  °K at the peak of helium burning and  $r = 6.5 \times 10^8$  cm from Kutter (1971), then for  $M = M_{\odot}$ ,  $F = 3.5 \times 10^{-4}$ .

This mass fraction of the star corresponds to about  $10^{-3}$  of the ejected matter and is shown in Fig. 1 as occurring at roughly  $10^{10}$  cm sec $^{-1}$  ejection velocity or roughly 100 MeV per nucleon. The energy absorption for low energy cosmic rays due to ionization loss is roughly 100 Mev per nucleon for the path from the Vela pulsar to earth so that the composition observed at the earth at least could not be greatly enriched in silicon-burning products from the ejecta of the presumed Vela supernova.

#### IV. Conclusion

The high ejection velocity of the high atomic number elements silicon through iron is needed for producing the ionization of the Gum Nebula within the estimated time available without at the same time requiring too much mass ( $\geq 1 M_{\odot}$ ) and without at the same time producing too much of the light elements lithium, beryllium and boron by spallation. In addition, a small outer mass fraction must correspond to an enriched solar abundance with or without hydrogen. These conditions are consistent with current supernova models.

#### References

- Kutter, G. S. 1971, Ap. J., 164, 115.
- Kutter, G. S., Savedoff, M. P., and Schuerman, D. W. 1969, Astrophys. and Space Sci., 3, 182.



## DISCUSSION

*G. S. KUTTER:*

Why should the planetary nebula shell still be around when the supernova explodes?

*S. A. COLGATE:*

It might not be. The ejection velocity is of the order of 20-30 km/sec. The evolution time from the ejection of the shell to the explosion of the supernova varies from  $2 \times 10^8$  years in the Finzi and Wolf models down to  $10^2$  years in the Arnett models.

*QUESTION:*

Wouldn't the core temperature be a few times  $10^8$  °K?

*COLGATE:*

You are thinking of a core that is entirely supported by degeneracy pressure. That assumes that the mass is cut off at about 1.4 solar masses, using the Finzi and Wolf model. Arnett has discussed models up to 2.5 solar masses, that arrive in this state with a helium-burning shell — of course, the central temperature has to be higher in order to support the pressure. In other words, the star evolves along a high temperature track.

## COSMIC RAYS FROM SUPERNOVAE AND COMMENTS ON THE VELA X PRE-SUPERNOVA

A. G. W. Cameron  
*Belfer Graduate School of Science*  
*Yeshiva University*  
*New York, New York 10033*

The discussion of the Gum Nebula which has taken place at this conference has relied to a great extent upon postulates about the character of supernova explosions and of the ionizing particles which can be ejected from them. I will first discuss the average properties of supernova explosions which were found in a recent study of chemical evolution of the galaxy, carried out by J. W. Truran and myself, and then make some remarks on the Vela X supernova.

In this study we have been playing a kind of game in which we try to account for the history of the production of elements in the galaxy by making a fairly large number of assumptions about the end points of stellar evolution and of the general evolution of the galaxy. We try to fit a wide range of observable quantities involving the relative abundances of the different products of nucleosynthesis observed in the solar system, and various galactic quantities such as the current rate of supernova production and the present gas content of the galaxy. The game consists of making these assumptions about the production of different products of nucleosynthesis at the end of stellar evolution, and utilizing them in a computer program in which the gas content of the galaxy is gradually turned into stars, being continually enriched in the products of nucleosynthesis as the stars which are formed come to the ends of their evolutionary lifetimes. We assume that the gas content of the galaxy decreases exponentially with time, to become only 5 percent of the galactic mass at the present age of the galaxy, which we find to be 12 billion years. Except for the first generation of stars, which we take to be all massive, we assume the stellar birth function which was first put together by Salpeter and by Limber. The computer code keeps track of the numbers of stars which are formed at different galactic evolutionary times, and mixes back the nucleosynthesis products from these stars into the interstellar medium when the stars come to the end of their evolutionary lifetimes. The mixing is assumed to take place instantaneously in the interstellar medium. The galaxy is taken to be structureless and featureless, since we are interested in the effects which occur when mass is cycled repeatedly between stars and the interstellar medium.

In addition to obtaining the right relative proportions of the products of nucleosynthesis at the time of formation of the solar system, which we find to be 7.4 billion years, we also wish to obtain consistency among the ratios of the radioactivities which are produced during nucleosynthesis, and which were incorporated into the solar system at the time of its birth. These radioactivities include thorium 232, uranium 235 and 238, and the extinct radioactivities plutonium 244 and iodine 129. We also wish to obtain a supernova rate in the galaxy at the present time of about one event per 25 years, to be consistent with the rate found by Tammann in a study of spiral galaxies similar to our own.

Time does not permit a lengthy exposition of the features of the model of galactic nucleosynthesis which we have studied. The aspects of this study which are most relevant to the present discussion concern the parameters which we found necessary to assign to supernova explosions in order to account for the abundances of the different products of nucleosynthesis in the solar system.

Figure 1 shows the assumptions which we had to make about the end points of stellar evolution in order to obtain a consistent picture of the chemical evolution of the galaxy. I shall discuss only the aspects of the supernova explosions shown in this figure. However, it should first be remarked that in the smaller mass range, where white dwarfs are found, Paczynski has found that the mass loss rates in the formation of planetary nebulae become sufficiently great so that the Chandrasekhar limit on the degenerate core is not reached until a main sequence mass of about 3.5 or 4 solar masses. Beyond this point, the degenerate core in the late state of stellar evolution would exceed the Chandrasekhar limit, and therefore something more catastrophic than the formation of a white dwarf remnant should occur.

An estimate was made by Gunn and Ostriker of the mass range of the stars needed to form the observed number of pulsars. They found that this mass range should lie about from 3.5 to 8 solar masses, which is consistent with our assumed range of 4 to 8 solar masses. Barkat has recently shown, as mentioned by Colgate, that there is a range of mass, from 4 to 8 solar masses, where the cores of stars in advanced stages of evolution evolve in essentially the same way.

These independent approaches all suggest that supernova explosions are to be associated with the mass range of about 4 to 8 solar masses.

The lower limit of 4 solar masses cannot be changed very much without changing significantly the number of supernovae which should currently be observed in the galaxy. The lower limit which we have chosen gives one

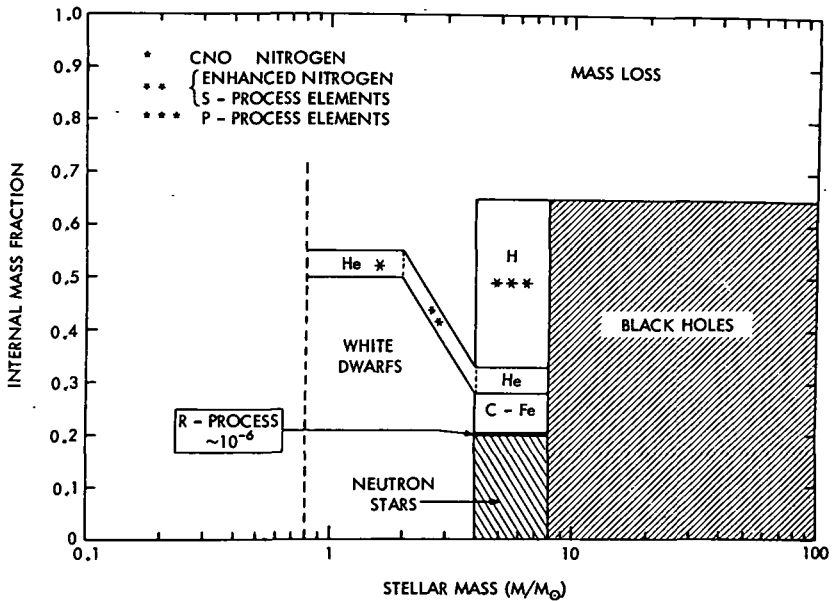


Figure 1. The adopted compositional structures for stars in their final stages of evolution. The fractional stellar masses, both in the appropriate remnant and in various nuclear burning zones, are indicated as a function of main sequence mass.

supernova per 25 years, although this rate is specifically linked to the assumptions about the stellar birth function, which falls off rapidly toward higher masses, and to the assumed rate of depletion of the interstellar gas in the formation of stars. However, even if these quantities were to be significantly modified, the lower limit of 4 solar masses could not be changed very much. On the other hand, the upper limit of the assumed supernova range is very much more uncertain.

Note that in Fig. 1 the combined masses of the assumed neutron star remnant and the layer in which the range of elements from carbon to iron is formed by explosive nucleosynthesis account for 28 percent of the stellar mass. This is about the fraction of the star which can be expected to lie in the stellar core following helium burning. We find that we require 8 percent of the stellar mass to give the products of explosive nucleosynthesis which lie in the range carbon-to-iron. Consequently, it is strongly indicated on the basis of our overall mass balance that a reimplosion must occur during the supernova explosion in order to form the neutron star. If the entire core were to be exploded, giving the products of explosive nucleosynthesis, then we would have to restrict the range of stellar masses involved in supernova explosions to be a very narrow strip in this diagram, and that would seem to be physically unreasonable.

A fantastically small amount of material must be ejected in the average event to give the r-process elements. Only  $10^{-6}$  of the stellar mass, or of the order of  $5 \times 10^{-6}$  solar masses can be ejected in the form of heavy neutron-rich elements. This is much less than the amount of mass which is ejected in the axial jets in the model of two-dimensional supernova explosions investigated by LeBlanc and Wilson. This raises some interesting questions about the r-process, but these lie beyond the scope of this talk.

Beyond the region of explosive nucleosynthesis, there is a helium layer, assumed to be 5 percent of the mass, and then some sort of outer layer of hydrogen which has never been subjected to nuclear burning. We have assumed that the star has lost mass in the red giant phase of its evolution, amounting to of order 35 percent of the main sequence mass. However, in the remaining hydrogen outer layer of the star, the supernova shock wave will be required to convert heavy elements into the p-process products, in which protons are added on to the heavy elements which have been formed by the s- and r-processes in previous generations of stars and stored in this outer hydrogen envelope since the time of formation of the star undergoing supernova explosion.

We have found that mass balance in the chemical evolution of the galaxy requires the processing of half the original content of the heavy elements in the outer hydrogen layer shown in Fig. 1. In order to produce the p-process elements, the supernova shock wave must heat the outer hydrogen layer to around  $3 \times 10^9$  °K in the region near the base of the hydrogen layer where the density will be of the general order of 1 gram per cubic centimeter or perhaps higher. Since much of the mass in the outer hydrogen layer will certainly be at much lower densities than this, it seems unlikely that the total content of heavy elements in this hydrogen layer can be converted to p-process products, and hence we feel that our assumed processing of half of the mass of these elements into p-process products is quite reasonable. In any case, there is a minimum requirement that about half to one solar mass of material should take place in the p-process in the average supernova explosion.

The type of stellar explosive event which emerges from this picture is obviously the type II supernova, in which hydrogen lines are observed in the spectrum. This approach, based upon accounting for the processes of nucleosynthesis, has not produced an explosive event which can easily be identified with the type I supernova.

Mrs. Charlotte Gordon, in an extensive study soon to be published, has interpreted the spectra of type I supernovae to represent the expansion of a supernova envelope in which hydrogen is quantitatively missing. She has

identified a large number of emission features in the spectrum as involving forbidden coronal emission lines of a variety of elements, initially formed at kinetic temperatures near  $10^6$  °K in the inner layer of the expanding supernova shell. Later on, less highly-ionized elements produce lines when the temperature falls to around  $10^5$  °K.

Evidently our nucleosynthesis-based approach has missed the type of supernova explosion which would be represented by the type I spectrum. Since type I supernovae often occur in elliptical galaxies where there is currently very little formation of stars, it appears that such supernovae should arise from stars with masses not very different from that of the sun. J. W. Truran and I therefore make a suggestion for the origin of type I supernovae which may be consistent with the above constraints. If the Vela X supernova remnant is to be identified with the nearby young association of stars, then it is evident that it cannot have produced a type I supernova explosion, and hence our suggestions for the type I explosion will be given only briefly.

Consider a pair of binary stars with masses initially approximately equal to that of the sun. One of them, slightly more massive than the other, will evolve off the main sequence first, and will then transfer most of its mass to the other, leaving behind a helium white dwarf which is not very massive. When the second star evolves, at a later date, there will be a reverse transfer of mass. Presumably this will result in a series of nova explosions occurring as mass addition occurs on the white dwarf star, accompanied by a great deal of hydrogen burning near the surface, which gradually builds up a helium white dwarf toward the Chandrasekhar limit. When this occurs, ignition of helium thermonuclear reactions will occur, leading to a thermonuclear explosion which will blow the star apart. One of my students, Mr. T. Mazurek, is currently carrying out supernova hydrodynamic calculations to investigate this process. This type of explosion, in which the thermonuclear ignition occurs at densities near  $10^{10}$  grams per cubic centimeter, should result in a reimplosion of the interior to form a neutron star, and hence a pulsar. It will also contribute somewhat to the abundance of the products of explosive nucleosynthesis in the galaxy.

Table 1 shows the mass fractions which are involved in our adjusted assumptions about the end points of stellar evolution.

Of particular concern here is that in a supernova range, 4 to 8 solar masses, only 8 percent of the region from carbon-to-iron is produced in the average event. The part of this which results in the formation of iron, which is expelled as nickel 56, is only 5 percent of this, which implies the ejection of only about 0.02 of solar masses of nickel 56 per average event. If much more than this is to be produced in the supernova which created the Vela X pulsar,

Table 1  
Compositional Structure at End of Life  
(by mass fraction)

Mass Range	Description	Conventional Model	Consistent Model	
			First Generation	Subsequent Generations
$M > 8 M_{\odot}$	{ Black Hole Remnant Mass Loss	0.65 0.35	0.95 0.05	0.65 0.35
$4 \leq M \leq 8 M_{\odot}$	{ Neutron Star Remnant r-Process Synthesis Carbon-to-Iron Synthesis Helium Shell Hydrogen Envelope* Mass Loss	0.20 $1.3 \times 10^{-6}$ 0.075 0.05 0.325 0.35	0.20 $1.4 \times 10^{-6}$ 0.08 0.05 0.32 0.35	0.20 $1.4 \times 10^{-6}$ 0.08 0.05 0.32 0.35
$M < 4 M_{\odot}$	{ White Dwarf Remnant Helium Shell** Mass Loss	0.50 (1.12 $M_{\odot}$ maximum) 0.05 (Remainder)		0.50 (1.12 $M_{\odot}$ maximum) 0.05 (Remainder)

\*Site of p-Process Synthesis: 50% of the primordial r-process and s-process nuclei are converted to p-process nuclei.

\*\*Site of s-Process and Nitrogen Synthesis:

- (a) all initial CNO-nuclei converted to nitrogen in masses  $1 \leq M \leq 2 M_{\odot}$ ;
- (b) for stars of mass  $2 \leq M \leq 4 M_{\odot}$ , 6.3% of the mass if converted to nitrogen and 0.375% of the C-Fe nuclei are s-processed (4.7% and 0.375%, respectively, for the Conventional Model).

then it would be necessary to conclude that the Vela supernova differed radically from the average event, ejecting an order of magnitude or more of nickel 56 than the average event.

Figure 2 shows the galactic history of nucleosynthesis which results from our assumptions. The figure shows the abundances, relative to those in the solar system, of various processes of nucleosynthesis in the interstellar medium as a function of galactic age. The various lines should go through unity at some galactic age which can be identified with the formation of the solar system. We find this to occur at 7.4 billion years, at which time we also have consistency from the cosmochronology. This gives the present age of the galaxy at 12 billion years. Note that the most abundant of the heavy elements are only moderately increased in abundance between the time of the formation of the solar system and the present epoch.

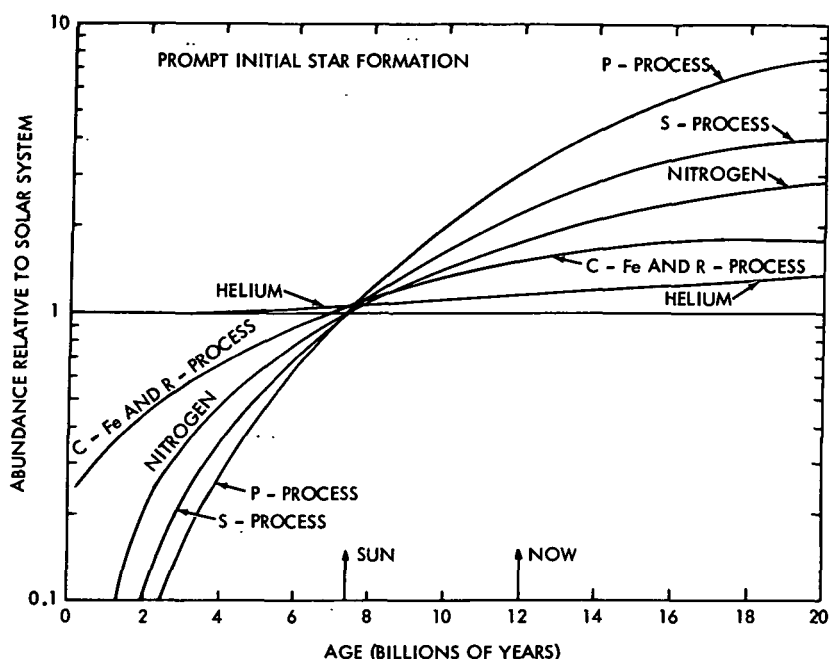


Figure 2. The abundances of nuclei formed by the various mechanisms of nucleosynthesis, relative to their solar system values, are shown as a function of galactic age for the adopted galactic model.

Thus the first major point I would like to make is that if the Vela supernova event resembled the average properties of the supernovae of type II which we find in this galactic history, then it could not have produced as much nickel 56 as Colgate would like to have in his theory of the supernova light curve, nor could it have produced the fluxes of heavily ionizing particles, consisting of ions such as nickel 56, which would be required in the theory of Colgate et al. to produce the ionization in the Gum Nebula.

The second major point that I would like to make is that we can use our model of galactic history to set limits on the amount of cosmic ray production by the average supernova explosion. These limits arise from the calculations of the production of lithium, beryllium, and boron by cosmic ray bombardment of the carbon, nitrogen, oxygen, and neon in the interstellar medium throughout past galactic history.

For this purpose we have taken the spallation production cross sections of the lithium, beryllium, and boron which have been estimated on the basis of experimental data by Henri Mitler at the Smithsonian Astrophysical



Observatory. We have scaled the present interstellar cosmic ray flux back in time in proportion to the rate of supernova activity predicted in the model to exist in the galaxy as a function of past time. We have also adopted Mitler's values for the low-energy cosmic ray flux, demodulated from solar system values to the interstellar medium. We believe that at low energies his demodulation factor may have been somewhat too large, and that it may therefore predict too much production of the beryllium and boron. This demodulated cosmic ray spectrum is shown in Fig. 3. We have used the dashed line shown in this figure for the demodulated flux.

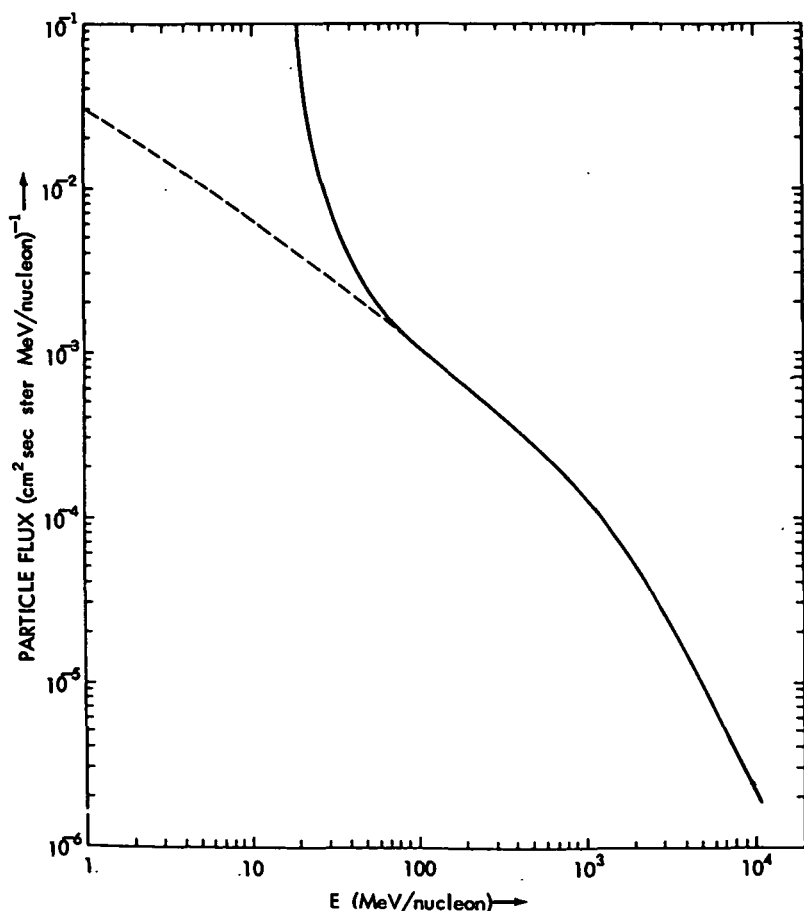


Figure 3. The observed  $p + \alpha$  cosmic ray flux, demodulated with  $\eta = 0.5$  GV and  $R_0 = 0.4$  GV. The dashed line is an approximate extrapolation of the high-energy part of the curve, tangent at  $E = 100$  MeV/nucleon.

Figure 4 shows the calculated supernova activity rate throughout galactic history. The present rate is about one per 25 years. The rate in the early history of the galaxy is an order of magnitude greater than that. It is evident in Fig. 2 that the CNO-Ne abundances rise fairly rapidly in early galactic history, so that the main production of the lithium, beryllium, and boron in the interstellar medium will be concentrated in the early history of the galaxy.

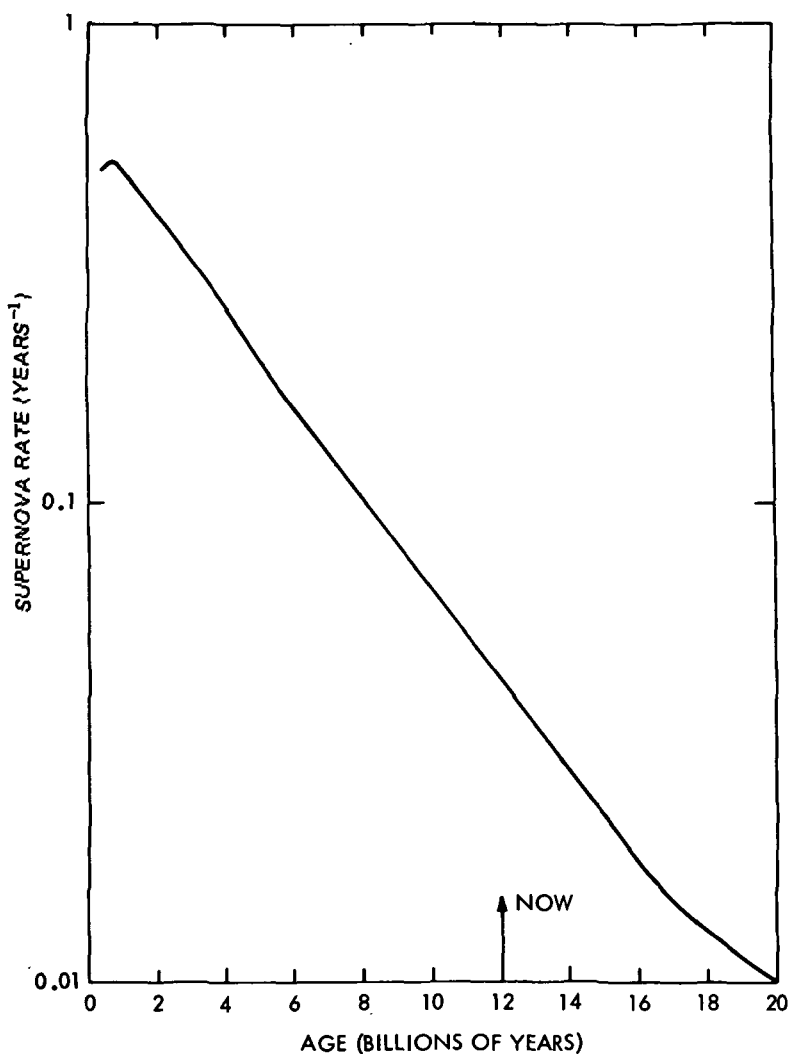


Figure 4. The rate of occurrence of supernovae (events per year) in the galaxy is plotted as a function of galactic age.

Figure 5 shows our calculated abundances of the two isotopes of lithium, and of beryllium plus boron in the interstellar medium as a function of galactic age. In the case of the beryllium and boron, there are two assumptions that have been made, in one of which it is assumed that the beryllium and boron have been destroyed in the mass which is ejected from stars by stellar winds, and the alternative assumption is that the beryllium and boron survived in the lower temperature regions of the mass which is ejected from the stars by stellar winds. It may be seen that there is not a great deal of difference in the results of these two assumptions.

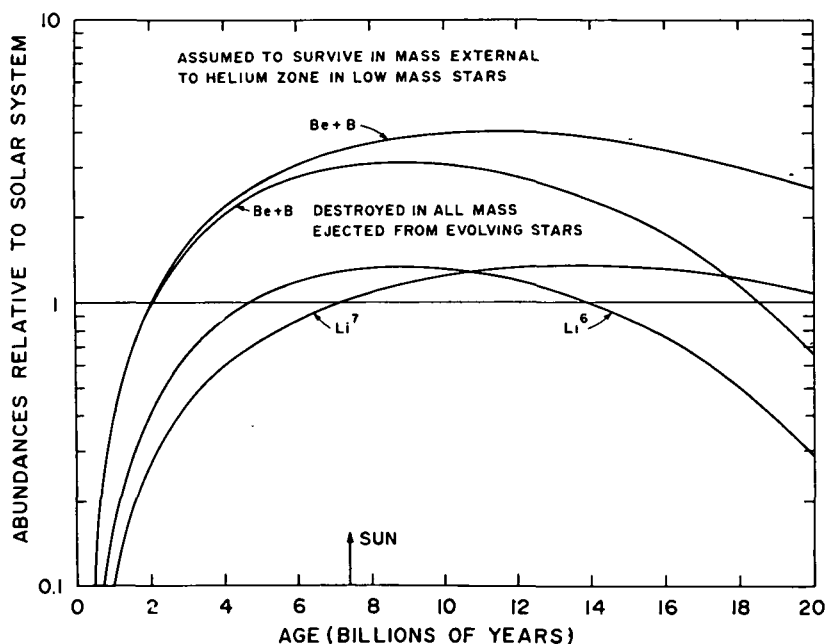


Figure 5. The abundances of  $\text{Li}^6$ ,  $\text{Li}^7$  and the isotopes of beryllium and boron in the interstellar medium, relative to solar system matter, are plotted as a function of galactic age. The two curves for  $\text{Be} + \text{B}$  correspond to limiting assumptions concerning their destruction in stellar envelopes.

The abundance of lithium 6 agrees reasonably well with the amount observed in the solar system. Beryllium and boron are too high by about a factor of 3. We believe that the discrepancy corresponds in part to the assumed demodulation of the cosmic ray spectrum, and in part to errors in the spallation production cross sections.

The cosmic ray spallation processes do not make enough lithium 7. The lithium 7 shown in Fig. 5 is made partly by cosmic ray spallation, and partly by another mechanism involving production in stellar interiors which has been suggested in a recent paper by W. A. Fowler and myself.

The basic point that I wish to make here is that the nucleosynthesis of the lithium, beryllium, and boron can be quite adequately explained by cosmic ray bombardment of the interstellar medium throughout past galactic history. The results are in quantitative agreement with the amounts found in solar system materials, subject to the uncertainties in cosmic ray fluxes and production cross sections which I have already discussed.

The reason for emphasizing this point is that one may suggest that ionizing particles ejected from the Vela supernova event may be responsible for the ionization produced in the Gum Nebula. In our picture we assume that the supernova explosions are responsible for the production of the present fluxes of cosmic rays in interstellar space. The average production rate of cosmic ray particles from supernova remnants can be estimated if one assumes an average age for the cosmic rays present in the galaxy. Such a production rate for the average supernova event seems inadequate to explain the ionization produced in the Gum Nebula. If one wishes to assume an additional flux of ionizing particles which would be needed to account for the ionization in the Gum Nebula, then these particles would have to be concentrated in the lower energy region, of less than about 10 MeV per nucleon, in order to avoid an excessive production of lithium, beryllium, and boron in the interstellar medium, which is already accounted for quantitatively by the demodulated flux shown in Fig. 3, or by a somewhat smaller flux at lower energies.

The net conclusions from this approach to the average supernova event are therefore that a medium energy flux of energetic protons and alpha particles seems unlikely to account for the ionization in the Gum Nebula. Also, it seems unlikely that enough heavier ions, such as nickel 56 and its decay products, can be ejected from the supernova event to account for the ionization of the H II clouds in the Gum Nebula region.

This seems to leave us with the requirement that about  $10^{52}$  erg of ultraviolet radiation should be produced in order to account for the ionization in the Gum Nebula. The source of this ultraviolet radiation may very well be the pulsar formed in the supernova explosion, where the initial rotational energy may easily be of the order of magnitude of  $10^{52}$  erg. The bulk of this energy is likely to be lost fairly early in the lifetime of the Vela X pulsar, in the first few years. Much of the energy may be emitted in X-rays from the pulsar region, which would be scattered from the expanding envelope

once the density of the expanding nebulosity has become sufficiently low. In addition, if the slowing of the pulsar rotation occurs as a result of magnetic dipole radiation, which accelerates particles in the circumstellar region, then a great deal of the ultraviolet emission may be produced by the accelerated electrons releasing synchrotron radiation when they spiral in the surrounding system of magnetic fields. The detailed investigation of such ultraviolet emission mechanisms remains a task for the future.

### References

- Barkat, Z. 1971, Astrophys. J. 163, 433.
- Cameron, A. G. W., and Fowler, W. A. 1971, Astrophys. J., 164, 111.
- Gunn, J. E., and Ostriker, J. P. 1970, Astrophys. J., 160, 979.
- LeBlanc, J. M., and Wilson, J. R. 1970, Astrophys. J., 161, 541.
- Limber, D. N. 1960, Astrophys. J., 131, 168.
- Mitler, H. E. 1967, in High Energy Reactions in Astrophysics, ed. B. S. P. Shen, W. A. Benjamin, Inc., New York.
- Paczynski, B. 1970, Acta Astr., 20, 47.
- Reeves, H., Fowler, W. A., and Hoyle, F. 1969, Nature, 226, 727.
- Salpeter, E. E. 1959, Astrophys. J., 129, 243.
- Tammann, G. A. 1970, Astron. Astrophys., 8, 458.
- Truran, J. W., and Cameron, A. G. W. 1971, Astrophys. Space Sci., 14, 179.

## DISCUSSION

*A. B. UNDERHILL:*

Why is the rate of supernova activity much greater in the early history of the universe?

*A. G. W. CAMERON:*

The gas content of the galaxy is assumed to decrease exponentially with time in our galactic history models. Since we assume that most of the supernovae arise from the mass range 4 to 8 solar masses, in which the evolution time is short, then the supernova rate becomes fairly accurately proportional to the star formation rate throughout past galactic history.

*A. BUNNER:*

Why does the abundance of lithium, beryllium, and boron decrease in the interstellar medium late in galactic history?

*CAMERON:*

The interstellar medium is enriched in the products of cosmic ray bombardment continually in time. However, since cosmic ray fluxes go down later in the history of the galaxy, the production rate becomes fairly small late in galactic history. The gas content of the galaxy also becomes quite small. Many stars were formed early in galactic history with a low content of lithium, beryllium, and boron, and this content may have been substantially destroyed in the stellar envelopes of these stars. When these stars reach the red giant phase, then mass ejection occurs by stellar winds, diluting the interstellar medium by gas with a lower content of the lithium, beryllium, and boron. This will cause an eventual downturn in the abundances of these elements.

*F. W. STECKER:*

Do you assume that the helium was made primordially or as a result of stellar evolution?

*CAMERON:*

We assume that most of the helium was made by cosmological nucleosynthesis. Our specific assumption is that the initial content of helium in the galaxy was 23 percent, and by the time of formation of the solar system, only about another 2 percent of the mass had been converted to helium in the interstellar medium.

*M. SHAPIRO:*

My recollection is that when Reeves et al. tried to make light elements by cosmic ray bombardment of the interstellar medium, they did not succeed too well. What is it that you did that changes this picture?

*CAMERON:*

Reeves, Fowler and Hoyle did succeed in principle in forming the lithium, beryllium, and boron in the interstellar medium by cosmic ray bombardment. We make somewhat more than their estimate because we allow for the higher rate of supernova activity and cosmic ray fluxes in past galactic history. However, we have not produced any qualitative change in the picture.

*QUESTION:*

Is this a promising method of getting the deuterium as well?

*CAMERON:*

No.

*S. A. COLGATE:*

If you integrate under the curve for the supernova rate times the time, you would find that the total number of supernovae is no more than two or three times the number you would get if you take the current rate and multiply it by the total age of the galaxy. Therefore, the total amount of iron produced in the supernovae should be no more than three times the current rate multiplied by the age of the galaxy. If you assume for the iron that 0.25 solar masses are produced in a supernova every 50 years, then this still gives you less mass of iron than is needed if you take something like 5 times the amount of iron that you would get in the solar composition, multiplying it by the mass of the galaxy. Can you comment on the discrepancy between your estimate of the needed production rate and mine?

*CAMERON:*

In our model, the average composition of iron in the total mass of the galaxy is somewhat less than that in the sun, so that we need only produce about  $5 \times 10^7$  solar masses of iron, contrasted to your estimate of about  $2 \times 10^8$ , based upon the solar composition. We find that about 2 percent of a solar mass of iron is formed in the average supernova explosion. We have one supernova explosion every 25 years. In your estimates previously you have generally taken one supernova explosion every century, so that if that rate

were to be correct, it would be necessary to produce 8 percent of a solar mass of iron per event. The remaining discrepancy between 0.08 solar masses and your estimate of 0.25 solar masses appears to lie in the fact that our detailed model shows that a total production of iron of only  $5 \times 10^7$  solar masses is needed, which is less than the amount you have estimated.

*F. W. STECKER:*

To what extent does your success in producing the lithium, beryllium, and boron in the galaxy depend upon fitting parameters, and how strongly do the lithium, beryllium, and boron abundances imply a high rate of supernova activity in the early history of the galaxy?

*CAMERON:*

We did not do any fitting in the calculations of the production of lithium, beryllium, and boron. All of the fitting which we did in producing the model had to do with the other main processes of nucleosynthesis, and we used the resulting model in a purely predictive sense to calculate the production of the lithium, beryllium, and boron. If anything, we make too much of these elements, but I am not concerned about this due to the various uncertainties which I have described. I do not think that this quantitative success demonstrated the validity of the precise curve which we have shown for the supernova activity in the early history of the galaxy, but I do believe it demonstrates the need for a higher average supernova rate throughout past galactic history than at the present time.

*J. R. GOTT:*

In connection with your diagram of the composition of the end points of stellar evolution, I have a concern about the runaway stars observed by Blaauw. There are about 20 of them that range in spectral class all the way out to about O7. This would seem to indicate that the companion stars which underwent a supernova explosion would have to be still more massive, and would have to lose the bulk of their mass in the explosion.

*CAMERON:*

Our assumed supernova range of 4 to 8 masses is not inconsistent with the existence of a lower mass stellar companion with a spectral class of early B or late O. In the explosion itself, we assume that 20 percent of the main sequence mass will remain behind as a remnant, and 45 percent of the main sequence mass will be ejected in the explosion. This does not seem to be inconsistent with the dynamics required to form runaway stars.



# COSMIC-RAY EFFECTS IN THE GUM NEBULA

R. Ramaty and E. A. Boldt

*Laboratory for High Energy Astrophysics  
Goddard Space Flight Center  
Greenbelt, Maryland 20771*

## Abstract

We investigate the effects of low energy heavy nuclei from the supernova explosion on nearby interstellar space. In addition to the ionization and heating of the Gum Nebula, these particles may produce detectable fluxes of X-rays and gamma rays, both as continuum radiation and line emission.

## Introduction

The possibility that the ionization of the Gum Nebula may have been produced by energetic charged particles from the supernova Vela X has been suggested by Ramaty *et al.* (1971). The principal features of this model are the existence of a prolonged source of ionization and heating and the possibility of direct detection of hard photon emissions from contemporary fluxes of energetic particles in the nebula. In the present paper, we shall summarize the model and discuss its main features. We shall also present an estimate of gamma-ray line emission from the interaction of energetic nuclei with the ambient gas and we shall discuss some additional ideas regarding the maintenance of a possible high temperature in the filaments of the nebula.

## Particle Propagation and Energy Deposition

A necessary requirement of a cosmic-ray model of the Gum Nebula is that in a time less than or equal to the age of the supernova remnant the particles should be capable of both reaching the outer edges of the nebula and depositing a significant fraction of their energy as ionization loss to the ambient gas.

A lower limit on the velocity  $c\beta$  of the ionizing nuclei can be obtained by assuming rectilinear propagation of particles in the nebula; i.e.:

$$\beta > L/ct \quad (1)$$

where  $L$  and  $t$  are the nebular radius and age respectively. If we adopt an age of about  $10^4$  years, as deduced from the period and rate of change of

period of PSR 0833-45 (Reichley, Downs and Morris 1970), and a nebular radius of about 360 pc, as obtained (Alexander et al. 1971) from  $\text{La}$  absorption data and a local hydrogen density of  $0.24 \text{ cm}^{-3}$ , the lower limit on  $\beta$  is about 0.1 corresponding to an energy per nucleon  $e \geq 5 \text{ MeV/nucleon}$ . It should be remembered that this lower limit is subject to considerable uncertainties in both  $t$  and  $L$ . In particular, if the age is larger than  $10^4$  years (Shklovsky 1970), the Gum Nebula may have been produced by even lower energy particles.

Cosmic-ray particles in general do not propagate along rectilinear paths but follow magnetic field lines and are scattered by irregularities in the field. The mean distance traversed in such diffusive motion may be approximated by

$$L \simeq (2 \lambda c \beta t)^{1/2} \quad (2)$$

where  $\lambda$  is the diffusion mean free path. For  $L \simeq 360 \text{ pc}$  and  $t \simeq 10^4$  years,  $\lambda \beta \simeq 20 \text{ pc}$ . If  $\beta = 0.15$  ( $e = 10 \text{ MeV/nucleon}$ ),  $\lambda \simeq 130 \text{ pc}$ . This value is quite large but not inconsistent with recent ideas on cosmic ray propagation (Ramaty and Lingenfelter 1971). In particular, if cosmic rays propagate by compound diffusion (Lingenfelter, Ramaty and Fisk 1971) or if cosmic rays are confined to the galactic disk by reflecting boundaries, both the low anisotropy and abundances of fragmentation products of galactic cosmic rays are not inconsistent with the long diffusion mean free path required for the ionization of the Gum Nebula. Finally, a relatively scatter-free motion in the nebula is also supported by the low values of both the ambient gas density and magnetic field in this region of interstellar space.

The ionization loss rate and the time for the deposition of half the energy of a nonrelativistic particle of mass number  $A$  and nuclear charge  $Ze$  in neutral hydrogen of density  $n_H$  are given by

$$\frac{de}{dt} \simeq 1.46 \times 10^{-12} Z_{\text{eff}}^2 / A n_H e^{-0.3} \text{ MeV/nucleon. sec}^{-1} \quad (3)$$

and

$$t_{1/2} \simeq 10^4 e^{1.3} A / (Z_{\text{eff}}^2 n_H) \text{ years} \quad (4)$$

where  $e$  and  $n_H$  are in  $\text{MeV/nucleon}$  and  $\text{cm}^{-3}$ , respectively. As a result of electron capture during the slowing down process the effective charge  $Z_{\text{eff}}$  becomes smaller than the nuclear charge  $Z$ .  $Z_{\text{eff}}/Z$  may be approximated by (Pierce and Blann 1968)

$$Z_{\text{eff}}/Z \simeq 1 - \exp(-130 \beta / Z^{2/3}) \quad (5)$$

Since even for  $\text{Fe}^{56}$  at 10 MeV/nucleon  $Z_{\text{eff}}/Z \simeq 0.9$ , we shall use  $Z$  instead of  $Z_{\text{eff}}$  in the evaluation of equations (3) and (4).

In Table 1,  $n_{\text{H}} t_{1/2}$  is given for various 10 MeV/nucleon particles. As can be seen, in  $10^4$  years these particles will deposit a major fraction of their energy only if  $n_{\text{H}} \gg 1 \text{ cm}^{-3}$ . The average electron density  $\langle n_e \rangle$  in the Gum Nebula is only  $0.16 \text{ cm}^{-3}$ , but the density in filaments is much higher,  $n_e \simeq X \langle n_e \rangle$  where  $X \simeq 65$  is the clumping factor in the nebula (Brandt *et al.*, 1971). A possible model, therefore, is one in which initially the nebular region consisted of neutral clouds or clumps with hydrogen densities approximately equal to the presently observed electron densities in filaments. The particles ejected from the supernova propagate in a scatter-free manner in the intercloud medium and subsequently penetrate clouds and lose their energy in a time scale shorter than the trapping time in the cloud. A possible trapping mechanism, based on wave-particle interactions, has been discussed by Ramaty *et al.* (1971).

If the initial hydrogen density in clouds is equal to the present electron density of about  $10 \text{ cm}^{-3}$ , it is very unlikely that low energy protons have ionized the Gum Nebula, since, as can be seen from Table 1, it would take about  $2 \times 10^4$  years for these particles to lose half their energy. On the other hand, if the ionization were produced by heavy nuclei such as Si and Fe, these particles would deposit sizable fractions of their energy in clouds on a time scale of 2000 to 3000 years leaving about 7000 to 8000 years for scatter-free propagation in the intercloud medium. This is consistent with the estimates of the transit times to the edges of the nebula given above.

Table 1

	$n_{\text{H}} t_{1/2} (\text{cm}^{-3} \text{ years})$
$\text{H}^1$	200000
$\text{C}^{12}$	67000
$\text{Si}^{28}$	29000
$\text{Fe}^{56}$	16000

A specific consequence of this model is that the degree of ionization of the intercloud medium is much smaller than that of the filaments. This is not the case for models in which the ionization is produced by photons since these lead to the complete ionization of both the clouds and intercloud medium out to an appropriate Strömgren radius.

### Mass and Energy Requirements of Supernova Ejecta

A fast particle of energy  $\geq 0.1$  MeV/nucleon expends some 36 eV to produce an ion pair (Bethe and Ashkin 1953). Therefore, if the nebula contains  $N_e \simeq 2 \times 10^{62}$  electrons, as suggested by Brandt et al. (1971), the particles ejected by the supernova must lose at least  $1.2 \times 10^{52}$  ergs. For the present value of  $N_e$ , this is a lower limit, since a fraction of the energetic particles may slow down in an ionized medium, thereby converting their energy directly to heat, and the total number of electrons produced could be larger than  $N_e$  since some recombination in the filaments may have already taken place.

The velocity distribution of the ejected material from a supernova explosion may be approximated by (Colgate and McKee 1969)

$$v = \begin{cases} v_1 (1 - F)^{1/3}; & 0.75 \geq F \geq F_0 = 3/7 \\ 0.67 v_1 F^{-1/4}; & F < F_0 \end{cases} \quad (6)$$

where  $F$  is the external mass fraction. The corresponding number spectrum of nuclei of mass number  $A$  in the nonrelativistic region is given by

$$N(e) = \frac{6}{7} \frac{M_{ej}(A)}{A m_p} \frac{1}{e} \begin{cases} (e/e_0)^{3/2}; & e \leq e_0 \\ (e_0/e)^2; & e > e_0 \end{cases} \quad (7)$$

Upon integration, the total kinetic energy  $W$  of the ejected material is

$$W = \frac{6}{5} \frac{M_{ej}}{m_p} e_0 \quad (8)$$

where  $m_p$  is the proton mass.

Since  $W \geq 1.2 \times 10^{52}$  ergs, the ejected mass in units of a solar mass and the characteristic ejection energy in MeV/nucleon must obey

$$\frac{M_{ej}}{M_\odot} e_0 \gtrsim 5 \text{ MeV/nucleon} \quad (9)$$

As discussed above,  $e_0$  cannot be smaller than about 5 MeV/nucleon, since otherwise the particles will not reach the edge of the nebula in the available time of about  $10^4$  years. On the other hand,  $e_0$  cannot be much larger than

about 20 MeV/nucleon, since, as can be seen from Table 1 and equation (4), the ejected nuclei, even if they are all  $\text{Fe}^{56}$ , will not have enough time to deposit their energy in clouds. For the range  $5 < e_0 < 20$  MeV/nucleon, the lower limits on the ejected mass range from  $0.25 M_\odot$  to  $1 M_\odot$ . For the efficient ionization of the nebula, the ejected material must consist of nuclei heavier than at least  $\text{C}^{12}$ .

We now proceed to examine the observational consequences of the model.

### Hard Photon Emissions by Energetic Particles in the Nebula

X-ray emission by bremsstrahlung is a necessary consequence of the interaction of fast nuclei with interstellar gas (Boldt and Serlemitsos 1969). The photon energy spectrum that would result from the particle distribution given in equation (7) is essentially flat with an end point  $h\nu_0$  at  $(m_e/m_p) e_0$ , where  $m_e$  is the electron mass.

Let  $M/(Am_p)$  nuclei of mass number  $A$  and atomic number  $Z$  be currently trapped in clouds of density  $n_e$ . The average bremsstrahlung volume emissivity in the Gum Nebula (independent of the ionization state of the gas) is given by

$$\eta = \frac{2a}{\pi} Z^2 \sigma_0 m_e c^2 \frac{n_e}{V} \frac{M}{Am_p} \langle c\beta \rangle \quad (10)$$

where  $\sigma_0 = 6.7 \times 10^{-25} \text{ cm}^2$ ,  $a = 1/137$ ,  $V$  is the volume of the Gum Nebula, and  $\langle c\beta \rangle$  is the particle velocity averaged over the energy spectrum of the particles. For  $\langle \beta \rangle = 0.15$ ,  $Z^2/A = 8.7$  (average of  $\text{Si}^{28}$  and  $\text{Fe}^{56}$  in a ratio of 2 to 1),  $n_e = 10 \text{ cm}^{-3}$  and  $V = 1.35 \times 10^{63} \text{ cm}^3$  (Brandt et al., 1971) we get

$$\eta \simeq 9 \times 10^{-28} \frac{M}{M_\odot} \text{ erg cm}^{-3} \text{ sec}^{-1} \quad (11)$$

According to the geometry of the Gum Nebula described by Brandt et al. (1971), we expect it to appear as a disk source of X-rays, extended in galactic longitude ( $\Delta l \simeq 90^\circ$ ) and relatively thin in galactic latitude ( $\Delta b \simeq 7^\circ$ ). Collecting radiation from an interval of length  $L$  penetrating the nebula, the intensity viewed by a detector of aperture  $(\Delta b)_0 < \Delta b$  would be expressed by

$$dI/dl = (\Delta b)_0 / (4\pi) \eta L \text{ erg cm}^{-2} \text{ sec}^{-1} \text{ rad}^{-1} \quad (12)$$

Using a detector of  $(\Delta b)_0 = 4^\circ$ , viewing at  $\ell \simeq (260 \pm 40)^\circ$ , which spans the Gum Nebula, Cooke, Griffiths and Pounds (1969) observed an enhanced X-ray emission associated with the galactic disk of about  $3 \times 10^{-9}$  erg (cm<sup>2</sup> sec rad)<sup>-1</sup> above 1.4 keV, with an essentially flat energy spectrum extending to about 10 keV. The upper limits to this flux at energies above 12.5 keV, as set by Hudson, Peterson, and Schwartz (1971), provide evidence that the spectrum is characterized by a break in the vicinity of about 10 keV. Using the volume emissivity as obtained from equation (11),  $L = 400$  pc and  $(\Delta b)_0 = 4^\circ$ , we get  $dI/d\ell = 6 \times 10^{-9}$  M/M<sub>⊙</sub> erg sec<sup>-1</sup> cm<sup>-2</sup> rad<sup>-1</sup>. Since a significant part of the apparently diffuse background observed from the direction of the Gum Nebula may be coming from undetected discrete sources (Cooke and Pounds 1971), the flux of  $3 \times 10^{-9}$  erg cm<sup>-2</sup> sec<sup>-1</sup> rad<sup>-1</sup> must be considered as an upper limit. This then sets an upper limit  $M/M_\odot < 0.5$  on the mass of energetic charged particles currently trapped in clouds.

In addition to bremsstrahlung X-rays, contemporary fluxes of energetic heavy nuclei in dense clouds may also produce detectable gamma-ray line emission in the few MeV range. As an example, we consider the 1.78 MeV line of Si<sup>28</sup>. The cross section  $\sigma_\gamma$  for the reaction Si<sup>28</sup> (p, p') Si<sup>28\*</sup> 1.78 MeV has a threshold at about 5 MeV, peaks at about 9 MeV and has a value of about 300 mb at 10 MeV (McGowan *et al.* 1969, 1970).

As above we assume that  $M/(Am_p)$  particles are currently trapped in clouds. The average volume emissivity of the Gum Nebula in line emission at a photon energy  $e_j$  is then given by

$$\eta(e_j) = \sigma_j e_j (n_p/V) (2M/3 Am_p) \langle c \beta \rangle \quad (13)$$

where  $n_p$  equal to  $n_e$  is the proton density in clouds, and the factor of 2/3 is the assumed fraction of silicon nuclei in the supernova ejecta. For the values of  $n_p = n_e$ ,  $V$  and  $\langle \beta \rangle$  given above

$$\eta(1.78 \text{ MeV}) \simeq 8 \times 10^{-28} \frac{M}{M_\odot} \text{ erg cm}^{-3} \text{ sec}^{-1} \quad (14)$$

Since present measurements of gamma rays at these energies have been made with omnidirectional detectors only (Vette *et al.* 1970), we shall make the simplifying assumption that the flux at earth is produced by a point source at the center of the Gum Nebula. The flux seen by an omnidirectional detector will then be given by

$$F(e_j) \eta(e_j) V / (4 \pi r^2 e_j) \quad (15)$$

For  $r \simeq 460$  pc,  $e_j = 1.78$  MeV and  $M/M_\odot < 0.5$ ,  $F(1.78 \text{ MeV}) < 8 \times 10^{-3}$  photon  $\text{cm}^{-2} \text{sec}^{-1}$ . This flux should be compared with the omnidirectional counting rate of  $1.2 \times 10^{-1}$  photon  $\text{cm}^{-2} \text{sec}^{-1}$  in the 1 to 2 MeV range (Vette et al. 1970). Since the energy of the photon-emitting nuclei is about 10 MeV/nucleon or less, line broadening should be less than 15%. Therefore, detectable gamma-ray line emission could be observed with detectors of moderate energy resolution.

It is of some interest to speculate about line emission at 4.43 MeV from  $\text{C}^{12}$  and 6.14 MeV from  $\text{O}^{16}$ . The cross sections for the excitation of these levels were plotted as a function of energy by Lingenfelter and Ramaty (1967). At 10 MeV/nucleon  $\sigma_\gamma \simeq 200$  mb for  $\text{C}^{12}$  and  $\sigma_\gamma \simeq 100$  mb for  $\text{O}^{16}$ . If  $M_c$  and  $M_o$  are the present masses of energetic carbon and oxygen nuclei in clouds the expected photon fluxes from the Gum Nebula are  $F(4.43 \text{ MeV}) \simeq 4 \times 10^{-2} M_c/M_\odot$  photon  $\text{cm}^{-2} \text{sec}^{-1}$  and  $F(6.14 \text{ MeV}) \simeq 1.5 \times 10^{-2} M_o/M_\odot$  photon  $\text{cm}^{-2} \text{sec}^{-1}$ . When compared with the observed counting rate of about  $5.6 \times 10^{-2}$  photon  $\text{cm}^{-2} \text{sec}^{-1}$  in the 4 to 6 MeV band (Vette et al. 1970), we see that line emission from carbon and oxygen could be detected and, moreover, it could account for at least part of the excess radiation above the intergalactic background as calculated by Brecher and Morrison (1969).

In addition to the gamma ray region, line emission should also be produced in the X-ray region as a result of charge exchange between energetic nuclei and H atoms resulting in the capture of electrons to excited states. Cascades down to the ground state occur, which produce the analogue of Ly  $\alpha$  and Ly  $\beta$  emission for the case of capture of K-electrons. Silk and Steigman (1969) have given a discussion of this process, with application to low energy galactic cosmic rays. The contemporary flux of X-ray line emission, however, is difficult to determine, since unlike bremsstrahlung and nuclear collision which do not depend on the ionization state of the ambient matter, charge exchange takes place in neutral hydrogen only. Estimates of the time integrated fluxes in the 7 keV line of iron and 2 keV line of silicon were given by Ramaty et al. (1971).

### Cooling of the Nebula

Alexander et al. (1971) suggested that the temperature of the nebula as a whole is quite high, probably in excess of  $5 \times 10^4$  °K. While it is possible that the dense filaments could at present be cooler than  $10^4$  °K, it is of some interest to examine the effects of a contemporary source of ionization and heating on the thermal state of the filaments.

According to Cox and Tucker (1969), for a gas of cosmic abundances in ionization equilibrium, the radiative loss rate at  $5 \times 10^4$  °K is  $P \simeq 2 \times 10^{-22} n_e^2 \text{ erg cm}^{-3} \text{ sec}^{-1}$ . The corresponding cooling time is  $t_c \simeq (3/2) n_e kT/P \simeq 1700/n_e$  years. For  $n_e = 10 \text{ cm}^{-3}$ ,  $t_c \simeq 170$  years, much shorter than the age of the nebula.

The rapid cooling of the filaments can be partially compensated by a contemporary source of heat such as a large flux of energetic particles presently trapped in clouds. The rate of energy loss of a particle of mass number  $A$  and nuclear charge  $Ze$  in a plasma of density  $n_e$  is approximately given by equation (3) with  $n_H$  replaced by  $4n_e$  (Hayakawa and Kitao 1956). If  $M/(Am_p)$  nuclei are currently trapped in clouds, the contemporary heat input is given by

$$Q \simeq 5.6 \times 10^{-22} (Z^2/A) e^{-0.3} n_e \frac{M}{M_\odot} \text{ erg cm}^{-3} \text{ sec}^{-1} \quad (16)$$

For  $Z^2/A = 8.7$ ,  $e = 10 \text{ MeV/nucleon}$ ,  $n_e = 10 \text{ cm}^{-3}$  and  $M/M_\odot < 0.5$ ,  $Q < 0.6 P$ . Thus, even though a contemporary flux of energetic particles, equal to the upper limit determined from the calculated bremsstrahlung emission and the observed disk component of diffuse x-rays could make a contribution to the maintenance of the temperature in the filaments, it is not quite sufficient to balance the radiative energy loss of the plasma. The characteristic time scale for contemporary heating,  $t_h$ , is given by equation (4) with  $n_H$  replaced by  $4n_e$ . For  $Z^2/A = 8.7$ ,  $e = 10 \text{ MeV/nucleon}$  and  $n_e = 10 \text{ cm}^{-3}$ ,  $t_h \simeq 800$  years.

The radiation loss  $P$ , however, could be smaller than the value calculated by Cox and Tucker (1969) if the abundances of carbon and oxygen in the Gum Nebula are below universal abundances or if the ions  $C^{+1}$  to  $C^{+3}$  and  $O^{+1}$  to  $O^{+5}$  are significantly depleted from their values corresponding to ionization equilibrium by the initial ionization process. If the maintenance of a high temperature in the filaments is achieved by the latter mechanism, the characteristic time of interest is the recombination time of  $O^{+6}$  to  $O^{+5}$  and  $C^{+4}$  to  $C^{+3}$ ,

Up to temperatures of a few times  $10^5$  °K dielectronic recombination for  $O^{+6}$  and  $C^{+4}$  is negligible. Using Seaton's (1959) hydrogenic approximation, the radiative recombination coefficient to all levels of an ion  $X^{+m}$  is given by (e.g.: Allen and Dupree 1969)

$$\alpha \simeq 2 \times 10^{-11} (m+1)^2 T^{-1/2} \left( 0.43 + \frac{1}{2} \ln \lambda + \frac{0.47}{\lambda^{1/3}} \right) \text{ cm}^3 \text{ sec}^{-1} \quad (17)$$



where  $\lambda = 157890 (m_H)^2/T$ . For  $n_e = 10$  and  $T = 2 \times 10^5$  °K, the recombination time for both  $O^{+6} \rightarrow O^{+5}$  and  $C^{+4} \rightarrow C^{+3}$  is about 900 years. By combining this time scale with the contemporary heating time  $t_h$ , we see that the onset of rapid cooling could be delayed by as much as 1500 to 2000 years. A high temperature in the filaments could then be consistent with a delayed mechanism for the ionization and heating of the Gum Nebula.

### Ionization and Heating of the Interstellar Medium

Several recent theoretical descriptions (Pikel'ner 1967; Balasubrahmanyam et al. 1968; Spitzer and Tomasko 1968; Spitzer and Scott 1969; Goldsmith, Habing, and Field 1969) of ionization and thermal equilibria for interstellar H I regions, based upon current models for the interstellar gas, indicate that the rate of ionization per hydrogen atom is  $\zeta \simeq 10^{-15} (\text{sec H atom})^{-1}$ . Hjellming, Gordon, and Gordon (1969) find that observed pulsar dispersion measures may be best fitted with such a model for  $\zeta = (2.5 \pm 0.5) \times 10^{-15} (\text{sec H atom})^{-1}$ . For an equilibrium situation, the rate of electron-ion recombination is the most direct measure of  $\zeta$ ; recent observations of H  $\beta$  hydrogen line emission from interstellar H I (Reynolds 1971) yield a direct measure of the recombination rate, and the corresponding ionization rate in the regions examined could be as high as  $10^{-14} (\text{sec H atom})^{-1}$ .

Since essentially all the gas in the Gum Nebula has been ionized by the supernova explosion, the average rate of ionization in interstellar hydrogen by such events would be given by

$$\zeta \langle n_H \rangle = f_{SN} N_e \quad (18)$$

where  $\langle n_H \rangle$  is the mean interstellar hydrogen density and  $f_{SN}$  is the average supernova frequency per unit volume in the galaxy. If supernovae occur at a rate of 1 per 100 years in a volume of  $4 \times 10^{66} \text{ cm}^3$ ,  $f_{SN} \simeq 8 \times 10^{-77} \text{ cm}^{-3} \text{ sec}^{-1}$ . For  $N_e \simeq 2 \times 10^{62}$  electrons (Brandt et al. 1971), we obtain  $\zeta \langle n_H \rangle \simeq 1.6 \times 10^{-14} \text{ sec}^{-1} \text{ cm}^{-3}$ . Radio observations at 21 cm indicate a mean value for the neutral hydrogen density in the galactic plane of about  $0.7 \text{ cm}^{-3}$  (Spitzer 1968); however, optical depth effects probably raise  $\langle n_H \rangle$  to  $\sim 1 \text{ cm}^{-3}$ . A further increase by about a factor of 2 in the value of  $\langle n_H \rangle$  may be due to the presence of molecular hydrogen in dense clouds. Hence the mean galactic value of  $\zeta$  as indicated by the parameters deduced for the Vela X supernova is about  $8 \times 10^{-15} \text{ sec}^{-1} (\text{H atom})^{-1}$ . This ionization rate could be reduced if the frequency of supernova explosions of the type that produced the Gum Nebula is lower than the assumed rate of 1 per 100 years or if the actual free electron content of the Gum Nebula is less than that estimated by Brandt et al. (1971). Furthermore, even if the

average supernova output is similar to that of Vela X but occurs in a region with larger magnetic fields, so that the particles propagate over a shorter distance before they lose their energy, the ionized volume produced by the supernova would be smaller than that of the Gum Nebula. In this case, the total ionization per supernova would be reduced since a larger fraction of the total energy would go into heating. Also, those supernovae which occur at more than about 100 pc away from the galactic plane (e.g.: the Crab) will produce energetic particles which may escape from the disk without producing significant ionization.

In order for H II regions such as the Gum Nebula to merge into the H I of the interstellar medium, the recombination and cooling times of the clouds should be much less than the time between supernova explosions  $t_{\text{SN}}$  in the volume of the nebula. For  $f_{\text{SN}} = 8 \times 10^{-77} \text{ cm}^{-3} \text{ sec}^{-1}$  and  $V = 1.35 \times 10^{63} \text{ cm}^3$ ,  $t_{\text{SN}} \simeq 3 \times 10^5$  years.

The recombination time of hydrogen is approximately  $t_{\text{rec}} \simeq 130 T^{0.7}/n_e$  (Bates and Dalgarno 1962). For  $n_e = 10 \text{ cm}^{-3}$  and  $T = 5 \times 10^4 \text{ }^\circ\text{K}$ ,  $t_{\text{rec}} \simeq 2.5 \times 10^4$  years. Since the recombination rate increases with decreasing temperature, both  $t_c$  and  $t_{\text{rec}}$  are much smaller than  $t_{\text{SN}}$ , so that the ionized clouds in the Gum Nebula will rapidly merge into the H I of the interstellar medium.

In the intercloud medium, for a density  $\langle n_e \rangle \simeq 0.16 \text{ cm}^{-3}$ , the temperature will not decrease appreciably below  $10^4 \text{ }^\circ\text{K}$  in  $3 \times 10^5$  years. The recombination time then becomes comparable to  $t_{\text{SN}}$  so that the degree of ionization is approximately constant as a function of time. The fact that the inferred degree of ionization of the intercloud medium probably does not exceed about 10% (Hjellming, Gordon, and Gordon 1969) is consistent with a cosmic-ray model for the ionization of the Gum Nebula, since as discussed above, the energetic charged particles from the supernova will deposit most of their energy in clouds and not in the intercloud medium.

## References

- Alexander, J. K., Brandt, J. C., Maran, S. P., and Stecher, T. P. 1971, Ap. J., 167, 487.
- Allen, J. W., and Dupree, A. K. 1969, Ap. J., 155, 27.
- Balasubrahmanyam, V. K., Boldt, E. A., Palmeira, R. A. R., and Sandri, G. 1968, Can. J. Phys., 46, S633.
- Bates, D. R., and Dalgarno, A. 1962, Atomic and Molecular Processes, ed. D. R. Bates, (New York: Academic Press) p. 245.
- Bethe, H. A., and Ashkin, J. 1953, Experimental Nuclear Physics, Vol. 1, ed. E. Segre, (New York: John Wiley and Sons) p. 166.
- Boldt, E., and Serlemitsos, P. 1969, Ap. J., 157, 557.
- Brandt, J. C., Stecher, T. P., Crawford, D. L., and Maran, S. P. 1971, Ap. J. (Letters), 163, L99.
- Colgate, S. A., and McKee, C. 1969, Ap. J., 157, 623.
- Cooke, B. A., Griffiths, R. E., and Pounds, K. A. 1969, Nature, 224, 134.
- Cox, D. P., and Tucker, W. H. 1969, Ap. J., 157, 1157.
- Goldsmith, D. W., Habing, H. J., and Field, G. B. 1969, Ap. J., 158, 173.
- Hayakawa, S., and Kitao, K. 1956, Prog. Theor. Phys. 16, 139.
- Hjellming, R. M., Gordon, C. P., and Gordon, K. J. 1969, Astron. Astrophys., 2, 202.
- Hudson, H. S., Peterson, L. E., and Schwartz, D. A. 1971, Nature, 230, 177.
- Lingenfelter, R. E., and Ramaty, R. 1967, High-Energy Nuclear Reactions in Astrophysics, ed. B.S.P. Shen, (New York: W. A. Benjamin) p. 99.
- Lingenfelter, R. E., Ramaty, R., and Fisk, L. A. 1971, Astrophys. Letters, 8, 93.
- McGowan, F. K., Milner, W. T., Kim, H. J., and Hyatt, W. 1969, Nuclear Data Tables, A6, 353.
- McGowan, F. K., Milner, W. T., Kim, H. J., and Hyatt, W. 1970, Nuclear Data Tables, A8, 199.
- Pierce, T. E., and Blann, M. 1968, Phys. Rev., 173, 390.

- Pikel'ner, S. B. 1967, Astrophys. Letters, 1, 43.
- Ramaty, R., Boldt, E. A., Colgate, S. A., and Silk, J. 1971, Ap. J., 169, 87.
- Ramaty, R., and Lingenfelter, R. E. 1971, Isotopic Composition of the Primary Cosmic Radiation, (Danish Space Research Institute), p. 203.
- Reichley, P. E., Downs, G. S., and Morris, G. A. 1970, Ap. J. (Letters), 159, L35.
- Reynolds, R. 1971, Ph.D. Thesis, University of Wisconsin.
- Seaton, M. J. 1959, M.N.R.A.S., 119, 81.
- Shklovsky, I. S. 1970, Nature, 225, 252.
- Silk, J., and Steigman, G. 1969, Phys. Rev. Letters, 23, 597.
- Spitzer, L., Jr. 1968, Diffuse Matter in Space (New York: Interscience).
- Spitzer, L., and Scott, E. H. 1969, Ap. J., 158, 161.
- Spitzer, L., and Tomasko, M. G. 1968, Ap. J., 152, 971.

## DISCUSSION

*R. McCRAY:*

Why did you use a density of  $10 \text{ cm}^{-3}$  for the filaments? The low frequency radio measurements refer to the general mass of the nebula, so the temperature reported by Alexander does not apply to the dense regions.

*R. RAMATY:*

Better H-alpha observations are needed. Then we can determine if there is an emission measure of at least  $600 \text{ pc cm}^{-6}$  over the entire beam of the RAE-1 instrument, or whether that brightness (the lowest value recorded by Gum) is very localized.

*H. M. JOHNSON:*

It is not clear how Gum determined the emission measure.

*B. J. BOK:*

I think that the emission measure will probably come out to be of order  $400 \text{ pc cm}^{-6}$ .

*J. C. BRANDT:*

I want to emphasize that our estimate of the number of electrons and the ionization energy does not depend on the emission measure, but only on the dispersion measure.

*D. P. COX:*

On the particle ionization theory, would the Gum Nebula be gradually getting larger?

*RAMATY:*

It might; it depends on how many ionizing nuclei are left. If you assume a simple model with spherical clouds and a clumpiness factor of 60 or 65, then the distance that one can travel in a straight line before encountering a cloud is equal to the radius of the cloud times the clumpiness factor. So there is a good chance that the average nucleus has already hit a cloud and lost its energy.

*COX:*

But the excess X-ray luminosity requires that the ionizing nuclei are still present.

*RAMATY:*

The excess luminosity may not originate in the nebula. It may be due to discrete sources or to a general galactic background. It might be due to charge exchange, if there is still some neutral hydrogen present. A search for gamma rays is probably the best test for whether the cosmic ray nuclei are still present in the nebula.

# THE EARLY EVOLUTION OF GIANT H II REGIONS FORMED BY SUPERNOVA EXPLOSIONS\*

Minas C. Kafatos

*Department of Physics and Center for Space Research  
Massachusetts Institute of Technology  
Cambridge, Massachusetts 02139*

## Abstract

Brandt *et al.* (1971) have shown that consistency in the combined observations of the Gum Nebula requires a giant H II region, presumably formed by the Vela X supernova explosion. Morrison and Sartori (1969) had concluded on the basis of their He II fluorescence theory of type I supernovae, that a giant H II region would be formed as result of the UV burst. In this paper the evolution of such a region, which cools after an initial ionization, is discussed. This discussion is then applied to the Vela X and Tycho supernovae. Other giant H II regions might not in general be as easily detectable as the Vela X region. The Tycho region may just be detectable in the O[II], O[III] optical lines or as a "hole" in the 21-cm emission line profiles (the latter is already suggested in the data). These giant H II regions last appreciably longer than the continuum radio sources within them.

## Introduction

In the fluorescence model of Morrison and Sartori (1969), only a small part of the total energy is emitted in the visible (the "bolometric correction" is about 8 magnitudes). Most of the total energy leaves the supernova neighborhood in the form of He II Lyman-alpha photons ( $h\nu = 40.8$  eV). The estimated photon number is  $\sim 10^{62}$ , corresponding to a primary energy of  $\sim 10^{52}$  erg. The mean free path of these photons at  $n_H = 1 \text{ cm}^{-3}$  is a couple of parsecs. An H II region with a sharp boundary will be formed, its radius at  $n_H = 1 \text{ cm}^{-3}$  being about 100 pc. In this model the ionization of the Gum Nebula is attributed to those UV photons; it follows that the initial temperature is fairly high, about  $10^5$  °K.

Once the H II region is formed it cools because there is no further radiation ionizing the gas, while it grows slowly in size, since the emission during cooling is predominantly beyond the Lyman limit of hydrogen. The

---

\*Supported in part by NASA Grants NSG-496, NGL-22-009-019, and also in part by NSF Grant GP-11453.

ionization of the interstellar gas starts immediately after the explosion; other theories which attribute the ionization to cosmic rays (Ramaty et al. 1971), or to UV photons from the expanding shock wave (Tucker 1971), predict a delayed formation (the region is formed  $\sim 10^4$  years after the initial explosion occurred). Recent supernovae, like Tycho, are critical in deciding if the supernova explosion produces an ionized region much later than the time of the explosion or not.

We will discuss the evolution of a gas, having the cosmic abundances of Aller (1961), that is initially ionized to a high temperature (above  $\sim 20,000^\circ\text{K}$ ) and then cools with no further heat input to keep the temperature more or less constant.\* We emphasize that this time-dependent treatment applies to any case in which the gas cools after an initial ionization and a high initial temperature, no matter what gave rise to the initial ionization. However, the discussion will be restricted to the Morrison-Sartori theory, with appropriate general remarks made whenever needed.

Most of the ideas in this paper, particularly the discussion on Tycho, were developed in a previous paper, herein referred to as Paper I (Kafatos and Morrison 1971).

### Non-Steady State Cooling

Cox and Tucker (1969) showed that in the temperature range  $10^4 - 10^5^\circ\text{K}$  the cooling of a cosmic gas is mostly due to ions of the elements H, He, C, O. These ions, once collisionally excited from the ground state, relax back to the ground state by allowed radiative transitions ("ions" includes the neutral stage too).

In their "steady state" treatment, Cox and Tucker assumed that collisional ionizations balance recombinations (dielectronic and radiative). In this case the abundance ratio for any ion  $z$  of an element  $i$  is:

$$\frac{n_z^i}{n_{z+1}^i} = \frac{a_{z+1,z}^{\text{Di}}(T) + a_{z+1,z}^{\text{Ri}}(T)}{C_{z,z+1}^i(T)} = \frac{a_{z+1,z}^i(T)}{C_{z,z+1}^i(T)} \quad (1)$$

( $C_{z,z+1}^i$  is the collisional ionization coefficient of ion  $z$ , while  $a_{z+1,z}^i$  is the total (dielectronic and radiative) recombination coefficient of ion  $z+1$ ; note

---

\*The heating of the galactic gas and cloud formation due to supernova explosions are discussed by McCray and Schwarz (1971). In the present paper the early evolution of Fossil Strömgren Spheres is discussed (the cooling is only followed down to  $10^4^\circ\text{K}$ ).



that this ratio is a function of  $T$  only.) Since the abundance of any ion is fixed by temperature, it follows that the radiative power loss is only a function of  $T^*$ ; as was mentioned above, in the range  $10^4$  °K -  $10^5$  °K this radiative power loss is mostly due to cooling resulting when ions that were collisionally excited from the ground state radiate back to the ground state by dipole emission.

On the other hand, if the gas cools with no heat input to keep the temperature more or less constant (as in the present case where after the initial sudden UV ionization there is no further heat or ionization input, other than collisions in the gas) the ionic abundances are found from the solution of the coupled system of equations:

$$\frac{dT}{dt} = -\Lambda(t, \dots, n_z^i, \dots) \quad (2)$$

$$\text{All } z, \text{ all } i \left| \frac{dn_z^i}{dt} = -a_z^i n_z^i n_e + a_{z+1}^i n_{z+1}^i n_e - C_z^i n_z^i n_e + C_{z-1}^i n_{z-1}^i n_e \right.$$

(where  $a_z^i, C_z^i$  refers to  $a_{z, z-1}^i, C_{z, z+1}^i$ ). Thermal expansion in system (2) is assumed negligible, i.e.:  $n_T = n_e + n_H = \text{const}$ . The ionic abundances found from system (2) might be different than the Cox and Tucker abundances. This is particularly prominent in hydrogen. If  $dT/dt = T/f(T)$  is the Cox and Tucker energy loss rate, then the total cooling time  $t_c = \int f(T) dT/T$  to cool down to 15,000 °K is  $t_c \sim 10^4/n_T$  years, if  $T \sim 10^5$  °K initially. According to the steady state model, hydrogen is half-neutral at 15,000 °K. The time for half of hydrogen to recombine is about  $10^5/n_T$  years, i.e.: it cools down to 15,000 °K before it recombines appreciably. We thus expect the collisionally induced hydrogen Lyman-alpha cooling, which in the steady state is peaked around 20,000 °K, to be appreciably reduced. In Paper I the approximation  $\Lambda(T, \dots, n_z^i, \dots) = \Lambda(T) \propto T^{1.857}$  was used in system (2). This approximation makes the computing much easier, since one may solve the ionization equations of a particular atom, e.g.: oxygen, along with  $dT/dt = -\Lambda(T)$ , instead of the complete system involving all atoms. It was found that this approximation yields similar results to the exact solution of system (2), except below 20,000 °K. If the density  $n_T = n_e + n_H$  is  $1 \text{ cm}^{-3}$  \*\* the total time to cool from  $10^5$  °K to  $10^4$  °K is  $1.2 \times 10^4$  years in this approximation.

\*The radiative power loss  $dE/dt dV$  (erg  $\text{cm}^{-3} \text{ sec}^{-1}$ ) is related to  $dT/dt$  by:  $dE/dt dV = (3/2) k (1+x) n_T dT/dt$ , where  $n_T = n_e + n_H$  and  $x = n_e/n_T$ . In the non-steady state case one has to be careful since  $dx/dt \neq 0$ .

\*\*From here on we assume that  $n_T = 1 \text{ cm}^{-3}$ . For other  $n_T$ , notice that the transformation  $t' = (1/\lambda) t$ ,  $n_T' = \lambda n_T$  leaves (2) unchanged.

System (2) was solved exactly by including the following ions of the atoms H, He, C, O: hydrogen, both stages; helium all three stages; carbon, the first five stages; oxygen, the first four stages (the other carbon and oxygen stages are not important unless the initial temperature is higher than  $2 \times 10^5$  °K). The cooling due to the forbidden lines O[II] 3727, 3729 Å and O[III] 5007, 4959 Å was also included in  $\Lambda$ ; above  $10^4$  °K these are the strongest forbidden lines of any ion (the infrared forbidden lines of the ions C II, N III, O IV, Ne II are important below  $10^4$  °K, while the O[I], N[I], N[II], Ne[III], Ne[IV], Ne[V] lines are not as strong as the O[II], O[III] lines). The O[II], O[III] cooling should be appreciable below  $\sim 30,000$  °K. At higher temperatures this cooling is small compared to the allowed line cooling. Hydrogen Lyman-alpha is dominant below  $20,000$  °K along with the O[II], O[III] cooling. Carbon and helium are important up to  $\sim 8 \times 10^4$  °K, while oxygen is dominant above  $8 \times 10^4$  °K. We should point out that the cooling equation when the predominant cooling agent is hydrogen is:

$$\frac{dU}{dt} = \frac{3}{2} k(1+x) n_T \frac{dT}{dt} + n_T \left( \frac{3}{2} kT + I_H \right) \frac{dx}{dt} = -\mathcal{L}_{La}^H - \mathcal{L}_{Rec}^H - \mathcal{L}_{fob}$$

where  $I_H$  is the I. P. of hydrogen,

$$\frac{dx}{dt} = -x^2 a_{10}^{RH}(T) + x(1-x) C_{01}^H(T)$$

and  $\mathcal{L}_{La}^H$ ,  $\mathcal{L}_{Rec}^H$ ,  $\mathcal{L}_{fob}$  are the cooling coefficients due to collisional excitation of the  $n=2$  level, due to recombinations and due to oxygen forbidden line emission respectively (see also Defouw 1970). If the region is optically thick in the Lyman continuum, then recombinations to the ground state are not taken into account in the above equations (for neutral hydrogen density  $n_H \sim 10^{-3} \text{ cm}^{-3}$ , the mean free path at the Lyman threshold is  $\sim 50$  pc).

It was found that the total time to cool from  $10^5$  °K down to  $10^4$  °K under various initial ionic abundances is about  $2 \times 10^4$  years.

In Fig. (1) the Cox and Tucker radiative power loss curve is shown along with the approximation  $\Lambda(T) \propto T^{1.857}$ . In Fig. (2) the exact cooling curve (initial relative ionic abundances  $H^+ = 1$ ,  $He^+ = 1$ ,  $C^{++} = 1$ ,  $O^{++} = 1$ ) calculated by solving system (2) is shown, along with the above mentioned approximation. It was shown that the exact cooling curve, found from (2), doesn't depend very much on the assumed initial abundances and that the behavior of the system is the same after about  $10^3$  years. This is because the cooling time and the dielectronic recombination time or collisional ionization time (whichever is shorter) of the dominant cooling agents are comparable at high temperatures; around  $10^5$  °K they all are a few hundred

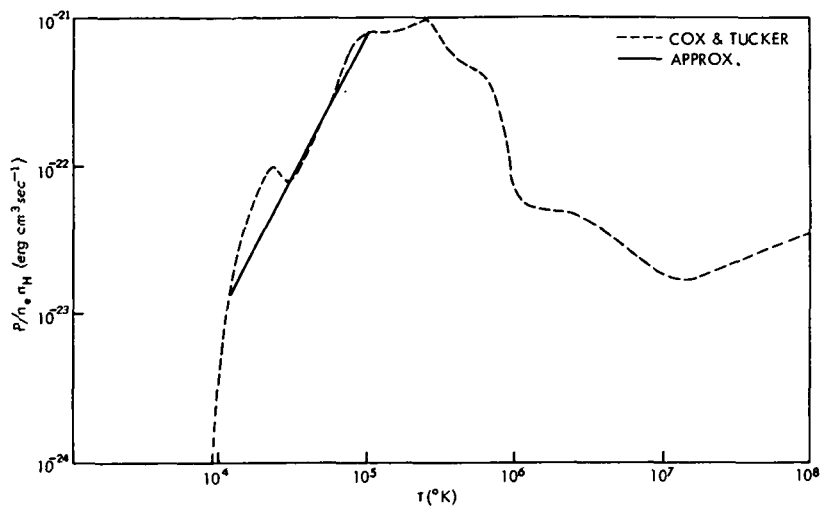


Figure 1. Total radiative power loss assuming cosmic abundances. Dotted line is by Cox and Tucker (1969); solid, the approximation  $\Lambda(T) \propto T^{1.857}$ .

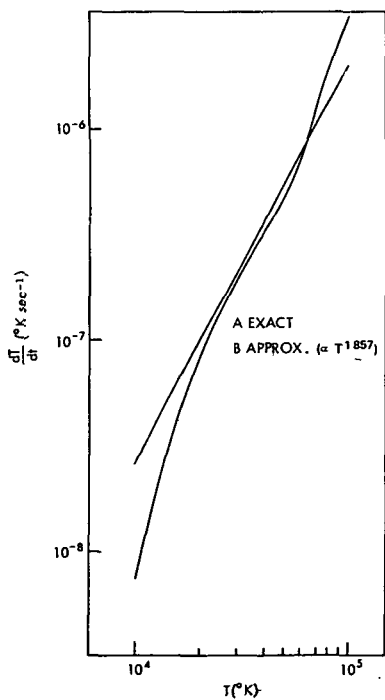


Figure 2. Curve A: exact cooling curve,  $dT/dt$ , found by solving system (2); the initial relative ionic abundances are  $H^+ = 1$ ,  $He^+ = 1$ ,  $C^{++} = 1$ ,  $O^{++} = 1$ . Curve B: the approximation  $dT/dt \propto T^{1.857}$ .

years. If one starts the cooling at lower temperatures (as low as  $20,000^\circ\text{K}$ ) the cooling curve might initially be quite different for various initial abundances; for example, around  $20,000^\circ\text{K}$  a 10 percent change in the initial abundance of  $\text{H}^+$ , or  $x$ , makes a big difference in the cooling curve, since the collisional Lyman-alpha cooling rate depends on  $1 - x$ . However, the cooling curve settles to curve A of Fig. 2 after a few thousand years. We therefore expect slight changes in the cooling curve depending on the temperature at which the cooling begins and on the initial abundances, but the overall shape of the curve should be the same after some time has elapsed.

In any case the relative ionic abundances are not the same as those expected from the steady state theory (e.g.: hydrogen is almost completely ionized,  $x = n_e/n_T \sim 0.87$ , at  $T \sim 10^4^\circ\text{K}$  while according to the steady state theory it should be mostly neutral etc.).

As expected the collisional hydrogen Lyman-alpha emission rate is appreciably reduced from the values expected under steady state conditions (by a factor of 10 around  $2 \times 10^4^\circ\text{K}$ ). The emission rate of hydrogen Lyman-alpha under steady state conditions and non-steady state conditions as a function of  $T_e$  is shown in Fig. (3) (if recombinations balance ionizations this emission rate is mostly due to collisional excitation of the  $n = 2$  level; in the time-dependent model, the Lyman-alpha emission rate from recombinations dominates the emission rate due to collisions only if  $T \sim 10^4^\circ\text{K}$ ).

The time evolution of the oxygen ions (initial conditions as before) is shown in Fig. (4). What is interesting is that the  $\text{O[II]}$ ,  $\text{O[III]}$  forbidden lines compete with the hydrogen Lyman-alpha in the cooling. These forbidden lines are much stronger than the hydrogen Balmer lines; H-alpha begins to compete with  $\text{O[II]}$ ,  $\text{O[III]}$  only below  $10^4^\circ\text{K}$ . The volume emission rates ( $\text{erg cm}^{-3} \text{ sec}^{-1}$ ) of the hydrogen Lyman-alpha line (due to collisions and recombinations) and the oxygen forbidden lines as a function of time are shown in Fig. (5). The temperature of the region is also shown. The initial conditions assumed were: relative ionic abundances  $\text{H}^+ = 1$ ,  $\text{He}^+ = 1$ ,  $\text{C}^{++} = 1$ ,  $\text{O}^{++} = 1$ ,  $T = 10^5^\circ\text{K}$  (for different initial conditions the exact values of the  $\text{O[II]}$ ,  $\text{O[III]}$  lines may vary but always, at least  $\text{O[II]}$ , compete with the hydrogen Lyman-alpha).

In solving system (2) the hydrogenic radiative recombination coefficients of Seaton (1959) and the formula of Burgess (1965) for the dielectronic recombination coefficients were used. The collisional ionization coefficients were those of Cox and Tucker (1969).

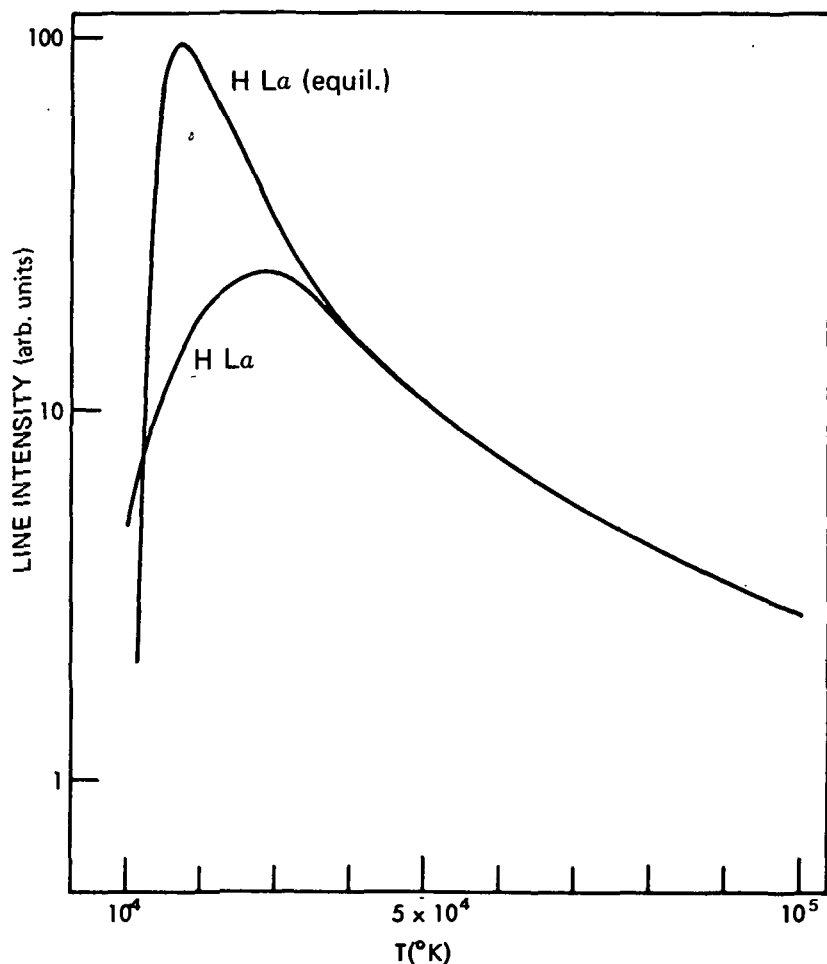


Figure 3. Intensity of the hydrogen Lyman-alpha line if recombinations balance ionizations (H La (equil.)), and in the time dependent case (H La) for the initial conditions of Figure 2.

#### Application to Gum Nebula and Tycho

Brandt et al. (1971), by combining the known emission measure, the dispersion measure of the pulsar in Vela X, the neutral hydrogen measure, and the optical extinction, reach the conclusion that a giant H II region of low density ( $n_e \sim 0.16 \text{ cm}^{-3}$ ,  $R \sim 400 \text{ pc}$ ) engulfs the Gum Nebula, while its

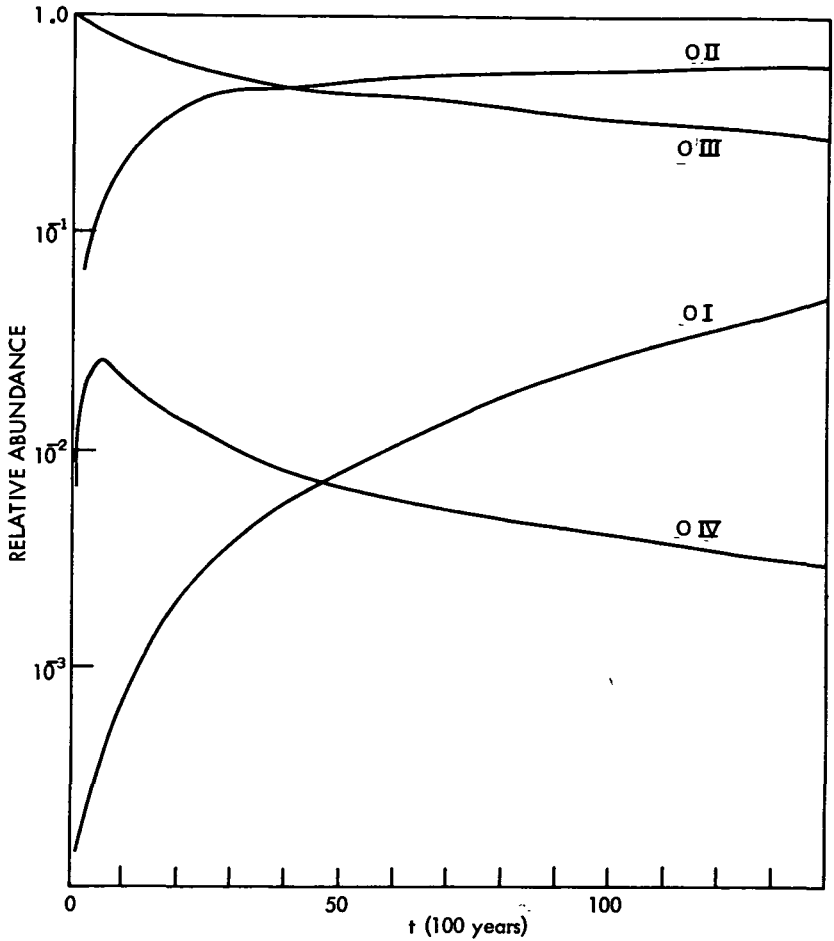


Figure 4. Relative abundances of oxygen ions as a function of time (initial conditions same as before). The unit of time is 100 years.

edge is only about 60 pc away from the Sun. The filaments seem to have densities appreciably higher than the mean. Brandt *et al.* find the root mean square electron density to be about  $1.28 \text{ cm}^{-3}$ ; this is based on the assumption that the mean emission measure is  $\sim 1300 \text{ cm}^{-6} \text{ pc}$ . The Gum Nebula may be the composite of a large diffuse and not very bright region, which was formed by the supernova explosion, and a smaller denser region,

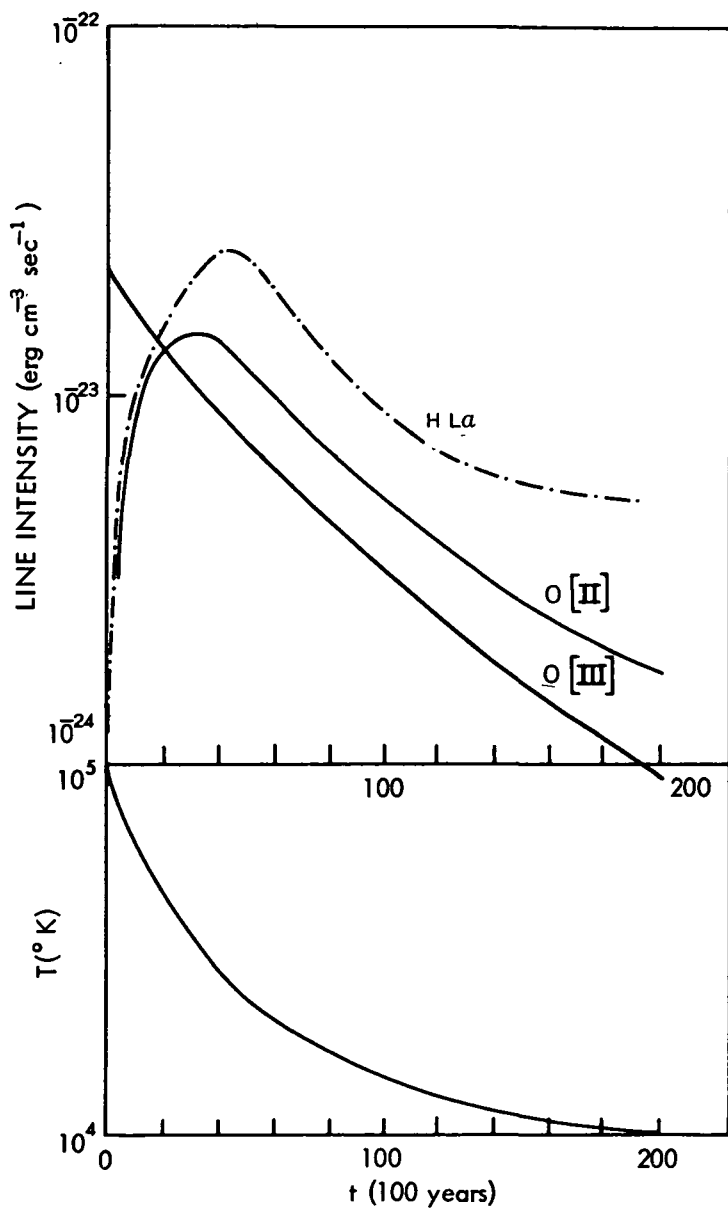


Figure 5. Volume emission rate ( $\text{erg cm}^{-3} \text{sec}^{-1}$ ) of the hydrogen Lyman-alpha and the O[II], O[III] lines as a function of time. The temperature of the region is also shown (initial conditions same as before).

which surrounds the stars  $\gamma^2$  Vel and  $\zeta$  Pup and which is probably kept ionized by those stars (e.g.: discussion by Bok 1971). Although the above mentioned value of the emission measure is questionable (as discussed during the present conference) it seems that there is appreciable concentration of the nebular matter in the weakest part of the nebula.

The age of the pulsar PSR 0833-45 (Reichley et al. 1970) is  $1.1 \times 10^4$  years. If the nebula was ionized  $1.1 \times 10^4$  years ago by a UV burst and the initial temperature was quite high ( $\sim 10^5$  °K), as expected from the fluorescence theory of type I supernovae, the diffuse region should still be quite hot. In Table 1 the temperature of a diffuse region ( $n_e \sim 0.1 \text{ cm}^{-3}$ ) as well as that of denser regions ( $n_e \sim 1 \text{ cm}^{-3}$ , which is more appropriate for the filaments) is given for various ages of the nebula, assuming that the initial temperature was  $\sim 10^5$  °K. These temperatures are consistent with the high temperatures of Alexander et al. (1971). On the other hand, regions which are appreciably denser than  $1 \text{ cm}^{-3}$  would cool down fairly fast after the initial explosion and their present temperature ( $\sim 10^4$  °K) would have to be attributed to sources other than the initial UV burst. This is the case for the very dense ( $n_e \sim 300 \text{ cm}^{-3}$ ) filaments near Vela X observed by Milne (1968a,b) and maybe the smaller, dense region around  $\gamma^2$  Vel and  $\zeta$  Pup. The former very dense filaments are probably excited by the remnant itself, while the latter region is probably excited by  $\gamma^2$  Vel and  $\zeta$  Pup. In any case the Gum Nebula is fairly rich in H II emission clouds, stars, filaments etc. and one shouldn't expect to attribute everything to the supernova.

Table 1  
Age and Corresponding Temperature Assuming  
an Initial Temperature of  $10^5$  °K

$n_e \text{ (cm}^{-3}\text{)}$	Age (years)	$T_e \text{ (}^\circ\text{K)}$
1	5,000	25,000
	11,000	15,000
	20,000	10,000
0.1	5,000	75,000
	11,000	55,000
	20,000	40,000

The estimated total number of electrons in the H II region is, according to Brandt et al. (1971), about  $2 \times 10^{62}$  at present. The region in cooling from  $10^5$  °K to its present  $T \sim 50,000$  °K, doubles its size, since the predominant



radiation, when cooling, is beyond the hydrogen Lyman limit. This gives  $\sim 10^{62}$  \* for the initial UV photon number in accordance with the Morrison-Sartori estimates.

The Vela X H II region is made easy to detect by a combination of fortunate circumstances, the most important being its relatively nearby location. As pointed out in Paper I (see also discussion by Sartori 1971), the essential difference between an ionized region produced by the UV photons of the fluorescence theory and other mechanisms (such as the cosmic rays of Ramaty *et al.* 1971), or the UV photons from the blast wave of Tucker (1971) is the time to form the region. The Gum Nebula could have been produced by any of the above mechanisms. However a recent supernova (not older than  $\sim 10^3$  years) should have already formed its "Gum Nebula" if the UV-burst is produced in the initial explosion but not if the formation of the ionized region takes place after  $10^4$  years. The known galactic supernovae younger than  $10^3$  years are the following: SN 1054 (the Crab Nebula Supernova), SN 1006, SN 1572 (Tycho's Supernova), SN 1604 (Kepler's Supernova) and Cas A. Of these only Tycho and Kepler are definitely of type I; of the others the Crab might be a unique remnant, not much is known about SN 1006, and Cas A is probably of type II and furthermore it is heavily obscured by dust. Kepler is further away than Tycho. Therefore the best supernova to test whether an ionized region is formed right after the explosion or much later, is Tycho (the following discussion is similar to that in Paper I).

The Tycho remnant is only 400 years old. We expect the H II region to be quite hot still. Menon and Williams (1966) determined a distance of 3.5 kpc to Tycho, from their 21-cm absorption line measurements and a density of  $n_H \sim 0.1 \text{ cm}^{-3}$ , at a distance about 100 pc above the galactic plane. Minkowski (1964, 1968) uses the distance 5 kpc and interstellar absorption for the remnant of  $\sim 2.1$  magnitudes. (There is still considerable uncertainty at present as to the correct value of distance, according to Williams 1971.) We present in Table 2 the expected surface brightness of the large H II region ( $n_e = 1, 0.1 \text{ cm}^{-3}$  and  $10^{62}$  electrons), as well as denser, small clouds ( $n_e = 10 \text{ cm}^{-3}$ ), in the O[II], O[III] lines for Tycho at present. A constant optical absorption of 2 magnitudes was assumed. We also show the expected\*\* H-alpha surface brightness for the above regions and the observed surface brightness of some weak normal H II regions in H-alpha (see Pottasch 1965).

\*The total mass changes by at most a factor of 4 in the recent work of Alexander *et al.* (1971).

\*\*As long as  $x = n_e/(n_e + n_H)$  is close to the equilibrium value, the H-alpha emissivity is as calculated by Parker (1964) for collisional excitation; this was found to be the case for  $T \gtrsim 30,000^\circ \text{K}$ .

Table 2  
Expected Surface Brightness of Tycho Model Regions and Observed Brightness in  
H-alpha of Normal H II Regions

A. Tycho Model Regions:

$n_e$ ( $\text{cm}^{-3}$ ) (assumed)	R (pc)	T ( $^{\circ}\text{K}$ )	Angular Radius (arc min)		Surface Brightness ( $\text{erg cm}^{-2} \text{sec}^{-1}$ )		
	(expected)		d = 3.5 kpc	d = 5 kpc	$S_{[\text{OIII}]}$	$S_{[\text{OII}]}$	$S_{\text{H}\alpha}$
1	95	80,000	94	66	$3 \times 10^{-4}$	$7 \times 10^{-5}$	$8 \times 10^{-7}$
0.1	130*	$10^5$	127	90	$5 \times 10^{-6}$	$2 \times 10^{-7}$	$7 \times 10^{-9}$
10	10	27,000	10	7	$1.3 \times 10^{-3}$	$2 \times 10^{-3}$	$10^{-4}$

B. Normal H II Regions:

Name	$n_e$ ( $\text{cm}^{-3}$ )	R (pc)	Observed Angular Radius (arc min)	Observed $S_{\text{H}\alpha}$ ( $\text{erg cm}^{-2} \text{sec}^{-1}$ )
IC 405	28	3.2	16 (d = 0.7, 0.525 kpc)	$5 \times 10^{-4}$
$\lambda$ Ori	10	11	100 (d = 0.37, 0.4 kpc)	$3 \times 10^{-4}$
NGC 7000	16	19	65 (d = 1, 1.13 kpc)	$8 \times 10^{-4}$

\*The light flash has only had time to travel 130 pc since the supernova occurred; the expected equilibrium radius is  $\sim 200$  pc. The H II region would still be growing with the speed of light if the density were this low.

We conclude the following: If  $n_e \sim 0.1 \text{ cm}^{-3}$  the H II region will not be seen in any optical lines. If  $n_e \sim 1 \text{ cm}^{-3}$  it may be possible to detect it in the O[III] lines 5007, 4959 Å. Finally, small clouds with  $n_e \sim 10 \text{ cm}^{-3}$ ,  $R \sim 10 \text{ pc}$  (which should lie within 40 pc from the supernova in order to become completely ionized) would probably be seen in the O[II], O[III] lines. No H-alpha, H-beta radiation is detectable, except for the denser clouds; i.e.: those regions will not show the characteristic H-alpha, H-beta radiation of an H II region. The  $R = 10 \text{ pc}$ ,  $n_e = 10 \text{ cm}^{-3}$  clouds would have a free-free radio flux of 1.5 f.u. at 1,000 MHz (3 f.u. if  $d = 3.5 \text{ kpc}$ ) while the giant region ( $R \sim 100 \text{ pc}$ ,  $n_e \sim 1 \text{ cm}^{-3}$ ) flux is 10 f.u. (if  $d = 3.5 \text{ kpc}$ , 20 f.u.). The small cloud fluxes are too weak to be detected, while the giant H II region is so large that it may be hard to distinguish from the background or from other sources (the remnant itself has a flux of 40 f.u. at 1,400 MHz). A more promising test of the situation would be to see if there is a deficiency of 21-cm emission in the neighborhood of the supernova.

At the position of Tycho, the velocity gradient across the cloud will be a couple of km/sec, comparable to the Doppler broadening at  $100^\circ \text{K}$ . Such a "hole" in 21-cm line profiles would be hard to detect, but not impossible. Williams and Weaver (Williams 1971) have perhaps detected the H II region around Tycho. Their survey indicates that there is no doubt that a 21-cm deficiency exists around Tycho but it is uncertain whether it has anything to do with the supernova. The feature they see shows for several km/sec either side on the  $-45.2 \text{ km/sec}$  velocity map; its diameter is approximately  $1.5^\circ$ . Williams and Weaver see similar holes in places where there is no known supernova remnant. This might be partially explained by the following argument: once an H II region is formed it lasts  $10^6 - 10^7$  years (if  $n_e \sim 0.1 - 1 \text{ cm}^{-3}$ ) while the supernova remnant survives not longer than  $\sim 10^5$  years (Milne 1970).

Therefore the H II region should be seen long after the remnant has disappeared, in the same way that most pulsars (with a lifetime of  $\sim 10^7$  years, Hewish 1970) are not associated with observable remnants.

In concluding it seems appropriate that the following observations should be made to increase our knowledge about the Gum Nebula and supernovae in general:

Interstellar clouds near Tycho, if they indeed exist, should be observed at the O[II], O[III] wavelengths; a survey of the Gum Nebula at the same wavelengths should be made. A survey of Tycho in the radio (21-cm as well as in the recombination lines of helium as pointed out by Dupree 1971) should be conducted. Finally, a survey for large H I "holes" around the galaxy should be conducted and a correlation of these with known supernova remnants or pulsars should be made.

### Acknowledgments

The ideas in this paper were developed jointly with Dr. P. Morrison. I would like to thank Dr. R. A. McCray, Dr. L. Sartori, and Dr. W. H. Tucker for very helpful discussions, Dr. D. R. Williams for kindly giving me permission to publish his 21-cm Tycho map, and Dr. S. P. Maran for providing early information on the Gum Nebula.

## References

- Alexander, J. K., Brandt, J. C., Maran, S. P., and Stecher, T. P. 1971, Ap. J., 167, 487.
- Aller, L. H. 1961, The Abundance of the Elements (New York: Interscience).
- Bok, B. J. 1971, this volume.
- Brandt, J. C., Stecher, T. P., Crawford, D. L., and Maran, S. P. 1971, Ap. J. (Letters), 163, L99.
- Burgess, A. 1965, Ap. J., 141, 1588.
- Cox, D. P., and Tucker, W. H. 1969, Ap. J., 157, 1157.
- Defouw, R. T. 1970, Ap. J., 161, 55.
- Dupree, A. K. 1971, this volume.
- Hewish, A. 1970, Ann. Rev. Ast. Ap., 8, 265.
- Kafatos, M. C., and Morrison, P. 1971, Ap. J., 168, 195. (Paper I.)
- McCray, R. A. and Schwarz, J. 1971, this volume.
- Menon, T. K., and Williams, D. R. 1966, A. J., 71, 392.
- Minkowski, R. 1964, Ann. Rev. Astr. Ap., 2, 247.
- Minkowski, R. 1968, Stars and Stellar Systems, Vol. 7, (Chicago: U. of Chicago Press), p. 623.
- Milne, D. K. 1968a, Austral. J. Phys., 21, 201.
- Milne, D. K. 1968b, ibid., 21, 501.
- Milne, D. K. 1970, ibid., 23, 425.
- Morrison, P., and Sartori, L. 1969, Ap. J., 158, 541.
- Parker, R. A. R. 1964, Ap. J., 139, 208.
- Pottasch, S. R. 1965, Vistas in Astronomy, 6, 149.
- Ramaty, R., Boldt, E. A., Colgate, S. A., and Silk, J. 1971, Ap. J., 169, 87.
- Reichley, P. E., Downs, G. S., and Morris, G. A. 1970 Ap. J. (Letters), 159, L35.
- Sartori, L. 1971, this volume.

Seaton, M. J. 1959, M.N.R.A.S., 119, 81.

Tucker, W. 1971, Ap. J., 167, L85.

Williams, D. R. 1971, private communication.

## DISCUSSION

*A. B. UNDERHILL:*

Shouldn't you see the forbidden N II lines in the H-alpha region, for Tycho?

*M. C. KAFATOS:*

We have not calculated their brightness.

### THREE PROPOSED B-ASSOCIATIONS IN THE VICINITY OF ZETA PUPPIS

Edward K. L. Upton

*University of California, Los Angeles  
Los Angeles, California 90024*

It has recently been suggested by Brandt et al. (1971) that some of the bright B stars within  $4^\circ$  of  $\gamma$  Velorum may comprise a physical association. This suggestion coincides with the conclusions of Robert Altizer and myself from an unpublished study of the distribution of B stars in this part of the Milky Way. Our study tends to confirm the reality of the association around  $\gamma$  Vel. It also indicates the existence of one or two additional associations of B stars in neighboring regions, and gives some indication of the ages of all three groups.

We were interested not so much in stars associated with  $\gamma$  Vel or the pulsar PSR 0833-45, as in those which might be associated with  $\zeta$  Puppis. An O5 star so close to the Sun (about 400 parsecs if  $M_v = -6$ ), and without any obvious cluster or association as its place of origin, presents a strong challenge to the idea that all stars are formed in clusters or associations. The magnitude of the challenge was not entirely clear to begin with, for although no nearby OB-associations had been recognized in the Vela-Puppis area, it was by no means evident that no such association existed. A map of B stars in this area (e.g.: Becvar's *Atlas Australis*) shows plenty of candidates for any number of associations. The problem is to separate out those with distances near 400 parsecs, and to locate the high-density regions at that distance.

With a very low interstellar absorption such as is found in the Vela-Puppis area, the members of an association at a distance of 400 to 500 parsecs and of spectral type B2.5 and earlier will be within the magnitude limit of the Bright Star Catalog. The stars of later spectral types will be mostly below the limit of that Catalog, except that close binaries and evolved stars (luminosity classes III and IV) will still be included to B4 or B5. These considerations indicate that any associations of the type postulated should be discoverable from a study of the distribution of O - B5 stars in the Bright Star Catalog. Fortunately, Hiltner et al. (1969) have included precisely these stars in a new and complete list of revised MK types on a uniform system. These spectrum and luminosity classifications, together with UBV or  $U_c$  BV photometry of the same stars from various sources, are the basis for our present results on the location of B-associations in Vela and Puppis. Some data on fainter stars have also been included in our studies, but this material is so incomplete that it will not be discussed here.

A  $40^\circ \times 30^\circ$  area with limits  $\ell = 235^\circ$  to  $275^\circ$ ,  $b = +10^\circ$  to  $-20^\circ$ , contains 151 HR stars of spectral types B5 and hotter. (This area is centered approximately on  $\zeta$  Puppis, and it includes most of the Gum Nebula.) Distance moduli for all 151 stars have been estimated on the basis of their revised MK types, with suitable allowance for interstellar absorption (small in most cases) derived from 3-color photometry, or from 2-color photometry and spectral types in a few cases. The distance moduli also include some rough corrections, in the case of known visual or spectroscopic binaries, for the excess luminosity of the system over that of a single star. The absolute magnitudes adopted for each MK class are those of Mrs. Lesh (1968).

The stars have been divided into a number of groups, according to the estimated distance moduli, and maps of the apparent distribution in the sky have been made for each group. The most interesting results are obtained for the group with  $7.6 < (m - M)_0 < 8.6$  (Figure 1). This map shows apparent clustering in the four regions labelled A, B, C, D. Region A coincides approximately with the association proposed by Brandt *et al.*

Before accepting the reality of these clusterings, it is well to check whether the same areas stand out on maps of the more distant stars. If they do, they would be more plausibly explained as holes or clear lanes in a nearby dust cloud, than as real clusters. The map of the more distant stars does in fact show a concentration in region D. Furthermore, the distant stars in region D have very small color excesses. Region D is therefore probably a hole in the dust, and not a real cluster. But regions A, B, and C are practically empty on the map of stars with  $(m - M)_0 > 8.6$ . Therefore they appear to be regions where the B-star density at 400 parsecs is really higher than normal.

It is also of interest to see whether the apparent clusterings A, B, and C show up on maps of stars with smaller estimated distance moduli. Clusters B and C are not seen at all for any distance moduli less than 7.6. Cluster A persists for  $(m - M)_0$  as low as 7.0, but not for lower values of the modulus, with a shift of the apparent cluster center toward the bottom of the region outlined in Fig. 1 as the stars with smaller  $(m - M)_0$  are included. All of this suggests that the groups are real, that the accidental errors in the assumed distance moduli do not exceed 0.5 magnitude and that group A is somewhat elongated along the line of sight. Since none of these regions contain any O stars, with the possible exception of the spectroscopic companion to  $\gamma^2$  Vel, it seems appropriate to call them B-associations.

The color-magnitude diagrams for the three proposed B-associations are shown in Figures 2 and 3. These diagrams include stars with estimated distance moduli 7.0 to 7.5, as well as those in the range 7.6 to 8.6 shown in Fig. 1. Symbols refer to luminosity classes and (in class V only) to a star's



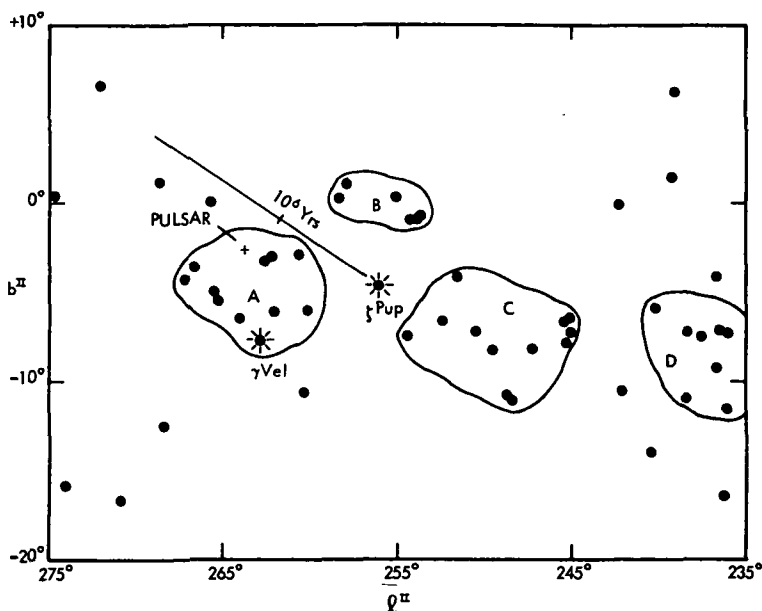


Figure 1. Projection on the sky of O-B5 stars in the Catalogue of Bright Stars with estimated distance moduli 7.6 to 8.6.

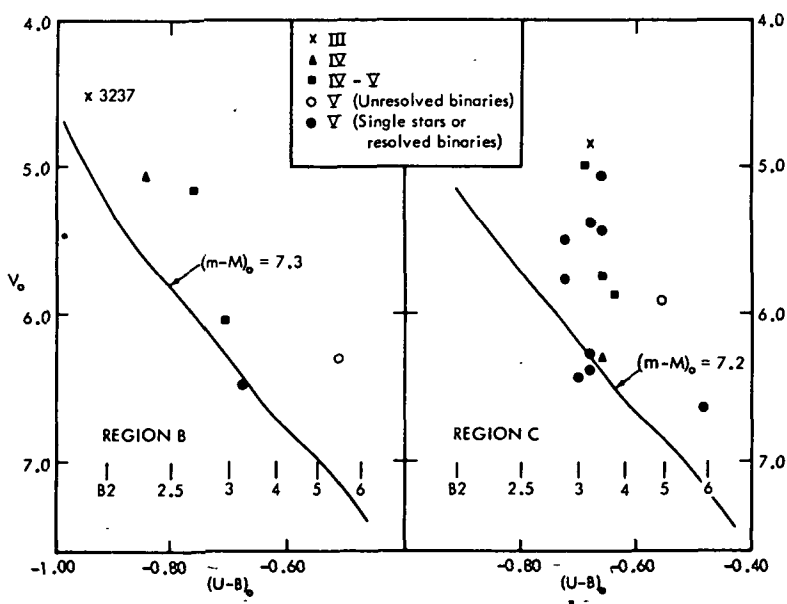


Figure 2. Color-magnitude diagrams for the stars in regions B and C, with estimated distance moduli 7.0 to 8.6.

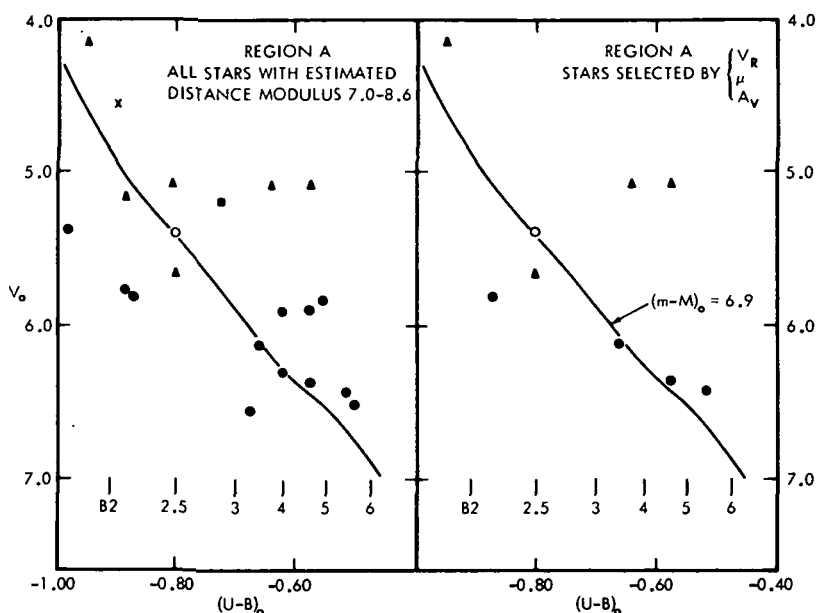


Figure 3. Color-magnitude diagrams for the stars in region A, with estimated distance moduli 7.0 to 8.6. Symbols have the same meaning as in Figure 2.

status as single, resolved binary, or unresolved binary. (A number of visual binaries are counted as "resolved," in the sense that photometry of the combined pair has been reduced to the light of the primary alone, on the basis of visual estimates of  $\Delta V$  and the assumption that both stars lie on the main sequence.) The zero-age main-sequence curve in each diagram is that of Blaauw (1963), fitted to the single stars and resolved binaries of luminosity class V.

The color-magnitude diagram for association C shows a well-defined main sequence turnoff at B3, corresponding to an age of about 50 million years. The main sequence itself appears to be barely reached at apparent magnitude 6.5. The distance of this group cannot be accurately deduced from the stars shown in Figure 2, but it appears to be more nearly 300 parsecs than 400. A similar result is found for associations A and B as well. All three groups appear to have mean distance moduli much closer to 7 than to 8, on the basis of the color-magnitude diagrams. The original estimates of distance modulus appear to have been systematically too large. In part this is due to the fact that Lesh's  $M_V$  values for luminosity class V are systematically brighter than the Blaauw values for the zero-age main sequence.

It should also be remarked that the interpretation just given for the color-magnitude diagram of association C implies that the MK luminosity classes do not mean very much, at least not in the range IV to V. Alternatively, if these classifications do correspond closely to luminosity, then this group of stars must have a substantial spread in depth, corresponding to  $0^m 8$  or more in  $(m - M)_0$ . The angular size of region C would lead one to expect a total spread of about  $0^m 3$  in  $(m - M)_0$ .

Concerning association B, little can be said beyond the fact that its distance is approximately the same as that of C, but its age is evidently considerably smaller.

Association A, which contains both  $\gamma$  Vel and PSR 0833-45 within its limits, is situated in the larger bright area of the Gum Nebula. It may be the place of origin of  $\zeta$  Puppis, a question to which I shall return in a moment. Its color-magnitude diagram (Figure 3, left) does not show any well-defined turnoff, but the diagram is not easy to interpret because of the apparent spread in distance moduli of the stars. I have tried to obtain a clearer diagram by excluding all stars which lie outside the main distribution in radial velocity, proper motion, or color excess. The results of this elimination appear in Figure 3, right. This reduced list of high-probability association members is the basis for the main-sequence curves drawn in both halves of the figure. As in groups B and C, the color-magnitude diagram indicates a smaller mean distance than the original estimates based on luminosity classes. If we assume that most of the stars in Figure 3 are on the zero-age main sequence, their range in distance modulus is about 6.5 to 7.6.

The question whether any of the stars in association A have significantly evolved off the zero-age main sequence is important in connection with the origin of  $\zeta$  Puppis. The proper motion of  $\zeta$  Pup, relative to the mean value for association A, is shown projected backward in time in Figure 1. An interpretation of  $\zeta$  Pup as a "runaway star" of moderate velocity from the northern part of region A is plausible, if the stellar types in this association are compatible with an age of  $3 \times 10^6$  years or less. This figure is approximately the main-sequence life-time of a normal O5 star. The age of  $\zeta$  Pup as a runaway would have to be 1 million years or less, if it originated in region A, but its total age could be as high as 3 million years.

Association A does not contain any stars of spectral class earlier than B1.5, except for  $\gamma^1$  and  $\gamma^2$  Vel. But this circumstance by itself does not rule out a very young age compatible with  $\zeta$  Pup. The proposed cluster is not a rich one, and it might very well have been formed with no more than one or two stars in the range O5-B1. NGC 2264 may be mentioned as a well-established cluster of this kind.

The most serious obstacle to the identification of association A as the birthplace of  $\zeta$  Puppis is the presence in it of some B1-B5 stars of luminosity classes III and IV. There are seven such stars in the area, when the limits of estimated distance modulus are taken as 7.0 and 8.6. But the one star of class III has an anomalously high color excess, as have two of the six stars of class IV. These stars may be tentatively assigned a larger distance than the main group. The remaining four stars of class IV cannot be eliminated on the basis of velocity or reddening. In order to assign a very young age to the association it is necessary to assume either that the luminosity classifications of Hiltner *et al.* are sometimes wrong by one class, so that these stars are really all class V; or else that the four stars in question are not true members. At this stage of our knowledge it does not seem difficult to accept one or both of these assumptions, and we therefore consider association A as a likely birthplace of  $\zeta$  Puppis. But much remains to be learned about association A, especially since its reality as a physical group is not yet entirely established.

To summarize, there appear to be three loose B-associations in the general vicinity of  $\zeta$  Puppis, all at distances of approximately 300 to 400 parsecs from the Sun. Their diameters perpendicular to the line of sight are 20 to 50 parsecs, and their separations are of similar size. All three of them are situated in bright areas of the Gum Nebula. The proposed associations A and C lie in the two brightest parts of the nebula. The three associations are not all of the same age. Association C is about 50 million years old, whereas A and B are decidedly younger. The ages of A and B cannot be determined from the present data, as their color-magnitude diagrams show no clear signs of turnoff from the main sequence. Association A may be young enough to qualify as the birthplace of  $\zeta$  Puppis, but no definite conclusion on this point is yet possible. It can be asserted with confidence that there is no other identifiable association in which  $\zeta$  Puppis can have originated, unless its age is substantially greater than the 3 million years I have assumed.

Aside from the question of origin of  $\zeta$  Pup, association A is in any case the locus of a Wolf-Rayet star and, apparently, a pulsar. Further investigations of this region will therefore be of great value. If the pulsar is indeed a member of the association, its original mass must have been at least  $15 M_{\odot}$ . An even higher figure can be set if it is established that  $\zeta$  Pup is also a member.

## References

- Becvar, A. 1964, Atlas Australis (Prague: Czechoslovak Academy of Sciences).
- Blaauw, A. 1963, in Basic Astronomical Data, ed. K. Aa. Strand (Chicago: University of Chicago Press), p. 407.
- Brandt, J. C., Stecher, T. P., Crawford, D. L., and Maran, S. P. 1971, Astrophys. J. (Letters), 163, L99.
- Hiltner, W. A., Garrison, R. F., and Schild, R. E. 1969, Astrophys. J., 157, 313.
- Lesh, J. R. 1968, Astrophys. J. Supplement, 17, No. 151.

## COMMENTS ON AN ASSOCIATION IN VELA

W. C. Straka

*Department of Astronomy, Boston University  
Boston, Massachusetts 02215*

I was aware of Dr. Upton's excellent work on O- and B-Associations, since he was my thesis advisor on a quite different topic. However, I did not know he had worked on this specific region.

In November 1970, when I became aware of the Brandt et al. (1971) suggestion of an association in the Vela pulsar region, I went to the catalogs to see what evidence was available on motions, distances, and so on. This work has been submitted for publication.

I found that the proper motions do not correlate very well with the suggestion of an association. Of the 10 stars looked at by Brandt et al., 5 seem to be moving together, and the other 5 in widely scattered directions. The radial velocities do not correlate with the proper motions or the distances found by Brandt et al.

I then looked at all O and B stars in a  $10^\circ$  radius region around  $\gamma$  Vel, about 500 in all. Again the proper motions do not correlate. Few radial velocities are available. However, most of the proper motions are of the order of the errors of measurement.

I next looked at the H-R diagram of the 500 stars. Here a strong suggestion of an association appears. There is a definite bunching in the diagram around the mean line. The indicated distance is about 500 parsecs, in good agreement with the pulsar distance and with the Brandt et al. stars, and also in agreement with Upton. The sample will clearly include background stars. I therefore tried several ways of eliminating the non-member stars. The first method was a selection by proper motion to match  $\gamma^2$  Vel. As mentioned earlier, this also eliminates half the Brandt et al. stars. The second method was to eliminate those stars at each spectral type which were more than 1 rms deviation away from the mean apparent magnitude. At each spectral type, the rms spread is about  $\pm 1$  mag. The third method involved eliminating only those stars more than 1 rms deviation fainter than the mean apparent magnitude at each spectral type. None of these methods of elimination altered the diagram in shape significantly, although elimination of the faint stars produced a mean magnitude for the remaining stars at each spectral type about 1/2 mag. brighter for the B8 and B9 stars, but much less for the earlier types.

The mean line lies close to a main sequence up to about B2 or B3. Then earlier types (mostly the Brandt et al. stars) tend upward from a zero age main sequence. Upton's region A corresponds closely to my selected stars, and his color-magnitude diagram is in agreement. He does not, however, include all of the Brandt et al. stars and thus finds no definite turnoff from the main sequence.

The evidence, then, for the association near the Vela pulsar rests on the H-R diagram, and is not supported by the motions. But the H-R diagram, both as done by Upton and by me is strongly suggestive.

It is interesting to note that, if the Vela pulsar is a member of this association, a rather large mass is implied. Some of the Brandt et al. stars are quite massive, notably  $\gamma^2$  Vel at 46 and 16 solar masses for the two components. A coeval hypothesis would call for a pre-supernova mass for the pulsar of more than 30 solar masses. If we take a spread in formation times of  $10^8$  or so years, as suggested by Iben and Talbot, we can get down to about 10 solar masses. This agrees with the suggestion made by Gott on a dynamical basis, although I know that Professor Cameron is quite unhappy with such a large mass.

#### References

- Brandt, J. C., Stecher, T. P., Crawford, D. L., and Maran, S. P. 1971, Ap. J. (Letters), 163, L99.
- Gott III, J. R., and Ostriker, J. P. 1971, this volume.
- Iben Jr., I., and Talbot, R. J. 1966, Ap. J., 144, 968.
- Upton, E. K. L. 1971, this volume.

# A DISCUSSION OF THE H-ALPHA FILAMENTARY NEBULAE AND GALACTIC STRUCTURE IN THE CYGNUS REGION

Thomas A. Matthews and S. Christian Simonson, III  
*Astronomy Program, University of Maryland*  
*College Park, Maryland 20742*

## Abstract

From a discussion of the galactic structure in Cygnus, the system of filamentary nebulae is found to lie at a distance of roughly 1.5 kpc, in the same region as about half the thermal radio sources in Cygnus X, the supernova remnant near  $\gamma$  Cygni, and the association Cygnus OB2, in the direction of which the X-ray source Cygnus XR-3 is observed. The source of excitation seems likely to have been the pulse of radiation from a supernova explosion, as has been proposed in the case of the Gum Nebula, but continuing excitation by early-type stars in the region of Cygnus X cannot be excluded.

## Introduction

The region in Cygnus from  $l = 70^\circ$  to  $90^\circ$ ,  $b = -10^\circ$  to  $+10^\circ$ , is unusual for the large number of sharp filaments found on either side of the galactic plane (Figure 1). We shall first discuss the location of the filaments with regard to that of other galactic features in this region, and then we shall discuss the question of whether the source of their excitation might have been the pulse of radiation from a supernova explosion such as has been suggested by Brandt *et al.* (1971) for the Gum Nebula.

### I. The Distance to the Filaments and their Relation to Other Features

The galactic structure in the Cygnus region is difficult to untangle. We are looking almost tangentially along a spiral feature containing a large number of dense dust clouds which hide much of the region from us optically. In addition, the velocity-distance relation gives velocities in the range  $\pm 5 \text{ km s}^{-1}$  at  $l = 80^\circ$  out to a distance of 4 kpc.

Notable features of the region, in addition to the filaments and the dark clouds, include the following objects: i) The complex of thermal radio sources Cygnus X contains many H II regions, a few of which are associated with visible emission nebulae. ii) Several OB associations range in distance from 1 kpc to 2.3 kpc (Alter, Balázs, and Ruprecht 1970). One of these, Cygnus OB2 ( $l = 80^\circ.1$ ,  $b = +0^\circ.9$ ), lies at a distance of 1.5 kpc (Schulte 1958) in the direction of the center of Cygnus X and of the system of filaments.



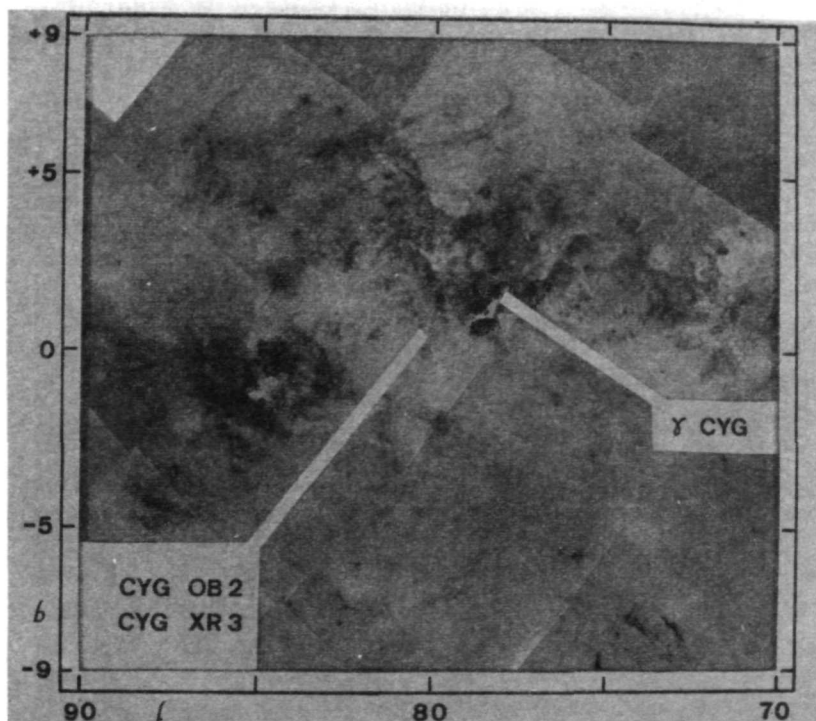


Figure 1. Region of filamentary nebulae in Cygnus (montage of Sky Survey Red prints). Copyright by National Geographic Society-Palomar Observatory Sky Survey.

iii) The X-ray source Cygnus XR-3 is observed within the projected boundaries of Cygnus OB2 at  $l = 80^{\circ}.0$ ,  $b = +0^{\circ}.7$  (Giacconi *et al.* 1967). Gorenstein, Giacconi, and Gursky (1967) point out that the low-energy attenuation observed in the spectrum of Cygnus XR-3 indicates a column density of neutral hydrogen of  $3 \times 10^{22} \text{ cm}^{-2}$ . Although this could be intrinsic to the source, it could also indicate a distance of a few kiloparsecs (Gursky, Gorenstein, and Giacconi 1967). iv) The supernova remnant near  $\gamma$  Cygni, designated by its galactic coordinates (Wendker 1970) G 78.2 + 1.8, has a diameter of 8 arc min and a flux density  $S(400 \text{ MHz}) = 630$  flux units (Higgs and Halperin 1968). Using the relation given by Poveda and Woltjer (1968), we estimate its distance as 1.4 kpc; Downes (1971) estimates its distance as 3.4 kpc.

At present the most practical way of obtaining distances to the emission nebulosities in the region is by associating them with dust whose distribution

can be estimated from star counts and from measurements of the reddening of early-type stars. According to Miller's (1937) analysis of star counts, the nearby dust clouds in this direction begin about 600 pc from the sun. The most extensive observations of the interstellar reddening of stars in this region are those of Ikhsanov (1959), who gives curves of absorption against distance for eight regions in a  $6^\circ$  square area NW of  $\gamma$  Cygni, an area where many filaments are seen. His curves appear to be reliable out to distances of 1.5 to 2 kpc. He confirms Miller's results, and in addition, he finds that the more distant dark clouds between  $\ell = 78^\circ$  and  $85^\circ$  set in at about 1 kpc. These results are further confirmed by Neckel's (1967) analysis of existing photoelectric measurements and MK spectroscopic classifications. Neckel's results show that significant absorption in otherwise clear regions sets in between 2 and 3 kpc.

#### a) Filaments

The Palomar Observatory Sky Survey shows numerous sharp filaments from  $\ell = 75^\circ$  to  $87^\circ$  between  $b = +2^\circ$  and  $+7^\circ$ . Some fainter filaments are found between  $\ell = 77^\circ$  and  $83^\circ$ ,  $b = -3^\circ$  to  $-8^\circ$ . Filaments of this nature are uncommon on the Sky Survey plates. Van den Bergh's (1960) search of the Sky Survey yielded nine examples of this type of filaments, including this region; the remaining eight are well-known supernova remnants. Thus, it is highly likely that the Cygnus filaments have been produced by a single event. Although there is no well-defined geometric center of these filaments, a circle of radius 8.5 degrees centered at  $\ell = 80^\circ$ ,  $b = +1^\circ$ , includes most of them. Morgan, Strömgren, and Johnson (1955) noted that the filaments north of the galactic plane seem oriented perpendicularly to the line toward Cygnus OB2; this has been confirmed quantitatively by Dickel, Wendker, and Bieritz (1970). The association Cygnus OB4 ( $\ell = 82^\circ.5$ ,  $b = -7^\circ.3$ ) lies in the direction of some of the filaments south of the galactic plane, and a weak X-ray source, Cygnus XR-4, has been reported in this region (Giacconi et al. 1967).

In estimating a distance to the filaments, we first note, as has been remarked by Ikhsanov (1960), that because an insignificant amount of radio continuum emission is seen in their direction, the filaments are unlikely to be intrinsically very bright structures that are obscured by dust. This is confirmed by comparison of the filaments appearing in the list of H-alpha sources by Dickel, Wendker, and Bieritz (1969) and the list of discrete radio sources in the same region by Wendker (1970). We identify 86 of the H-alpha sources of Dickel et al. with filaments; nine of these appear in Wendker's list. However, since their flux is very low, the uncertainty in the background corrections makes a determination of the reddening meaningless.

In the area of the sky that he surveyed, Ikhsanov's (1959) regions 1 and 7 contain most of the bright filaments. The filaments appear to be obscured or in some cases partially obscured by dark clouds in regions 2, 6, and 8; essentially no filaments are observed in regions 3, 4, and 5. According to the results of both Ikhsanov and Neckel (1967), in the regions where filaments are obscured or absent, significant absorption amounting to several magnitudes sets in at distances around 1 kpc. By contrast, in regions 1 and 7, which contain most of the bright filaments, there is no significant absorption before a distance of 1.6 kpc; however, by 2.5 kpc significant absorption has set in. The small number of stars observed beyond 1.6 kpc does not allow the onset of absorption to be defined more accurately. We tentatively conclude that the filaments lie in the range 1 to 2 kpc, and we shall adopt a mean distance 1.5 kpc.

### b) Thermal Radio Sources

A detailed radio map of Cygnus X (Wendker 1970) shows 76 discrete thermal radio sources in this area, which are probably all more or less obscured H II regions. By comparing the H-alpha radiation and the radio continuum flux, Dickel et al. (1969) estimated the absorption in front of these regions and then determined distances from Ikhsanov's (1959) curves of absorption against distance. Only 20 percent of the H II regions are more distant than 4 kpc. Most of them are found in the interval from 1 kpc to 2.5 kpc; slightly more than half are in the range 1.2 to 1.8 kpc.

In addition to these discrete sources, Wendker (1970) finds an unresolved background thermal source containing about half the total flux of Cygnus X lying within an area of size  $5.6 \times 3.5$  (at the  $T_b = 1^\circ\text{K}$  level) covering essentially the same area where the discrete thermal sources are found.

## II. The Source of Excitation of the Filaments

We now turn to a discussion of the objects observed near the location of the filaments to consider the possibilities for their excitation. At the distance 1.5 kpc near  $l = 80^\circ$ ,  $b = +1^\circ$ , we find the association Cygnus OB2, more than half the discrete radio sources in the Cygnus X complex, and the supernova remnant G 78.2 + 1.8. The distance of Cygnus XR-3 is uncertain, but it too could be at this same distance. We shall also consider the suggestion of van den Bergh (1960) that the filaments are themselves a supernova remnant similar to the Cygnus Loop.

## a) The State of the Filaments

We consider two possibilities for the state of excitation of the filaments: i) steady state, in which the flux of Lyman continuum photons is proportional to the product of the densities of ions and electrons, and ii) ionization by a radiant pulse, in which the total energy of radiation above the Lyman limit, in terms of 15-eV photons, is equal to the number of electrons.

No pulsars have as yet been detected in the region of the filaments in Cygnus (Maran and Modali 1970). Therefore we have relied on the H-alpha emission measurements of Dickel *et al.* (1969) to obtain the parameters listed in Table 1. In order to calculate the r.m.s. electron density  $(n_e^2)^{1/2}$  for the filaments we need to know the thickness  $L$  in the line of sight. We have considered two cases: i) "sheets" seen edge-on, for which  $L$  has been taken to be the larger dimension, and ii) "cylinders", for which  $L$  has been taken to be the smaller dimension. We have adopted the electron temperature  $T_e = 6000^\circ\text{K}$  used by Dickel *et al.* (1969), which can be considered reasonable for case i), and we note the dependence of the resulting energy in case ii) as  $T_e^{0.425}$  (Seaton 1959). We have expressed the ionizing flux for case i) in terms of the ionization parameter,

$$U = [(3/4 \pi) \int n_e^2 dV]^{1/3}$$

where the integral is taken over the ionized region, and in terms of O5 stars, for which we have adopted an effective temperature of  $49,500^\circ\text{K}$  (Hjellming 1968a) and an ionization parameter  $U = 74 \text{ pc cm}^{-2}$  (Hjellming 1968b).

The number of filaments seen is strongly influenced by obscuration. In order to estimate the total number of filaments we have chosen a sector of angle  $60^\circ$  from position angle  $310^\circ$  to  $10^\circ$  centered on  $\ell = 80.0$ ,  $b = +0.7$ , as being a typical unobscured region. No filaments are seen closer than  $2^\circ$  to this center because of the foreground dust clouds. In the unobscured region there are 71 sources from the list of Dickel *et al.* (1969) that we identify as filaments. Within a circle of radius  $8.5$  we estimate there are about six times this number of filaments, or about 430 in all. The parameters in Table 1 for 86 observed filaments are then multiplied by a factor 5 to refer to the expected total number of filaments.

## b) Cygnus OB2 and Cygnus X

We have used Wendker's (1970) observations at 2695 MHz to derive the size and radio flux from the H II regions in Cygnus X. We have examined his map and have summed all the 66 discrete thermal sources not associated with visible filaments. The parameters for the sum of these sources are given in Table 1. According to Dickel *et al.* (1969) slightly more than half

Table 1  
Parameters of extended emission regions in Cygnus

Type of Object	Number of Objects	Total Area (deg <sup>2</sup> )	Total Volume <sup>(3)</sup> (cm <sup>3</sup> )	Total Flux	Average Emission Measure (pc cm <sup>-6</sup> )	$n_e^{2,1/2}$ <sup>(6)</sup> (cm <sup>-3</sup> )	Total Electrons	Mass (M <sub>⊙</sub> )	Ionization Parameter (pc cm <sup>-2</sup> )	Energy Required for Ionization	
										(erg) <sup>(7)</sup>	(O5 stars) <sup>(8)</sup>
<u>Filaments</u>											
(observed)	44+	3.1	—	2.6 <sup>(4)</sup>	500	—	—	—	69	—	0.8
"sheets"	42 <sup>(1)</sup>	—	9.6 × 10 <sup>59</sup>	—	—	4.0	3.9 × 10 <sup>60</sup>	3.2 × 10 <sup>3</sup>	—	1.6 × 10 <sup>50</sup>	—
"cylinders"	—	—	2.6 × 10 <sup>59</sup>	—	—	8.2	2.1 × 10 <sup>60</sup>	1.7 × 10 <sup>3</sup>	—	8.8 × 10 <sup>48</sup>	—
<u>Filaments</u>											
(estimated)	430	15.5	—	13.0 <sup>(4)</sup>	500	—	—	—	118	—	4.0
"sheets"	—	—	4.8 × 10 <sup>60</sup>	—	—	4.0	2.0 × 10 <sup>61</sup>	1.6 × 10 <sup>4</sup>	—	8.0 × 10 <sup>50</sup>	—
"cylinders"	—	—	1.3 × 10 <sup>60</sup>	—	—	8.2	1.1 × 10 <sup>61</sup>	8.5 × 10 <sup>3</sup>	—	4.4 × 10 <sup>49</sup>	—
<u>H II Regions</u>											
1	66	8.8	2.0 × 10 <sup>60</sup>	2060 <sup>(5)</sup>	7050	21.0	4.2 × 10 <sup>61</sup>	3.5 × 10 <sup>3</sup>	217	—	25
<u>Thermal Background</u>											
1	1	40.4 <sup>(2)</sup>	1.1 × 10 <sup>61</sup>	2990 <sup>(5)</sup>	2260	2.9	3.2 × 10 <sup>61</sup>	2.7 × 10 <sup>4</sup>	245	—	36

(1) Dickel et al. (1969) list 42 sources for which no H-alpha flux is given. We have arbitrarily assumed 0.1 (10<sup>-4</sup> cgs).

(2) Area observed by Wendker (1970) and appropriate for his total flux of 2990 for unresolved and "unaccounted for" H II emission.

(3) Distance assumed to be 1.5 kpc.

(4) S(Hα) 10<sup>-14</sup> W m<sup>-2</sup> (flux).(5) S(2695 MHz) 10<sup>-26</sup> W m<sup>-2</sup> Hz<sup>-1</sup> (flux density).

(6) Calculated as uniform sphere.

(7) Calculated on assumption of one 15-eV photon per electron.

(8) Flux necessary to sustain ionization based on ionization parameter of 74 pc cm<sup>-2</sup> for an O5 star.

of these sources are near the distance 1.5 kpc. The results for the unresolved thermal background are also taken from Wendker (1970). Although the distance distribution of this source is unknown, from its location and extent we have considered it likely that it is largely concentrated in the region near 1.5 kpc where most of the discrete sources are found and near a possible source of excitation, Cygnus OB2.

As given in Table 1, the value of  $U$  for the discrete sources is  $217 \text{ pc cm}^{-2}$  and that for the thermal background is  $245 \text{ pc cm}^{-2}$ . These have been calculated using the relations given by Hjellming (1968a) for mean temperature  $6000^\circ\text{K}$ , frequency 2695 MHz, and distance 1.5 kpc. Véron (1965) has calculated the ionization parameter of Cygnus OB2 to be  $170 \text{ pc cm}^{-2}$  for stars with MK spectral types. Using the calibration of Hjellming (1968a, b), this value should be adjusted to  $120 \text{ pc cm}^{-2}$ . Since Cygnus OB2 has only weak H-alpha and continuum emission in its immediate vicinity (Wendker 1970), it seems a likely source of excitation for much if not all of the thermal background, especially in view of the incomplete spectral classification for Cygnus OB2, the uncertainties in the calibration of spectral type and effective temperature, and the possible existence of additional obscured members. On the other hand, the discrete thermal sources may well be excited by one or more early-type stars embedded in them and heavily obscured by dust. For instance, on the average, eight O9 V stars ( $U = 25 \text{ pc cm}^{-2}$ ) would be required, these being obscured by 6 magnitudes to fall below the limit of discovery (roughly  $V = 12 \text{ mag}$ ). Obscuration of this amount certainly occurs in this region. Thus, it seems possible to account for the thermal radiation from the complex by attributing the source of the excitation to obscured early-type stars.

In view of the relatively small flux required to ionize the filaments in the steady-state hypothesis (case i) in addition to that required for the excitation of the whole Cygnus X complex, Cygnus OB2, augmented by other early-type stars and perhaps also by Cygnus XR-3, must be considered a possible source of their excitation.

### c) Excitation by a Supernova Explosion

The amount of energy required in case ii), ionization by a pulse of radiation in a brief event, is roughly  $10^{50} \text{ erg}$ . The only likely source of such an amount of energy is a supernova explosion (Morrison and Sartori 1969).

The appearance of the filaments tends to support this interpretation. It is important to note that the filaments do not resemble in any way Barnard's Loop in Orion; most significantly the filaments contain no "elephant trunk"

structures indicative of expansive motion from a long-lasting center of thermal energy. Rather, they have the appearance of intrinsic structures in the interstellar medium such as those seen in the form of dark clouds and reflection nebulae. Brandt *et al.* (1971) have also suggested a similar interpretation in the case of the Gum Nebula. The filamentary structures in the Gum Nebula are similar in appearance to those in the Cygnus region if they are a factor 10 closer to the sun.

The supernova explosion must have occurred at a time longer than the light travel time but shorter than the recombination time. The light travel time is about 700 years. Spitzer (1968) gives the recombination rate as  $2.6 \times 10^{-13} n_e^2 \text{ cm}^{-3} \text{ s}^{-1}$  at  $T_e = 10^4 \text{ }^\circ\text{K}$ , varying as  $T_e^{-1/2}$ . This corresponds to a recombination time of  $1.2 \times 10^5 n_e^{-2}$  years assuming  $T_e = 10^4 \text{ }^\circ\text{K}$ . For the filaments the recombination time is  $8 \times 10^3$  years (sheets), or  $1.8 \times 10^3$  years (cylinders). However, in the case of ionization by a supernova explosion the temperature could well be much higher and the recombination time longer.

If a supernova flash illuminated the filaments at a time on the order of  $10^3$  years in the past, we should expect to observe the supernova remnant. We consider the following candidates: i) the supernova remnant G 78.2 + 1.8, ii) the nonthermal radio sources G 78.4 + 2.5 (Wendker 1970) and iii) G 78.6 + 1.0, and iv) the X-ray source Cygnus XR-3. The distance to G 78.2 + 1.8 is 1.4 kpc as derived from Poveda and Woltjer's (1968) relation or 3.4 kpc as given by Downes (1971). Both are probably uncertain by a factor  $\sim 2$ , but the distance seems likely to be in the same range of distance as the filaments. By comparison with other supernova remnants in the list of Poveda and Woltjer (1968) its radius of 3 pc at the distance 1.4 kpc would seem to imply an age of roughly  $10^3$  years. According to Downes (1971), its surface brightness indicates an age of less than  $2 \times 10^3$  years. These ages are of the same order of magnitude as the light travel time and the recombination times discussed above. The supernova remnants G 78.4 + 2.5 and G 78.6 + 1.0 are both probably more distant than the region containing the filaments (Downes 1971). While observed within the projected area of the Cygnus X complex, these sources are  $2^\circ$ ,  $2.5^\circ$ , and  $1.4^\circ$ , respectively, away from the geometric center of the filaments. Cygnus XR-3 is observed in the direction of the filaments, but it has no associated nonthermal radio source; consequently, it is not similar to X-ray sources associated with known supernova remnants (Palmieri *et al.* 1971). On the basis of our present knowledge we consider G 78.2 + 1.8 to be the most likely candidate of the three.

A third alternative to the above models is collisional ionization by the expanding shell of gas thrown off in a supernova explosion, as has been suggested by

van den Bergh (1960). If the filaments represent a late stage in expansion of a supernova remnant, as would be suggested under this hypothesis by the size of the structure, which is ten times that of the largest supernova remnants in the list of Poveda and Woltjer (1968), then their age would be expected to be at least of the order of  $10^6$  years. Given a rate of supernova explosions in the galaxy of roughly one per 100 years then the entire galactic plane would be expected to be covered with such luminous filaments. This inference does not agree with observations, and thus the model is unattractive.

### III. Conclusion

We find the distance of the filaments to lie in the range 1 to 2 kpc from an analysis of their distribution with respect to dust clouds. Thus, they lie in the same region as Cygnus OB2, half the radio sources in the Cygnus X complex, probably the supernova remnant G 78.2 + 1.8, and probably Cygnus XR-3. The excitation of the discrete and spread thermal sources seems likely to be supplied by early-type stars. While the excitation of the filaments could also be due to early-type stars, their form suggests that they are more likely to have been ionized by a brief event, such as a radiant pulse from a supernova. It seems unlikely that their ionization is caused by the late stages of expansion of a supernova shell.

### Acknowledgment

We thank Mr. J. L. Saba for constructing the photomontage in Figure 1.



## References

- Alter, G., Balázs, B., and Ruprecht, J. 1970, Catalogue of Star Clusters and Associations, 2nd edition (Budapest: Akademiai Kiadó).
- Bergh, S. van den 1970, Z. Astrophys., 51, 15.
- Brandt, J. C., Stecher, T. P., Crawford, D. L., and Maran, S. P. 1971, Ap. J. (Letters), 163, L99.
- Dickel, H. R., Wendker, H., and Bieritz, J. H. 1969, Astron. Astrophys., 1, 270.
- \_\_\_\_\_. 1970, in The Spiral Structure of Our Galaxy, ed. W. Becker and G. Contopoulos (Dordrecht: Reidel), p. 213.
- Downes, D. 1971, A. J., 76, 305.
- Giacconi, R., Gorenstein, P., Gursky, H., and Waters, J. R. 1967, Ap. J. (Letters), 148, L119.
- Gorenstein, P., Giacconi, R., and Gursky, H. 1967, Ap. J. (Letters), 150, L85.
- Gursky, H., Gorenstein, P., and Giacconi, R. 1967, Ap. J. (Letters), 150, L75.
- Higgs, L. A., and Halperin, W. 1968, M.N.R.A.S., 141, 209.
- Hjellming, R. M. 1968a, Ap. J., 154, 533.
- \_\_\_\_\_. 1968b, in Interstellar Ionized Hydrogen, ed. Y. Terzian (New York: W. A. Benjamin), p. 171.
- Ikhsanov, R. N. 1959, Izv. Krymsk. Astrofiz. Observ., 21, 257.
- \_\_\_\_\_. 1960, Sov. Astr.-AJ, 4, 258.
- Maran, S. P., and Modali, S. B. 1970, Earth Extraterr. Sci., 1, 147.
- Miller, F. D. 1937, Proc. Nat. Acad. Sci., 23, 405.
- Morgan, W. W., Strömgren, B., and Johnson, H. M. 1955, Ap. J., 121, 611.
- Morrison, P., and Sartori, L. 1969, Ap. J., 158, 541.
- Neckel, T. 1967, Veröffentl. Landessternwarte Heidelberg-Königstuhl, 19, 1.
- Palmieri, T. M., Burginyon, G., Grader, R. J., Hill, R. W., Seward, F. D., and Stoering, J. P. 1971, Ap. J., 164, 61.
- Pottasch, S. 1960, Ap. J., 132, 269.

Poveda, A., and Woltjer, L. 1968, A. J., 73, 65.

Schulte, D. H. 1958, Ap. J., 128, 41.

Seaton, M. J. 1959, M.N.R.A.S., 119, 81.

Spitzer, L., Jr. 1968, Diffuse Matter in Space (New York: Interscience).

Thompson, A. R., Colvin, R. S., and Hughes, M. P. 1969, Ap. J., 158, 939.

Véron, P. 1965, Ann. Ap., 28, 391.

Wendker, H. J. 1966, Mitt. Astr. Inst. Univ. Münster, No. 10.

\_\_\_\_\_. 1970, Astron. Astrophys., 4, 378.

# RADIOFREQUENCY RECOMBINATION LINES FROM THE INTERSTELLAR MEDIUM

A. K. Dupree

*Harvard College Observatory  
Cambridge, Massachusetts 02138*

## Abstract

A selective discussion is given of observations of recombination lines from "normal" H II regions, extended H II regions, nonthermal sources, and the H I medium. Detection of recombination lines from elements other than hydrogen may provide a means of identifying "fossil Strömberg spheres" at high temperature.

## I. Introduction

The capture of an electron by an ion into a highly excited level (principal quantum number  $n \gtrsim 60$ ) and the subsequent cascade to the ground term can produce line emission in the radiofrequency portion of the spectrum. The emission frequency is given by  $\nu = cRZ^2 [n^{-2} - (n + \Delta n)^{-2}]$  where  $R$  is the Rydberg constant for an element of charge  $Z$ . When  $\Delta n = 1$ , the transition is denoted as an  $\alpha$ -transition; when  $\Delta n = 1$ , a  $\beta$ -transition; etc. Such lines are observed in the spectra of H II regions, where transitions over a wide range in principal quantum number,  $n = 57 \rightarrow 56$  (56  $\alpha$ ) at 36.5 GHz to  $n = 254 \rightarrow 253$  (253  $\alpha$ ) at 400 MHz, have been detected from hydrogen (Sorochenko *et al.* 1969; Penfield *et al.* 1967). Higher order transitions, involving a change in principal quantum number greater than one, have also been observed up to  $\Delta n = 5$  (so-called  $\epsilon$ -transitions). The strongest recombination lines found to date are those of hydrogen; lines from helium are present if the excitation of the H II region is sufficiently high, but the intensity is about a factor of 10 less than that of hydrogen because of the lower helium abundance. Narrow recombination lines observed in the spectra of H II regions appear to be formed in H I clouds between the source H II regions and the observer.

Study of recombination lines has extraordinary value. They can be used as diagnostic tools in determining the physical parameters of the emitting region: radial velocity, electron temperature, electron density, turbulent velocity, and emission measure. In addition, the fractional ion concentration can be derived from intensity ratios of two lines originating in the same region and produced by different elements.

In the following sections we note selected results on studies of recombination lines from thermal and nonthermal sources and suggest observations that may be useful in studying "Gum Nebulae" and related objects.

## II. Thermal Sources

### A. Normal H II Regions

To understand how recombination lines vary in different sources, it is useful to briefly describe the solutions to the transfer equation for the line and continuum intensities in a normal H II region. Here ionization results from the ultraviolet radiation field or nearby exciting stars. Recombination takes place via radiative processes also, and the high levels of atoms producing recombination lines are not populated in equilibrium at the local electron temperature. The continuum emission however is due to thermal bremsstrahlung. The line-to-continuum ratio for a recombination line formed by a transition from upper level  $m$  to lower level  $n$  in an isothermal, homogeneous, optically-thin gas is given by

$$\frac{T_L}{T_C} = \frac{\tau_L^*}{\tau_C} \left[ b_m - \frac{1}{2} b_n \beta_{nm} (\tau_C + b_m \tau_L^*) \right] \quad (1)$$

where the optical depths in local thermodynamic equilibrium (LTE) of the line and continuum are given by  $\tau_L^*$  and  $\tau_C$  (Dupree and Goldberg 1970). The non-LTE departure coefficient for level  $n$  is denoted by  $b_n$ , and the correction factor for stimulated emission is given by (Goldberg 1966)

$$\beta_{nm} = \frac{b_m}{b_n} \left[ 1 - \left( \frac{k T_e}{h\nu} \right) \left( \frac{b_m - b_n}{b_m} \right) \right] \quad (2)$$

In H II regions where  $T_e \sim 10^4$  °K, the  $b$  factors for hydrogen and helium for  $n \sim 100$  are less than but approximately equal to one. The quantity  $\beta$  can be negative and have an absolute value much greater than one owing to the amplification of small population differences between levels by the factor  $kT_e/h\nu$ . Inspection of equation (1) shows that the line intensity depends on the value of the upper level population as expected ( $b_m \equiv 1$  in LTE) and on the amount of stimulated emission due to both the continuum and the line self-emission. If the atomic levels are populated in LTE, the line-to-continuum ratio for  $n\alpha$  transitions ( $\Delta n = 1$ ) is given by

$$\frac{T_L}{T_C} \cong \frac{2.33 \times 10^4 Z^2 \nu^{2.1}}{\Delta \nu_L T_e^{1.15}} \left( \frac{E_L}{E_C} \right) \exp(X_n) \quad (3)$$

where  $Z = (m + 1)$  for an atom  $X^{+m}$ ;  $\nu$  (GHz) is the frequency of the transition;  $\Delta\nu_L$  (kHz) is the full line width at half-power;  $(E_L/E_C)$  is the ratio of the emission measures of the line and the continuum ( $E_L/E_C \cong 0.91$  for H II regions); and  $X_n = 157800 Z^2/n^2 T_e$ .

The H109a transition at 5 GHz has been surveyed in sources in both the northern and southern hemispheres (Reifenstein *et al.* 1970; Wilson *et al.* 1970). The line-to-continuum ratio in H II regions varies from 2 to 22 percent and averages about 5 percent. The southern survey has included observations of three sources which happen to lie within the extended boundaries of the Gum Nebula, as noted by Abt *et al.* (1957); G265.1 + 1.5; G267.8 - 0.9; G268.0 - 1.1. One of the sources, G267.8 - 0.9 (RCW 38), has been mapped at 5 points in the H109a and H126a, H127a transitions (McGee and Gardner 1968; Wilson 1969). All three show a continuum spectrum indicative of an optically-thin thermal source (Milne *et al.* 1969). The LTE electron temperatures determined by substitution in equation (3) range from 6000-7900°K; however, such LTE values usually underestimate the actual temperature in H II regions.

To determine the parameters of line-emitting regions, observations are needed at many frequencies and should include higher order transitions as well. Several methods (Hjellming and Davies 1970; Goldberg and Cesarsky 1970) are being used to obtain the parameters of H II regions. These rely on observations at a number of frequencies to determine the emission measure  $E$ ,  $T_e$ , and  $n_e$  (see Table 1). Unfortunately, only the brightest H II regions have been studied in such detail, and the emission measures are probably not representative of H II regions generally. H II regions in the surveys have  $E \gtrsim 10^4$  pc cm<sup>-6</sup>; NGC 7000 and the Rosette Nebula appear to be among the H II regions of lowest emission measure ( $<10000$  pc cm<sup>-6</sup>) in which a recombination line has been detected (Dieter 1967; Penfield *et al.* 1967). Clearly "normal" H II regions can be profitably studied with recombination line measurements of hydrogen at various frequencies and at several points within the nebula.

A helium line is present in many H II regions if there are ultraviolet photons of sufficient energy available to ionize neutral helium. At temperatures of  $10^4$  °K, we expect the departures from LTE for high levels of the helium atom to be the same as for hydrogen. Hence, with the assumption of well-mixed emitting regions, the ratio of line energies  $T_L/\Delta\nu_L$  for corresponding helium and hydrogen transitions gives directly the ratio of ion densities  $n_{He^+}/n_{H^+}$ . Assuming the helium to be all in the form of He II, Palmer *et al.* (1969) find an average value 0.084 of the helium abundance in H II regions.

Table 1  
Parameters of H II Regions

Object	$n_e$ ( $\text{cm}^{-3}$ )	$T_e$ ( $^{\circ}\text{K}$ )	L (pc)	EM ( $\text{pc cm}^{-6}$ )	Ref.
<u>"Normal" H II Regions</u>					
Orion	17000	10000	0.066	$1.9 \times 10^7$	1
M8	4900	7700	0.042	$1.0 \times 10^6$	2
M17	16000	7500	0.063	$8.2 \times 10^6$	1
W51	44000	10000	0.028	$5.5 \times 10^7$	2
NGC 7000	$\sim 10$	$\sim 10000$		$2-8 \times 10^3$	7,8
<u>Supernova (H II Region)</u>					
Gum Nebula	0.2	$\sim 57000$	800	$3 \times 10^1$	6
Tycho Model I	1.	80000	190	$2 \times 10^2$	3
Tycho Model II	0.1	100000	260	2.6	3
Tycho Model III	10.	27000	20	$2 \times 10^3$	3
<u>Supernova (Filament)</u>					
Gum Nebula	$\sim 300$	$10^4-10^5$	0.03	$\sim 1.3 \times 10^3$	6
Cygnus Loop (O III)		$\sim 10^5$	0.01-0.02		4,5
Cygnus Loop (O II, S II, N II)	80-400	15000-20000	0.01-0.02	$10^2-10^3$	4,5

<sup>1</sup>Hjellming, R. M., and Gordon, M. A. 1971, Ap. J., **164**, 47.

<sup>2</sup>Andrews, M. H., Hjellming, R. M., and Churchwell, E. 1971, Ap. J., **167**, 245.

<sup>3</sup>Kafatos, M., and Morrison, P. 1971, Ap. J. **168**, 195.

<sup>4</sup>Parker, R. A. R. 1964, Ap. J., **139**, 493.

<sup>5</sup>Harris, D. E. 1962, Ap. J., **135**, 661.

<sup>6</sup>Brandt, J. C., Stecher, T. P., Crawford, D. L., and Maran, S. P. 1971, Ap. J. (Letters), **163**, L99; also Alexander, J. K., Brandt, J. C., Maran, S. P., and Stecher, T. P. 1971, Ap. J., **167**, 487.

<sup>7</sup>Westerhout, G. 1958, BAN, **14**, 215.

<sup>8</sup>Downes, D., and Rinehart, R. 1966, Ap. J., **144**, 937.

## B. Fossil Strömgren Spheres

Recent theoretical and observational results suggest (Brandt et al. 1971; Morrison and Sartori 1969) that there may also be large H II regions that have been ionized by ultraviolet or x-ray radiation or by cosmic rays associated with supernovae. Physical conditions in these regions — so-called fossil Strömgren spheres — at early stages of their evolution could differ

markedly from conditions in a normal H II region. Some representative parameters included in Table 1 show that the electron temperatures may reach  $10^5$  °K, while the electron density can be  $10 \text{ cm}^{-3}$  or less (Kafatos and Morrison 1971).

It is interesting to speculate on the recombination line spectrum from such a configuration. Such conditions of high temperature and low density lead to strong departures from LTE conditions in the populations of high levels. In particular, certain atoms and ions of abundant heavy elements (such as helium, oxygen, or carbon) can experience severe overpopulation of high levels (Goldberg and Dupree 1967) that may lead to greatly enhanced intensities of radiofrequency recombination lines. This can result from an increased  $b_n$  and/or  $\beta$  factor [see equation (1)] as compared to the values for hydrogen. The He II atom, for instance, recombines to He I predominantly by dielectronic recombination at temperatures  $\gtrsim 50000$  °K. Calculations of high level populations of He I for electron densities of  $10^4 \text{ cm}^{-3}$  show that overpopulation of levels  $n \sim 40$  leads to  $b_n \sim 100$  at  $T \sim 10^5$  °K (Burgess and Summers 1969); preliminary estimates for lower densities of  $n_e \sim 1 \text{ cm}^{-3}$  at  $T \sim 80000$  °K indicate that  $b_n > 100$  at  $n \sim 100$ . By contrast, hydrogenic atoms recombine directly onto a singly-excited level by radiative recombination, a process that usually proceeds more slowly than dielectronic recombination. And the departure coefficients,  $b_n$  for hydrogenic atoms are close to, but less than one. Thus if helium is in the singly ionized state (He II) in a high temperature medium, a recombination line of He I may very well be stronger than the corresponding hydrogen transition. Recombination lines from atoms populated by dielectronic recombination will have a frequency dependence that differs from that of lines arising from hydrogen. The hydrogen-to-helium line ratio should not be constant with  $n$  as it is at temperatures near  $10^4$  °K. With increasing  $n$ , it is possible that the emission line will turn into an absorption line when the  $b_n$  factors decrease as the levels approach their LTE populations and  $\beta$  becomes positive [see equation (2)].

Ions such as O II and O III can also experience overpopulations ( $b > 1$ ) of high levels at  $T \gtrsim 40000$  °K. However, detailed calculations are required to see whether the  $b_n$  and  $\beta$  factors are sufficiently large to compensate for the oxygen abundance and to make the line intensities comparable to those of hydrogen and helium. At present, calculations for high temperatures are available for only a few neutral atoms and ions (Dupree 1969; Burgess and Summers 1969).

In the proposed fossil Strömgren spheres, helium may be completely ionized, in which case recombination lines from He II would be produced. We do not expect enhancement of high level populations in the He II atom because

dielectronic recombination is not possible; however, the behavior of the  $b_n$  factors will differ in detail from that of hydrogen, because of a charge dependence of atomic parameters such as collision cross sections and radiative lifetimes. Detection of recombination lines from He II would be of particular interest because the character of the ionization source may well be inferred from its presence.

### III. Nonthermal Sources

A small proportion of sources observed at H109 $\alpha$  in the northern and southern surveys displayed a nonthermal continuum spectrum. The hydrogen line in such sources is weaker than in most normal H II regions (Milne et al. 1969; Wilson and Altenhoff 1969). This apparent weakness can result from a number of conditions. The electron temperature may be higher in a non-thermal source than in an H II region. Evaluation of equation (1) shows that if the H109 $\alpha$  line has a value of  $T_L/T_C$  that equals 5 percent at 10000 °K, its intensity will decrease to 2 percent at 20000 °K. Alternately, a non-thermal contribution to the continuum intensity will also cause the line to appear weaker than normal. In addition, the level populations may be affected by a strong nonthermal continuum. Stimulated emission can also be enhanced by the continuum. Details of the effect of a non-thermal continuum source upon atomic level populations and line intensities have not yet been investigated. It is possible too that in a nonthermal source a recombination line may be excessively broadened by turbulent velocity; this possibility should be verifiable if optical observations of forbidden-line emission are available.

Several searches have been made for recombination lines in two supernova remnants. The Cygnus Loop was searched at H158 $\alpha$  and C158 $\alpha$  (Downes 1970), and Cas A at H166 $\alpha$  and C166 $\alpha$  (Zuckerman and Ball 1970); both attempts were unsuccessful. However, a recent study of the supernova remnant W 28 shows an admixture of thermal and nonthermal sources with detectable recombination lines at H109 $\alpha$  (Milne and Wilson 1971).

If the high temperature and a nonthermal background are the principal reasons for the weakness of recombination lines in nonthermal sources, it would appear that investigations at high frequencies are an optimum choice for several reasons: the line-to-continuum ratio increases with increasing frequency (equation 3); the nonthermal continuum makes less of a contribution relative to a thermal continuum at high frequencies; a smaller beam-width may minimize the nonthermal contribution to the measured continuum temperature.



## IV. The H I Component

The detection of recombination lines from cold clouds (Ball *et al.* 1970; Gottesman and Gordon 1970) is potentially one of the most powerful diagnostics of the neutral hydrogen component of the interstellar medium. Transitions from both carbon and hydrogen have been observed (Palmer *et al.* 1969; Ball *et al.* 1970). The detection of corresponding transitions in two elements allows the ratio of ionized fractions to be determined directly from the ratio of energy in the line, *viz*:

$$\frac{(T_L \Delta \nu_L)_H}{(T_L \Delta \nu_L)_C} = \frac{n_H^+}{n_C^+} = \frac{n_H^+/n_H}{n_C^+/n_H} \quad (4)$$

In this case, carbon is believed to be fully ionized by the local radiation field because its ionization potential is less than that of hydrogen. The carbon abundance is assumed to be known, and carbon and hydrogen are taken to be well mixed in the line-forming region. Hence, such observations lead directly to the degree of hydrogen ionization. The quantity  $n_{H^+}/n_H$  has been found to equal  $2.7 \times 10^{-4}$  in one cloud along the line of sight to NGC 2024 (Ball *et al.* 1970).

Observations of the carbon line at several frequencies, when combined with calculations of the line intensities, are expected also to yield values of (or at least constraints on) other physical parameters of H I clouds. Recent theoretical results indicate that atomic populations of high levels can be modified by thermal radiation fields similar to those observed in H II regions. Hence, detailed models of the cloud configurations may be needed.

Detection of similar lines from the "hot" H I component may allow one to discriminate among various models of the interstellar medium. In particular, the degree of ionization of helium as compared with hydrogen is greater for models heated by X-rays or UV radiation than for models with energetic particle heating (Jura and Dalgarno 1971; Bergeron and Souffrin 1971).

Search for recombination lines from neutral hydrogen requires knowledge of the 21-cm profiles near the source, so that corresponding radial velocities may be searched with appropriate velocity resolution. Observations indicate that the carbon line (formed in cold H I clouds) becomes stronger at lower frequencies relative to lines originating in H II regions (Churchwell 1969). This suggests that low frequencies are most appropriate for its detection in order to facilitate separation of an H I and H II profile. However, some consideration must also be given to the size of the beamwidth to ensure that the signal from the H I region is measurable against an extended background H II region or nonthermal source.

The author wishes to thank L. Goldberg and J. Black for a number of useful suggestions. This work was supported in part by NASA under Grant NGL-22-007-006.

### References

- Abt, H. A., Morgan, W. W., and Strömberg, B. 1957, Ap. J., 126, 322.
- Ball, J. A., Cesarsky, D., Dupree, A. K., Goldberg, L., and Lilley, A. E. 1970, Ap. J. (Letters), 162, L25.
- Bergeron, J., and Souffrin, S. 1971, Astron. Astrophys., 11, 40.
- Brandt, J. C., Stecher, T. P., Crawford, D. L., and Maran, S. P. 1971, Ap. J. (Letters), 163, L99.
- Burgess, A., and Summers, H. P. 1969, Ap. J., 157, 1007.
- Churchwell, E. 1969, Ph.D. Thesis, Indiana University.
- Dieter, N. H. 1967, Ap. J., 150, 435.
- Downes, D. 1970, Ph.D. Thesis, Harvard University.
- Dupree, A. K. 1969, Ap. J., 158, 491.
- Dupree, A. K., and Goldberg, L. 1970, Ann. Rev. of Astronomy and Astrophysics, 8, 231.
- Goldberg, L. 1966, Ap. J., 144, 1225.
- Goldberg, L., and Cesarsky, D. 1970, Astrophys. Letters, 6, 93.
- Goldberg, L., and Dupree, A. K. 1967, Nature, 215, 41.
- Gottesman, S. T., and Gordon, M. A. 1970, Ap. J. (Letters), 162, L93.
- Hjellming, R. M., and Davies, R. D. 1970, Astron. Astrophys., 5, 53.
- Jura, M., and Dalgarno, A. 1971, Astron. Astrophys., 14, 243.
- Kafatos, M., and Morrison, P. 1971, Ap. J., 168, 195.
- McGee, R. X., and Gardner, R. F. 1968, Austral. J. Phys., 21, 149.
- Milne, D. K., and Wilson, T. L. 1971, Astron. Astrophys., 10, 220.
- Milne, D. K., Wilson, T. L., Gardner, F. F., and Mezger, P. G. 1969, Astrophys. Letters, 4, 121.
- Morrison, P., and Sartori, L. 1969, Ap. J., 158, 541.

- Palmer, P., Zuckerman, B., Penfield, H., Lilley, A. E., and Mezger, P. G. 1969, Ap. J., 156, 887.
- Penfield, H., Palmer, P., and Zuckerman, B. 1967, Ap. J. (Letters), 148, L25.
- Reifenstein, E. C., III, Wilson, T. L., Burke, B. F., Mezger, P. G., and Altenhoff, W. 1970, Astron. Astrophys., 4, 357.
- Sorochenko, R. L., Ruzanov, V. A., Salomonovich, A. E., and Shteinshleger, V. B. 1969, Astrophys. Letters, 3, 7.
- Wilson, T. L. 1969, Ph.D. Thesis, M.I.T.
- Wilson, T. L., and Altenhoff, W. 1969, Astrophys. Letters, 5, 47.
- Wilson, T. L., Mezger, P. G., Gardner, R. F., and Milne, D. K. 1970, Astron. Astrophys., 6, 364.
- . Zuckerman, B., and Ball, J. 1970, personal communication.

## THE APPEARANCE OF THE GUM NEBULA

Bart J. Bok

*Steward Observatory  
University of Arizona  
Tucson, Arizona 85721*

According to Brandt *et al.* (1971), the center of the Gum Nebula is at a distance of 460 parsecs from the Sun. The outer dimensions quoted by these authors are  $40^\circ \times 90^\circ$ , and they suspect that the inner boundary of the emission region lies at about 100 parsecs from the Sun. They assign a radius of 360 parsecs to the nebula, which they suspect of being slightly flattened, with the huge volume  $1.4 \times 10^{63} \text{ cm}^3$ ! Obviously, tremendous amounts of energy must have been available to ionize so large a volume. Brandt estimates that  $10^{52}$  erg of energy were required to do the job. The Wolf-Rayet star  $\gamma^2$  Velorum and the O5f star  $\zeta$  Puppis would obviously not be equal to this task. However, I wish to challenge the distances and dimensions quoted by Brandt *et al.*

First of all, I question the assumption that the Gum Nebula complex is as large as suggested by Brandt *et al.* The quoted dimensions of  $40^\circ \times 90^\circ$  seem like gross overestimates, since they are based on the assumption that some minor outlying patches of nebulosity fix the outer boundary of the region of ionization;  $35^\circ$  seems like a more reasonable value for the diameter of the complex. We should stress the non-homogeneous appearance of the nebular complex. There is a region of brightest nebulosity centered upon  $\gamma^2$  Velorum, a WC8 star. It has an apparent diameter of  $9^\circ$ , to which would correspond a radius for the Strömgren sphere of ionization of about 50 parsecs at the estimated distance of 460 parsecs. It seems quite reasonable that  $\gamma^2$  Velorum would supply sufficient energy to keep this part of the nebula going. The section near  $\zeta$  Puppis must similarly be ionized and made luminous by the intrinsically very brilliant O5f star, the brightest O-star in the heavens in apparent magnitude!

Other speakers at the Symposium, notably Gott and Ostriker and also Upton, have questioned the distance of 460 parsecs assigned by Brandt *et al.* to the pulsar and to the B-association that contains  $\gamma^2$  Velorum.

My general impression is that Brandt *et al.* have overestimated the dimensions of the Gum Nebula complex, that their distance to the central pulsar of 460 parsecs is rather on the large side and that they have underestimated the likely contributions from  $\gamma^2$  Velorum and  $\zeta$  Puppis.

The section of the Gum Nebula that is covered by the radio supernova remnant and the area near the pulsar both show a highly filamentary structure on the nebular photographs. The sample applies to the section further out, as distinct from the smoother appearance of the nebula near  $\gamma^2$  Velorum. It seems reasonable to accept the estimate that not more than 1% or 2% of the total volume is filled with gas and free electrons. The "clumpiness factor" for the part of the Gum Nebula identified with the supernova remnant may be 100, or greater.

The multiple-origin character of the Gum Nebula seems assured. The big problem is now what parts of the Gum Nebula are produced principally by traditional ultraviolet thermal radiation and what parts mainly by processes directly related to the supernova outburst. These matters can be decided only by careful observational studies of the spectra of different parts of the Gum Nebula; one can be certain that the nebular spectrographs and interferometers are going to be very busy starting in November 1971, when the Gum Nebula will be well placed for observations from southern hemisphere observatories: Cerro Tololo, La Silla and Las Campanas Observatories in Chile, Radcliffe Observatory in South Africa and Mount Stromlo and Siding Springs Observatories in Australia. Related radioastronomical work at all accessible wavelengths, X-ray observations and cosmic ray studies, as well as Lyman-alpha observations are obviously desired. The general properties of the spiral features for the section of the Milky Way that contains the Gum Nebula must be studied with minimum delay, for there are obviously present many optical and radio features that lie at distances greater than 1000 parsecs, far beyond the nearby Gum Nebula and its associated phenomena. A comprehensive study of the distribution and radial velocities of the OB stars in the section seems especially urgent.

#### Reference

Brandt, J. C., Stecher, T. P., Crawford, D. L., and Maran, S. P. 1971, Ap. J. (Letters), 163, L99.

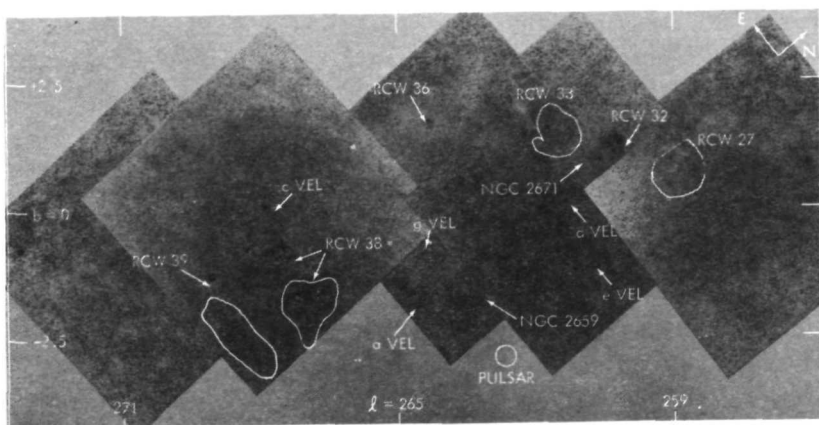


Figure 1. A composite of red 098-02 plates in a region of the Gum Nebula as obtained by Gaston Araya with the Schmidt telescope at Cerro Tololo Inter-American Observatory.

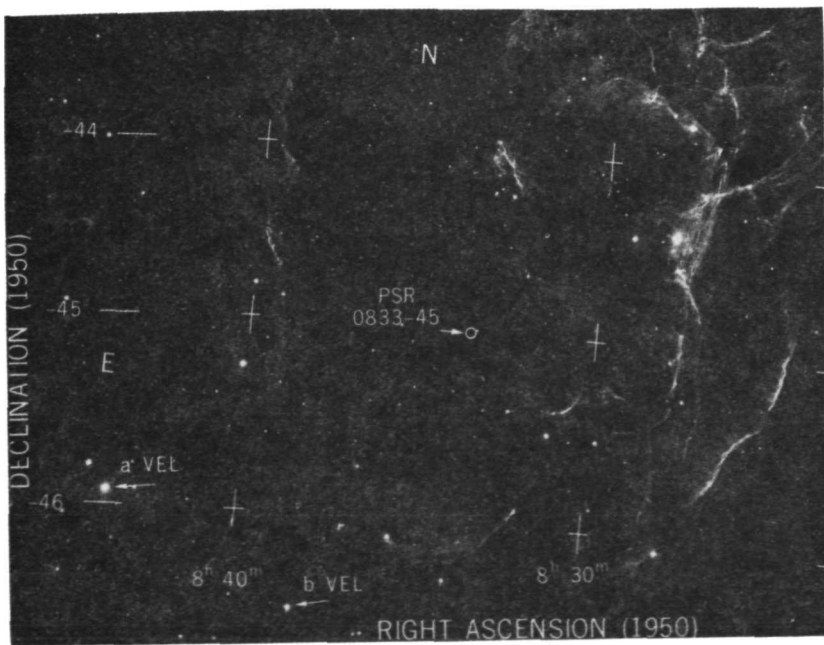


Figure 2. Photograph of the UV network of nebulosity associated with the Vela pulsar and supernova remnant. (B. J. Bok, Schmidt telescope at C.T.I.O.)

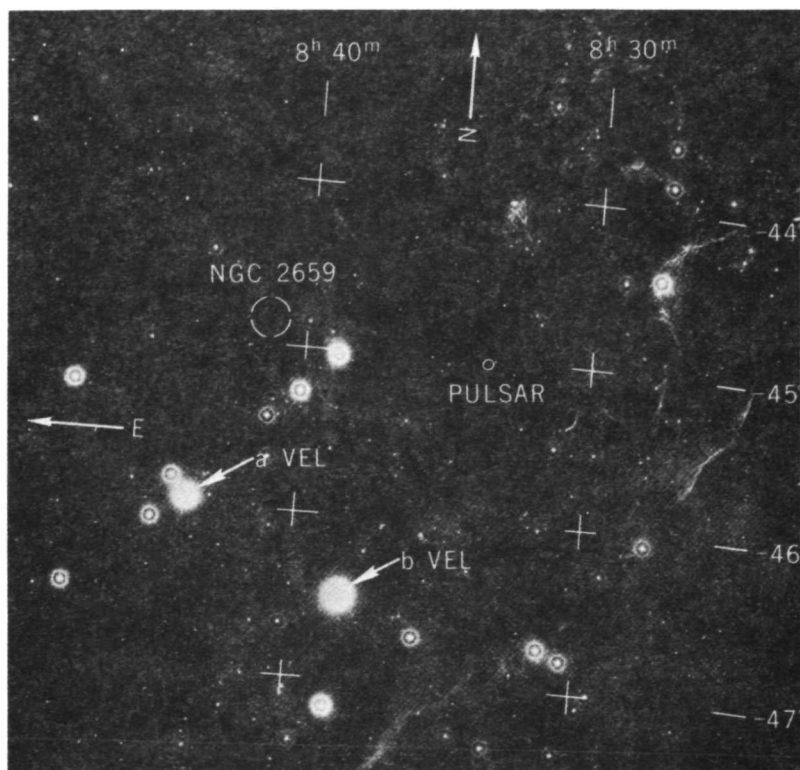


Figure 3. The region of Figure 2 in red light; 90-minute exposure on 098-01 emulsion, with RG2 filter. (B. J. Bok, Schmidt telescope at C.T.I.O.)

# THE DIFFICULTY OF ULTRAVIOLET EMISSION FROM SUPERNOVAE

Stirling A. Colgate

*New Mexico Institute of Mining and Technology  
Socorro, New Mexico 87801*

I would like to point out the conceptual difficulties of generating the ultraviolet radiation that has been presumed for the creation of both the optical fluorescence mechanism of supernova light emission as well as the ionization of a nebula as large as the Gum Nebula.

The efficiency of the helium optical fluorescence mechanism is roughly  $10^{-3}$  so that at least  $10^{52}$  erg must be emitted in the ultraviolet to create the observed  $10^{49}$  erg of optical emission. Similarly, we have recognized here today that at least  $10^{52}$  erg are needed in ultraviolet emission to create the Gum Nebula.

There are several obvious requirements concerning the energy distribution of the ultraviolet photons:

1. The energy of the greater fraction of the photons must be sufficient to cause both helium fluorescence as well as hydrogen ionization. The former implies  $51 \leq h\nu \leq 54$  eV and the latter implies  $h\nu \geq 15$  eV.
2. In addition, if the photons are emitted in an approximate black-body spectrum, the fraction of the energy emitted in the optical must be no more than what is already observed in the optical. The bolometric correction, therefore, must be  $10^3$  or greater in order that the optical emission associated with the ultraviolet radiation not be greater than observed. Since the integral energy of the low energy part of the spectrum is proportional to  $(h\nu_{\max})^3$ , this implies that  $kT \simeq 17$  eV in both cases.

The question of ultraviolet black-body emission depends primarily upon the energy source. The supernova explosion as described by the author elsewhere in this volume, converts explosion energy to kinetic energy of expansion in a highly efficient fashion. Consequently, we expect by far the major fraction of the energy released in the explosion to appear as kinetic energy of ejecta. Since the upper limit of the explosion energy is of the order of  $10^{52}$  erg, essentially all the kinetic energy of expansion must be reconverted into heat and then emitted as black-body radiation or go directly into photons by atom-atom impact. The latter direct atom-atom or transparent emission



depends in detail upon the available atomic states. The probability that the wide mixture of elements present in the interstellar medium as well as supernova ejecta should result in an emission spectrum localized to the limited region of the spectrum for either ionization or fluorescence ultraviolet with less than  $10^{-3}$  emission in the visible is remote indeed. We therefore exclude transparent emission as being highly unlikely and emphasize black-body or at least quasi-black-body emission.

Presumably  $1/2$  to  $1 M_{\odot}$  is ejected with  $10^{52}$  erg. The ejection velocity therefore becomes

$$1/2 U^2 M_{\odot} = 10^{52} \text{ erg}$$

or

$$U = 3 \text{ to } 4 \times 10^9 \text{ cm sec}^{-1}$$

In order that at least half of this kinetic energy be converted into heat by collision, the stationary mass must be  $\geq$  moving mass. In order that the radiation associated with the heat can escape, the integral opacity must be less than several mean free paths; otherwise, the re-expansion of the hot gas will again reconvert the heat to kinetic energy of motion rather than emitted radiation. The ultraviolet opacity of such a mixture of heavy elements is at least  $1 \text{ cm}^2 \text{ gm}^{-1}$  so that the stationary matter can be no thicker than  $1 \text{ gm cm}^{-2}$ .

The energy source is kinetic and this energy must be delivered to a shell  $1 \text{ gm cm}^{-2}$  thick,  $1 M_{\odot}$ , and at a rate so that this layer will radiate as a black-body at  $kT \simeq 17 \text{ eV}$ . This places a similar density limit on both moving and stationary matter.

The energy conversion rate depends slightly on details of the shocks propagating in both the moving and stationary gases and is limited to

$$(1/4) \rho U^3 \geq (c/3) a T^4.$$

Then  $\rho \geq 1.5 \times 10^{-11} \text{ gm cm}^{-3}$ . Since the shell mass thickness must be no greater than  $1 \text{ gm cm}^{-2}$ , the linear thickness must be  $\delta < 10^{11} \text{ cm}$ . On the other hand the mass of these shells  $\simeq M_{\odot}$ , requires that

$$4\pi r^2 \rho \delta = M_{\odot}$$

or

$$r = 1.4 \times 10^{16} \text{ cm}.$$

Therefore the moving and stationary matter must be distributed in shells with a ratio of thickness to radius of less than  $10^{-5}$ . This seems highly unlikely (1) in view of the velocity distribution of supernova ejecta and (2) in view of the present theories of quasi-static mass loss leading to planetary nebulae. Both observations and theory lead to a nearly uniform distribution. From both standpoints then, intense ultraviolet emission seems unlikely from supernova explosions.

# A NOTE ON THE POSSIBLE IMPORTANCE OF THE GUM NEBULA

D. P. Cox

*Department of Physics  
University of Wisconsin  
Madison, Wisconsin 53706*

I would like at this time to develop my first astronomical catalog to which future generations of Gum Nebulists may refer. It is a catalog of

## Theories and Vested Interests

- C-I There are a number of people for whom it is important that the Gum Nebula be some kind of fossil H II region, directly and almost wholly associated with the Vela X supernova remnant. Two groups come to mind:
  - C-IA is the group who have studied the region and proposed the possibility (Brandt, Stecher, Crawford, Maran, Alexander, ...);
  - C-IB is the group who have proposed the time-dependent theory for heating and ionization of the interstellar medium, and who are studying the possible consequences on growth of instabilities and star formation (Bottcher, McCray, Dalgarno, Jura, ...).
- C-II There are several groups who are more particular about the kind of fossil H II region they want:
  - C-IIA formed by the immediate outburst of UV radiation from the SN explosion (Morrison, Sartori, Kafatos, ...)
  - C-IIB formed by the gradual emission of UV radiation from the expanding, shock-heated remnant (Tucker, me\*)
  - C-IIC formed by the immediate release of low-energy cosmic rays from the SN explosion, cosmic rays which are able to spiral along the magnetic field lines without sweeping those lines into a wall and thereby be confined within a shock, and which instead are able to escape beyond the mechanical

---

\*Ph.D. thesis, LaJolla 1970, p. 105.

shock front to penetrate and ionize the medium beyond. These cosmic rays, although released immediately, require a substantial length of time to ionize the nebula because of their low velocities (Ramaty, Colgate, Boldt, Silk, ...).

C-III One final group is not so much concerned with the remnant, but instead with the possible relationship between the pulsar(s), high-velocity stars, and the nearby B-associations in this region (Gott and Ostriker).

It seems to me that there are really two fundamental questions which need to be answered by the students of the Gum Nebula in order to make some of these catalog entries retire to the realm of pure historical interest:

- (1) To what degree and scale is the ionization of the Gum Nebula region really due to the occurrence of one supernova event?
- (2) What evidence exists which would indicate the mode or modes of energy transport from the SN to the interstellar medium, and the amount of energy transported?

In this regard, I think a two-step cooperative process between observers and theoreticians is required:

- (1) Detailed observations of the  $5^\circ$ -diameter supernova remnant proper, coupled with a complete and credible model of the remnant which is capable of explaining the entire presently-observed spectrum, must be made.
- (2) Detailed observations of the much larger H II region outside the remnant must be made over the complete spectral range. In addition, the model of the present remnant must be extrapolated backward in time to get its spectrum at earlier epochs. The necessary consequences of this earlier radiation on the surrounding interstellar medium must be subtracted from the presently "observed" distribution of ionization, temperature, cosmic rays and magnetic field to discover those residual effects attributable to other possible modes of energy transport from the SN explosion, not included in the model of the present remnant.

There are several measurements of the Gum Nebula which seem potentially very useful:

- (1) We need a good series of spectra of some of the optical filaments in the SNR proper. There is some chance that these spectra can be matched by calculations of the cooling behind a shock wave, such as

I have performed for the Cygnus Loop. If so, this might help pin down the shock velocity and ambient density.

- (2) I would like to see density and temperature measured by using [OII] and [OIII] lines in the regions in the Gum Nebula lying outside the SNR, but which show high emission measures. These can then be compared with calculations such as those by Kafatos and Morrison to determine whether it is possible for this material to have been impulse-heated 10,000 years ago. The studies should also measure the relative populations of various ions in order to determine the current ionization structure.
- (3) It would be worth checking to see if the characteristic X-rays expected from the cosmic ray model of Ramaty, Boldt, Colgate, and Silk are found in emission outside the SNR.
- (4) The  $\text{He}^+$  radio recombination lines, enhanced by dielectronic recombination as described by Dupree, should be studied, as should
- (5) The intensity and spectrum of continuous X-ray emission outside the SNR.
- (6) If the bright emission regions are actually found to be very hot, one might search for cooler ( $T \sim 10^4$  °K) H II regions around the B stars, imbedded in the hotter material as predicted by Stecher in the discussions here.

In closing, I think that the idea advanced by Colgate to argue against the impulsive emission of UV by a SN explosion should be evaluated after relaxing the restriction (or verifying its validity) that the emission spectrum would resemble a black-body.

# X-RAYS FROM THE VELA-PUPPIS COMPLEX

A. N. Bunner

*Department of Physics*

*University of Wisconsin*

*Madison, Wisconsin 53706*

## Abstract

A review of X-ray observations in the vicinity of the Gum Nebula is presented. There is little doubt that the filamentary nebula Stromlo 16, the radio source Vela X and the extended X-ray object Vel XR-2 are indications of the same, relatively nearby, supernova remnant. X-ray absorption measurements are consistent with a distance of  $500 \pm 100$  pc. The observed X-ray spectra have not yet distinguished between thermal bremsstrahlung and synchrotron radiation as the source mechanism. A search for low energy X-ray emission lines, both within the  $5^\circ$  diameter remnant and in the larger Gum Nebula, may provide an important test for models of supernova remnant evolution.

---

Present views on the age and distance of the Vela supernova remnant place it as the nearest ( $\sim 460$  parsecs) such object with age less than 50,000 years yet discovered. As such, its effect on the nearby interstellar medium may be considerable. With an associated radio source, magnetic field pattern, filaments bright in optical emission lines, an active pulsar, and possibly a large, high temperature fossil H II region, it is clear that this area provides a fine laboratory for investigating supernova remnants at close hand. It is therefore in order to review the X-ray observations in this region and to suggest ways in which measurements at X-ray wavelengths may shed light on the physics of supernova remnants and the properties of the interstellar medium.

Three distinct X-ray sources have been discovered to date in the  $\sim 40^\circ$  diameter region termed the Gum Nebula. The first found was labelled Vel XR-1 by its discoverers (Chodil *et al.* 1967) and is now located by the Uhuru satellite at  $9^h 00^m 27^s \pm 15^s$ ,  $-40^\circ 22' \pm 4'$  with the new designation 1AS&E 0900-40 (Uhuru Source Position Bulletin Apr. 10, 1971, AS&E X-Ray Astronomy Group). This object appears as a point source of 3 to 11 keV X-rays with an intensity  $\sim 0.4$  photon  $\text{cm}^{-2} \text{sec}^{-1}$ . There is no evidence to associate this source with the Vela supernova remnant.

Also coincidentally close in position to the Vela X radio and optical object is the X-ray source found by Palmieri *et al.* (1971) and identified with the Puppis A nonthermal radio source. This object is classed as a supernova remnant by Harris (1962) who suggests a distance of 1400 pc, much farther than the Vela X remnant. The low-energy cutoff observed by Seward *et al.* (1971) in the Pup A X-ray spectrum indicates an average gas density along the line of sight to the source of 0.14 to 0.5 atoms  $\text{cm}^{-3}$  if the distance is 1400 pc. The Puppis A radio shell is about  $1^\circ$  in diameter. Seward *et al.* find the associated X-ray source to be  $\leq 0.5^\circ$ .

The X-ray object of principal interest here is the strong soft source Vel XR-2 first observed by Grader *et al.* (1970). The location coincides with the extended radio source Vela X, which includes the pulsar PSR 0833-45, and with a network of fine optical filaments (catalogued Stromlo 16) which are seen in the emission lines of  $\text{O}^{++}$ ,  $\text{O}^+$  and H (Milne 1968b). The radio spectrum, the high degree of radio polarization, the indications of collisionally excited gas and the presence of a young pulsar all point to an identification of the  $5^\circ$  diameter region as a supernova remnant.

Energetically, the remnant is primarily, like the Crab nebula, an X-ray object. The X-ray emission from 150 eV to 2 keV corresponds to about  $2.3 \times 10^{35}$  erg  $\text{sec}^{-1}$  (Seward *et al.* 1971). It is evidently the brightest object in the night sky for  $150 \text{ eV} < E < 500 \text{ eV}$ .

According to the LRL study (Seward *et al.* 1971) the angular size of the X-ray emitting region is smaller at 0.2 to 0.3 keV than at 0.3 to 2 keV. Referring to Figure 1, the brightest filaments form a D shape which Milne (1968a) suggested was formed by a non-uniform radial expansion. 90% of the Vela X radio emission occurs within this D region, which includes the pulsar, while the LRL group reports the lower energy X-ray emitting region borders the D to the east. The higher energy X-rays, on the other hand, appear to come from a larger area consistent with the circle formed by completing the D. These authors suggest that there may be obscured filaments forming the rest of a shell. Support for this suggestion is seen in a diminished star count on the east side of the filaments approaching the galactic equator. As in the case of the Cygnus Loop, there is some indication that the X-ray emission is correlated with the optically bright, sharp filaments.

The associated pulsar PSR 0833-45 has not been clearly identified in either the optical spectrum or X-ray spectrum. A search for pulsed X-ray emission has led to upper limits for the fraction of the 0.15 to 2 keV flux contained in a pulse of 2.4% from Wisconsin data and 1% from LRL data, taken May 29, 1970 and May 13, 1970 respectively. Pacini and Rees (1970) have shown that if the high energy (optical and X-ray) emission from pulsars

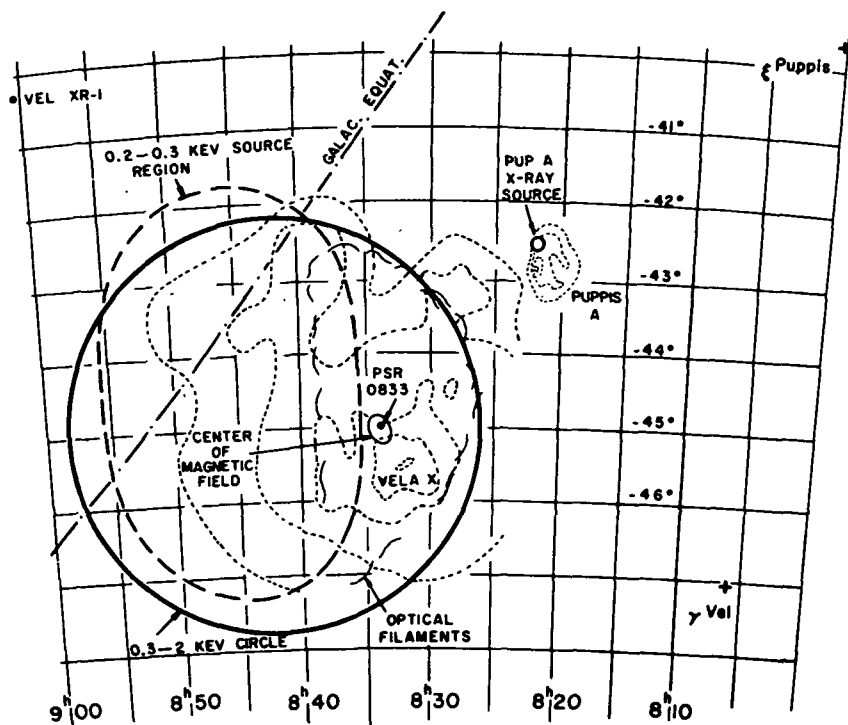


Figure 1. A map of the Vela-Puppis region. The radio brightness contours are 2650 MHz isotherms from Milne (1968a) and from Milne and Hill (1969). The X-ray source positions of LRL and ASE are shown. The large solid circle is a shell model used to fit the Vel XR-2 0.3 - 2 keV data of Seward *et al.* (1971). The dashed ellipse indicates the 0.2 - 0.3 keV emission. The accuracy of the location of the X-ray source Pup A is 0.3. Also shown is the center of a circumferential magnetic field pattern (Milne 1968a), the location of the pulsar PSR 0833-45 and the optical filaments (wispy lines).

comes from synchrotron radiation at the speed of light circle, then the power radiated may vary as  $(\text{Period})^{-6}$ . In this case, by comparison with the Crab pulsar NP 0532, detection of the Vela pulsar in X-rays must await experiment sensitivities of  $10^{-3}$  photon  $\text{cm}^{-2}$   $\text{sec}^{-1}$ .

The analysis of spectra obtained by proportional counters is complicated by the fact that these detectors have a complex response function. The usual procedure is to fit models to the data which may have a physically meaningful interpretation and which make use of a number of free parameters consistent with the quality of the data. X-ray spectra of Vel XR-2 have been obtained by the LRL group (Palmieri *et al.* 1971, Seward *et al.* 1971) and by the Wisconsin group (unpublished results) using 3 types of models: (a) thermal bremsstrahlung with an input spectrum  $(1/E) e^{-E/kT}$



photon  $\text{cm}^{-2} \text{sec}^{-1} \text{keV}^{-1}$ ; (b) a power law spectrum  $e^{-\alpha}$  photon  $\text{cm}^{-2} \text{sec}^{-1} \text{keV}^{-1}$ ; and (c) an emission line spectrum, based on the predictions of Tucker and Koren (1971) for a collisionally excited plasma.

Each model also makes use of an additional parameter which relates to interstellar absorption. If the neutral atomic hydrogen column density along the line of sight is  $N_H$  atoms  $\text{cm}^{-2}$  with other elements present according to the abundance ratios chosen by Brown and Gould (1970), then the effective photoelectric cross-section per H atom at energy  $E$  is

$$\sigma_{\text{eff}}(E) = \frac{\sum_i N_i \sigma_i}{N_H} \quad (1)$$

and the optical depth at energy  $E$  is

$$\tau(E) = N_H \sigma_{\text{eff}}(E) \quad (2)$$

Table 1 summarizes the results of this model fitting including the parameter  $N_H$ .

It is important to emphasize that these models are little more than mathematical artifices since, even if the radiation were entirely thermal, it is unlikely that a single temperature could adequately represent a region 40 pc in diameter. Figure 2 shows the spectrum of the Vela X remnant from radio, optical and X-ray data. The radio data are from Milne (1968a), the optical point is based on emission measurements on filaments (Milne 1968b), and the X-ray sector is drawn for a 3.3 index power law without absorption for illustrative purposes.

However, regardless of the choice of model above, the observed pulse height spectra indicate a mass of absorbing gas along the line of sight equivalent to the "standard" interstellar gas of Brown and Gould (1970) containing 2.4 to  $5.6 \times 10^{20}$  hydrogen atoms per  $\text{cm}^2$  (about one optical depth at 270 eV). The X-ray absorption measurement actually determines the concentration of elements heavier than hydrogen because of the strong dependence of the photoelectric cross-section on  $Z$ . At 270 eV, assuming the Brown and Gould composition, the optical depth is 69% due to He and 26% to H. Above 526 eV, oxygen is the principal contributor. In principle, provided a reasonably well-established source spectrum is available, the X-ray absorption measurements allow a determination of the elemental and ionic composition along the line of sight to a source. This technique has been used recently to study the interstellar gas along the path to the Crab Nebula (Coleman 1970).

Table 1  
Spectral Models of Vel XR-2

Reference	Thermal without emission lines		Power law		Thermal with emission lines	
	kT	$10^{-20} N_H$	$\alpha$	$10^{-20} N_H$	$10^6 T$	$10^{-20} N_H$
	keV	H-atoms $\text{cm}^{-2}$	—	H-atoms $\text{cm}^{-2}$	$^{\circ}\text{K}$	H-atoms $\text{cm}^{-2}$
Palmieri et al. 1971	$0.2 \pm 0.14$	$2.4 \pm 0.8$	$2 \pm 1.2$	$5.6 \pm 1$	—	—
Seward et al. 1971	$0.23^{+0.07}_{-0.03}$	$2.5 \pm 1.2$	$4.2 \pm 0.5$	$5.6 \pm 2.5$	—	—
Wisconsin (unpublished)	$0.27 \pm 0.03$	$3.6 \pm 0.5$	$3.3 \pm 0.5$	$4.0 \pm 1$	$2 \pm 1$	$4 \pm 1$

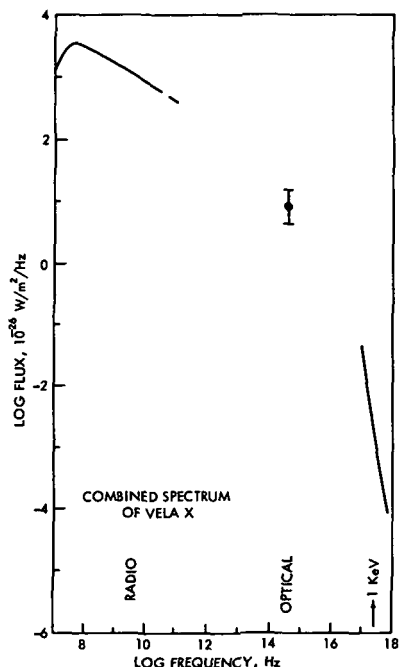


Figure 2. The spectrum of the Vela X remnant from radio frequencies to X-ray frequencies.

For Vel XR-2, neither the source spectrum nor the observed pulse height distribution are known with the accuracy necessary for a detailed analysis. However, the estimate above is sufficient to place some constraints on models for the line of sight to the X-ray source. It is unlikely that any absorption occurs within or near the filamentary nebula itself. Milne (1968a) estimates the mass swept up by the expanding nebula at  $30$  to  $170 M_{\odot}$ ; therefore, if the diameter is  $40$  pc, an upper limit to the column density within the nebula is  $0.15 \text{ H-atom cm}^{-2}$ . If the distance is  $500 \pm 100$  parsecs, the line of sight is completely within our local spiral arm and the X-ray absorption indicates an average density of  $0.24 \pm 0.10 \text{ atom cm}^{-3}$ , in agreement with the model of Brandt *et al.* (1971) and Alexander *et al.* (1971). A density as high as  $0.4 \text{ protons cm}^{-3}$  could be accommodated if a large fraction of the line of sight is at a temperature of  $50,000^{\circ}\text{K}$ , as suggested by Alexander *et al.* (1971), since hydrogen is transparent to X-rays for  $T > 15,000^{\circ}\text{K}$  and  $\text{He}^{+}$  is semi-transparent for  $30,000^{\circ}\text{K} < T < 80,000^{\circ}\text{K}$ . Above  $80,000^{\circ}\text{K}$  the effective cross-section drops drastically and the observed absorption would be difficult to explain.

By way of comparison with radio observations, a search for the 21-cm absorption line in the continuum radiation of PSR 0833-45 by Gordon and Gordon (1970) has yielded an upper limit of  $\tau(21 \text{ cm}) < 0.08$ . These

authors conclude that either the line of sight to this pulsar is unusually lacking in cool hydrogen, or that whatever hydrogen is present must be sufficiently clumped that the line of sight happens to miss all such cool clouds. Evidence for the existence of such clouds comes from a study of several pulsar neutral hydrogen absorption measurements, in which a gap is found between the smallest 21-cm optical depth detected and upper limits set on others (Gordon *et al.* 1969). In contrast to the X-ray absorption measurement, which averages over a beam  $5^\circ$  in diameter, the pulsar measurement is a truly stellar line of sight and so has a higher probability of missing all clouds. Therefore, the radio observations are not inconsistent either with the X-ray data or with the model of Brandt *et al.* (1971).

Refined X-ray measurements with thin window proportional counters and/or Bragg spectrometers will allow better estimates of the line of sight parameters. An observation of X-ray polarization would establish the emission mechanism as synchrotron radiation, but such a measurement is extremely difficult for  $\lambda > 6 \text{ \AA}$ . The most promising attack will be the search for X-ray emission lines. If the X-rays are from a hot plasma at  $2$  to  $3 \times 10^6 \text{ }^\circ\text{K}$ , the lines of  $\text{Fe}^{15+}$  at 227 eV,  $\text{Si}^{9+}$  at 245 eV and  $\text{O}^{7+}$  at 652 eV, among others, should be prominent (Tucker and Koren 1971). A clear identification of even one emission line would establish a temperature reasonably well. Failure to observe lines with higher resolution devices would support synchrotron radiation as the source.

It is interesting to consider the possibility that emission lines may be found from a diffuse region surrounding the supernova remnant. If a large quantity of heavy element enriched material is ejected in the supernova outburst at energies above 10 MeV/nucleon, as suggested by Ramaty *et al.* (1971), these stripped nuclei may be carried beyond the remnant proper before slowing down to velocities at which electrons can be captured into excited states with subsequent K and L characteristic line emission.

In this connection, it should be mentioned that a systematic survey of the diffuse soft X-ray background in the  $\sim 40^\circ$  diameter Gum Nebula region has not yet been published. Both spectral features and spatial structure are of interest in this respect.

Including Vela X and Puppis A, the number of plausible identifications of X-ray sources with supernova remnants now reaches 16 (Table 2). Of these, Cep XR-3 and Oph XR-1 have not been confirmed as X-ray sources since they were reported in 1964-67. However, it would seem that it is yet too early to conclude that a majority of X-ray sources are not associated with supernovae.

That the 3 sources discovered to date which are strong sources below 1 keV, Vel XR-2, Pup A and the Cygnus Loop, all correspond to supernova remnants with relatively large angular diameters may be largely a reflection of their proximity to the sun and corresponding low interstellar attenuation. It is also possible, as Palmieri et al. (1971) suggest, that the soft spectra are an indication of age and that a steepening of the power-law index results from a decay of the high-energy electrons in the remnant. Alternatively, if the X-ray emission is thermal, the effect could indicate deceleration of shock waves leading to a decrease of effective temperature with age. A search for further very soft X-ray sources may lead to other large diameter remnants in this age class.

This work was supported in part by the National Aeronautics and Space Administration under grant NGL 50-002-044.

Table 2  
Supernova Remnants as X-Ray Sources

Supernova Remnant	X-Ray Source	Position Error	Distance	Age	X-Ray Power	Ref.
			(pc)	(yr)	( $10^{36}$ erg/sec)	
Crab 1054	Tau X-1	—	1700	917	10	
Vela X	Vel XR-2	—	460	11,000	0.23	1,4
Puppis A	Pup A	0°.3	1200-1400		2.6	1,17
Cygnus Loop	Cyg X-5	—	770	50,000	1.0	10,12
Tycho 1572	Cep XR-1	0.2	3500	399	1.4	2,7,13
Cas A	Cas XR-1	—	3400	260	2.8	13,17
CTA 1	Cep XR-3	1.1	1000-2000		0.9	2,3,9
P1439-62	Cen XR-1	1.5	2000-2300		1.3	2,9
P1548-55	Nor XR-2	1.8	1600-3200		3.9	2,9,14
P1613-50	Nor XR-1	1.7	4300-5700		27	2,9,14
W28	Sgr XR-3/GX9+1	1.8	1300-1500		1.0	2,6,9,15
3C392	3C392	0.2	1500-1600		0.05	2,8,9
3C396	3C396	0.5	1800		0.07	8,9
13S6A (SN of 185 ?)	Cen XR-2 (UAT)	0°.6 in R <sup>II</sup>	2300-5300	1786 ?	Flared in 1967	2,9,11,16
Kepler 1604	Oph XR-1	1.5	5300-10,000	367		2,3
Milne 56	GX5-1	0.2	2400		10	5,6,9

#### REFERENCES TO TABLE 2:

- <sup>1</sup>Seward, F. D., Burginoy, G. A., Grader, R. J., Hill, R. W., Palmieri, T. M., and Stoering, J. P. 1971, *Ap. J.*, **169**, 515.
- <sup>2</sup>Poveda, A., and Wolter, L. 1968, *A. J.*, **73**, 65.
- <sup>3</sup>Friedman, H., Byram, E. T., and Chubb, T. A. 1967, *Science*, **156**, 374.
- <sup>4</sup>Brandt, J. C., Stecher, T. P., Crawford, D. L., and Maran, S. P. 1971, *Ap. J.*, **163**, L99.
- <sup>5</sup>Milne, D. K., and Dickel, J. R. 1971, *Nature*, **231**, 33.
- <sup>6</sup>Brandt, H., Burnett, B., Mayer, W., Rappaport, S., and Schnopper, H. 1971, *Nature*, **229**, 96.
- <sup>7</sup>Gorenstein, P., Gursky, H., Kellogg, E. M., and Giacconi, R. 1970, *Ap. J.*, **160**, 947.
- <sup>8</sup>Schwartz, D., Bleach, R. D., Boldt, E. A., Holt, S. S., and Serlemitsos, P. J. 1972, *Ap. J.*, **173**, L51.
- <sup>9</sup>Milne, D. K. 1970, *Aust. J. Phys.*, **23**, 425.
- <sup>10</sup>Gorenstein, P., Harris, B., Gursky, H., Giacconi, R., Novick, R., and Vanden Bout, P. 1971, *Science*, **172**, 369.
- <sup>11</sup>Fransky, R. J. 1971, *Nature Phys. Sci.*, **229**, 229.
- <sup>12</sup>Grader, R. J., Hill, R. W., and Stoering, J. P. 1970, *Ap. J.*, **161**, L45.
- <sup>13</sup>Gorenstein, P., Kellogg, E. M., and Gursky, H. 1970, *Ap. J.*, **160**, 199.
- <sup>14</sup>Cook, B. A., and Pounds, K. A. 1971, *Nature*, **229**, 114.
- <sup>15</sup>Kellogg, E. M., 1971, A Catalog of Soft X-Ray Sources, ASE Report 2536.
- <sup>16</sup>Hamilton, P. A., and Haymes, R. F. 1968, *Aust. J. Phys.*, **21**, 895.
- <sup>17</sup>Harris, D. E. 1962, *Aust. J. Phys.*, **135**, 661.

## References

- Alexander, J. K., Brandt, J. C., Maran, S. P. and Stecher, T. P. 1971, Ap. J., 167, 487.
- Brandt, J. C., Stecher, T. P., Crawford, D. L., and Maran, S. P. 1971, Ap. J., 163, L99.
- Brown, R. L., and Gould, R. J. 1970, Phys. Rev. D, 1, 2252.
- Chodil, G., Mark, H., Rodriques, R., Seward, F. D., and Swift, C. D. 1967, Ap. J., 150, 57.
- Coleman, P. L., 1970, thesis, University of Wisconsin.
- Gordon, C. P., Gordon, K. J., and Shalloway, A. M. 1969, Nature, 222, 129.
- Gordon, K. J., and Gordon, C. P. 1970, Astrophys. Lett., 5, 153.
- Grader, R. J., Hill, R. W., Seward, F. D., and Hiltner, W. A. 1970, Ap. J., 159, 201.
- Harris, D. E. 1962, Ap. J., 135, 661.
- Milne, D. K. 1968a, Aust. J. Phys., 21, 201.
- Milne, D. K. 1968b, Aust. J. Phys., 21, 501.
- Milne, D. K., and Hill, E. R. 1969, Aust. J. Phys., 22, 211.
- Pacini, F., and Rees, M. J. 1970, Nature, 226, 622.
- Palmieri, T. M., Burginyon, G., Grader, R. J., Hill, R. W., Seward, F. D., and Stoering, J. P. 1971, Ap. J., 164, 61.
- Ramaty, R., Boldt, E. A., Colgate, S. A., and Silk, J. 1971, Ap. J., 169, 87.
- Seward, F. D., Burginyon, G. A., Grader, R. J., Hill, R. W., Palmieri, T. M., and Stoering, J. P. 1971, Ap. J., 169, 515.
- Tucker, W. H., and Koren, M. 1971, Ap. J., 168, 283.

## THE BASIC ASSUMPTION

Theodore P. Stecher  
*Laboratory for Optical Astronomy*  
*Goddard Space Flight Center*  
*Greenbelt, Maryland 20771*

As the last of the panel speakers, it is perhaps my duty to examine the basic assertion underlying this conference; i.e., when a supernova occurs there is a release of sufficient energy to ionize a large amount of the surrounding interstellar material and that the Gum Nebula is an example of this process.

The validity of this statement must be checked by examining the observational facts available in the case of the Gum Nebula since theoretical arguments are seldom completely convincing by themselves when the subject is so complex. The first fact would appear to be the establishing of the pulsar in the supernova remnant and the two of them near the center of the Gum Nebula. This pulsar was the first to be found in a supernova remnant and there can be little doubt from both the position and age of the two objects that they are associated. The distances derived by Milne and by Harris for the supernova remnant are relatively uncertain but the finding that the stars previously thought to be the source of ionization of the nebula are located at this same distance may argue in favor of the pulsar being a member of the B-association.

The dispersion measure gives the total number of electrons in the path independent of distance to the pulsar and therefore the total number of electrons in the nebula depends not on the distance to it but only on the height assumed for the nebula. The total estimate of the energy involved, i.e., about  $5 \times 10^{51}$  erg can not easily be changed by a large amount.

This amount of energy is near the total released during the main sequence lifetime of a star. It is also comparable to the binding energy of a neutron star and hence presumably to the energy released by a supernova. A star whose energy output is mostly at wavelengths below the Lyman limit could produce the observed number of electrons if no recombination occurs. Since with the interstellar densities involved recombination is fast with respect to the main sequence lifetime of the stars, an ordinary stellar source for the nebula may be ruled out. The supernova explanation becomes plausible.

Before the supernova explosion a nebula must have existed around each of the hot stars, with the largest one surrounding the pre-supernova itself. These nebulae would be unaffected by the supernova explosion since the gas is

already ionized and their temperatures remain the same, i.e. about  $10^4$  °K. The Morrison-Sartori model of a supernova explosion predicts a temperature of a few times  $10^5$  °K, and this distinction may suggest a way of determining which of the bright nebulae correspond to stellar ionization and which have their origin in ionization by the supernova.



# LOW-INTENSITY H-BETA EMISSION FROM THE INTERSTELLAR MEDIUM\*

R. J. Reynolds, F. Roesler, and F. Scherb

*Physics Department  
University of Wisconsin  
Madison, Wisconsin 53706*

and

E. Boldt

*Laboratory for High Energy Astrophysics  
Goddard Space Flight Center  
Greenbelt, Maryland 20771*

## Abstract

A search for diffuse galactic H-beta emission not associated with any known H II regions was conducted using a 2-inch diameter pressure-scanned Fabry-Perot spectrometer at the coudé focus of the 36-inch telescope at Goddard Space Flight Center.

Observations were made near the directions of four pulsars (PSR 0532, PSR 1508, PSR 1541 and PSR 1642) between November 1969 and June 1970. Emissions with intensities from  $4 \times 10^4$  to  $40 \times 10^4$  photons/cm<sup>2</sup> sec ster (corresponding to emission measures of approximately 10 - 100) were detected in three of the directions. The data indicate an average ionization rate (assuming steady state) of  $\simeq 10^{-14}$ /H-atom sec for the interstellar hydrogen in these directions and temperatures between  $10^3$  °K and  $10^4$  °K for the emitting regions.

Plans have been made to continue the investigation of these very faint hydrogen emission sources using a 6-inch diameter Fabry-Perot spectrometer.

## Introduction

Before the discovery of pulsars, the state of ionization in H I regions was generally attributed to the ionizing effect of starlight on elements whose ionization potentials are smaller than that of hydrogen. For example, ultraviolet radiation escapes from H II regions surrounding hot stars and can

---

\*Supported in part by National Aeronautics and Space Administration grants No. NGL 50-002-044 and No. 50-002-162, and by the University of Wisconsin Graduate School.

produce ions such as  $C^+$ ,  $Si^+$ , and  $Fe^+$  in H I regions. From the known abundances of these elements in the Galaxy, this model for the ionization state in H I regions leads to an electron density  $n_e$  given by

$$n_e/n_H \simeq 5 \times 10^{-4}, \quad (1)$$

where  $n_H$  is the neutral hydrogen density.

Since the discovery of pulsars, observations of pulse dispersions give direct information on electron densities in the interstellar medium. In particular these observations determine the dispersion measure d.m. given by

$$\text{d.m.} = \int_0^d n_e ds, \quad (2)$$

where  $d$  is the distance to the pulsar. In addition, observations of the 21-cm line of atomic hydrogen can determine the columnar density  $N_H$  of neutral hydrogen in the Galaxy, given by

$$N_H = \int n_H ds. \quad (3)$$

Some idea of the order of magnitude of the quantity  $n_e/n_H$  can be obtained from the ratio of d.m. to  $N_H$ . Values of  $\text{d.m.}/N_H \simeq 0.05$  are typical, implying electron densities roughly 100 times larger than expected from ionization by starlight. Therefore, either the number densities of  $C^+$ ,  $Si^+$ , and  $Fe^+$  are 100 times larger than the generally assumed values or additional ionization processes occur which also ionize hydrogen.

Ionization of the interstellar hydrogen, whatever the mechanism, leads to the emission of recombination radiation. In general, the intensity of a particular hydrogen line is given by

$$I_y = \frac{1}{4\pi} \int \epsilon_y \alpha(T_e) n_e n_{H^+} e^{-\tau_y(s)} ds, \quad (4)$$

where  $y$  denotes a particular recombination line,  $\epsilon_y$  is the probability of a  $y$ -photon being emitted per recombination,  $T_e$  is the electron temperature,  $\alpha(T_e)$  is the effective recombination coefficient,  $n_{H^+}$  is the proton density, and  $\tau_y(s)$  is the optical depth to  $y$ -photons of a point at a distance  $s$ . Assuming a steady state,  $I_y$  is also given by

$$I_y = \frac{1}{4\pi} \int \epsilon_y \zeta n_H e^{-\tau_y(s)} ds, \quad (5)$$

where  $\zeta$  is the ionization rate per hydrogen atom. It can be shown that  $\epsilon_y$  varies slowly with  $T_e$ . For H-beta,  $\epsilon_{H\beta}$  has a nearly constant value of 0.12 for  $10^2 < T_e < 10^5$  °K. Therefore, if  $\zeta$  is assumed to be constant throughout the interstellar medium,  $\zeta$  is given by

$$\zeta = \frac{4\pi}{\epsilon_{H\beta}} \cdot \frac{I_{H\beta}}{\int n_H e^{-\tau_{H\beta}} ds} \quad (6)$$

In directions of low 21-cm absorption, e.g., in high galactic latitudes, the columnar density of neutral hydrogen can be directly determined from 21-cm emission measurements. Assuming small optical absorption in these directions, measurements of  $I_{H\beta}$  result in a direct determination of  $\zeta$ , given by

$$\zeta = 105 \frac{I_{H\beta}}{N_H}, \quad (7)$$

where  $I_{H\beta}$  is in units of  $\text{cm}^{-2} \text{sec}^{-1} \text{ster}^{-1}$  and  $N_H$  is in units of  $\text{cm}^{-2}$ . If the value of  $\zeta$  is not assumed to be a constant along the line of sight, then  $I_{H\beta}$  determines an average ionization rate  $\langle \zeta \rangle$ .

In addition, measurements of  $I_{H\beta}$  and a knowledge of the temperature can be combined with pulsar dispersion measures to determine various parameters of the interstellar medium including limits on the electron densities and sizes of the emitting regions. In directions of little reddening or where the reddening is accurately known, the emission measure e.m., defined by

$$\text{e. m.} = \int n_e^2 ds \quad (8)$$

can be computed from  $I_{H\beta}$  and  $T_e$  using values for the  $H\beta$  emissivity of hydrogen computed by Pengelly (1963). The values of e.m. and d.m. can then be used to set limits on both the total length  $L$  along the line of sight occupied by the emitting regions and on the average electron density  $\langle n_e \rangle$  within these regions, defined by

$$\langle n_e \rangle = N_e / L, \quad (9)$$

where  $N_e$ , the columnar electron density through the galactic disk, is defined by

$$N_e = \int n_e \, ds. \quad (10)$$

(Assuming the pulsars are confined to the galactic disk, d.m. must always be a lower limit to  $N_e$ .) The mean square deviation,  $\Delta^2 n_e$ , of  $n_e$  from  $\langle n_e \rangle$  along the line of sight within these regions is defined by the relation

$$\Delta^2 n_e = \frac{1}{L} \int (n_e^2 - \langle n_e \rangle^2) \, ds. \quad (11)$$

From this relation and the definition (9) of  $\langle n_e \rangle$  it follows that

$$\langle n_e \rangle = \frac{1}{\left[ 1 + \frac{\Delta^2 n_e}{\langle n_e \rangle^2} \right]} \cdot \frac{e.m.}{N_e}, \quad (12)$$

and

$$L = \left[ 1 + \frac{\Delta^2 n_e}{\langle n_e \rangle^2} \right] \frac{N_e^2}{e.m.}. \quad (13)$$

Since

$$N_e \geq d.m., \quad (14)$$

and

$$\frac{\Delta^2 n_e}{\langle n_e \rangle^2} \geq 0, \quad (15)$$

the limits on  $\langle n_e \rangle$  and  $L$  are given by

$$\langle n_e \rangle \leq e.m./d.m. \quad (16)$$

and

$$L \geq \frac{(d.m.)^2}{e.m.}. \quad (17)$$

For regions having an approximately uniform electron distribution

$$\left( \frac{\Delta^2 n_e}{\langle n_e \rangle^2} \ll 1 \right),$$

and in a direction where the pulsar dispersion measure is approximately the total columnar electron density ( $d.m. \simeq N_e$ ), the computed limits given by (16) and (17) would be close to the actual values of  $\langle n_e \rangle$  and  $L$ . A comparison of  $(d.m.)^2/e.m.$  with the total distance through the galactic disk in that direction would then be a measure of the "clumpiness" of these regions within the interstellar medium.

Assuming a steady-state ionization process, the intensity of H-beta from the H I interstellar medium can be estimated.\* For X-ray or cosmic ray ionization, the ionization rate  $\zeta$  for equilibrium models has been estimated as  $10^{-15}/H$  atom sec (Field *et al.* 1969, Werner *et al.* 1970, Hjellming *et al.* 1969). Therefore, for an H I cloud occupying 20 pc along the line of sight with a density of 20 hydrogen atoms/cm<sup>3</sup> ( $N_H = 12.3 \times 10^{20}/cm^2$ ) at a distance  $s$  from the earth such that  $\tau_{H\beta} \ll 1$  ( $\tau_{H\beta} \simeq 1$  for  $s = 1$  kpc in the galactic plane), equation (5) gives

$$I_{H\beta}^{cloud} = 1 \times 10^4/cm^2 \text{ sec ster.} \quad (18)$$

The intensity from the intercloud medium in the plane of the galaxy is estimated by integrating over one absorption mean free path for H-beta (1 kpc). Assuming that  $n_H = 1.0 \text{ cm}^{-3}$  ( $N_H = 31 \times 10^{20}/cm^2$ ),

$$I_{H\beta}^{intercloud} = 3 \times 10^4/cm^2 \text{ sec ster.} \quad (19)$$

The H-beta emission from a "classical" H II region is normally the result of ionization due to ultraviolet radiation from nearby O and B stars. Assuming a diameter of 20 pc and  $n_e = 3 - 10 \text{ cm}^{-3}$ , then

$$I_{H\beta}^{HII} = 10^6 - 10^7/cm^2 \text{ sec ster.} \quad (20)$$

In general, the hydrogen emission from a particular direction could include radiation from all these sources: H II regions, H I clouds, and the intercloud medium. With a spectrometer of sufficient sensitivity and resolving power

\*The expected intensities of various radiations resulting from cosmic ray ionization and heating have been calculated in detail by Hayakawa *et al.* (1960) and Balasubrahmanyam *et al.* (1967).

these sources may be distinguished from one another. For example, the position and shape of the H-beta emission profiles could be compared with the position and shape of 21-cm features. Such a comparison should then help determine whether the H-beta emissions were originating from H I regions. Also, it could be possible to distinguish these three sources from one another on the basis of the measured widths of the emission lines and the intensity ratio  $I_{H\alpha}/I_{H\beta}$ . For example, a cloud at a temperature of about  $100^\circ\text{K}$  would emit H-beta with a characteristic line width  $\Delta\lambda \simeq 0.03\text{\AA}$  and  $I_{H\alpha}/I_{H\beta} \simeq 8$ , whereas for an H II region at  $10^4\text{ }^\circ\text{K}$ ,  $\Delta\lambda \simeq 0.34\text{\AA}$  and  $I_{H\alpha}/I_{H\beta} \simeq 4$ . (Actually these line widths  $\Delta\lambda$  are the widths of the two fine structure components of the H-beta line, which are separated by  $0.078\text{\AA}$ .)

The results of the preceding discussion are summarized in Table 1.

Table 1

H-beta Source	$T_e$ ( $^\circ\text{K}$ )	$n_H$ ( $\text{cm}^{-3}$ )	$n_e$ ( $\text{cm}^{-3}$ )	$N_H$ ( $\times 10^{20}\text{ cm}^{-2}$ )	$\left( \frac{I_{H\alpha}}{\text{photons}} \right)$ $\frac{\text{cm}^2}{\text{cm}^2 \text{ sec ster}}$	$\frac{\Delta\lambda}{\text{\AA}} \frac{I_{H\alpha}}{I_{H\beta}}$
H I cloud	$10^2$	20	0.050	12	$1 \times 10^4$	0.03 8
Intercloud medium	$10^3$	1.0	0.025	31	$3 \times 10^4$	0.10 5
H II region	$10^4$	$\sim 0$	3-10	$\sim 0$	$10^6 - 10^7$	0.34 4

Faint H-beta emissions that did not appear to be associated with any known H II regions have been observed by Johnson (1970) using wide-band filters and by Hindle *et al.* (1967), Daehler *et al.* (1968), and Reay and Ring (1969) using relatively low resolution ( $0.6\text{ \AA}$ ) Fabry-Perot spectrometers. Because of the low resolution they could not accurately discriminate between galactic and local emissions, nor could they measure the line profiles of the emission.

A search for faint galactic H-beta emission with relatively high resolution ( $0.13\text{\AA}$ ) was conducted using a 2-inch diameter pressure-scanned Fabry-Perot etalon at the coudé focus of the 36-inch telescope at Goddard Space Flight Center. The observations were conducted between October 1969 and June 1970.

## Instrumentation

The Fabry-Perot etalon as a spectrometer has been discussed widely in the literature (Mack *et al.* 1963, Roesler 1967, Jacquinot 1954). In general, a spectrometer can be characterized by two quantities: the resolving power  $R$ , and the luminosity  $L$ , which is proportional to the flux transmitted by the spectrometer. The fact that the product  $LR$  of a Fabry-Perot etalon can be made much greater (30 to 400 times) than that for a prism or grating of equal area (Jacquinot 1954) makes the Fabry-Perot spectrometers particularly well suited for observations of emission lines from faint extended sources, *i.e.*, for a given resolution, the light can be collected over a relatively large solid angle.

Figure 1 illustrates the combined transmission curve of an etalon and  $6\text{\AA}$  FWHM interference filter used in the observations. The filter was necessary to suppress all etalon transmission peaks except those near the wavelength of interest.

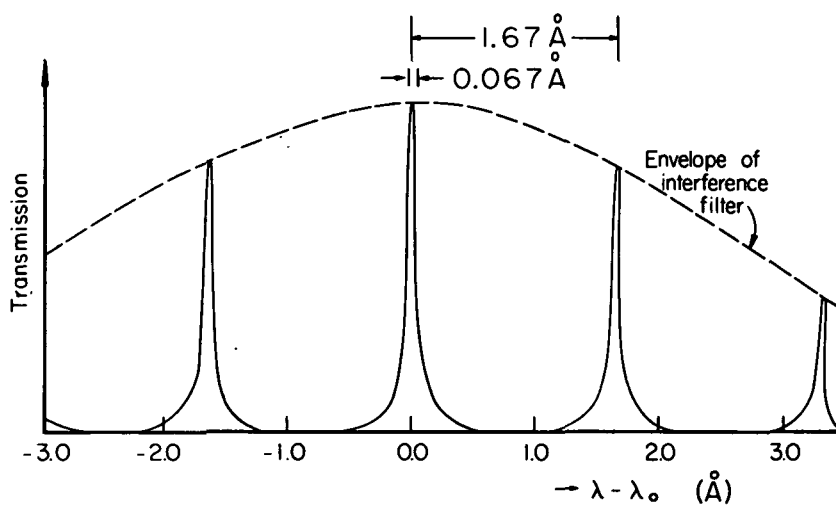


Figure 1. Transmission of etalon for small apertures in series with a  $6\text{\AA}$  interference filter centered on wavelength  $\lambda_0 = 4861\text{\AA}$ .

## Observations

The H-beta recombination line was chosen because its wavelength is near the peak of the S20 photocathode response curve and because the local sky background is low in this wavelength region relative to H-alpha (Eather 1969). Although observations of both the H-beta and H-alpha fluxes are desirable, as will soon be evident, the combination of weak line intensity, low instrumental quantum efficiency, and the limited time available did not permit the study of both H-beta and H-alpha emissions.

In order to maximize the signal-to-noise ratio, in addition to using optical coatings and a cooled photocathode, virtually all observations were restricted to moonless nights with low atmospheric extinction, and, using the 6-inch finder telescope, care was taken to eliminate any stars brighter than 11th magnitude from the 1.5 arc minute field of view. The various contributions to the photomultiplier count rate on a clear, moonless night in and out of the galactic plane are given in Table 2. The signal count rate has been normalized to 0.1/sec and represents the rate at the peak of the line. Such a rate roughly corresponds to the intensities observed.

Table 2  
Contributions to Total Count Rate

Source	in galactic plane	out of galactic plane
dark count	0.6/sec	0.6/sec
sky background	1.0/sec	0.4/sec
emission line	0.1/sec	0.1/sec
total	1.7/sec	1.1/sec
signal/noise	0.08	0.10

Regions near the pulsars PSR 0532 (Crab Nebula pulsar), PSR 1508, PSR 1541, and PSR 1641 were studied. The bulk of the observations in the direction near the Crab were made in January and February 1971, while those in the directions of the other three pulsars were made in the interval from May 29 through June 7, 1970.

It was assumed that the emission would be approximately centered about the local standard of rest (LSR) velocity because, by definition, this is the velocity about which the local intercloud medium and the individual H I clouds are expected to be centered on the average. Since the Crab is close to the galactic anticenter direction ( $l^{\text{II}} = 182^\circ$ ,  $b^{\text{II}} = -6^\circ$ ), there are no



galactic rotation effects in this direction, and all the material along the line of sight should have velocities centered about the LSR velocity. Figures 2 and 3 give 21-cm data for the four regions studied and show that the assumption is justified.

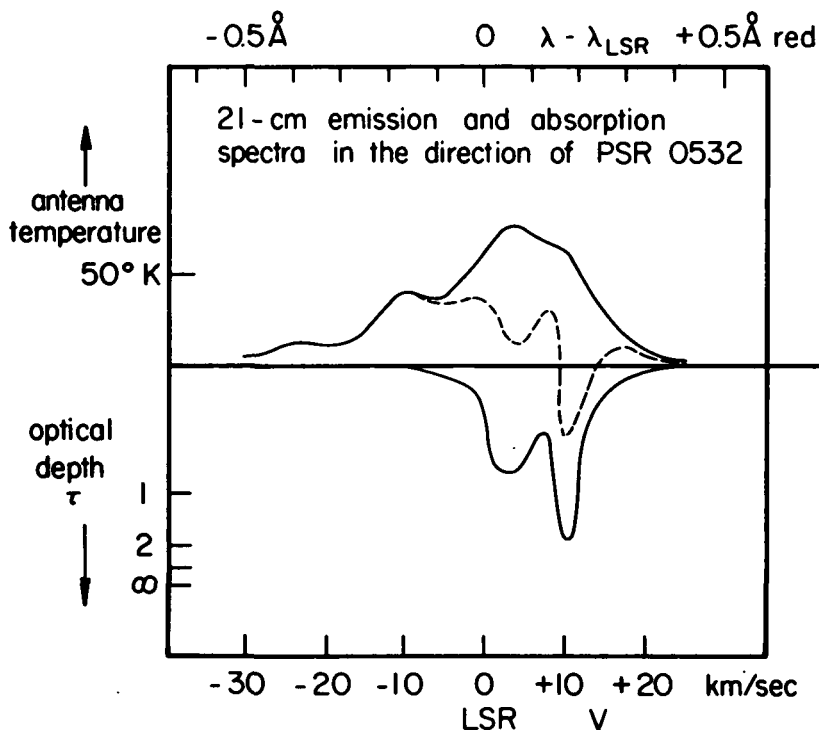


Figure 2. 21-cm emission and absorption spectra in the direction of PSR 0532 as given by Müller (1959). The dashed curve represents the observed profile from which are derived:

- upper curve: the expected emission profile.
- lower curve: the expected absorption profile.

The observations near PSR 0532 were made on a 1.5 arc minute diameter region (the field of view of the spectrometer) located approximately 9 arc minutes from the center of the Crab. The observational results in this direction are presented in Figure 4 where the accumulated counts are plotted as a function of wavelength (and velocity). The data were obtained by two different procedures. In the top two graphs, Figures 4a and 4b, the points

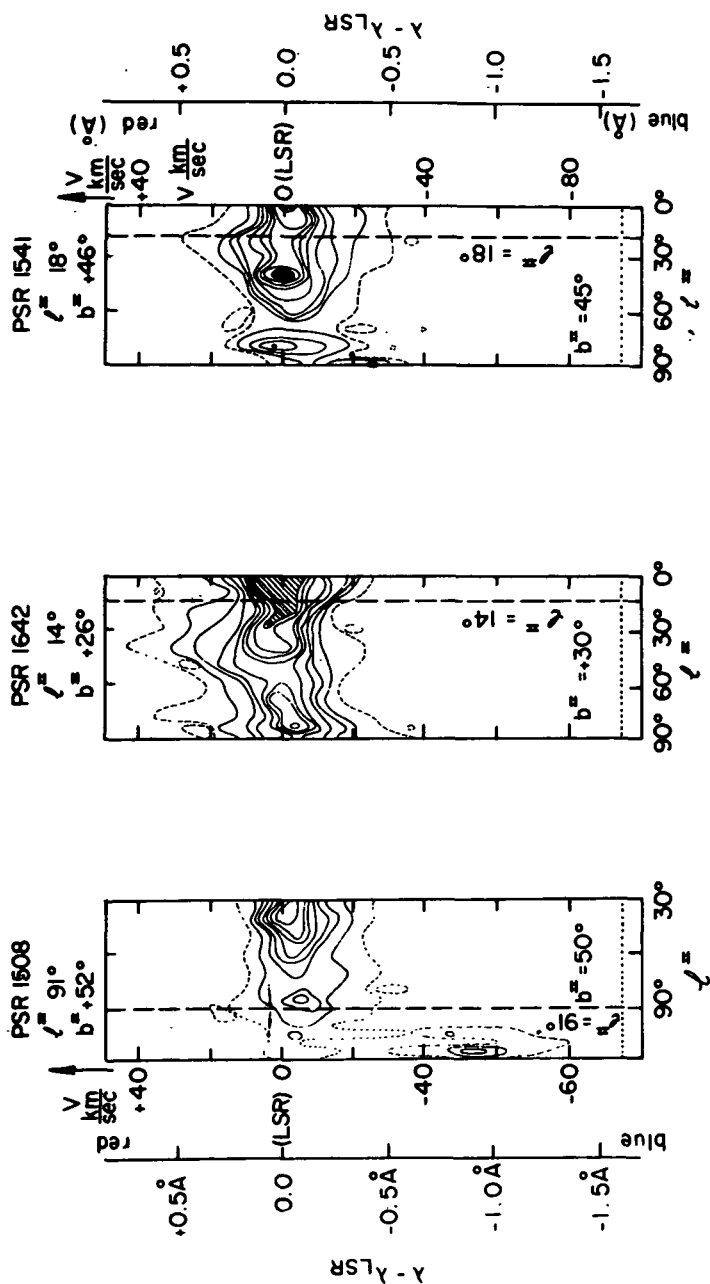


Figure 3. 21-cm emission data as given by Tolbert and Fejes (1969): a) near direction of PSR 1508, b) near direction of PSR 1642, c) near direction of PSR 1541. The contour values, indicated by varying line thickness, are 1 (dashed line), 2, 3, 4, 6, 8, 10, and 14 units, where 1 unit equals  $\sim 1^\circ\text{K}$  in brightness temperature. All intensities greater than 18 units are shaded. Note that the 21-cm emission is centered on the LSR (0 km/sec) velocity in all three directions.

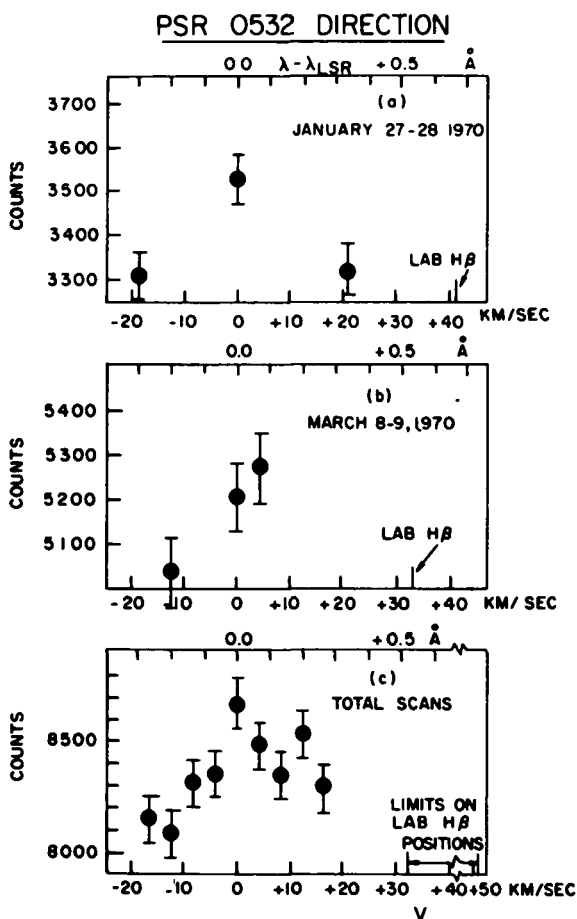


Figure 4. Data in the direction of PSR 0532. LSR at 0 km/sec.

(a) data of January 27-28, 1970; 2000 sec/point.

(b) data of March 8-9, 1970; 3000 sec/point.

(c) sum of all 62 continuous scans from November 16, 1969 through February 28, 1970; 3720 sec/interval; 0.067 Å/interval; direction of observations:

RA = 05<sup>h</sup>32<sup>m</sup>6.4<sup>s</sup>

DEC = +22° 00' 05" 1970

represent the count rates at discrete wavelength positions near the LSR wavelength of H-beta. The bottom graph, Figure 4c, represents the result of an attempt to measure the line profile of the emission. It is the summation of 62 individual continuous pressure scans taken between November 15, 1969 and February 28, 1970. Each point represents an accumulation time of 3720 seconds over a wavelength interval of  $0.066\text{\AA}$ .

There is little doubt that the data in Figure 4 represent real emission, but to establish that the emission was galactic H-beta requires some additional discussion. Because a single etalon produces an ambiguity in the position of a line, the emission could have been an atmospheric line at any one of the permitted wavelengths:  $\lambda_{\text{LSR}} \pm 1.23k\text{\AA}$ , where  $k = 0, 1, 2, 3, \dots$ . However, observations were also made in another direction at the same wavelengths at which the emission was observed from the Crab direction and no emission was detected. Therefore, it appears unlikely that the emission was an atmospheric line. The emission also could not have been H-beta from the geocorona or solar system, since all the data were obtained when the LSR velocity for the Crab direction was about 35 km/sec ( $0.6\text{\AA}$ ) to either side of the H-beta rest wavelength. Any emission at the rest wavelength of H-beta would have appeared as a flat background since it would have been just half-way between two transmission peaks of the etalon. Also any emission at rest with respect to the sun would have been centered about 11 km/sec ( $0.2\text{\AA}$ ) to the blue of the observed emission.

During the observing period from May 30 through June 7, 1970, observations were made in the directions of PSR 1508 ( $l^{\text{II}} = 91^\circ$ ,  $b^{\text{II}} = +50^\circ$ ), PSR 1541 ( $l^{\text{II}} = 18^\circ$ ,  $b^{\text{II}} = +46^\circ$ ) and PSR 1642 ( $l^{\text{II}} = 14^\circ$ ,  $b^{\text{II}} = +26^\circ$ ). The resulting data are shown in Figures 5, 6, and 7. Although the statistics are poor, emissions appear to be present at the LSR velocities in the first two directions. There is some ambiguity as to whether the emissions from the PSR 1508 and PSR 1541 directions are galactic or local since the rest and LSR velocities in these two cases are separated by an amount equal to or less than the resolution of the spectrometer ( $\approx 8$  km/sec). However, the expected flux of H-beta photons from the geocorona is much too low to have contributed significantly to the observed flux. Meier (1969) estimates the H-alpha intensity from the geocoronal absorption of solar Lyman-beta in directions greater than  $90^\circ$  from the Sun to be less than  $4 \times 10^5/\text{cm}^2$  sec ster. Therefore, from the ratio of fluxes of solar Lyman-beta to Lyman-gamma (Hinteregger 1961), and using the values for the absorption cross sections of these two lines and the branching ratios from the  $n = 3$  and  $n = 4$  levels given by Allen (1955) and Bethe and Salpeter (1957), we have

$$I_{\text{H}\beta}^{\text{geocorona}} < 5.5 \times 10^3/\text{cm}^2 \text{ sec ster} \quad (21)$$

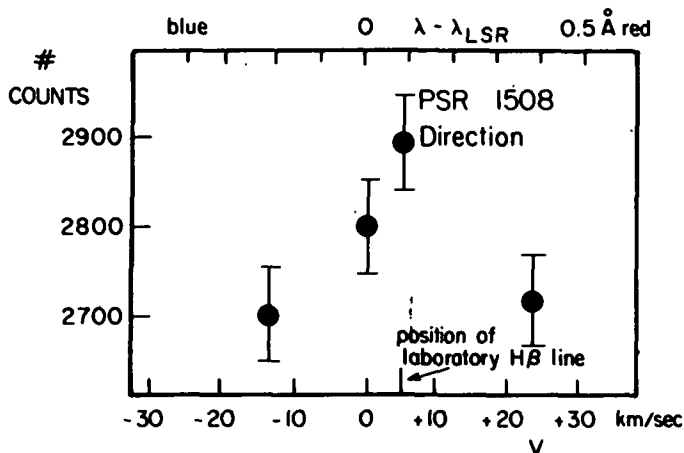


Figure 5. Data in the direction of PSR 1508 obtained May 29-30, 1970; 2700 sec/point; direction of observation:

RA =  $15^{\text{h}} 08^{\text{m}} 03^{\text{s}}$   
 DEC =  $+55^{\circ} 46' 00''$  1970

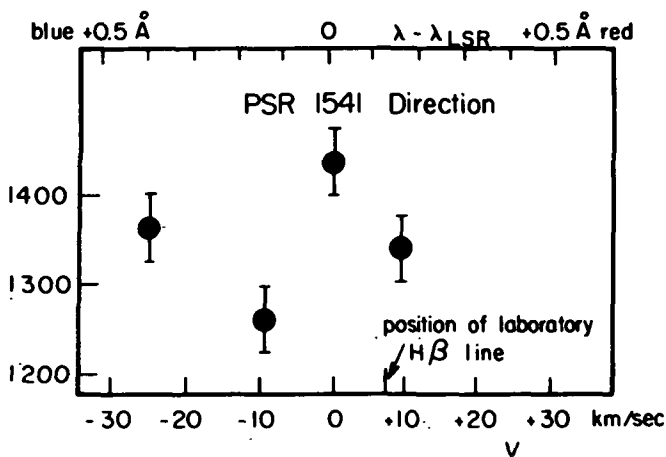


Figure 6. Data in direction of PSR 1541 obtained May 31 – June 2, 1970. 1400 sec/point; direction of observation:

RA =  $15^{\text{h}} 41^{\text{m}} 35.0^{\text{s}}$   
 DEC =  $+09^{\circ} 38' 00''$  1970

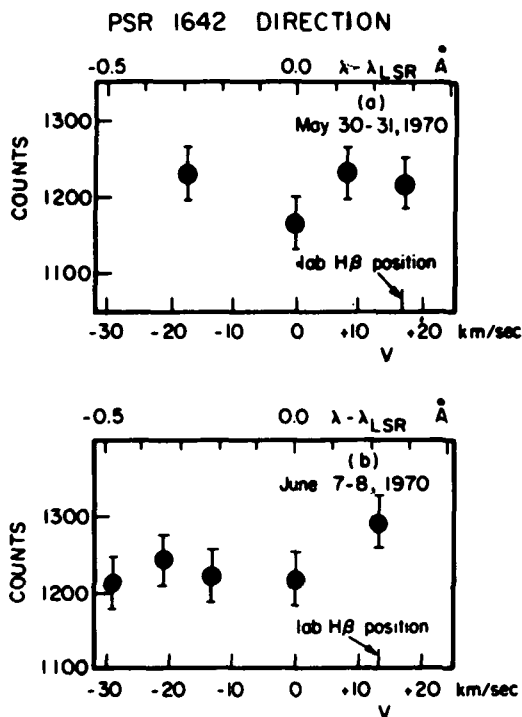


Figure 7. Data in the direction of PSR 1642.  
 (a) data of May 30-31, 1970; 900 sec/point  
 (b) data of June 7-8, 1970; 1000 sec/point.

which is (as will be seen) about one order of magnitude below the observed intensities. The possibility that the observed emissions were due to the absorption of solar Lyman-gamma by a much larger amount of hydrogen perhaps within the solar system cannot be excluded.

In the direction near PSR 1642 no emission was detected at the LSR wavelength.

Because of the rather poor statistics, the widths of the emission lines could not be accurately measured. Therefore,  $I_{H\beta}$  and the quantities that can be derived from  $I_{H\beta}$  ( $\langle \xi \rangle$ , e.m., and limits on  $\langle n_e \rangle$  and  $L$ ) can only be determined as functions of the assumed temperature and turbulent velocities within the emitting regions.

Tables 3 and 4 list these quantities computed from the observed emission near the Crab direction and from the extinction in this region as given by O'Dell (1960). In Table 3 the emission was assumed to be originating from regions occupying a total distance  $L$  along the line of sight and distributed uniformly out to the distance of the Crab. The rms random velocity  $V_{\text{rms}}$  of these regions (or the combination of random velocities and internal turbulent motions) was assumed to be 10 km/sec. The quantity  $\alpha$  is the fraction of the line of sight distance occupied by the emission regions. In Table 3,  $\alpha$  was computed from the relation

$$\alpha = \frac{L}{2000} \geq \frac{(\text{d.m.})^2 / \text{e.m.}}{2000}. \quad (22)$$

In Table 4, the emission was assumed to be originating from a region centered on the Crab at a distance of 2 kpc. Attributing the observed value of d.m. to such a region implies that the value of the columnar electron density  $N_e$  used in the calculations was given by  $n_e = 2 \text{ d.m.}$

Table 3  
PSR 0532  
d.m. =  $56 \text{ cm}^{-3} \text{ pc}$ ;  $V_{\text{rms}} = 10 \text{ km/sec}$

$T_e$ (°K)	$I_{H\beta} \times 10^{-4}$ ( $\text{cm}^{-2} \text{ sec}^{-1} \text{ ster}^{-1}$ )	e.m. ( $\text{cm}^{-6} \text{ pc}$ )	$\langle n_e \rangle$ ( $\text{cm}^{-3}$ )	$L$ (pc)	$\alpha$
100	16	2.8	$\leq 0.050$	$\geq 1100$	$\geq 0.55$
1000	18	11	$\leq 0.19$	$\geq 300$	$\geq 0.15$
10000	39	130	$\leq 2.3$	$\geq 24$	$\geq 0.01$

Table 4  
Emitting Region Centered on PSR 0532  
 $V_{\text{rms}} = 0 \text{ km/sec}$

$T_e$ (°K)	$I_{H\beta} \times 10^{-4}$ ( $\text{cm}^{-2} \text{ sec}^{-1} \text{ ster}^{-1}$ )	e.m. ( $\text{cm}^{-6} \text{ pc}$ )	$\langle n_e \rangle$ ( $\text{cm}^{-3}$ )	$L$ (pc)	$\alpha$
100	12	7.1	$\leq 0.063$	$\geq 1800$	$\geq 0.90$
1000	14	28	$\leq 0.25$	$\geq 440$	$\geq 0.22$
10000	32	371	$\leq 3.3$	$\geq 34$	$\geq 0.02$

Tables 5, 6, and 7 list the parameters for the directions near PSR 1508, PSR 1541, and PSR 1642 respectively. Because of the high galactic latitudes of these pulsars, extinction was neglected in the calculations. The values of  $a$  were computed from the relation,

$$a = L \frac{\sin b^{\text{II}}}{H} \geq \frac{(\text{d.m.})^2}{\text{e.m.}} \cdot \frac{\sin b^{\text{II}}}{H} \quad (23)$$

where  $H$ , the half-thickness of the galaxy, was assumed to be 200 pc and  $b^{\text{II}}$  is the galactic latitude of the direction of the observation. Since in the PSR 1642 direction only an upper limit to the peak count rate could be determined, the values computed for  $I_{\text{H}\beta}$  and e.m. are upper limits with a 90% confidence limit at each temperature.

Table 5  
PSR 1508  
d.m. =  $19.6 \text{ cm}^{-3} \text{ pc}$ ;  $V_{\text{rms}} = 10 \text{ km/sec}$

$T_e$ (°K)	$I_{\text{H}\beta} \times 10^{-4}$ ( $\text{cm}^{-2} \text{ sec}^{-1} \text{ ster}^{-1}$ )	e.m. ( $\text{cm}^{-6} \text{ pc}$ )	$\langle n_e \rangle$ ( $\text{cm}^{-3}$ )	$L$ (pc)	$a$
100	4.0	0.28	$\leq 0.014$	$\geq 1400$	—
1000	4.5	1.1	$\leq 0.055$	$\geq 360$	—
10000	9.0	12	$\leq 0.62$	$\geq 32$	$\geq 0.13$

Table 6  
PSR 1541  
d.m. =  $35 \text{ cm}^{-3} \text{ pc}$ ;  $V_{\text{rms}} = 10 \text{ km/sec}$

$T_e$ (°K)	$I_{\text{H}\beta} \times 10^{-4}$ ( $\text{cm}^{-2} \text{ sec}^{-1} \text{ ster}^{-1}$ )	e.m. ( $\text{cm}^{-6} \text{ pc}$ )	$\langle n_e \rangle$ ( $\text{cm}^{-3}$ )	$L$ (pc)	$a$
100	11	0.79	$\leq 0.023$	$\geq 1600$	—
1000	12	3.0	$\leq 0.085$	$\geq 410$	—
10000	20	26	$\leq 0.75$	$\geq 47$	$\geq 0.17$

The data presented in the tables imply that the observed emission could have originated from any one of a variety of possible regions. For example, the data in Table 3 suggest that the emission may have been from either regions occupying approximately 15 percent of the line-of-sight distance with  $T_e \approx 10^3 \text{ °K}$  and  $n_e \approx 0.19 \text{ cm}^{-3}$  or from a tenuous H II region about 24 pc in diameter with  $n_e \approx 2 \text{ cm}^{-3}$  and  $T_e \approx 10^4 \text{ °K}$ .



Table 7  
PSR 1642  
d.m. =  $40 \text{ cm}^{-3} \text{ pc}$ ;  $V_{\text{rms}} = 10 \text{ km/sec}$

$T_e$ (°K)	$I_{\text{H}\beta} \times 10^{-4}$ ( $\text{cm}^{-2} \text{ sec}^{-1} \text{ ster}^{-1}$ )	e.m. ( $\text{cm}^{-6} \text{ pc}$ )	$\langle n_e \rangle$ ( $\text{cm}^{-3}$ )	L (pc)	$a$
100	$\leq 3.4$	$\leq 0.24$	$\leq 0.006$	$\geq 6700$	—
1000	$\leq 3.7$	$\leq 0.89$	$\leq 0.022$	$\geq 1800$	—
10000	$\leq 7.5$	$\leq 10$	$\leq 0.25$	$\geq 160$	$\geq 0.35$

There are some further statements that can be made about the interstellar medium using the data that were obtained. First, a lower limit can be placed on the average ionization rate  $\langle \zeta \rangle$  along the line of sight, given by Eq. (7). Columnar hydrogen densities  $N_{\text{H}}$  in the directions of pulsars are given by Davies (1969) and a more recent compilation of values of  $N_{\text{H}}$  has been made by Daltabuit (1970). For each direction the lower limit to  $\langle \zeta \rangle$  was computed by choosing the largest value of  $N_{\text{H}}$  from the two compilations and the lowest possible value for  $I_{\text{H}\beta}$ . This latter limit corresponds to assuming a continuous, uniform emitting region ( $T_e < 10^3 \text{ }^\circ\text{K}$ ) along the total line of sight distance through the galaxy. In the direction of PSR 1642 it was not possible to place a lower limit on  $\langle \zeta \rangle$  since no emission was observed.

Secondly, lower limits can be set on the temperatures in the directions of PSR 1508, PSR 1541, and PSR 1642. Since the path lengths through the galactic disk in these directions are less than 300 or 400 pc, the data in Tables 5, 6, and 7 suggest that the temperatures of the emitting regions are greater than  $10^3 \text{ }^\circ\text{K}$ . From the line profile obtained in the Crab direction an upper limit on the temperature can be placed in that direction:

$$T \leq 2 \times 10^4 \text{ }^\circ\text{K} \text{ (90\% confidence interval)}$$

$$T \leq 1 \times 10^4 \text{ }^\circ\text{K} \text{ (60\% confidence interval)}$$

More restrictive limits on the temperatures can be obtained from the radio absorption measurements of Ellis and Hamilton (1966). By assuming that the absorption of the galactic radio radiation below 20 MHz is caused by free-free transitions of ionized hydrogen, they were able to compute as a function of galactic latitude a quantity they call the absorption index a.i. defined by

$$\text{a.i.} = \int \frac{n_e^2}{(T/10^4)^{3/2}} ds. \quad (24)$$

Table 8  
Limits On  $\langle \zeta \rangle$

Direction	$I_{H\beta}$ Minimum ( $\times 10^4/\text{cm}^2 \text{ sec ster}$ )	$N_H$ Maximum ( $\times 10^{20} \text{ cm}^{-2}$ )	$\langle \zeta \rangle$ Minimum ( $\times 10^{-15}/\text{sec atom}$ )
PSR 0532	16 $\pm$ 4	43†	9.5 $\pm$ 2.4
PSR 1508	4.0 $\pm$ 1.6	4.9†	8.6 $\pm$ 3.5
PSR 1541	11 $\pm$ 5	8.0*	14 $\pm$ 7

†Davies (1969).

\*Daltabuit (1970).

They found that a.i. varied smoothly\* with galactic latitude in a way consistent with a uniform disk-like distribution of ionized hydrogen. The values for a.i. were computed for southern galactic latitudes, but, assuming galactic symmetry about the solar position†, values for a.i. could be estimated in the directions of the H-beta observations. If uniform temperatures are assumed in the regions occupied by the electrons, the emission measure can be written as

$$e.m. = a.i. (T/10^4)^{3/2} \quad (25)$$

Since these values for e.m. determined by radio absorption techniques have a different functional dependence on temperature than the values determined by observations of H-beta recombination lines, a graphical comparison of both data as shown in Figure 8 can be used to determine the temperatures which are compatible with both types of observations in a particular direction. These temperatures together with the temperature limits determined from previous considerations are summarized in Table 9. Depending upon the particular direction, temperatures from 1,600 °K to 11,000 °K are indicated for the emitting regions.

Referring back to Tables 3, 5, 6, and 7, the higher temperatures that are indicated by the comparisons with radio data suggest that the emission regions have electron densities (depending upon the particular direction) in the range 0.1 to 2.5  $\text{cm}^{-3}$  and occupy anywhere from 1% to 100% of the line of sight distance through the galactic plane.

\*The beamwidth of the radiotelescope was  $\sim 8^\circ$ .

†Rocket observations of the north galactic pole by Alexander and Stone (1965) are consistent with this assumption.

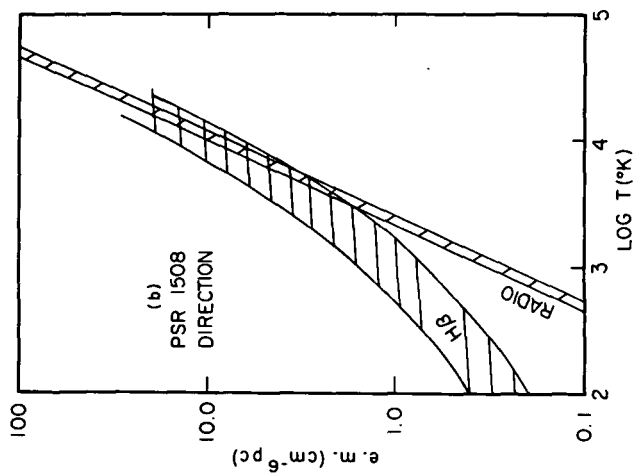
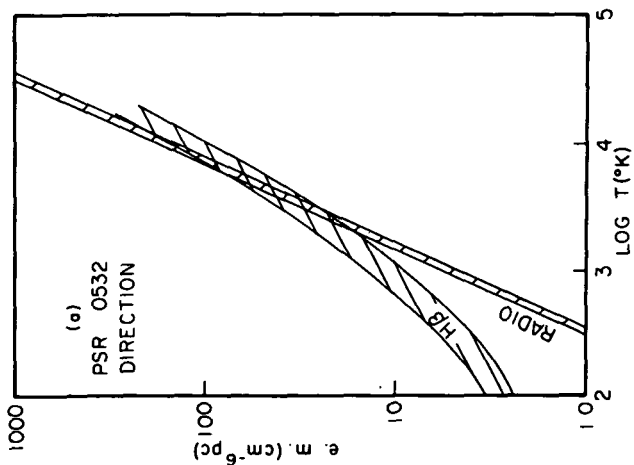


Figure 8. (b) direction near PSR 1508.

Figure 8. Comparisons of e.m. ( $T_e$ ) from the radio absorption measurements of Ellis and Hamilton (1966) with e.m. ( $T_e$ ) derived from the observed H-beta intensities. The cross-hatched regions represent the area bounded by  $\pm 1$  standard deviation in the data. (a) direction near PSR 0532.

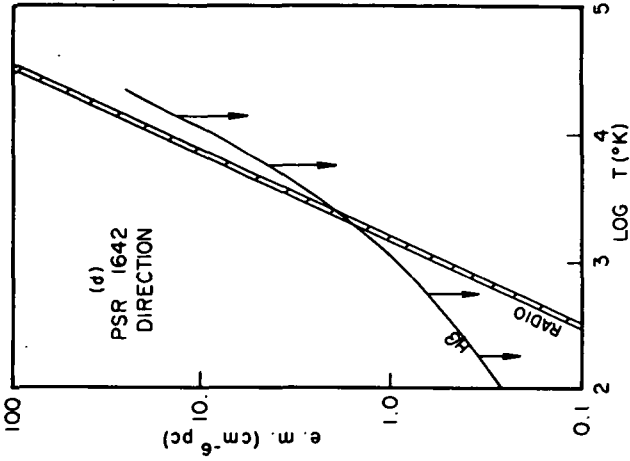


Figure 8. (d) direction near PSR 1642. The single solid line represents the upper limit to e.m. as derived from the H-beta observations assuming no extinction.

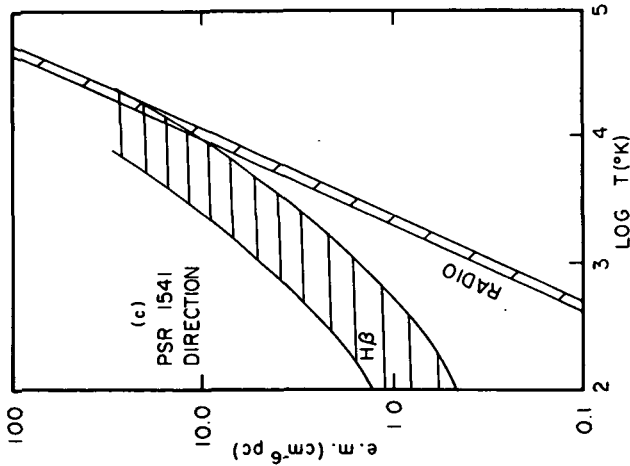


Figure 8. (c) direction near PSR 1541.

Table 9  
Limits on Emission Region Temperatures

Direction	$b^{\text{II}}$ (deg)	$T(^{\circ}\text{K})$		
		from line profile	from condition $a \leq 1.0$	from comparison of $\text{H}\beta$ and radio
PSR 0532	- 6	$<10^4$	—	$1.6 \times 10^3$ to $1.1 \times 10^4$
PSR 1508	+52	—	$\geq 1.4 \times 10^3$	$\geq 2.5 \times 10^3$
PSR 1541	+46	—	$\geq 1.6 \times 10^3$	$\geq 1.0 \times 10^4$
PSR 1642	+26	—	$\geq 4.3 \times 10^3$	$\leq 1.6 \times 10^3$

### Discussion

According to a model by Bottcher *et al.* (1970), large sections of the interstellar medium are ionized by ultraviolet photons from supernova explosions (Morrison and Sartori 1969). Such an effect could also arise from highly ionizing subrelativistic nuclei (e.g.: Si and Fe) ejected by these explosions (Ramaty *et al.* 1971). Since the cooling time for the medium is much shorter than the recombination time, the medium quickly cools after a supernova occurs, leaving behind a high residual amount of ionization. Therefore, along a given line of sight, various regions of the interstellar gas are in different stages of relaxation depending upon when the last supernova in each particular region occurred. The H-beta data at high galactic latitudes are consistent with this model, assuming that a sufficient time has elapsed (since the occurrence of supernovae in those directions) to have allowed the regions to cool from an initial  $10^5$  °K (Cox 1970) down to  $\sim 10^4$  °K. But in the vicinity of the Crab Nebula, since the Crab supernova occurred only  $10^3$  years ago, the hydrogen still should be nearly 100 percent ionized and at a temperature near  $8 \times 10^4$  °K (Lenzen and Cox 1970). Using a value of  $10^{61}$  photons/outburst and an interstellar hydrogen density of  $1 \text{ cm}^{-3}$ , the diameter of this region would be about 100 pc corresponding to a region on the sky  $3^{\circ}$  in diameter. The associated H-beta intensity from this region at the Earth would be  $1.1 \times 10^4 \text{ cm}^{-2} \text{ sec}^{-1} \text{ sterad}^{-1}$  in a line  $1 \text{ \AA}$  wide. The observed emission in the direction of the Crab, therefore, cannot be explained by such a model. This does not eliminate the possibility, however, that some or most of the dispersion measure may be due to such a region. This would have the effect of leaving fewer electrons available to produce the observed emission, thus increasing the limits on  $\langle n_e \rangle$  and decreasing the limits on  $L$  in Table 4, for example.

These investigations will be continued at the Goddard telescope, using a 6-inch diameter etalon system which has 10 times the collecting area of the 2-inch system. It should be remembered that the line intensities that have been observed correspond to emission measures as low as 10 for temperatures of  $10^4$  °K and emission measures less than one for temperatures as low as 100 °K. Therefore, it is hoped that the 6-inch system will be a powerful tool in the search for and investigation of extended emission sources which are too faint to have been observed by other methods.

#### Acknowledgments

It is a pleasure to thank Dr. V. K. Balasubrahmanyam for anticipating the value of the measurements and Dr. Pierre Connes for suggesting the use of a pressure-scanned Fabry-Perot spectrometer.

## References

- Alexander, J. K., and Stone, R. G. 1965, Ap. J., 142, 1327.
- Allen, C. W. 1955, Astrophysical Quantities (London: The Athlone Press).
- Balasubrahmanyam, V. K., Boldt, E., Palmeira, R. A. R., and Sandri, G. 1967, G.S.F.C. Report X-611-67-357.
- Bethe, H. A., and Salpeter, E. E. 1957, Quantum Mechanics of One- and Two-Electron Atoms (New York: Academic Press).
- Bottcher, C., McCray, R. A., Jura, M., and Dalgarno, A. 1970, Astrophys. Lett., 6, 237.
- Cox, D. P. 1970, private communication.
- Daehler, M., Mack, J. E., Stoner, J. O., Jr., Clark, D., and Ring, J. 1968, Planet. Space Sci., 16, 795.
- Daltabuit, E. 1970, private communication.
- Davies, R. D. 1969, Nature, 223, 355.
- Eather, R. 1969, private communication.
- Ellis, G. R. A., and Hamilton, P. A. 1966, Ap. J., 146, 78.
- Field, G. B., Goldsmith, D. W., and Habing, H. J. 1969, Ap. J., 155, L149.
- Hayakawa, S., Nishimura, S., and Takayanagi, K. 1961, Pub. Astr. Soc. Japan, 13, 184.
- Hindle, P. H., Reay, N. K., and Ring, J. 1968, Planet. Space Sci., 16, 803.
- Hinteregger, H. E. 1961, J. Geophys. Res., 66, 2367.
- Hjellming, R. M., Gordon, C. P., and Gordon, K. J. 1969, Astron. and Astrophys., 2, 202.
- Jacquinet, P. 1954, J. Opt. Soc. Amer., 44, 761.
- Johnson, H. M. 1971, Ap. J., 164, 379.
- Lenzen, A., and Cox, D. P. 1970, private communication.
- Mack, J. E., McNutt, D. P., Roesler, F. L., and Chabbal, R. 1963, Applied Optics, 2, 873.
- Meier, R. R. 1969, J. Geophys. Res., 74, 3561.
- Morrison, P., and Sartori, L. 1969, Ap. J., 158, 541.

- Müller, C. A. 1959, Paris Symposium on Radio Astronomy, ed. R. N. Bracewell (Stanford: Stanford University Press), p. 360.
- O'Dell, C. R. 1962, Ap. J., 136, 809.
- Pengelly, R. M. 1963, M.N.R.A.S., 127, 145.
- Ramaty, R., Boldt, E. A., Colgate, S. A., and Silk, J. 1971, Ap. J., 169, 87.
- Reay, N. K., and Ring, J. 1969, Planet. Space Sci., 17, 561.
- Roesler, F. L., and Mack, J. E. 1967, Journal de Physique, C2, 313.
- Tolbert, C. R. and Fejes, I. 1969, A General Survey of 21-cm Radiation at High Galactic Latitude, Netherlands Foundation for Radio Astronomy.
- Werner, M. W., Silk, J., and Rees, M. J. 1970, Ap. J., 161, 965.



# LARGE NEBULAR COMPLEXES IN THE NORTHERN PORTION OF THE GALAXY

William J. Webster, Jr.\*  
*Laboratory for Solar Physics*  
*Goddard Space Flight Center*  
*Greenbelt, Maryland 20771*

## Abstract

Several northern complexes of ionized hydrogen, stars and possibly non-thermal radio emission are known whose properties are similar to those of Gum's nebula. Among the best known complexes are the Ori I and Ceph IV associations and IC 1795-IC 1805-IC 1848. Each of these complexes contains an extended ring structure and requires more excitation than is available from the known early-type stars. We examine the properties of these objects and show that many of the properties of Gum's nebula are common to such galactic complexes.

## Introduction

Several of the better known nebular complexes have properties reminiscent of those ascribed to Gum's nebula by Brandt *et al.* (1971). Although none of the complexes we consider contains pulsars (Reifenstein, Brundage and Staelin 1969), four of them have nonthermal emission associated (Ori I, Ceph IV, W28, Monoceros). All (except W49) contain a low-surface-brightness ring structure surrounding a central star clustering. In these cases where a significant portion of the exciting stars can be identified (Ori I, Ceph IV, IC 1805), the stellar component is visible through the ring and may have dense H II associated with the stars (Ori I) or the individual stars may be highly reddened as if they were surrounded by dust clouds (Ceph IV; Reddish 1967). In any case, the dust distribution is highly irregular throughout the complexes.

The volume occupied by these complexes is larger than the typical H II regions studied by many observers (for example, Schraml and Mezger 1969). This can be attributed to the relatively extended associations which are responsible for at least part of the excitation of the nebulosities. In each case,

---

\*NAS-NRC Resident Research Associate.

a substantial amount of neutral hydrogen, ionized hydrogen, dust and molecules is scattered throughout the volume. Such data as are available indicate that each of these components is highly clumped. The gas and dust mass can be of the order of  $10^4 M_{\odot}$ , while each of the complexes contains at least  $10^2 M_{\odot}$  in stars.

In the following sections we will examine the data on each of these complexes. The available radio data will be stressed since the radio brightness is unaffected by optical absorption. In the final section we will compare these objects and Gum's nebula.

### The Orion I Association

The Orion I association contains several stellar groupings of a common origin but with different ages (Blaauw 1964). The youngest of these stellar groupings contains the stars responsible for the excitation of the Orion Nebula (M 42, M 43). In addition to the bright nebulosity around the Trapezium, bright nebulosity is associated with  $\lambda$  Orionis and the  $\zeta$  Orionis region (NGC 2024, and IC434; it is unlikely that  $\zeta$  Ori excites NGC 2024, M. A. Gordon 1969). Beside these bright nebulae, weak nebular emission pervades most of the region between the dense H II regions and dust clouds are present throughout. The most obvious dust clouds are the dark bay which enters M 42 on the east side and reaches almost to the Trapezium, the dark cloud which divides NGC 2024 into roughly equal parts and the dark bay associated with the Horsehead Nebula. A number of early type stars are scattered throughout the region (Walker 1969).

The extent of the stars and nebulosity of the Ori I association is best seen on very wide field, long exposure photographs. From these photographs (see, for example, the frontispiece to Baker's Astronomy) it is clear that the nebulosity covers the whole constellation and extends northward until it merges with the Milky Way in Gemini. A conservative estimate of the projected size is an ellipse with axes  $40^{\circ} \times 30^{\circ}$  with the major axis at position angle  $30^{\circ}$ . Within these boundaries, a number of extended structures can be seen. The brighter of these structures are associated with the Barnard Loop. In red light, the Barnard Loop appears to be an ellipse of axes  $14^{\circ} \times 10^{\circ}$  with the major axis at position angle  $0^{\circ}$  and centered roughly between the Sword and Belt regions of Orion.

Using Gemini-11 ultraviolet objective prism photographs, O'Dell, York and Henize (1967) showed that the Barnard Loop is extremely bright at short wavelengths. They suggested that the Barnard Loop represents the interface between predominantly ionized hydrogen and predominantly neutral hydrogen in the outskirts of the Ori I association. On this hypothesis, the Barnard

Loop is the result of the interaction between the stellar radiation field and the gas and dust from which the stars of the association formed. It appears that, if the Barnard Loop is radiatively excited, some Lyman continuum flux must leak through, since material beyond the Barnard Loop is ionized. The optical emission measure, however, is probably less than 600 because of the very low surface brightness. Because of the great extent of this low surface brightness component, a substantial source of energy is required to maintain it.

Continuum interferometry of the compact nebulosities (M 42, M 43, NGC 2024, etc.) shows that each contains considerable structure on a size scale of 10 arc sec (0.03 pc). These structures have been interpreted as the ionized remnants of the protostar complexes from which the exciting stars formed (Webster and Altenhoff 1970a; Wink, Webster, and Altenhoff 1972). Each of the compact nebulosities is surrounded by a less compact envelope which gradually merges into the surrounding background. Thus, the compact nebulae are core-halo sources (cf.: Schraml and Mezger 1969). At centimeter wavelengths, only the most dense nebulosity can be detected without difficulty in continuum measurements. To detect the least dense portions of the nebulosity, high sensitivity and low frequencies are required.

Rishbeth (1958a), has mapped the Orion complex at 85.5 MHz and 19.7 MHz using Mills Cross antennas. The half-power responses were  $50' \times 60'$  and  $85' \times 100'$  respectively. In addition to emission from the stronger sources, Rishbeth detected 85.5 MHz radiation which is clearly associated with the Barnard Loop. This radiation comes from a rough ring less than 15 pc thick with an electron density of about  $4 \text{ cm}^{-3}$  on the eastern side and  $\leq 1.5 \text{ cm}^{-3}$  in the faintest portions of the ring. A diffuse source about  $7^\circ \times 12^\circ$  in extent covers most of the Barnard Loop but extends beyond the northeast portion of the Loop (this object is called Orion X by Rishbeth). Since absorption from this diffuse source is not detected at 19.7 MHz, Rishbeth infers that the source might be nonthermal. This important observation needs confirmation. Should the interpretation prove correct, it suggests that a supernova might have occurred in the heart of the Ori I association a long time ago. If the source is thermal, however, its emission measure is  $\leq 300 \text{ pc cm}^{-6}$ .

Observations of the central portion of the association in the 21-cm hydrogen line (C. P. Gordon 1970) show that a considerable amount of neutral hydrogen is present ( $7 \times 10^4 M_\odot$ ). The spectral region is clearly recognizable on velocity-longitude plots because of its apparent rotation with respect to the surrounding gas (period  $\sim 5 \times 10^7 \text{ yr}$ ). The center of the Barnard Loop is not coincident with the area of increased H I density which could be said to define the center of the complex. The Loop center is more than  $3^\circ$  from

the peak of the H I and the Loop is wholly contained in the H I region bounded by the rotation. It is of considerable interest that radio recombination line observations of M 42 (Mezger and Ellis 1968) and NGC 2024 (M. A. Gordon 1969) indicate a rotation of the ionized gas in the opposite sense from the neutral gas.

The presence of considerable optical absorption is implied by the many dust clouds and reflection nebulae within the complex. Further, the 21-cm emission studies (C. P. Gordon 1970) and interferometric studies of the 21-cm absorption (Clark 1965) show that the hydrogen is highly clumped.

From these data, a picture of the Ori I association emerges. Within a volume whose projection is an ellipse with axes of at least 350 pc  $\times$  260 pc, is a vast complex of gas, dust, and stars. The highest surface brightness objects in the complex are high density, highly clumped H II regions. These objects are typically 2 pc in diameter and contain a few  $M_{\odot}$  of ionized gas and as much as 100  $M_{\odot}$  in stars. Surrounding these high density regions and their more diffuse halos is a ring of nebulosity with axes 100  $\times$  80 pc. Underlying these structures is a very diffuse low-frequency radio source which may either be very thin plasma or nonthermal emission. The amount of neutral hydrogen and dust and the clumpiness of the distribution suggests that the period of star formation is not over in the Ori I association.

#### The Cepheus IV Association

The optical structure of the Cepheus IV OB association has been studied extensively by MacConnell (1968). He found that it contains numerous T-Tauri stars and reflection nebulae and a substantial number of O and early B stars. The central portion of the association is obscured by a dust cloud which appears to have a fairly sharp edge. Bright rims occur on the southern edge of the cloud. The inner part of the association is surrounded by an irregular ring of emission nebulosity (NGC 7822) of diameter about  $2^{\circ}$ . The brightest portion of the ring is on the southern side, near the edge of the dust cloud, so that some sections of the ring are seen through the dust cloud.

Radio continuum emission from NGC 7822 has been studied by Churchwell and Felli (1970). They find that, as might be expected, the brightest portions of the ring are the strongest radio sources. The dust cloud, thus, does not completely absorb the optical radiation from the ring in these regions. Since the radio contours follow the overall optical emission well in most regions, the net absorption is light, although clearly spotty. The 6-cm radio contours show a well defined minimum in the center of the ring. From a comparison of the brightness temperatures of 20 cm and 6 cm, Churchwell and Felli

conclude that there is a nonthermal component contributing to the emission of the two bright regions which comprise the southern portion of the ring. They further conclude that the nonthermal component becomes increasingly important on the western side of this region. Although this conclusion can be disputed on the basis of the accuracy of the flux density and brightness temperature measurements, the available Lyman continuum flux is at least a factor of 2 less than that required by the assumption that the radio emission is wholly thermal.

MacConnell (1968) finds that the association has a diameter of 60 pc. On the basis of similar distances, he suggests that the Ceph I and Ceph III associations as well as the Ceph IV association might be part of a huge OB complex. The individual associations would be the Blaauw (1964) subgroups of the complex. Should this be true, the complex covers a region  $24^\circ \times 10^\circ$  on the sky and extends over a line of sight distance of more than 130 pc, centered 800 pc from the sun.

#### The IC 1795 – IC 1805 – IC 1848 Complex

This large complex which contains the Cassiopeia OB VI association, covers a region at least  $5^\circ \times 3^\circ$  on the sky and is about 3 kpc distant. It contains the radio sources W3, W4 and W5. W3 is a compact, high density H II region on the northwest edge of W4. W4 is an extended ring-like nebula which surrounds IC 1805, similar to NGC 7822 and Ceph IV (Akabane *et al.* 1967). W5 is associated with IC 1848 and S26. No evidence is available to suggest that any non-thermal emission comes from this complex (Caswell 1967).

W3 is associated with IC 1795. No exciting stars are known for all but the most diffuse portions of the object even though some of the brightest optical nebulosity of the entire complex occurs in this region. Thus, it is not surprising that single antenna (Schraml and Mezger 1969) and interferometer mapping (Webster and Altenhoff 1970b) show the presence of several small, extremely dense condensations near the peak of radio emission while most of the radio source is obscured by at least 7 magnitudes of dust (Ishida and Kawajiri 1968). One of the optically invisible, compact sources is associated with strong OH and  $\text{H}_2\text{O}$  emission (Aikman 1969; Schraml and Mezger 1969).

The H-alpha isophotes of Ishida and Kawajiri (1968) show that IC 1795 is a bright region on the northeast portion of a ring of emission nearly  $3^\circ$  in diameter which surrounds the cluster IC 1805. The cluster contains several OB stars, the earliest being of spectral type O5V (Ishida 1970). The ring surrounding IC 1805 is roughly defined at radio wavelengths and shows a minimum in the center. Several bright condensations mark the border of the ring. None of these condensations is as bright as IC 1795, however.

To the east of the ring around IC 1805 is another ring structure associated with IC 1848 and S26. The ring is not very obvious on optical photographs because of substantial absorption of light from the northern portion of the nebula. At centimeter wavelengths, the ring structure is very clear and the central minimum is well defined (Kaifu and Morimoto 1969). The dust clouds probably obscure both the optical emission corresponding to W5 and the total extent of the entire complex.

### Other Complexes

We have examined some of the best studied complexes. Other groupings may have similar properties. These merit additional study both in the radio and optical regions of the spectrum.

The complex W28 consists of a ring-type supernova remnant and two thermal sources. The nonthermal component is unique in that, although it has been identified as a supernova remnant (Goss and Robinson 1968), radio recombination line radiation has been detected from the brightest portion of the ring (Reifensten et al. 1969).

W49 (Mezger, Schraml and Terzian 1967) is on the other side of the galactic nucleus from the sun at a distance of 14 kpc. Although the total extent of the thermal component cannot be determined, the total excitation required to support the observed portion suggests that this component surrounds a very young association. More than 5 OB stars are needed in a volume of diameter 4 pc to account for the radio emission (Webster, Altenhoff and Wink 1971).

A recent study of the region of the Rosette nebula was made by Holden (1968) using a 178-MHz pencil beam array. The observations suggest that the Monoceros loop, which has been identified as a supernova remnant, may be directly associated with the Rosette nebula. Should further observations support this suggestion, the complex would be comparable with the structure of the inner region of the Ori I association.

### Discussion

Objects with many of the properties of Gum's nebula are rather common. In the past, such complexes have not been thought exceptional because of their size but rather due to the complexity of their structure and the diversity of their constituents. The angular size of Gum's nebula marks it as an exceptional object but it is not clear whether other complexes are as extensive. It may be that Gum's nebula is unique in that its outer portions can be traced optically to very low emission measures.

It should be noted that Gum called his nebula a "giant" H II region by virtue of its apparent size. More recently, "giant" H II regions have been characterized by the value of  $D^2 S$ , where  $D$  is the distance, usually in kpc, and  $S$  is the flux density emitted by the entire source at a frequency where both the H II region and the intervening medium are optically thin. For a "giant" H II region,  $D^2 S$  is required to be greater than some value, usually 400. Hjellming (1968) has shown that this parameter is a measure of the total Lyman continuum luminosity required for excitation of the observed radio emission. While each of the complexes we have discussed is a "giant" H II region by this criterion, the thermal portion of Gum's nebula is clearly not a giant H II region (see Rishbeth 1958b).

For most of the complexes we have discussed, the known sources of excitation are insufficient to account for the observed continuum radio emission by at least a factor of 2. Because of the extensive and irregular dust clouds associated with these complexes, it has been usual to ascribe the missing excitation to completely obscured O-stars. Some justification for this assertion is to be found in the fact that the overall spectral indices for the radio sources are thermal to within the errors of measurement.

Except for W49, the objects considered show a low surface brightness ring surrounding their inner parts. It is not clear in every case whether the rings can be explained by mechanisms connected with the early-type stars of the complexes or whether a primeval supernova explosion is required. Such evidence as is available suggests that the ring in W28 and the Monoceros loop are supernova remnants while the Barnard Loop, the Rosette nebula, W4 and W5 are thermal. Further work is required to settle the question for Orion X and NGC 7822. In the case of the clearly thermal rings, the areal extent of the associated surface brightness emission is large enough so that the required excitation must greatly exceed the excitation needed to sustain the emission of the denser regions.

The total angular size of these complexes is difficult to determine optically because of the associated dust clouds. The best hope seems to be low frequency, high sensitivity, high resolution radio observations. Since these observations detect the lowest density ionized material in emission, it might be possible to observe the ionized hydrogen of a complex almost to the density where it merges into the surrounding medium. It is, of course, important that the nonthermal foreground and background emission be properly accounted for. Some support for this suggestion comes from the work of Rishbeth (1958a), who detected 85 MHz emission from material in Ori I with emission measures as low as 300. Mills Cross antennas, because of their large collecting area and beam swinging capabilities seem ideal for this purpose.

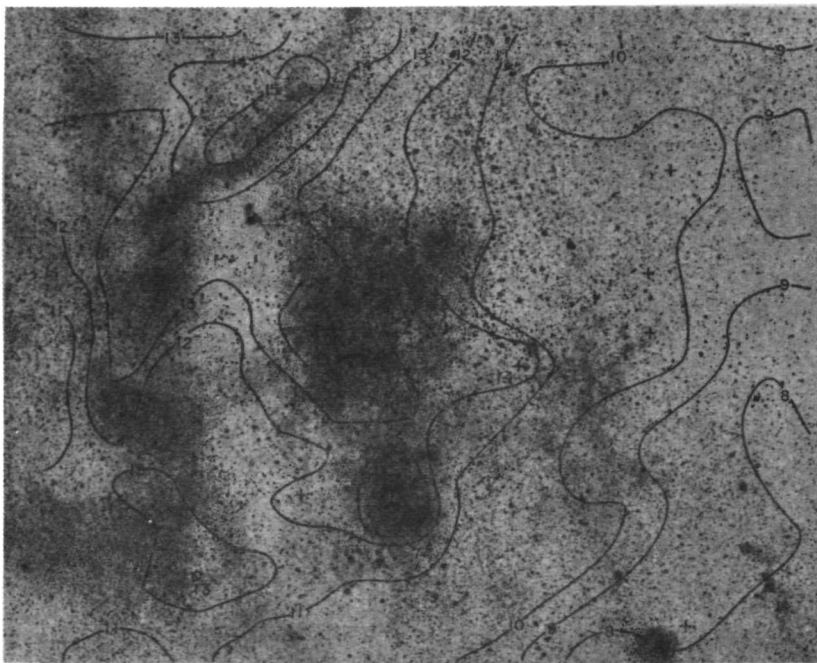


Figure 1. Overlay of Rishbeth's 3.5-m map of the radio emission from the inner regions of Ori I on a wide-field photograph. Contour unit =  $100^\circ\text{K}$ . + = unresolved source;  $\odot$  = extended source. Courtesy of R. M. Hjellming and C. S. Smith.

#### Acknowledgments

I acknowledge helpful discussions with W. J. Altenhoff, R. M. Hjellming, C. M. Wade, and J. E. Wink.



## References

- Aikman, G. C. 1968, unpublished Masters dissertation, Univ. of Toronto.
- Akabane, K., Miyazawa, K., Takahashi, T., Ishizawa, Y., and Nakajima, T. 1967, Tokyo Astr. Bul. 2nd Ser., No. 117, 241.
- Blaauw, A. 1964, Ann. Rev. Astr. and Ap., 2, 213.
- Brandt, J. C., Stecher, T. P., Crawford, D. L., and Maran, S. P. 1971, Ap. J., 163, L99.
- Caswell, J. L. 1967, M.N.R.A.S., 137, 141.
- Churchwell, E., and Felli, M. 1970, Astron. and Astrophys., 4, 309.
- Clark, B. G., 1965, Ap. J., 142, 1398.
- Gordon, C. P. 1970, A. J., 75, 914.
- Gordon, M. A. 1969, Ap. J., 158, 479.
- Goss, W. M., and Robinson, G. J. 1968, Astrophys. Letters, 2, 81.
- Hjellming, R. M. 1968, Ap. J., 154, 533.
- Holden, D. J. 1968, M.N.R.A.S., 141, 57.
- Ishida, K. 1970, Pub. Astron. Soc. Japan, 22, 227.
- Ishida, K., and Kawajiri, N. 1968, Pub. Astr. Soc. Japan, 20, 95.
- Kaifu, N., and Morimoto, M. 1969, Pub. Astron. Soc. Japan, 21, 203.
- MacConnell, D. J. 1968, Ap. J. Suppl., 16, 275.
- Mezger, P. G., and Ellis, S. A. 1968, Astrophys. Letters, 1, 59.
- Mezger, P. G., Schraml, J., and Terzian, Y. 1967, Ap. J., 150, 807.
- O'Dell, C. R., York, D. G., and Henize, K. G. 1967, Ap. J., 150, 835.
- Reddish, V. C. 1967, M.N.R.A.S., 135, 251.
- Reifenstein, E. C. III, Brundage, W. D., and Staelin, D. H. 1969, Ap. J., 156, L125.
- Reifenstein, E. C. III, Wilson, T. L., Burke, B. F., Mezger, P. G., and Altenhoff, W. J. 1970, Astron. and Astrophys., 4, 357.
- Rishbeth, H. 1958a, M.N.R.A.S., 118, 591.

Rishbeth, H. 1958b, Austral. J. Phys., 11, 550.

Schraml, J., and Mezger, P. G. 1969, Ap. J., 156, 269.

Walker, M. F. 1969, Ap. J., 155, 447.

Webster, W. J., Jr., and Altenhoff, W. J. 1970a, Astrophys. Letters, 5, 223.

Webster, W. J., Jr., and Altenhoff, W. J. 1970b, A. J., 75, 896.

Webster, W. J., Jr., Altenhoff, W. J., and Wink, J. E. 1971, A. J., 76, 677.

Wink, J. E., Webster, W. J., Jr., and Altenhoff, W. J. 1972, in preparation.

# PRELIMINARY RESULTS ON AN H-ALPHA MAP OF THE GUM NEBULA OBTAINED WITH THE D-2-A SATELLITE

J. E. Blamont and A. C. Levasseur  
*Service d'Aéronomie du C.N.R.S.*  
*B.P. No. 3*  
*91-Verrières, France*

## I. Introduction

Data on H-alpha emission from the Gum Nebula were obtained first by Gum and Allen in 1952. They discovered an intense emission centered at the galactic coordinates  $l = 226^\circ$ ,  $b = -8^\circ$ , with a diameter of at least  $15^\circ$ . However, the filter used had a large bandwidth, so that the limits of the nebula and its absolute intensity were not obtained.

A map of the Milky Way in the southern hemisphere was published by Johnson in 1960. The resolution was 2 to 3 arc minutes. The filter had a bandwidth of  $326\text{\AA}$ , centered on  $6560\text{\AA}$ , and was therefore transparent to the [N II] lines at  $6548\text{\AA}$  and  $6583\text{\AA}$  and to the telluric emissions of oxygen and OH. The maximum intensity found between  $07^{\text{h}}00^{\text{m}}$  and  $08^{\text{h}}00^{\text{m}}$  Right Ascension was about 60 Rayleighs, from which Johnson (1960) subtracted 5R of night sky emission ( $1.5 \times 10^{-5} \text{ erg cm}^{-2} \text{ s}^{-1} \text{ sterad}^{-1}$ ).

## II. H-alpha Experiment on D-2-A

The purpose of this experiment is to study the hydrogen emissions in the terrestrial atmosphere. These include the telluric H-alpha emission, which is supposed to have an intensity of a few R. This emission was discovered through ground-based observations; however, such measurements are strongly contaminated by night sky emissions, due largely to OH. It has been proven that the OH emissions arise between the altitudes of 80 km and 120 km. A further contamination of the ground-based observations is due to a strong continuum, originating from about the same altitudes, whose source has not yet been proven. The H-alpha experiment on D-2-A was, therefore, designed as a monochromatic photometer that would provide measurements of weak H-alpha emission originating at altitudes of a few hundred or thousand km, free of contamination by other telluric emissions. It was found immediately that the Gum Nebula was recorded by the instrument as a much more intense feature than the geocoronal emission; this note presents a map of the data that were obtained a few weeks before the GSFC Symposium on the Gum Nebula and Related Problems.

### A. Spacecraft

D-2-A, launched April 15, 1971 from Kourou (French Guyana), is a 96-kg, sun-stabilized spacecraft. The orbit parameters at launch were: apogee 702 km, perigee 453 km, and inclination  $45^\circ$ .

The satellite is a cylinder whose axis is kept parallel to the sun-spacecraft direction by an active stabilization system with an accuracy of a few arc minutes. The satellite rotates about this axis with a period of 60 seconds.

Two types of optical experiments are carried by D-2-A; the first kind has its optical axis parallel to the rotation axis, and the second kind has its optical axis perpendicular to the rotation axis. The H-alpha photometer is of the second type, and therefore every 60 seconds, its optical axis traces out a great circle on the celestial sphere, orthogonal to the sun-spacecraft direction (i.e.: orthogonal to the ecliptic plane). Forty of these circular scans are made per satellite orbit, and the circle rotates across the sky at  $1^\circ$  per day due to the orbital motion of the Earth. Thus a complete map of the sky can be obtained in six months.

### B. Optics

The photometer (Fig. 1) is a very simple system, comprising one lens, two filters, and a dual-cathode photomultiplier. The lens L (diameter = 100 mm, focal length = 500 mm) projects an image of the sky in its focal plane. The flat mirror M is used to rotate the beam by  $92^\circ$ , because of spacecraft geometrical constraints.

Before the focal plane, a shutter, actuated by a photodiode, protects the photomultiplier against a strong signal, as obtained during the daylight part of the orbit. This shutter also holds the two small mirrors  $M_1$  and  $M_2$  that are used, together with the light source C, for on-board calibration measurements.

In the focal plane, the two interference filters  $F_1$  and  $F_2$  are placed in front of a dual cathode photomultiplier; the wavelengths of peak transmissions for these filters are  $6563\text{\AA}$  and  $6530\text{\AA}$ . Thus, the incident beam is split into two beams, one at H-alpha and the other at (H-alpha -  $33\text{\AA}$ ). Each of these beams hits a separate photocathode.

The photomultiplier has two cathodes but only one multiplier system, and there is only one amplifier for the two channels. For 1/16 second, one photocathode is fed and the corresponding gate of the counter is open; thus a measure at one wavelength is obtained. For the next 1/16 second, the

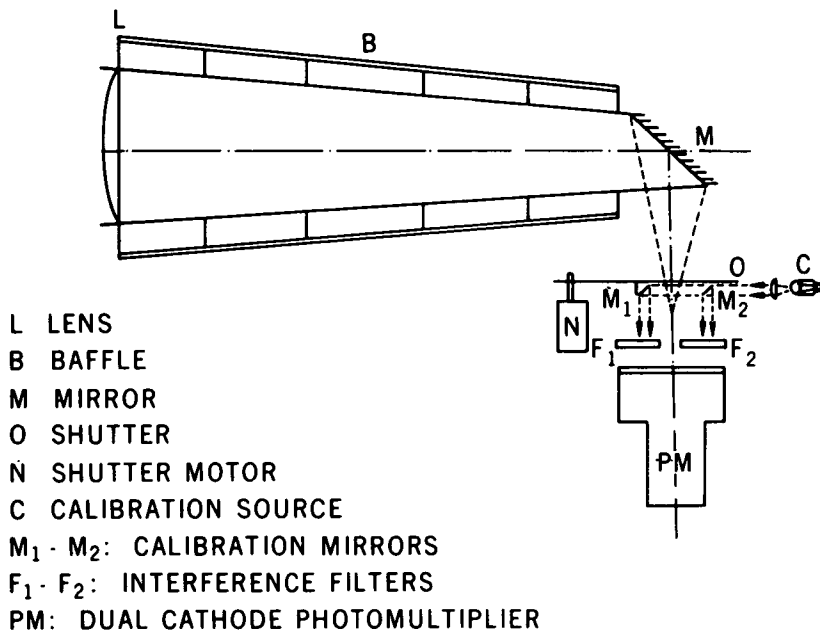


Figure 1. Optical schematic of the H-alpha photometer on satellite D-2-A.

other photocathode is fed and its gate is open, so that a measure at the second wavelength is obtained. This procedure is repeated 7 times and the results are integrated, providing one 7/8 second observation every 2 seconds. The signal is processed by a pulse-counting technique with threshold discrimination and a floating point counter, and transmitted via PCM telemetry.

The dark current is measured once every 236 seconds when the shutter is closed for 7/8 second.

Both wavelengths are recorded independently, and the H-alpha emission is determined by subtracting the 6530Å intensity from the 6563Å intensity while taking the proper ratio into account.

### C. Instrumental Performance

Field of view. For each channel, the field would be  $1^{\circ} 20' \times 2^{\circ} 40'$  for a stationary spacecraft. However, during a measurement interval of 1 second, the satellite rotates by  $6^{\circ}$ . Deconvolution of the signal allows us to reduce the field from  $(6 + 2)^{\circ}$  to  $2^{\circ}$ .

Spectral response. Figure 2 illustrates the response of the two channels; the bandwidth can be taken safely as about  $20.5\text{\AA}$ .

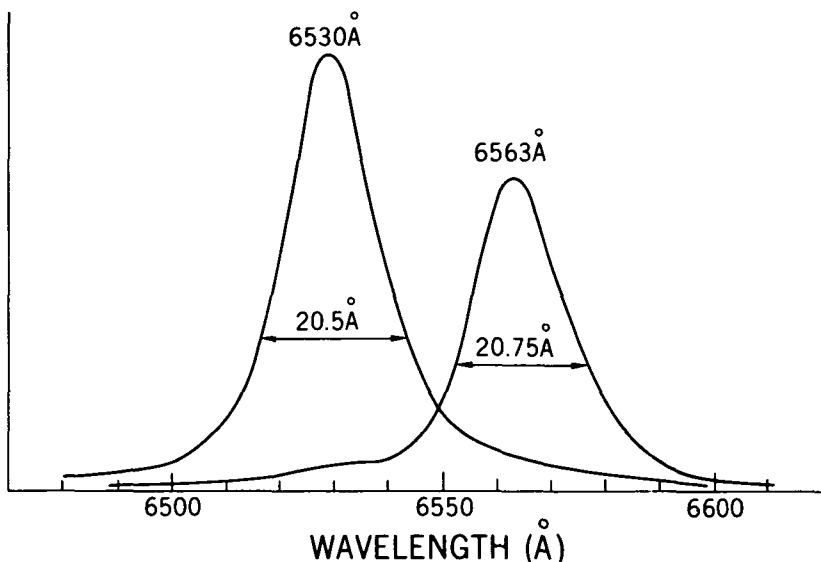


Figure 2. Transmission curves for the two channels of the H-alpha photometer.

Absolute calibration. The response of the instrument to a secondary source was determined. This source, a white Osram flat tungsten ribbon lamp, has been calibrated carefully against a primary standard from the Physikalisches Institut in Berlin. The estimated preliminary error in the absolute value is less than 50%; this error should be reduced when evaluation of the experiment is completed.

It is found that the instrument yields 75 pulses for 1R of H-alpha light; the dark current is less than 100 pulses per second.

Linearity. The linearity is excellent over the range of 0.5R to 120R.

In-flight performance. The instrument was turned on by ground command on April 19, 1971, and it functioned as planned. During the "day" portion of the orbit, the stray light is strong and the shutter remains closed. The dark current during the orbit "night" is 60 pulses per second (0.8R).

The ratio of the calibration signals in the two channels as measured in orbit is identical to the laboratory value, and the absolute values of the calibration signals are also unchanged.

We conclude that the equipment is providing accurate and reliable measurement.

### III. Results

The intensity of the continuum observed outside the Milky Way is  $0.6R/\text{\AA}$  and the intensity of the geocoronal H-alpha emissions is in the (5 to 1)R bracket. The brightest feature observed so far is the Gum Nebula. Figure 3 shows an example of a part of the maps obtained over the line AB (see the chart, Fig. 4). The intensity plotted in Fig. 3 is obtained, as explained above, by subtracting the  $6530\text{\AA}$  intensity from the  $6563\text{\AA}$  intensity, with an appropriate calibration factor. The great strength of the Gum Nebula H-alpha emission as compared to those of the geocorona and the Milky Way is obvious.

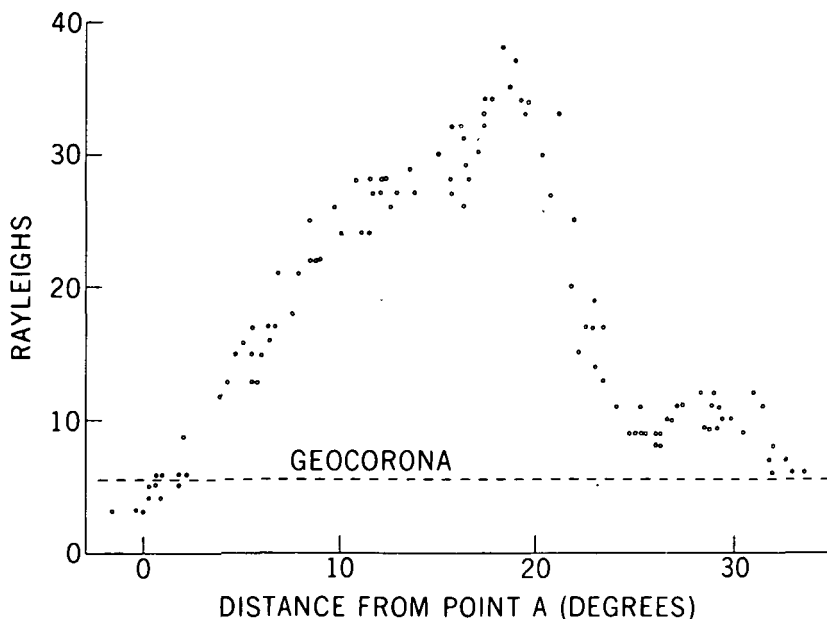


Figure 3. H-alpha intensity measured along the line segment AB in the Gum Nebula region on April 29 – May 2, 1971 (see Figure 4). The dashed horizontal line indicates the geocoronal intensity.

The maximum intensity recorded in the Gum Nebula in the present observations is  $44R$ , in good agreement with Johnson's results but definitely on the low side.

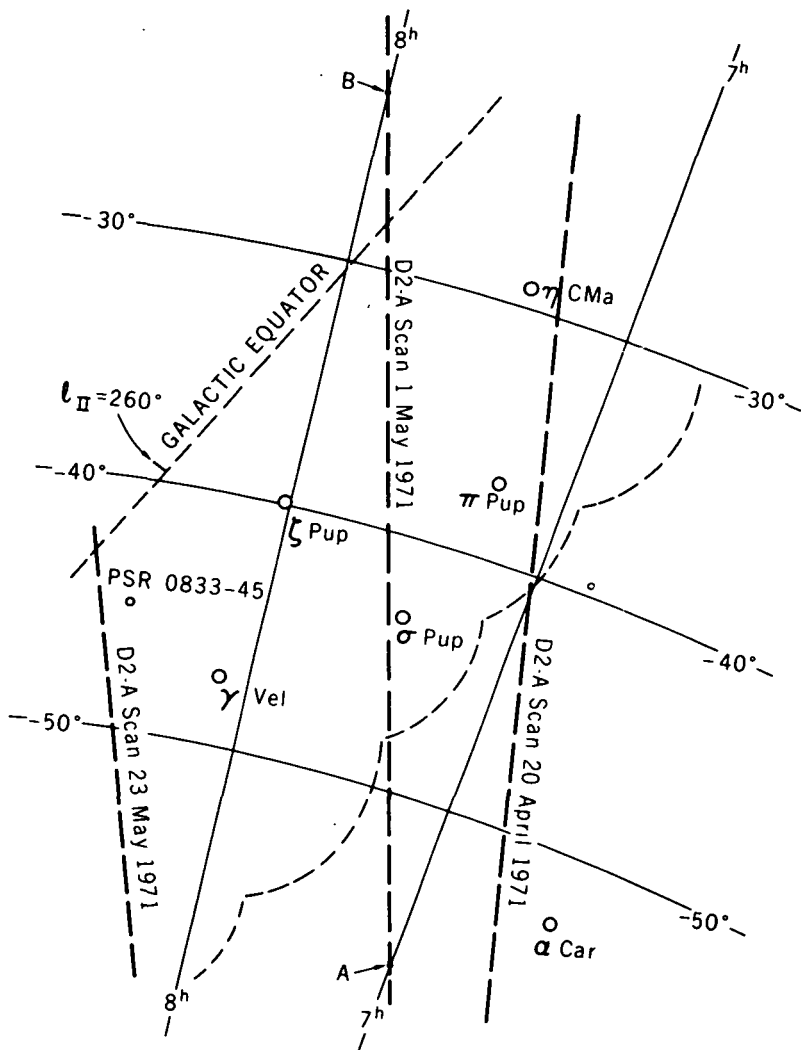


Figure 4. Sketch showing the position of line AB in the sky. The curved, dashed line indicates the western boundary of the region surveyed by H. M. Johnson. The coordinates are Right Ascension and Declination (1950).



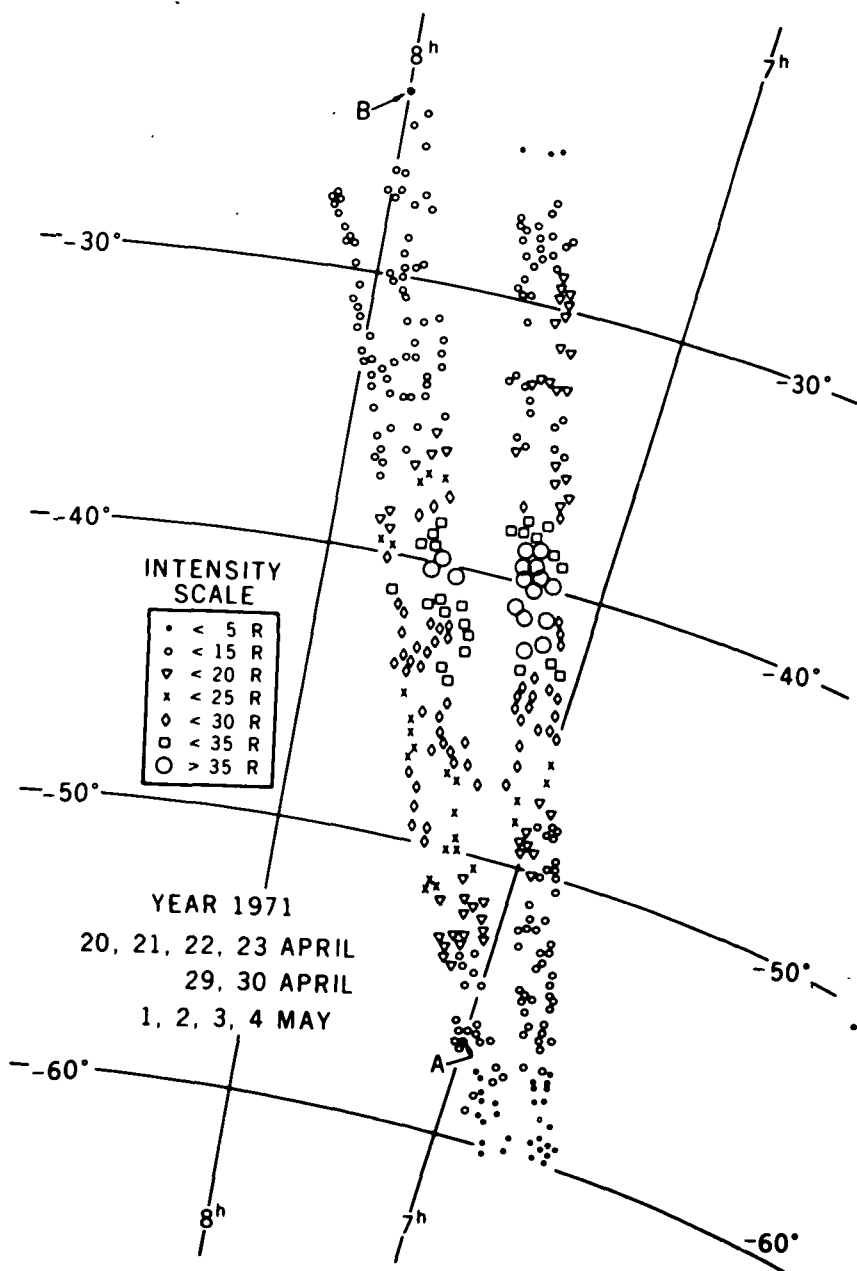


Figure 5. Measurements of the intensity of H-alpha emission from the Gum Nebula region, obtained by the D-2-A satellite during late April and early May, 1971. At each location, the size of the mark indicates the brightness in Rayleighs.

Figure 5 contains the essence of the results presented in this paper, a map obtained from the data collected during April 20 to May 4, 1971.\* Again, H-alpha data have been plotted after first subtracting the continuum. This map will be extended and completed, since good data have been obtained down to the data of writing (July 2, 1971). As of this date, the extent in declination of the Gum Nebula appears to be  $30^\circ$  to  $35^\circ$ . The resolution of the D-2-A map is inferior to that of the Johnson maps, but it is more extended, the intensity is given in steps of 5R instead of 15R, and since our bandwidth is  $20.5\text{\AA}$  there is no contamination by astrophysical emission features.

A complete map of the absolute intensities, with a resolution of  $2^\circ$  and a bandwidth of  $20.5\text{\AA}$  will be available at the end of 1971.

#### References

- Abt, H. A., Morgan, W. W., and Strömgren, B. 1957, Ap. J., 126, 322.  
Gum, C. S. 1952, Observatory, 72, 151.  
Gum, C. S. 1955, Mem. R.A.S., 67, 155.  
Johnson, H. M. 1960, Mem. Mt. Stromlo Obs., 3, 15.

---

\*Editor's Note: In Figure 5 we have had to lump together the author's data for intensities  $< 10R$  and  $< 15R$ , due to difficulties in presentation. SPM.

## HOW TO RECOGNIZE AND ANALYZE GUM NEBULAE\*

Gart Westerhout

*Astronomy Program, University of Maryland  
College Park, Maryland 20742*

In the course of this Symposium, it became clear that we expect something like one supernova in the Galaxy every 25 to 50 years. If their effect in terms of Gum Nebula type objects lasts  $10^4$  years, then on the average within about 1 kpc from us we would see one Gum Nebula — as we do. Within 2 kpc, which is the kind of region where one expects to be able to recognize filamentary structures, etc., we can expect about four of them. So when we talk about recognizing Gum Nebulae, we should be aware of the fact that we are really looking for only a few objects — maybe five to ten at the most.

The second point that became quite clear in today's discussion is that the theorists know a lot more about supernovae than the observers. This, of course, is a healthy state of affairs. The theorist has no bounds to restrict him; and the observer has hardly any data and thus is almost unbounded also. The theorist has a lot to show us. Theory predicts large quantities of iron, helium and other materials to be thrown out, and I think the observer should look for these. It is also clear that we need more and better equipment to solve the really important problems of the Universe, a point which I hope will be noted by the representatives of the Government's funding agencies present. Supernovae seem to be the objects which put the iron and all the other elements except hydrogen and helium in the Universe; and Man is made from these, which brings us back to the relation of Man to the Universe.

Now let us address ourselves briefly to the means of recognizing Gum Nebulae. There are a number of ways. Sky surveys, including those of X-ray sources, pulsars,  $H\alpha$  and radio emission need to be integrated; the searcher for Gum Nebulae should use all the means at his disposal, and could then follow the pattern set by Brandt *et. al.* which led to this Symposium.

I would submit also that low-frequency radio astronomy with a high-resolution instrument is a very powerful way to detect Gum Nebulae. Simple calculations for the free-free emission process show that an Emission Measure of  $1000 \text{ cm}^{-6} \text{ pc}$  will give an optical depth of around 5 at 10 MHz and around

---

\*Based on introductory remarks to the panel discussion at the Symposium, this contribution was received too late for inclusion in the Preliminary Edition of these proceedings. (Ed.)

$3 \times 10^{-3}$  at 1000 MHz for a medium at  $10^4$  K. In the central parts of the Gum Nebula, the Emission Measure is very much higher, and hence a very deep absorption hole is to be expected. But even the outlying regions, with Emission Measures of perhaps 500 or so, will reach considerable optical depths and thus will show in absorption. Of course, the satellite measurements, at an even lower frequency and with a very wide beam, show the Gum Nebula as a very prominent, very large feature. Narrow-beam measurements at say 10 MHz would almost certainly show the entire outline of the nebulosity. And more distant nebulae with that kind of Emission Measure, which optically would not be detectable or at least very hard to detect because of interstellar absorption, could be mapped with relative ease.

But why not do it at high frequencies, like 1000 MHz? The outlying parts of the Gum Nebula, with Emission Measures of 500 or less, would give rise to brightness temperatures of the order of 1K and would get lost in the jumbled nonthermal emission of several degrees, connected with loops and spurs.

A low-frequency wide-beam instrument will smear out the very deep absorption hole over the size of its beam. Hence, Alexander's RAE measurements show a very large feature with apparent optical depth of only 3 or so, as a combination of the effect of the very faint outlying regions and the central hole which probably has an optical depth of 100 or more. With a high-resolution low-frequency antenna we are almost sure to be able to detect almost all thin nebulae; the reason we have not done so is probably a lack of interest, so that appropriate instruments have not been constructed. Since such ground-based instruments are unbelievably cheap as compared to high-frequency instruments, I suggest that if indeed the interest in local (within 1000 pc) faint nebulosity is there, their construction should be pushed.

Finally, on the optical side, it is amazing that detailed spectroscopic investigations of faint nebulosities have hardly been made. Such measurements, done with the emerging electronic instruments such as Fourier Transform Spectrometers, Fabry-Perot/Image tube combinations and even ordinary Coudé-scanners, will be very important. They bear on the problem of the structure of the interstellar medium. For example, how much of the matter is in the form of filaments. Do "clouds" really exist? H II regions certainly seem cloudy, without much, if any, filamentary structure. So do many of the dark nebulae. But then there are the Gum Nebula type filaments — or the dust filaments like those in the Pleiades. If there is a 400 parsec diameter region in every square kiloparsec which has been influenced by a supernova outburst, then a big fraction of the interstellar medium should contain filaments.

Therefore, studies of filamentary structures will not only help in our understanding of Gum Nebulae and our models for these, but also in our understanding of the interstellar medium as a whole.

## INDEX

## A

- A 35 (S 313), 13  
 1AS&E 0900-40 (see also Vela XR-1), 158  
 Abell, G. O., 13, 18  
 Ables, J. G., 47, 51  
 absorption index, 185, 186  
 Abt, H. A., 141, 146, 210  
 Aikman, G. C., 197, 201  
 Akabane, K., 197, 201  
 Alexander, J. K., 5, 6, 9, 12, 18, 19, 31-37, 38, 40, 54, 90, 95, 99, 101, 112, 113, 117, 142, 155, 163, 166, 186, 191, 212  
 Allen, C. W., 1, 2, 3, 180, 191, 203  
 Allen, J. W., 96, 99  
 Aller, L. H., 26, 66, 104, 117  
 Altenhoff, W. J., 141, 144, 147, 195, 198, 200, 201, 202  
 Alter, G., 128, 137  
 Altizer, R., 119  
An Atlas of H-Alpha Emission in the Southern Milky Way, 47  
 Andrews, M. H., 142  
 Arnett, W. D., 73  
 Arnett model, 73  
 Ashkin, J., 99  
Astronomy, Baker's, 194  
Astrophysical Quantities, 1  
Atlas Australis, 119  
 Australia, observatories, 149

## B

- Baade, W., 11  
 Bailey, H. H., 9, 13, 18, 51  
 Baker, R. H., 194  
 Balasubrahmanyam, V. K., 97, 99, 173, 190, 191  
 Balazs, B., 128, 137  
 Ball, J. A., 144, 145, 146  
 Balmer lines (see also H-alpha and H-beta), 14, 108  
 Barkat, Z., 75, 85

- Barnard Loop, 134, 194-196, 199  
B-association, iii, 5, 42, 45-50, 55, 119-127, 148  
Batchelor, R. A., 51  
Bates, D. R., 98, 99  
Becker, M. A., ii  
Becker, W., 137  
Becvar, A., 119, 125  
Bergeron, J., 63, 66, 145, 146  
van den Bergh, S., 11, 130, 131, 136, 137  
Bethe, H. A., 99, 180, 191  
Bieritz, J. H., 130, 137  
binary stars, 119-120  
    dynamics of, 42-50, 53  
    evolution, 78  
Bird, M., ii  
Blaauw, A., 43, 51, 88, 122, 125, 194, 197, 201  
Black, J., 146  
blackbody spectrum, 21, 30, 58, 152, 153, 157  
black hole, 76, 79  
Blamont, J. E., ii, 203-210  
Blann, M., 90, 99  
blast wave theory, 26, 58, 113, 157  
Bleach, R. D., 165  
blueshift, 22  
Boersma, J., 43, 51  
Bok, B. J., ii, 7, 9, 10, 19, 38, 40, 54, 101, 112, 117, 148-151  
Boldt, E. A., iv, 28, 66, 89-100, 117, 156, 157, 165, 166, 169-192  
bolometric correction, 26, 29, 30, 57, 103, 152  
Bottcher, C., 56, 57, 62, 63, 66, 155, 189, 191  
Vanden Bout, P., 165  
Bracewell, R. N., 2, 3, 192  
Bradt, H., 165  
Brandt, J. C., ii, 4-11, 12, 18, 19, 20, 26, 28, 31, 35, 36, 41, 45-47, 51, 53, 54, 57, 66, 91, 92, 93, 97, 99, 101, 103, 110, 112, 117, 119, 120, 125-128, 135, 137, 142, 146, 148, 149, 155, 163-166, 193, 201, 211  
Brecher, K., 95  
Bright Star Catalog, 119, 121  
Broten, N. W., 37  
Brown, H., 19  
Brown, L. W., 35  
Brown, R. L., 161, 166  
Brundage, W. D., 193, 201

- B-star (see also B-association), 5, 43, 119-124, 126-127, 157  
     in Cepheus IV association, 196  
     ultraviolet emission, 173  
 Bunner, A. N., 86, 158-166  
 Burgess, A., 108, 117, 143, 146  
 Burginyon, G. A., 137, 165, 166  
 Burke, B. F., 147, 201  
 Burnett, B., 165  
 Byram, E. T., 165

## C

- Cameron, A. G. W., 29, 53, 54, 74-88, 127  
 Campbell, C. T., 9, 13, 18, 51  
 Carina spiral arm, 38  
 Cas A (Cas XR-1), 113, 144, 165  
 Cassiopeia OB VI association, 197  
 Caswell, J. L., 197, 201  
 Caulk, H., ii  
 Cen XR-1, 165  
 Cen XR-2, 165  
 Cep XR-1, 165  
 Cep XR-3, 164, 165  
 Ceph I association, 197  
 Ceph III association, 197  
 Cepheus IV association, 193, 196-197  
 Cerro Tololo Inter-American Observatory, 149  
 Cesarsky, C., 58, 66  
 Cesarsky, D., 141, 146  
 Chabbal, R., 191  
 Chandrasekhar limit, 75, 78  
 Chodil, G., 158, 166  
 Chubb, T. A., 165  
 Chupp, E., iv  
 Churchwell, E., 142, 145, 146, 196, 201  
 Clarke, B. G., 196, 201  
 Clark, D., 191  
 Clark, T. A., 35  
 cloud, cold, 145  
 Cole, D. J., 37  
 Coleman, P. L., 161, 166  
 Colgate, S. A., 26-29, 53, 66, 68-73, 75, 80, 87, 92, 99, 100, 117, 152-154,  
     156, 157, 166, 192  
 Colvin, R. S., 138



- condensation, in fossil H II regions, 56-65
- Connes, P., 190
- Contopoulos, G., 137
- Cooke, B. A., 94, 99, 165
- Cooke, D. J., 51
- Cox, D. P., 30, 60, 61, 66, 96, 99, 101, 102, 104-108, 117, 155-157, 189, 191
- CP 0329, 50
- CP 0834, 47
- Crab Nebula, 113, 159, 161, 165, 176, 177, 180, 183, 189
  - emitting region in line of sight, 183, 186, 189
  - fossil Strömgren sphere, 189
  - pulsar (NP 0532, also called PSR 0532), 160, 169, 176, 177, 179, 183, 187
  - supernova (1054 A.D.), 8, 98, 189
- Crawford, D. L., 9, 18, 28, 36, 51, 66, 99, 117, 125, 127, 137, 142, 146, 149, 155, 165, 166, 201
- Crimean catalog, 53
- CSIRO Radiophysics Laboratory, 1, 2
- CTA 1 (see Cep XR-3)
- $\gamma$  Cygni, 129
  - absorption, 130
- Cygnus, 10
  - dust clouds, 128-131
  - excitation of region by supernova, 134-136
  - filaments, 128-136
  - galactic structure of region, 128-136
  - H-alpha emission measurements, 132
  - interstellar reddening, 130
  - nebular complex at galactic coordinates ( $75^\circ, 0^\circ$ ), 17
  - nebular complex at galactic coordinates ( $80^\circ, +1^\circ$ ), 128-136
  - nonthermal radio sources, 135
  - physical parameters of emission regions, 133
  - pulsars absent, 132
  - star counts, 130
  - thermal radio sources, 131, 136
- Cygnus Loop, 131, 142, 144, 157, 159, 165
- Cygnus OB2, 128, 129, 130-134, 136
  - H-alpha, emission, 134
- Cygnus OB4, 130
- Cygnus X, 128, 131-136
- Cygnus XR-3, 128, 129, 131, 134-136
  - low-energy attenuation, 129
- Cygnus XR-4, 130
- Cygnus X-5 (see Cygnus Loop)

## D

- D-2-A (satellite), 203-210
  - H-alpha experiment, 203-210
- Dalgarno, A., 57, 66, 98, 99, 145, 146, 155, 191
- Daehler, M., 174, 191
- Daltabuit, E., 185, 186, 191
- Davies, R. D., 141, 146, 185, 186, 191
- Day, G. A., 38
- DeFouw, R. T., 106, 117
- Dickel, H. R., 130-133, 137
- Dickel, J. R., 165
- Dieter, N. H., 141, 146
- dispersion measure, 5, 6, 12, 170-173
  - inaccuracy in, 41
- Downes, D., 129, 135, 137, 142, 144, 146
- Downes, G. S., 9, 14, 18, 47, 51, 62, 66, 90, 100, 117
- Dupree, A. K., 40, 96, 99, 115, 117, 139-147, 157

## E

- Eather, R., 176, 191
- Ekers, R. D., 49, 51
- elephant trunks, 134-135
- Ellis, G. R. A., 33, 34, 36, 185, 187, 191
- Ellis, S. A., 196, 201
- emission measure, 5
- Ewing, M. S., 43, 51, 55

## F

- Fejes, I., 178, 192
- Felli, M., 196, 201
- Field, G. B., 63, 64, 66, 97, 99, 173, 191
- filaments (*see* Cygnus, Gum Nebula, fossil Strömgren sphere condensations)
- Finzi, A., 73
- Fisk, L. A., 90, 99
- Flinders Range, Australia, 1
- fluorescence theory, 20-30, 56, 58, 103, 112, 113, 152, 153
  - test, 41
- forbidden lines, 27, 78, 106, 111, 113-115
- Ford, W. K., Jr., 12, 18

- fossil Strömgren sphere, 12, 24, 27, 29, 42, 58, 59, 139, 142-144, 155
  - condensations in, 56-65
  - cooling, 104-110
  - evolution, 59-63, 103-115
  - ionization, 103-105, 113, 142-144, 189
  - physical parameters, 112, 114, 142
  - recognition of, 211-213
  - recombination lines, 143-144
- Fowler, W. A., 84, 85, 87
- Francey, R. J., 165
- free-free absorption, 31, 32, 185
- free-free emission, 211
- Friedman, H., 165
- Friefield, R. D., 51

## G

- G 78.2 + 1.8, 129, 131, 135, 136
- G 78.4 + 2.5, 135
- G 78.6 + 1.0, 135
- G 265.1 + 1.5, 141
- G 267.8 - 0.9, 141
- G 268.0 - 1.1, 141
- galactic spurs, iii
- galaxy
  - age, 79
  - chemical evolution, 74-88
  - H I "hole," 115
- Gardner, F. F., 146
- Gardner, R. F., 141, 146, 147
- Garrison, R. F., 125
- Gemini 11 (satellite), 194
- Giacconi, R., 129, 130, 137, 165
- giant loops, iii
- Goldberg, L., 140, 141, 143, 146
- Goldsmith, D. W., 63, 66, 97, 99, 191
- Gordon, Ch., 77
- Gordon, C. P., 63, 66, 97, 98, 99, 163, 164, 166, 191, 195, 196, 201
- Gordon, K. J., 63, 66, 97, 98, 99, 163, 166, 191
- Gordon, M. A., 142, 145, 146, 194, 196, 201
- Gorenstein, P., 129, 137, 165
- Goss, W. M., 198, 201
- Gott, J. R., III, ii, 42-55, 88, 127, 148, 156

- Gottesman, S. T., 145, 146  
Gould, R. J., 161, 166  
Gould's Belt, 17  
Grader, R. J., 137, 165, 166  
Griffiths, R. E., 94, 99  
Gum, C. S., iii, 1-3, 12, 13, 15, 18, 36, 101, 199, 203, 210  
Gum Nebula  
    age, 8, 11, 14, 47, 89, 112  
    ancient observations, 8  
    angular size, 6, 10, 12, 13, 40, 46  
    appearance, 148, 149  
    B-associations, 5, 42, 45, 46, 48, 50, 119-124, 126, 127, 156, 167  
    bremsstrahlung volume emissivity, 5  
    central pulsar (see PSR 0833-45)  
    charts, 3, 13, 14, 34, 39, 160, 208, 209  
    clumpiness, 5, 6, 16, 35, 40, 41, 91, 101, 149, 164  
    component nebulae, 10, 13, 38, 39, 110, 112, 149  
    cooling, 62, 67, 95-97, 112  
    cosmic ray electrons, 32, 54  
    cosmic ray propagation, 89-91, 101  
    density distribution, 39, 48, 91, 112, 163  
    discovery, 2  
    dispersion measure, 5, 12, 35, 41, 45, 47, 167  
    distance, 5, 12, 45, 47, 148, 167  
    electron content, 8, 10, 15, 92, 101, 112  
    electron density, 12, 15, 91, 110  
    emission measure, 5, 10, 15, 16, 19, 35, 101, 110, 112, 198  
    evolution, 112  
    expansion, 101  
    Faraday rotation, 49  
    filaments, 95-97, 101, 110, 112, 142  
    forbidden lines, 157  
    as fossil Strömgren sphere, 4-8, 155, 167, 168  
    free-free absorption, 31, 54  
    gamma-ray emission, iv, 94, 95, 102  
    H-alpha emission, 12, 14, 46, 203-210  
    H-II region within, 41, 110, 112, 148, 157  
    hydrogen absorption (21-cm line), 163-164  
    hydrogen measure in line of sight, 5, 45, 47  
    ionization,  
        by blast wave, 58, 113, 155  
        by cosmic rays from supernova, 58, 72, 80, 84, 89-102, 113,  
            155, 156

- energy requirement, 7, 8, 10, 12, 27, 29, 101, 152, 167
- by fluorescence mechanism, 103, 112, 113, 152, 155, 168
- by hot stars, 6, 11, 19, 148
- radii, 15, 16
- rate, 97
- by Vela X supernova, 7, 12, 14, 20, 47, 57, 103, 155, 167
- by young pulsar's ultraviolet emission, 84, 85
- magnetic field, 32
- mass, 113
- models, 5-8, 47, 48, 53, 54, 89, 142
- not a conventional "giant H II region", 199
- observations needed, 101, 102, 149, 156-157, 158, 164, 212
- origin (*see* ionization)
- photographs, 4, 150
- preionization structure, 14
- proton density, 163
- pulsars, in or near, 5, 41, 42, 45-50, 167
- radio observations, 31-36, 38, 39, 54, 101
- Razin effect, 32, 35
- recombination lines, 38, 40, 41, 157
- recombination of, 47, 62, 95, 96
- review articles, iii
- runaway stars in, 42-55
- satellite observations, iv, 31-36, 93-95, 101, 203-210
- shape, 12-17, 93, 148
- size, 6, 8, 12-17, 45, 90, 148
- "small Gum Nebula", 38-40
- stars within (*see also* B-associations), 5, 10, 46, 47
- structure, 14, 15
- temperature, 5, 31-36, 40, 95-97, 112, 163
- volume, 8, 10, 12, 15, 93, 148
- x-ray absorption, 158, 161, 164
- x-ray emission, 93-95, 102, 157, 158-165
- x-ray polarization, 164
- Gunn, J. E., 43, 49, 51, 53, 58, 66, 75, 85
- Gursky, H., 129, 137, 165
- GX5+1 (*see* Milne 56)
- GX9+1 (*see* W28)

## H

- H-beta, interstellar emission, 97, 169-192
- H I clouds, 145, 173, 174

- H I medium (*see also* Gum Nebula sub-entries on hydrogen absorption, hydrogen measure),  
clumpiness, 173  
column density, 170  
density in galactic plane, 97  
electron column density, 172  
emission measure, 186-188  
emitting region models, 183-186  
fraction occupied by emitting regions, 183  
H-beta emission, 97, 169-192  
heating, 97, 98  
ionization, 63, 97, 98, 145, 155, 169-192  
local density, 5, 6, 47  
principal plane, 2  
radio surveys (21-cm line), 20, 115, 145, 163, 164, 171, 195, 196  
recombination lines, 139-145, 169-192  
recombination rate, 97  
temperature, 185, 189  
thickness, 15, 184
- H II region, (*see also* fossil Strömgren sphere, Gum Nebula, Strömgren spheres),  
10, 16, 17, 41, 54, 148, 149, 157, 167, 168, 184  
emission measure, 141  
escape of ultraviolet radiation from, 169  
filamentary nebulae in Cygnus, 128-136  
H-alpha surface brightness, 113, 114  
H-beta emission, 173, 174  
helium, 141  
large nebular complexes in northern part of the galaxy, 193-200  
physical parameters, 142  
recombination lines, 139-142  
surveys, 1, 38, 39
- Habing, H. J., 63, 66, 97, 99, 191
- Halperin, W., 129, 137
- Hamilton, P. A., 33, 34, 36, 51, 165, 185, 187, 191
- Harris, B., 165
- Harris, D. E., 142, 159, 165-166, 167
- Harvard College Observatory, 57
- Hayakawa, S., 96, 99, 173, 191
- Haymes, R. F., 165
- He II  
Balmer lines, 26  
fluorescence, 22  
Lyman edge, 24  
Lyman-alpha emission, 26  
Paschen-alpha, 22

Healey, J. R., 38, 39

heating

    cosmic ray, 173

    by supernova shock wave, 77

heavy elements, abundance, galactic, 79, 80

Henize, K. G., 55, 194, 201

Hewish, A., 115, 117

Higgins, C. S., 33, 34, 37

Higgs, L. A., 129, 137

Hill, E. R., 160, 166

Hill, R. W., 9, 137, 165, 166

Hiltner, W. A., 119, 124, 125, 166

Hindle, P. H., 174, 191

Hinteregger, H. E., 180, 191

Hjellming, R. M., 63, 66, 97, 98, 99, 132, 134, 137, 141, 142, 146, 173, 191,  
199, 200, 201

Holden, D. J., 198, 201

Holt, S. S., 165

Horsehead Nebula, 194

Hoyle, F., 85, 87

HP 1508 (*see* PSR 1508)

Hromov, G. S., 13, 18

Hudson, H. S., 94, 99

Hughes, M. P., 138

Hunt, V. O., 9, 13, 18, 51

Hyatt, W., 99

hydrodynamic theory of supernovae, 27

hydrogen measure, 5

## I

Iben, I., Jr., 127

IC 434, 194

IC 1795-IC 1805-IC 1848 complex, 193, 197, 198

IC 4182, 21, 23, 25

Ikhsanov, R. N., 130, 131, 137

intercloud medium

    H-beta radiation, 173

    ionization, 91

    velocity, local, 176

International Astronomical Union, galactic coordinate system, 2, 13

interstellar absorption, 120, 161

- interstellar cloud, 65, 115
  - formation, 65
- interstellar density, effect on Gum Nebula, 15
- interstellar gas, (see also H I medium), 189
  - along path to Crab Nebula, 161
  - electron density, 56-57
  - formation of stars, 76
  - interaction, fast nuclei, 93
  - temperature, 56-57
- interstellar medium (see H I medium, H II regions, intercloud medium, interstellar gas, etc.)
- interstellar scintillation, 55
  - used to measure transverse velocity, 43, 45, 47, 50
- Ishida, K., 197, 201
- Ishizawa, Y., 201

## J

- Jacquinet, P., 174, 175, 191
- Jenkins, E. B., 47, 51
- Johnson, H. M., 4, 9, 12-18, 36, 38, 40, 101, 130, 137, 174, 191, 203, 207, 208, 210
- Jura, M., 57, 59, 60-63, 66, 145, 146, 155, 191

## K

- Kafatos, M. C., iii, 26, 27, 28, 61, 65, 66, 103-118, 142, 143, 146, 155, 157
- Kaifu, N., 198, 201
- Kaiser, M. L., 35
- Kalet, M., ii
- Kawajiri, N., 197, 201
- Kellogg, E. M., 165
- Kepler's supernova (see SN 1604)
- Kerr, F. J., iii, 1-3, 15, 18, 38-41
- Kim, H. J., 99
- Kitao, K., 96, 99
- Kohoutek, L., 13, 18
- Komesaroff, M. M., 51
- Koren, M., 161, 164, 166
- Kourou, 204
- Kutter, G. S., 71, 72, 73



## L

- Landecker, T. L., 33, 34, 37  
Lang, K. R., 45, 47, 51  
Large, M. I., 7, 9  
La Silla Observatory, 149  
Las Campanas Observatory, 149  
LeBlanc, J. M., 77, 85  
Leiden 21-cm survey, 2  
Lenzen, A., 189, 191  
Lequeux, J., 51  
Lesh, J. R., 120, 122, 125  
Levasseur, A. C., ii, 203-210  
Lilley, A. E., 146, 147  
Limber, D. N., 74, 85  
Lingenfelter, R. E., 90, 95, 99, 100  
Lyman-alpha  
    absorption, 5, 45  
    emission, 106, 108, 109, 111  
    solar, 6  
Lyman-beta, emission, solar, 180  
Lyman-gamma, emission, solar, 180, 182  
Lyman continuum, 106, 132, 195, 197, 199  
Lyman limit, 24, 106, 113, 132, 167  
Lynds, B. T., 13, 16, 17, 18

## M

- M 42 (*see* Orion Nebula)  
M 43, 194, 195  
MacConnell, D. J., 196, 197, 201  
McCray, R., iii, 40, 56-67, 101, 104, 116, 117, 155, 191  
McGee, R. X., 141, 146  
McGowan, F. K., 94, 99  
Mack, J. E., 175, 191, 192  
McKee, C., 26, 28, 92, 99  
McLaughlin, D. B., 28  
McNutt, D. P., 191  
Manchester, R. N., 41  
Maran, S. P., ii-iv, 9, 18, 19, 28, 35, 36, 51, 53, 66, 99, 116, 117, 125, 127, 132, 137, 146, 149, 155, 165, 166, 201  
Mark, H., 166  
mass loss, 76  
Mathewson, D. S., 33, 34, 37, 38, 39  
Matthews, T. A., 128-138

- Mayer, W., 165  
Mazurek, T., 78  
Meier, R. R., 180, 191  
Menon, T. K., 113, 117  
Mezger, P. G., 146, 147, 193, 195-198, 201  
Middlehurst, B. M., 66  
Milky Way, 194, 203  
    B-star distribution, 119  
    Gum Nebula region, 149  
    H-alpha emission, 207  
    Southern, photographic survey, 1  
Miller, F. D., 130, 137  
Miller, J. S., 49, 52  
Mills, B. Y., 9  
Milne, D. K., 5, 7, 9, 47, 51, 112, 115, 117, 141, 144, 146, 147, 159, 160,  
    161, 163, 165, 166, 167  
Milne 56 (GX5+1), 165  
Milner, W. T., 99  
Minkowski, R., 11, 21, 22, 28, 57, 66, 113, 117  
Mitler, H. E., 80, 81, 85  
Miyazawa, K., 201  
Modali, S. B., 132, 137  
Moffet, A. T., 51  
Molonglo Radio Observatory, 41  
Monoceros, 193  
Monoceros loop, 198, 199  
Morgan, W. W., 130, 137, 146, 210  
Morimoto, M., 198, 201  
Morris, D., 51  
Morris, G. A., 9, 14, 18, 47, 51, 62, 66, 90, 100, 117  
Morrison, P., iii, 20, 22, 23, 25, 26, 28, 41, 53, 56, 58, 65, 66, 95, 103, 104,  
    113, 116, 117, 134, 137, 142, 143, 146, 155, 157, 168, 189, 191  
Morton, D. C., 47, 51  
Mount Stromlo Observatory, 1, 4, 14, 149  
MP 0736 (see PSR 0736-40)  
MP 0818 (see PSR 0818-13)  
MP 0835, 5, 42, 45, 46, 48, 49  
    age, 42, 50, 53  
    dispersion measure, 5, 48  
    distance from Sun, 48  
    linear polarization, 50  
    parent star, 42  
    rotation axis position angle, 50

MP 0940, 5

Müller, C. A., 177, 192

## N

N II, forbidden emission, 12, 118

Nakajima, T., 201

Nebula

compact, as core-halo source, 195

ringlike, 197

thin, detection, 212

Neckel, T., 130, 131, 137

neutron star, 42, 43, 68, 76, 79, 167

NGC 1003, 23, 25

NGC 2024, 145, 194

recombination line, 196

structure, 195

NGC 2264, 123

NGC 4214, 23

NGC 4374, 25

NGC 6835, 25

NGC 7000, 141

NGC 7822, 196, 197, 199

Nishimura, S., 191

Nor XR-1, 165

Nor XR-2, 165

Novick, R., 165

NP 0532 (see Crab Nebula pulsar)

nucleosynthesis (see also p-process, r-process, s-process), 74-85  
carbon-to-iron, 76, 78-80

## O

O-association, 43, 126

OB-association, 119

OB-complex, 197

OB-star, 17, 149, 197, 198

O'Connell, D. J. K., 43, 51

O'Dell, C. R., 183, 192, 194, 201

OGO-5 (satellite), 6

Oph XR-1 (see SN 1604)

ζ Ori, 194

λ Ori, 194

- Orion (see also Barnard Loop), 40, 194-196
- Orion I association, 193-199
  - dust cloud, 194, 196
  - H II region, 194
  - nebula, reflection, 196
  - radio source, 195, 196
- Orion Nebula, 35, 194
- Orion X, 195, 199
- O-star, 10, 43, 88, 119-124, 126, 127, 148, 199
  - in Cepheus IV association, 196
  - ultraviolet emission, 173
- OSO-7 (satellite), iii
- Ostriker, J. P., ii, 42-55, 58, 66, 75, 85, 127, 148, 156

## P

- P1439-62 (see Cen XR-1)
- P1548-55 (see Nor XR-2)
- P1613-50 (see Nor XR-1)
- Pacini, F., 159, 166
- Paczynski, B., 75, 85
- Page, T. L., 29, 67
- Palmeira, R. A. R., 99, 191
- Palmer, P., 141, 145, 147
- Palmieri, T. M., 9, 135, 137, 159, 160, 162, 165, 166
- Palomar Observatory Sky Survey, 16, 129, 130
- Parker, R. A. R., 113, 117, 142
- Parkes, 38, 41
- Pawsey, J. L., 2, 3
- Penfield, H., 139, 141, 147
- Pengelly, R. M., 171, 192
- Peterson, L. E., 94, 99
- Pierce, T. E., 90, 99
- Pikel'ner, S. B., 97, 100
- Pleiades, 212
- Pottasch, S. R., 113, 117, 137
- Pounds, K. A., 94, 99, 165
- Poveda, A., 10, 19, 29, 53, 129, 135, 136, 138, 165
- p-process, 76, 77, 79, 80
- Price, R. M., 51
- PSR 0532 (see Crab Nebula pulsar)
- PSR 0628-28, 47
- PSR 0736-40, 5, 41

PSR 0818-13, 41, 47

PSR 0833-45 (Vela pulsar), iii, 5, 7, 11, 14, 16, 41, 42-50, 57, 119, 159,  
163, 164, 167

age, 8, 14, 47, 90, 112

B-association, 50, 123, 126, 127

dispersion measure, 5, 41, 45, 47, 109

distance, 47, 148

origin, 42-50, 57, 68, 78-80, 124, 127

period, 45

polarization, 49

position, 46, 160

rotational axis, 42, 49, 50

runaway star theory, 42-50

ultraviolet radiation, 84, 85

PSR 1508, 169-190

age, 50

PSR 1541, 169-190

PSR 1642, 169-190

PSR 1929 + 10, 41

pulsar (see also names of pulsars),

ages, 50, 53, 115

B-association, relation with, 156

emission, high-energy, 159-160

formation, 78

mass of stars needed, 75

galactic plane, distance from, 43, 55

high velocity star, relation with, 156

hydrogen absorption, 163, 164

H I "hole," correlation with, 115

interstellar scintillation, 43, 55

motion, 43, 45, 55

as oblique magnetic rotator, 49

as runaway objects, 43, 53

§ Puppis, 2, 4, 5, 7, 10, 11, 16, 47, 48, 53, 148

B-association, 119-125

as ionization source, 6, 10, 11

Lyman-alpha absorption, 5, 45, 47

origin, place of, 123, 124

proper motion, 123

Strömgen sphere, 10, 41, 42, 48, 54, 110, 112

temperature, 19

Puppis A, iii, 11, 159, 160, 164, 165

## R

- RAE-1 (Radio Astronomy Explorer 1), 31-36, 212  
RCW 38 (G 267.8 - 0.9), 141  
RCW 63, 13  
Radcliffe Observatory, 149  
Radhakrishnan, V., 49, 51  
Radio Astronomy Explorer 1 (see RAE-1)  
Ramaty, R., iv, 26, 27, 28, 58, 66, 89-102, 104, 113, 117, 156, 157, 164,  
166, 189, 192  
Rappaport, S., 165  
Razin effect, 32, 35  
Reames, D., 30  
Reay, N. K., 174, 191, 192  
Reber, G., 33, 34, 37  
recombination lines, radio frequency, 139-147  
red shift, 22  
Reddish, V. C., 193, 201  
Rees, M. J., 63, 66, 159, 166, 192  
Reeves, H., 85, 87  
Reichley, P. E., 8, 9, 14, 18, 47, 51, 62, 66, 90, 100, 112, 117  
Reifenstein, E. C., III, 141, 147, 193, 198, 201  
Reynolds, R. J., ii, 97, 100, 169-192  
Rinehart, R., 142  
Ring, J., 174, 191, 192  
Rishbeth, H., 195, 199, 200, 201, 202  
Robinson, G. J., 198, 201  
Rodgers, A. W., 4, 9, 13, 18, 46, 51  
Rodrigues, R., 166  
Roesler, F., 169-192  
Rohan, P., 33, 34, 37  
Rome, J. M., 38, 39  
Rosette Nebula, 141, 198, 199  
r-process, 76, 77, 79, 80  
Rubin, V. C., 12, 18  
runaway star, 42-55, 88, 123  
Ruprecht, J., 128, 137  
Ruzanov, V. A., 147

## S

- S26, 197, 198  
S 313 (see A 35)

- Salomonovich, A. E., 147  
Salpeter, E. E., 74, 85, 180, 191  
Sandri, G., 99, 191  
Sartori, L., 20-30, 41, 53, 56, 58, 66, 103, 104, 113, 116, 117, 134, 137,  
142, 146, 155, 168, 189, 191  
Savedoff, M. P., 71, 72  
Scargle, J. D., 49, 52  
Scherb, F., 169-192  
Schild, R. E., 125  
Schnöpper, H., 165  
Schraml, J., 193, 195, 197, 198, 201, 202  
Schuërmann, D. W., 71, 72  
Schulte, D. H., 128, 138  
Schwartz, D. A., 94, 99, 165  
Schwarz, J., iii, 56-67, 104, 117  
Scorpius, 17  
Sco X-1, 63  
Scott, E. H., 97, 100  
Seaton, M. J., 96, 100, 108, 118, 132, 138  
Segre, E., 99  
Seielstad, G. A., 51  
Serlemitsos, P., 93, 99, 165  
Seward, F. D., 7, 9, 135, 137, 159, 160, 162, 165, 166  
Sgr XR-3 (see W28)  
Shain, C. A., 33, 34, 37  
Shalloway, A. M., 166  
Shapiro, M., 87  
Sharpless, S., 13, 18  
Shen, B. S. P., 85  
Shklovsky, I. S., 57, 62, 66, 90, 100  
Shteinshleger, V. B., 147  
Siding Springs Observatory, 149  
Silk, J., iii, 28, 63, 66, 95, 100, 117, 156, 157, 166, 192  
Simonson, S. C., III, 128-138  
Smith, A. M., 47, 52  
Smith, C. S., 200  
Smith, L., 10  
Smithsonian Astrophysical Observatory, 80-81  
SN 1006, 113  
SN 1054 (Crab Nebula supernova), 113  
SN 1572 (Tycho's supernova, Cep XR-1), 113-116, 118, 165  
SN 1604 (Kepler's supernova), 25, 113, 164, 165  
Sobieski, S., 54  
Soden, L. B., 33, 34, 37

- Sorochenko, R. L., 139, 147  
 Souffrin, S., 63, 66, 145, 146  
 South Africa, 149  
 southern survey, 38  
 spallation, 80, 83, 84  
 spherical blast wave theory, 57  
 Spitzer, L., 6, 9, 35, 37, 48, 52, 97, 100, 135, 138  
 s-process, 76, 77, 79, 80  
 Staelin, D. H., 43, 51, 193, 201  
 Stecher, T. P., ii, 9, 18, 19, 28, 35, 36, 41, 51, 66, 99, 117, 125, 127, 137,  
 142, 146, 149, 155, 157, 165, 166, 167-168, 201  
 Stecker, F. W., 86, 88  
 Steigman, G., 95, 100  
 stellar wind, 83  
 Stoering, J. P., 9, 137, 165, 166  
 Stone, R. G., 35, 37, 186, 191  
 Stoner, J. O., Jr., 191  
 Straka, W. C., 126-127  
 Strand, K. Aa., 125  
 Strömgren, B., 130, 137, 146, 210  
 Strömgren radius (see also Strömgren sphere), 91  
 definition, 15  
 Strömgren sphere (see also fossil Strömgren sphere,  $\gamma$  Velorum, Gum Nebula  
 sub-entries, H II region, Strömgren radius,  $\zeta$  Puppis), 58, 59  
 Stromlo, 16, 158, 159  
 Summers, H. P., 143, 146  
 supernova (see also Crab Nebula, Gum Nebula, "SN" entries, Vela X)  
 in binary star system, 42-55, 78  
 composition, 79  
 core temperature, 73  
 cosmic rays from, 74-88, 89-102, 155-157  
 ejecta (see also cosmic rays from supernova), 152-154  
 velocity and composition, 68-73  
 electromagnetic theory, 58  
 as end product of stellar evolution, 74-88  
 energy release, 29, 152-154  
 envelope expansion, 77  
 fluorescence theory, 20-30, 152, 153  
 as heat source of interstellar medium, 62  
 hydrodynamic theory, 27  
 light curve, 21-25, 29, 58  
 mass of pre-supernova, 42-55, 74-78, 124, 127  
 mass loss, 76, 77



- model, 73, 79
- nucleosynthesis, 74-88
- rate of occurrence, 14, 57, 62, 75, 81, 82, 86-88, 211
- rocket effect, 53
- as source of iron in universe, 211
- spectrum, 21, 77, 78
- type I, 20-30, 77, 78, 103, 112, 113
- type II, 77, 80, 113
- supernova remnant (see also Crab Nebula, Cygnus Loop, G78.2 + 1.8,  
Monoceros Loop, Puppis A, supernova, "SN" entries, Vela X, W28)
  - 3C 392, 165
  - 3C 396, 165
  - 13S64, 165
- Swift, C. D., 166
- Sydney 21-cm survey, 2
- synchrotron emission, interstellar, 54
- synchrotron radiation, 160, 164
  - galactic, 31, 32

## T

- Takahashi, T., 201
- Takayanagi, K., 191
- Talbot, R. J., 127
- Tammann, G. A., 75, 85
- Taurus, 17
- Terzian, Y., 47, 48, 52, 137, 198, 201
- thermal condensation, 63-65
- thermal instability theory, linearized, 64
- Thompson, A. R., 138
- Tolbert, C. R., 178, 192
- Tomasko, M. G., 97, 100
- Trapezium, 194
- Truran, J. W., 74, 78, 85
- Tucker, W. H., 26, 27, 28, 58, 60, 61, 66, 96, 99, 104-108, 113, 116, 117,  
118, 155, 161, 164, 166
- Tycho's supernova (see also SN 1572, supernova remnant), 27, 28, 65, 103,  
104, 109-116

## U

- Uhuru (satellite), 158
- Underhill, A. B., 54, 86, 118
- Upton, E. K. L., 119-125, 126, 127, 148

## V

Vaughan, A. E., 9

Vela X (see also Gum Nebula, supernova, PSR 0833-45), iii, 15, 45, 46, 57, 155

age (see PSR 0833-45, age)

chart, 160

cosmic rays from, 89-102

distance, 5

expansion rate, iii, 11

filaments, 112, 161

fossil Strömgren sphere, 4-11, 103-116

mass of pre-supernova, 124, 127

models, 162

nature of pre-supernova, 74-85

nucleosynthesis in, 74-85

photographs, 150, 151

radio source, 7

x-ray source (Vel XR-2), 7, 158-165

$\gamma$  Velorum (see also  $\gamma^1$  Velorum,  $\gamma^2$  Velorum), 2, 4, 5, 7, 10, 11, 45, 47,

49, 50, 119, 126

B-association, 5, 42, 45, 48, 50, 126, 127

distance, 5, 45

as ionization source, 6, 10, 11

location in Gum Nebula, 123

Lyman-alpha absorption, 5, 45

Strömgren sphere, 10, 41, 42, 48, 54, 110, 112

$\gamma^1$  Velorum, 123

$\gamma^2$  Velorum, 2, 16, 112, 120, 123, 126, 127, 148, 149

Véron, P., 134, 138

Vette, J. I., 94, 95

## W

W3 (see also IC 1795-IC 1805-IC 1848 complex), 197

W4 (see also IC 1795-IC 1805-IC 1848 complex), 197, 199

W5 (see also IC 1795-IC 1805-IC 1848 complex), 197, 199

W28 (Sgr XR-3, GX9+1), 144, 165, 193, 199

W28, 198

W49, 193, 198, 199

Wade, C. M., 200

Walker, M. F., 194, 202

Wallerstein, G., iii

Wampler, E. J., 49, 52

Waters, J. R., 129, 130, 137  
Weaver, H., 115  
Weber, R. R., 33, 35, 37  
Webster, W. J., Jr., ii, 193-202  
Wendker, H. J., 129-135, 137, 138  
Werner, M. W., 63, 66, 173, 192  
Westerhout, G., ii, 3, 142, 211-213  
white dwarf, 70, 75, 76, 78  
Whiteoak, J. B., 9, 13, 18, 51  
Whiteoak Sky Survey, 11  
Wielebinski, R., 33, 34, 37  
Williams, D. R., 28, 113, 115, 116, 117, 118  
Wilson, J. R., 77, 85  
Wilson, T. L., 40, 141, 144, 146, 147, 201  
Wink, J. E., 195, 198, 200, 202  
Wisconsin, 160, 162  
Wolf-Rayet star, 10, 124, 148  
Woltjer, L., 129, 135, 136, 138

## X

X-ray source, 7, 63, 135, 158-165

## Y

Yates, K. W., 33, 34, 37  
York, D. G., 194, 201

## Z

Zuckerman, B., 144, 147  
Zwicky, F., 21, 28, 43, 52

NATIONAL AERONAUTICS AND SPACE ADMINISTRATION  
WASHINGTON, D.C. 20546

OFFICIAL BUSINESS  
PENALTY FOR PRIVATE USE \$300

SPECIAL FOURTH-CLASS RATE  
BOOK

POSTAGE AND FEES PAID  
NATIONAL AERONAUTICS AND  
SPACE ADMINISTRATION  
481



POSTMASTER: If Undeliverable (Section 1  
Postal Manual) Do Not Ret

*"The aeronautical and space activities of the United States shall be conducted so as to contribute . . . to the expansion of human knowledge of phenomena in the atmosphere and space. The Administration shall provide for the widest practicable and appropriate dissemination of information concerning its activities and the results thereof."*

—NATIONAL AERONAUTICS AND SPACE ACT OF 1958

## NASA SCIENTIFIC AND TECHNICAL PUBLICATIONS

**TECHNICAL REPORTS:** Scientific and technical information considered important, complete, and a lasting contribution to existing knowledge.

**TECHNICAL NOTES:** Information less broad in scope but nevertheless of importance as a contribution to existing knowledge.

**TECHNICAL MEMORANDUMS:** Information receiving limited distribution because of preliminary data, security classification, or other reasons. Also includes conference proceedings with either limited or unlimited distribution.

**CONTRACTOR REPORTS:** Scientific and technical information generated under a NASA contract or grant and considered an important contribution to existing knowledge.

**TECHNICAL TRANSLATIONS:** Information published in a foreign language considered to merit NASA distribution in English.

**SPECIAL PUBLICATIONS:** Information derived from or of value to NASA activities. Publications include final reports of major projects, monographs, data compilations, handbooks, sourcebooks, and special bibliographies.

**TECHNOLOGY UTILIZATION PUBLICATIONS:** Information on technology used by NASA that may be of particular interest in commercial and other non-aerospace applications. Publications include Tech Briefs, Technology Utilization Reports and Technology Surveys.

Details on the availability of these publications may be obtained from:

SCIENTIFIC AND TECHNICAL INFORMATION OFFICE

NATIONAL AERONAUTICS AND SPACE ADMINISTRATION  
Washington, D.C. 20546